SCREENING AND EVALUATION OF THE ANTICANCER POTENTIAL OF SCORPION VENOMS AND SNAKE VENOM L-AMINO ACID OXIDASE IN GASTRIC CANCER

DING JIAN

NATIONAL UNIVERSITY OF SINGAPORE

2014

SCREENING AND EVALUATION OF THE ANTICANCER POTENTIAL OF SCORPION VENOMS AND SNAKE VENOM L-AMINO ACID OXIDASE IN GASTRIC CANCER

DING JIAN

(*B.S.c*)

A THESIS SUBMITTED FOR THE DEGREE OF

DOCTOR OF PHILOSOPHY

VENOM AND TOXIN RESEARCH PROGRAMME

DEPARTMENT OF ANATOMY

YONG LOO LIN SCHOOL OF MEDICINE

NATIONAL UNIVERSITY OF SINGAPORE

2014

DECLARATION

I hereby declare that this thesis is my original work and it has been written by me in its entirety. I have duly acknowledged all the sources of information which have been used in the thesis.

This thesis has also not been submitted for any degree in any other university previously.

DING JIAN

(20, Mar, 2015)

ACKNOWLEDGEMENTS

I would like to take this opportunity to express my sincere gratitude to those who give me help during my pursuit of PhD degree for the last four years. It is obvious that this thesis could not be finished in time and with good quality without their support.

First, I would thank my supervisor **Prof Gopalakrishnakone, P**, who introduced this interesting project to me. As a supervisor, Prof Gopal helped me design experiments, guided me to learn the knowledge and skills in toxicology and cancer research, and more importantly encouraged me to be confident and move forward when the project was not going smoothly. His attitudes towards work and life also impressed me and let me know the importance of the balance between these two factors.

Second, I would deliver my deep appreciation to my co-supervisor **Prof Bay Boon-Huat**, Head of Anatomy department, NUS. Prof Bay interviewed me and enrolled me from Zhejiang University, China, to NUS. Furthermore, Prof Bay took me in as a member of team Anatomy and as part of his research group. I have benefited so much from the friendly and supportive environment in his group. Prof Bay also guided me and supported me with detailed instructions during the whole processes of my PhD project. He has discussed with me for most experimental problems and revised my drafts of publications, proposals and thesis as well.

Next, I would like to thank **Dr Wu Ya Jun**, **Ms Chan Yee Gek** for their help in sample processing and viewing of TEM and SEM, respectively. I appreciate the support on SILAC work from our collaborator **Dr Jayantha Gunaratne`s** team, Quantitative Proteomics Group, Institute of Molecular & Cell Biology, Singapore. The appreciation also goes to **Ms Ng Geok Lan, Ms Yong Eng Siang, Mr Poon Zhung Wei, Mr Gobalakrishnakone, Ms Pan Feng** and **Dr Cao Qiong** for their efforts in the lab management and the technique assistance to my bench work. Similarly, the support from **Ms Carolyne Ang, Ms Diljit Kour** and **Ms Violet Teo** for administrative issues should not be ignored.

I am also deeply grateful for the guidance and help from my seniors, **Dr Feng Luo, Dr VGM Naidu, Dr M M Thwin, Dr Yu Ying Nan, Dr Alice Zen Mar Lwin, Dr Chua Pei Jou** and **Dr Jasmine Li Jia En.** I would appreciate the partnership and friendship of my colleagues from Anatomy department, **Ms Guo Tian Tian, Ms Oliva Jane Sculy, Ms Eng Cheng Teng, Mr Denish Babu, Mr Ashwini Kumar, Ms Cynthia Wong, Ms Shao Fei, Dr Xiang Ping, Ms Ooi Yin Yin, Dr Parakarlane R, Mr Lum Yick Liang,** and **all the staff and students** in Department of Anatomy. The research wouldn`t be done in smooth and the life wouldn`t be joyful without their company.

The last but not the least, I would especially thank my parents who raise me up, support my education, teach me good behaviours and always encourage, care and love me. The love from my parents and my elder sister is the ever motivation to make progress.

TABLE OF CONTENTS

SUMMARY

Animal venoms and toxins from snakes, scorpions, spiders and bees, have been widely applied in both traditional medicine and current biopharmaceutical research. Possessing anticancer potential is another novel discovery for animal venoms and toxins. An increasing number of studies have shown the anticancer effects of venoms and toxins of snakes, scorpions and others *in vitro* and *in vivo*, which were achieved mainly through the inhibition of cancer growth, arrest of cell cycle, induction of apoptosis and suppression of cancer metastasis. However, more evidence is needed to support this concept and the mechanisms of anticancer actions are still not clearly understood. Therefore, in this study, several scorpion venoms were screened and the anticancer potential of *Hottentotta hottentotta* scorpion venom (BHV) and the L-amino acid oxidase (LAAO) from *Crotalus adamanteus* snake venom were extensively evaluated and investigated in NUGC-3 human gastric cancer cells and xenograft model.

Crude venoms of *Mesobuthus martensi karsch*, *Hottentotta hottentotta*, *Heterometrus longimanus* and *Pandinus imperator* scorpions, were screened for their anti-proliferative effects to gastric cancer cells, with results showing that BHV was the most inhibitory to NUGC-3 cell proliferation with low IC50 (8.12 µg/ml). Further studies indicated that BHV decreased the cell viability of NUGC-3 cells by cell cycle arrest at sub-G1 phase and

induction of apoptosis. In NUGC-3 gastric cancer mouse xenograft model, BHV inhibited tumor growth, histologically disrupted tumor homogeneity and induced apoptosis *in situ*. Interestingly, at low concentration (2 µg/ml), BHV also suppressed NUGC-3 cell migration and invasion.

BHV crude venom was partially purified and characterized by HPLC, SDS-PAGE and mass spectrometry, with the identification of L-amino acid oxidase (LAAO) as an active molecule. However, as crude BHV was almost used up and the supplier was not able to continue the supply, a commercially available LAAO from *Crotalus adamanteus* snake venom was applied to investigate the anticancer potential of LAAO in gastric cancer cells. Similarly, it was observed that LAAO decreased the cell viability of gastric cancer cells dose-dependently, arrested cell cycle at G2/M phase, induced cell apoptosis and inhibited cell migration at low concentration. These functional studies revealed (for the first time) that BHV and LAAO from *Crotalus adamanteus* snake venom exert anticancer effects in gastric cancer via cell cycle arrest, induction of apoptosis and inhibition of cancer metastasis.

Another contribution from this work is the clarification of the mechanisms for BHV and LAAO`s anticancer actions. A caspase-independent apoptosis (CIA) induced by BHV and LAAO was confirmed by western blot, caspase-3 activity assay and the presence of pan caspase inhibitor z-VAD-fmk. Increase of intracellular ROS, with permeabilization of mitochondrial membrane and the translocation of AIF from mitochondria to nucleus were

also observed in LAAO induced CIA. Moreover, using genomic and transcriptomic approaches, the MAPK/ERK pathway was found to be inhibited by both BHV and LAAO treatment. Finally, several gene and protein candidates were elucidated from microarray and SILAC data, such as EIF, HNRNP and HSP families as well as TUBB, TOP2A and SDHA, which could be good anticancer targets and deserve further investigations.

Taken together, this study evaluated and confirmed the anticancer potential of BHV and LAAO from *Crotalus adamanteus* snake venom using gastric cancer model. The MAPK/ERK pathway was identified as the mechanistic pathway responsible for the anticancer activities of BHV and LAAO. The novel findings shed light on the development of anticancer agents from scorpion venoms and L-amino acid oxidases, and provided biological insight into the targets for gastric cancer therapeutics.

LIST OF FIGURES

LIST OF TABLES

ABBREVIATIONS

5-FU	5-Fluorouracil
AGAP	Analgesic-antitumor peptide
AIF	Apoptosis inducing factor
ANOVA	Analysis of variance
AO/EB	Acridine orange / ethidium bromide
APS	Ammonium persulfate
ARS	Age standardized rate
BHV	*Buthus hottentotta* (*Hottentotta hottentotta*) venom
BmK	*Buthus martensii* (*Mesobuthus martensii*) *karsch*
BSA	Bovine serum albumin
caspase	Cysteine-containing aspartate-directed protease
CCCP	Carbonyl cyanide 3-chlorophenylhydrazone
CIA	Caspase independent apoptosis
CTX	Chlorotoxin
DAPI	4,6-diamidino-2-phenylindole
DAVID	Database for Annotation, Visualization and Integrated Discovery
DCF	2’,7’ - dichlorofluorescin
DCFDA	2’,7’ - dichlorofluorescein diacetate
DEPC	Diethyl pyrocarbonate
DMSO	Dimethylsulfoxide

Dox	Doxorubicin
DTT	Dithiothreitol
EDTA	Ethylenediaminetetraacetic acid
EGFR	Epidermal growth factor recepotr
EIF	Eukaryotic translation initiation factor
ERK	extracellular signal-regulated kinase
FBS	Fetal bovine serum
FDA	Food and drug administration
H. pylori	Helicobacter pylori
HER-2	Human epithelial growth factor 2
HNRNP	Heterogeneous nuclear ribonucleoprotein
HPLC	High performance liquid chromatography
HSP	Heat shock protein
JC-1	5,5',6,6'-tetrachloro-1,1',3,3'- tetraethyl-imidacarbocyanine iodide
JNK	c-Jun NH2-terminal kinase
kDa	Kilo dalton
KTxs	Potassium channel toxins
LAAO	L-amino acid oxidase
LDH	Lactate dehydrogenase
M.W.	Molecular weight
MALDI-TOF-MS	Matrix-assisted laser desorption/ionization time of flight mass spectrometry

MAPK	Mitogen-activated protein kinase
MDA	Malondialdehyde
MEK	MAPK kinase
MMP	Mitochondrial membrane potential
MMp	Mitochondrial membrane permeabilization
MMPs	Matrix metalloproteinases
MSI	Microsatellite instability
MSK	Mitogen- and stress-activated protein kinase
NaScTxs	Scorpion Na^+ channel toxins
NDBPs	Non disulfide-bridged peptides
OD	Optical density
p90RSK	90 kDa ribosomal S6 kinase
PARP	Poly (ADP-ribose) polymerase
PBS	Phosphate buffered saline
PI	Propidium iodide
PLA_2	Phospholipase A2
PS	Phospholipid phosphatidylserine
PTEN	Phosphatase and tensin homolog
PVDF	Polyvinyl difluoride
ROS	Reactive oxygen species
RT	Room temperature
RT-PCR	Real-time polymerase chain reaction
SDS-PAGE	Sodium dodecyle sulphate-polyacrylamide gel electrophoresis

SEM	Scanning electron microscopy
SEM	Standard error of the mean
SILAC	Stable Isotopic Labeling using Amino acids in Cell culture
TBS	Tris buffered saline
TBST	Tris buffered saline in 1% tween-20
TEM	Transmission electron microscopy
TEMED	N,N,N’,N’- tetramethylethylenediamine
TOP2A	Topoisomerase (DNA) II alpha
TUBB	Tubulin
TUNEL	Deoxynucleotidyl transferase (TdT) dUTP nick end labeling
VEGF	Vascular endothelial growth factor

PUBLICATIONS

Book Chapter

- **Jian Ding,** Boon-Huat Bay, P Gopalakrishnakone. Animal venoms and toxins, a novel approach in breast cancer treatment. *Advances In Breast Cancer Biology And Clinical Management.* G. Yip and B.H. Bay, 2012

Journals

- **Jian Ding**, Pei-Jou Chua, Boon-Huat Bay, P Gopalakrishnakone. Scorpion venoms as a potential source of novel cancer therapeutic compounds. *Exp Biol Med* 2014, **4**, 378-393 (IF=2.226).

Patent pending

- **Title:** L-Amino Acid Oxidase (LAAO) From *Crotalas Adamanteus* Venom Induces Caspase-Independent Apoptosis in Human Gastric Cancer Cells.

  Inventors: Jian Ding, P Gopalakrishnakone (PI), Boon-Huat Bay, Pei-Jou Chua.

  Status: patent filing by US Provisional Application No.: 61/976,567.

Conference Proceedings

- **Jian Ding,** Boon-Huat Bay, P Gopalakrishnakone. Scorpion venom induces cytotoxicity in human gastric cancer cells *in vitro*. The 2nd International Anatomical Sciences and Cell Biology Conference. Chiang Mai, Thailand, Dec.2012
- **Jian Ding,** Pei-Jou Chua, Boon-Huat Bay, P Gopalakrishnakone. Screening the anti-cancer potential of scorpion venom in gastric cancer *in vitro* and *in vivo*. XI Congress of Pan-American Society of the International Society on Toxicology. Brazil, Nov. 2013

- **Jian Ding,** Boon-Huat Bay, P Gopalakrishnakone. Transcriptomic Studies of Gastric Cancer Cells with Scorpion Venom Treatment. Yong Loo Lin School of Medicine 4th Annual Graduate Scientific Congress. Singapore, Mar. 2014
- **Jian Ding,** Boon-Huat Bay, P Gopalakrishnakone. L-amino acid oxidase from *Crotalus adamanteus* venom induces caspase-independent apoptosis in human NUGC-3 gastric cancer cells. American Association for Cancer Research (AACR) Annual Meeting 2014. USA, Apr. 2014

Other publication by the candidate

- VGM. Naidu, Bandari Uma Mahesh, Ashwini Kumar Giddam, Kuppan Rajendran Dinesh Babu, **Jian Ding**, K Suresh babu, B Ramesh, Rajeswara Rao Pragada, Gopalakrishnakone P. Apoptogenic activity of ethyl acetate extract of leaves of *Memecylon edule* on human gastric carcinoma cells via mitochondrial dependent pathway. *Asian Pac J Trop Med* 2013, 412-420 (IF=0.926).

CHAPTER 1

INTRODUCTION

1. INTRODUCTION

1.1 Gastric cancer

1.1.1 Epidemiology

According to the World Health Organization (WHO), cancer has surpassed heart disease to become the leading cause of death worldwide, accounting for 14.1 million new cases and 8.2 million deaths in 2012. Lung, liver, stomach, colorectal and breast cancers are the most common causes of cancer death. More than 60 percent of new cancer cases come from less developed regions such as Africa and Asia.

Gastric cancer, also called stomach cancer, refers to the tumors that arise from any part of the stomach, which is a J-shape gastrointestinal organ consisting of 5 parts: cardia, fundus, body, antrum and pylorus. The inner lining of the stomach has four layers: serosa, muscularis, submucosa and mucosa (Fig 1.1) (Clayburgh *et al.*, 2004).

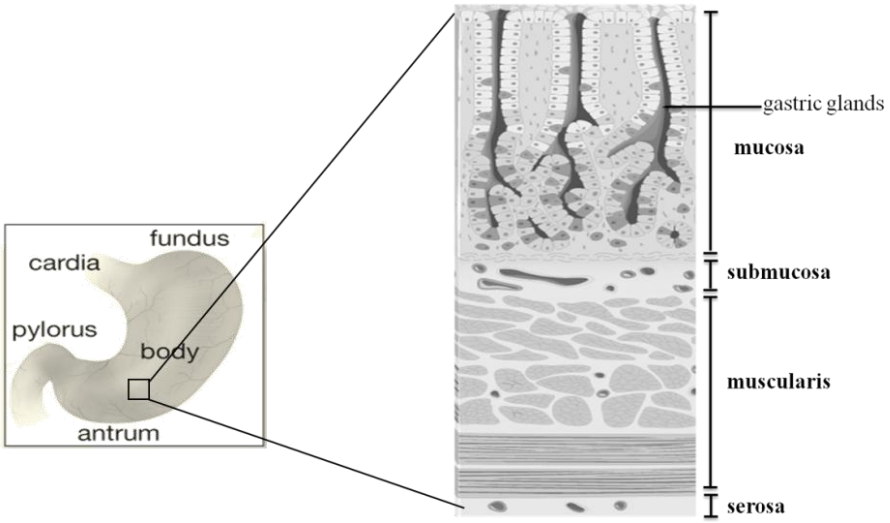

Fig 1.1 Structures of human stomach (modified from *stomach: structure*. Art. *Encyclopædia Britannica,2010*). Left, regions of the stomach; Right, the inner lining of stomach wall in inside-out direction.

Due to the high incidence and mortality rates, gastric cancer has become a major health burden for most countries in the last few decades. In 2012, gastric cancer accounted for 952,000 new cases, which makes it the 5th most common cancer worldwide. More perturbing is the fact that it causes 723,000 cancer deaths and ranks as the 3rd leading death of cancer in 2012, only behind lung and liver cancers (Ferlay *et al.,* 2013). Gastric cancer mostly occurs in patients between ages of 60 to 80 and shows a male preponderance with an approximate male: female ratio of 2:1. As most patients are diagnosed at advanced stages, the 5-year survival rate is low, at only about 20 percent (Nagini, 2012). From the geographical perspective, there are high incidence rates in Eastern Asia, Eastern Europe, and South America. In contrast, low incidence rates are documented in North America and most parts of Africa. Males in China, Korea and Japan now predominate with up to 30 new diagnosed cases per 100,000 population per year (Jemal *et al.*, 2011). This regional variation is attributed to genetic differences, dietary patterns and the high association of *Helicobacter pylori* infection (Parkin, 2006).

In Singapore, even though there is a declining trend in gastric cancer, it remains the 7th most frequent cancer in males and 8th most frequent cancer in females respectively, leading to 1611 cancer deaths for both gender (data 2008-2012) (Singapore Cancer Registry, 2014). Moreover, there is a difference between various ethnic groups in Singapore. Chinese males have the highest incidence rate with an age standardized rate (ASR, per 100

000 population per year) of 25.7. Whereas, Malay and Indian males have lower incidence rates as ASR decreases to 8.4 and 6.6, respectively (Look *et al.*, 2001).

1.1.2 Risk Factors

Gastric cancer is a multifactorial disease with complex interactions and combination effects between different risk factors. *Helicobacter pylori* (*H. pylori*) bacterial infection is considered as one primary risk factor for gastric cancer. Several meta-analyses performed in gastric cancer has proven that *H. pylori* chronic infection is associated with a two-fold increased risk of developing distal gastric carcinoma and gastric mucosal lymphoma in human (Eslick, 2006). In 1994, based on the evidences from numerous epidemiological and animal studies, the WHO International Agency for Research on Cancer has characterized *H. pylori* as a "Group 1 human carcinogen" (IACR, 1994). However, even though over 50% of the world population is infected by *H. pylori*, only 2 percent of the infected individuals progress to gastric cancer and *H. pylori* does not increase the risk of proximal or cardia gastric cancers (Group, 2001; Suerbaum *et al.*, 2002). Therefore, a combination of a virulent bacterial strain, environment factors (i.e. smoking and dietary factors) and the host genetic susceptibility is established to be responsible for *H. pylori* -induced gastric cancer (Kim et al., 2011). Studies show that strains possessing the cytotoxin-associated gene A (CagA) are more virulent and carcinogenic (Huang *et al.*, 2003). The molecular and cellular

driving forces for *H. pylori*-induced gastric carcinogenesis include generation of oxidative stress, DNA damage and cell cycle dysregulation as well as changes in epithelial gene expression (described in section 1.1.5) and loss of gastric acidity (Kim *et al.*, 2011). Preclinical and clinical data show that the eradication of *H. pylori* can inhibit or even regress the progression of precancerous lesions, shedding light on the potential to prevent gastric cancer by early screening and removal of *H. pylori* in patients. However, the time the *H. pylori* infection is detected should be taken into account as atrophic gastritis and intestinal metaplasia are irreversible where genetic changes have already occurred (Malfertheiner *et al.*, 2006).

Another important risk factor for gastric cancer is diet. High consumption of salt and salt-preserved foods is strongly associated with the increased risk of developing gastric cancer. It is found that salt intake will enhance *H. pylori* colonization, cause direct damage to gastric mucosa, and eventually lead to gastritis (Wang *et al.*, 2009; D'Elia *et al.*, 2012). Also, dietary nitrates and nitrites from processed meat, smoked foods as well as animal foods being grilled, baked, roasted and barbecued, can increase gastric cancer risk, because all these practices enhance the formation of carcinogenic N-nitroso compounds. On the other hand, non-starchy vegetables and fruits are considered as protective substances (Liu *et al.*, 2008).

Other risk factors include tobacco, alcohol and family history. The European Prospective Investigation into Cancer and Nutrition (EPIC) project observed a significant association between cigarette smoking and gastric cancer risk, with 1.45 hazard ratio (HR) for smokers (Gonzalez *et al.*, 2010). The risk is increased by two to three folds if the patient has first-degree relatives with gastric cancer (Dhillon *et al.*, 2001).

1.1.3 Classification

1.1.3.1 Types of gastric cancer

In terms of the origins of neoplastic cells, gastric cancers can be divided into different types. About 90% to 95% of gastric cancers are adenocarcinomas and generally the term "gastric cancer" refers to adenocarcinoma of the stomach (Lawrence, 2004). Stomach adenocarcinoma indicates the cancer starting in the glandular tissue that lines the lumen of the stomach. Other types of cancerous tumors that originate from the stomach include lymphoma, squamous cell cancer, gastrointestinal stromal tumour (GIST) and carcinoid tumors (Hu *et al.,* 2012). With respect to anatomical location, stomach cancers are classified into cardia (proximal) stomach cancer, non-cardia (distal) stomach cancer and diffused stomach cancer.

1.1.3.2 Histological classification of gastric cancer

Several classification systems have been proposed for gastric cancer based on microscopic-morphological features (Table 1.1). The two most commonly used systems are Lauren`s classification and WHO classification. The Lauren`s classification, which is coined early in 1965 based on the glandular architecture and

cell adhesion between tumor cells, defines gastric cancer as two major types: intestinal and diffuse (Lauren, 1965). The intestinal type is characterized by cohesive cells that form gland-like structure, whereas in diffuse type, cell adhesion is absent so that the individual cell can infiltrate and thicken the stroma wall. The development of intestinal type gastric cancer normally involves sequential histopathological changes in gastric mucosa, including atrophic gastritis, intestinal metaplasia and dysplasia that ultimately progresses to carcinoma (Correa *et al.*, 2012).

Table 1.1 Gastric cancer classification systems

WHO (2010)	Lauren (1965)	Ming (1977)
Tubular adenocarcinoma	Intestinal type	Expanding type
Papillary adenocarcinoma		
Mucinous adenocarcinoma		
Signet-ring cell carcinoma	Diffuse type	Infiltrating type
Other poorly cohesive carcinomas		

One detailed classification system is provided by WHO in which gastric cancers are recognized as four major histologic patterns: tubular adenocarcinoma, papillary adenocarcinoma, mucinous adenocarcinoma, signet-ring cell adenocarcinoma and others (Hu *et al.*, 2012). Tubular carcinoma and papillary carcinoma are two common types in early gastric carcinoma, which are characterized by irregular-shaped and fused neoplastic glands and epithelial projections supported by fibrovascular cores. Mucinous carcinoma contains mucous lakes filled with mucins secreted by tumor cells.

In signet-ring cell carcinoma, the nucleus of tumor cells is compressed to the edge of the cell by the unsecreted mucous in the cytoplasm.

Another practical classification was proposed by Ming in 1977 (refer to Table 1.1) on the basis of different growth and invasiveness patterns of the cancer: the expanding type contains discrete tumor nodules and is prognostically favourable, whereas the infiltrating type contains individually invaded tumor cells and has a poor prognosis (Ming, 1977).

1.1.4 Early screening, diagnosis and prognosis

One reason for the low 5-year survival rate of gastric cancer is that this disease is usually detected in late stage as most patients experience vague and nonspecific symptoms in the early period. Anemia, weight loss, weakness or fatigue, abdominal pain, vomiting may accompany tumor invasion and metastasis (Axon, 2006). There is a long period for the stomach epithelial lining to become cancerous and the development of early gastric cancer is slow (Tsukuma *et al.*, 2000). Thus, screening and early diagnosis are of great importance for gastric cancer intervention. In Japan, one third of gastric cancer cases are detected at an early stage due to rigorous screening processes (White *et al.*, 1985).

Radiographic investigation of upper gastrointestinal tract (barium meal) and endoscopy are two useful tools to screen pre-malignant gastric lesions. The double-contrast barium techniques are low cost, non-invasive

and convenient for initial screening. Endoscopy followed by pathologic assessments can provide higher detection sensitivity and is increasingly used for gastric cancer screening. However, the limitation is the dependence on the skills of the endoscopist and the instrument availability, which makes it unfeasible for mass screening (Leung *et al.*, 2008). Endoscopic ultrasound (EUS), computed tomography (CT) and magnetic resonance imaging (MRI) are now frequently used to facilitate diagnosis of gastric cancer, which provide more detailed information about tumor infiltration and metastasis.

Over the past years, many efforts have been made to search for biological markers for early detection and diagnosis of gastric cancer. Measurement of serum pepsinogen (PG) is considered as a convenient and non-invasive test for gastric cancer. Pepsinogen contains two types: PGI and PGII and the PG I/II ratio is a good indicator of atrophic gastritis. Based on the studies on Japanese, the combination of *H. pylori* serology and pepsinogen test has good prediction for intestinal gastric cancer (Watabe *et al.*, 2005).

The clinicopathologic stage is the most important indicator of resectability and prognosis for gastric cancer. The most commonly used system is the TNM classification (tumor stage, lymph node status and presence of metastasis) by the American Joint Committee on Cancer (AJCC) (Edge *et al.*, 2010). Early gastric cancer (EGC) is defined as adenocarcinoma that invades no more deeply than submucosa, irrespective of lymph node

metastasis. Thus, compared with the TNM classification, EGC refers to any gastric cancer with tumor stage less than T2.

1.1.5 Molecular changes in gastric cancer: genetic and epigenetic alterations

Gastric cancer is a heterogeneous disease and it is estimated that 80-90% gastric cancers are sporadically developed (Al Saghie, 2013). Understanding the molecular changes in gastric tumorigenesis is critical for the early detection and the identification of novel therapeutic targets. Studies from past few decades have shown that a number of genetic and epigenetic alterations occur in the multistep processes of gastric carcinogenesis. Such changes include point mutation, chromosome instability (loss of heterozygosity, translocation and amplification), microsatellite instability and hypermethylation, which are involved in the regulations of cell cycle, cell apoptosis, DNA repair, inflammation, invasion and angiogenesis (Hamilton *et al.*, 2006).

Microsatellite instability:

Microsatellites are short repetitive DNA sequences (2-7 nt) in the genome. Microsatellite instability (MSI) occurs in DNA replication as a result of defective DNA mismatch repair. MSI was initially reported in colorectal cancer and became a hallmark of the hereditary non-polyposis colorectal cancer (HNPCC) syndrome. MSI has also been found in 25% - 50% of sporadic

gastric cancers (Ottini *et al.*, 2006). Mutation or epigenetic inactivation of mismatch repair genes leads to MSI phenotype, such as *hMLH1* and *hMSH2*. In gastric cancer, more than 50% of patients showing high levels of MSI, are due to the hypermethylation of *hMLH1* promoter. The affected genes by MSI are normally tumor suppressor genes in cell cycle, apoptosis and DNA repair, including TGFβ RII, IGFIIR, BAX, MSH6, MSH3, *et al.* (Hudler, 2012). All these genomic alterations further enhance genomic instability and promote gastric carcinogenesis. However, one interesting finding is that high MSI is reported to be associated with unique clinical-pathological features, favourable prognosis and better survival outcome. Patients with high MSI display a higher frequency of intestinal histotype, antral location, and a decreased prevalence of nodal metastasis (Iacopetta *et al.*, 1999; Beghelli *et al.*, 2006; Corso *et al.*, 2009). This phenomenon is proposed to be related to the increased host immune response (Chiaravalli *et al.*, 2006).

Involvement of p53:

p53, a tumor suppressor gene, regulates cell growth and apoptosis in response to DNA damage. More than 50% of human cancers contain *p53* gene mutation. Similarly, mutation and inactivation of p53 by loss of heterozygosity, missense mutation or frameshift deletion, are widely documented in gastric cancer and its precursor lesions: intestinal metaplasia (38%), dysplasia (58%) and gastric carcinoma (67%), suggesting its critical role in early events of gastric carcinogenesis (Shiao *et al.*, 1994; Chen *et al.*, 2011).

Although the p53 mutation is more frequent in patients with *H pylori* infection, the mechanism of p53 mutagenesis by *H pylori i*nfection has not been elucidated (Kubicka *et al.*, 2002).

HER-2:

Human epithelial growth factor receptor 2 (HER-2), also called c-erbB-2, is a membrane receptor of the tyrosine kinase family. With IHC and FISH techniques, it is found that HER2 is over-expressed in approximately 20% of gastric cancer, especially in intestinal type gastric carcinoma (Gravalos *et al.*, 2008). Moreover, according to clinical data, high level expression of HER2 is significantly associated with tumor size, serosal invasion, lymph node metastases as well as poorer prognosis and 10-year survival (Uchino *et al.*, 1993; Vizoso *et al.*, 2004). All these evidence indicate that HER2 could be an effective prognostic marker and a target for molecular targeted therapy for intestinal gastric cancer.

E-cadherin:

E-cadherin is a protein that controls cell-cell adhesion and cell polarity. Abrogation of E-cadherin results in the loss of adherens junction, cellular polarity and contact inhibition, reduces cell adhesiveness and enhances cancer cell migration and invasion (Vleminckx *et al.*, 1991; Handschuh *et al.*, 1999). The germline mutation of E-cadherin gene, CDH1, has been described in a subset of hereditary diffuse gastric cancers and CDH1 mutations are the most common somatic alterations in diffuse gastric cancers, accounting for

about 50% of cases or more (Graziano *et al.*, 2003). In susceptible individuals with CDH1 germline mutation in one allele, the loss or inactivation of the other normal allele is achieved by deletion of the whole gene or promoter hypermethylation. Finally, loss of function of E-cadherin is linked with enhanced metastasis and poor survival, further highlighting its importance in the pathogenesis of diffuse gastric cancer (Kawanishi *et al.*, 2000).

Other molecular abnormalities and research interests include K-*ras* and K-*sam* (oncogenes), RUNX3 and SMAD4 (tumor suppressors), APC/β-catenin (cell adhesion), COX-2 (inflammatory mediator), EGFR and VEGF (invasion and angiogenesis), p16, p21, p27 and Cyclin E (cell cycle regulation), Bcl-2 and Bax (apoptosis regulation), as well as matrix metalloproteinases (MMPs) and microRNAs (miRNAs) (Hamilton *et al.*, 2006; Nobili *et al.*, 2011; Resende *et al.*, 2011; Nagini, 2012). The molecular alterations in the pathogenesis of gastric cancer are illustrated in Fig 1.2.

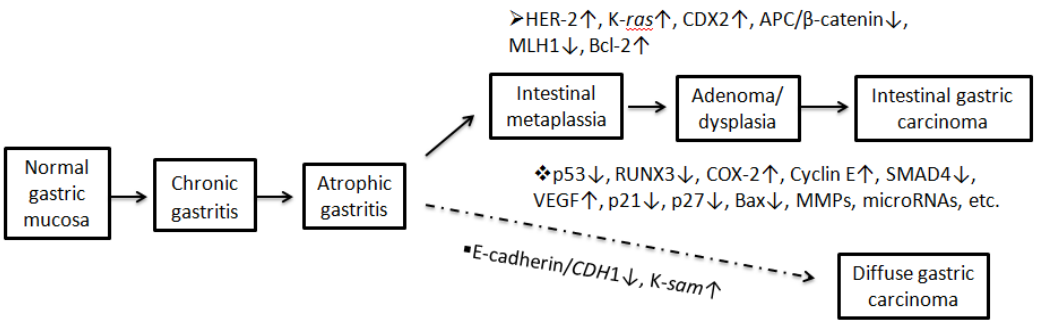

Fig 1.2 Diagrammatic representations of the molecular alterations in the progress of gastric carcinogenesis. ➢, genes mainly involved in the progression of intestinal GC; ❖, genes involved in both intestinal and diffuse GC; ▪, genes mainly involved in diffuse GC. ↑ indicates over-expression or up-regulation; ↓ indicates inactivation, reduced-expression or down-regulation (Modified and redrawn with reference to Correa *et al.,* 2012).

1.1.6 Treatment of gastric cancer: conventional and targeted therapies

With the advances in surgical and adjuvant chemo- or radio-therapy, treatment of gastric cancer has improved over the last 30 years. Nevertheless, the overall survival rate is still low for gastric cancer, because the majority of patients are diagnosed at advanced stages with locally advanced tumors, regional lymphnode involvement, or metastasis to distant organs. Endoscopic mucosal resection and submucosal dissection can be only applied in very early stage, when the primary tumor is small and limited to the mucosa (Gotoda *et al.*, 2013). Surgical gastrectomy remains the mainstay of treatment to remove localised tumors. 30-50% of gastric cancer patients are fortunate to receive a curative-intent surgery, with 5-year survival rates of 60% and 34% for stage I and stage II diseases, respectively (Morabito *et al.*, 2009). Preoperative, perioperative and postoperative chemotherapy or radiotherapy are normally conducted to reduce the tumor size, lower the risk of recurrence and improve survival and life quality of patient.

Results from meta-analyses show a significant benefit of adjuvant chemotherapy in the treatment of completely resected gastric cancer (Earle *et al.*, 1999; Panzini *et al.*, 2002). The efficacy of neoadjuvant therapy (chemotherapy, chemoradiotherapy and immunotherapy) for locally advanced tumors and those with high risk of recurrence after surgery is under investigation. For unresectable locally advanced or metastatic gastric cancers, systemic chemotherapy is considered as a gold standard of palliative

treatment. Combination chemotherapy with docetaxel, cisplatin and 5-FU (DCF) has been shown to improve the overall survival (OS) and has advantage compared with single drug or CF (Van Cutsem *et al.*, 2006). New generation of cytotoxic drugs in systemic chemotherapy include S1 (block thymidine synthesis), oxaliplatin (crosslink DNA) and irinotecan (topoisomerase inhibitor) (Power *et al.*, 2010).

However, poor outcome of survival of advanced gastric cancer shows that conventional therapies are still not optimum. Moreover, toxicity to normal tissues, resistance to treatment and recurrence of tumors are needed to be taken into account. Therefore, the emergence of targeted therapy opens a new way for researchers and doctors to treat gastric cancer. An increased understanding of gastric cancer biology such as genetic and epigenetic alterations and signal transduction pathways that are involved in cell proliferation, apoptosis and metastasis, has lead to the development of molecular targeted drugs. A number of targeted molecule-based drugs, which target vascular endothelial growth factor (VEGF), epidermal growth factor receptor (EGFR) and HER-2, cyclin-dependent kinase (CDK), mammalian target of rapamycin (mTOR) and matrix metalloproteinase (MMP) (Fig 1.3), are in clinical phase II/III trial and giving promising outcome (Zagouri *et al.*, 2011; Kasper *et al.*, 2014).

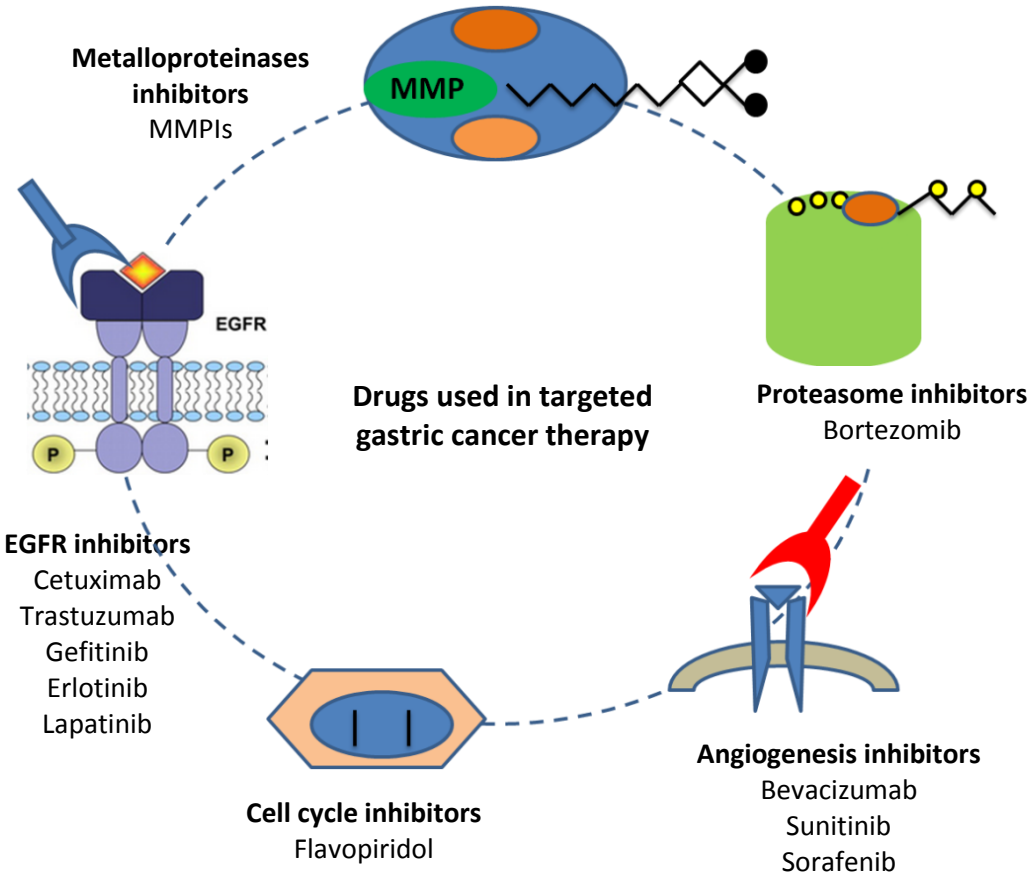

Fig 1.3 A diagrammatic representation of novel target-based drugs in gastric cancer treatment (redrawn with reference to Morabito *et al.*, 2009).

For targeted therapies, two common strategies are being used for drug development, viz. monoclonal antibodies and small molecule inhibitors. Antibodies can directly bind and block signal factors and receptors in cancer cells or trigger the immune system mediated-cell killing (Scott *et al.*, 2012). Such examples in gastric cancer targeted therapies include trastuzumab and pertuzumab (anti-HER-2), cetuximab (anti-EGFR), bevacizumab and ramucirumab (anti-VEGF). Small molecule inhibitors are compounds that can enter cancer cells and interfere with the enzymatic function of receptor

tyrosine kinases or intracellular signaling molecules to inhibit or stop aberrant signal transduction. Most inhibitors will compete with ATP binding in the catalytic domain of the respective target (Zhang *et al.*, 2009a). The small molecule inhibitors under investigation in gastric cancer therapy include erlorinib and gefitinib (anti-EGFR), lapatinib (dual inhibitor of EGFR and HER-2), sunitinib and sorafenib (anti-VEGF), everolimus (mTOR inhibitor), bortezomib (proteasome inhibitor) (Yamada, 2012).

Trastuzumab (Herceptin®, Genentech), is a humanized immunoglobulin G1 monoclonal antibody against the HER-2/neu receptor. It has been approved by FDA in combination with chemotherapy as adjuvant treatment of HER-2 positive breast cancer (Smith *et al.*, 2007). More than 20 percent of gastric cancers show HER-2 overexpression, predominantly in intestinal type (Albarello *et al.*, 2011). One phase III clinical trial, ToGA, has been conducted to evaluate the combination effect of trastuzumab with cisplatin/5-FU in the treatment of metastatic HER-2 positive gastroesophageal and gastirc cancers. Results have shown that trastuzumab can significantly increase the objective response rate (ORR), median progression-free survival (PFS) and median overall survival (OS) (Bang *et al.*, 2010).

1.2 Scorpion venoms and toxins and their effects on cancer

1.2.1 Animal venoms and toxins, an introduction

Venomous animals produce venoms/toxins from specialized organs named venom glands. Venomous animals have long history of evolution and cover a wide range of species, e.g. snakes, scorpions, spiders, bees, lizards, cone snails and sea anemones. The venoms can be secreted from teeth, stingers, claws or even skins of these animals, to paralyze and kill the prey or to protect themselves from predation and other dangers.

Venomous animals often have negative reputations because of the morbidity and mortality inflicted by their bites or stings. The signs and symptoms after exposure to venoms vary from mild allergic reactions, itch, pain, swelling to respiratory arrest, paralysis, necrosis or even death (Weinstein *et al.*, 2009). Envenomation has become a global health concern and the antivenom strategies are needed to be established and developed.

Nevertheless, animal venoms and toxins are also beneficial to human beings in terms of their applications in medical and pharmaceutical research and industry. The usage of animal venoms in folk medicine has been documented since long-time ago in some countries, like China, India and Middle East. For example, Chan Su, the dried toad venom from skin glands, first recorded in traditional Chinese medicine more than 1,000 years ago, has been long used as a diuretic, cardiotonic and anesthetic agent (Meng *et al.*,

2009). Animal venoms are complex cocktails with various bioactive proteins and peptides and they are quite variable between different species, making animal venoms a rich source for drug discovery. For the last 30 years, animal venoms and toxins have been widely investigated in the treatment of human disorders, such as diabetes, hypertension, chronic pain, HIV, cancer, etc. Up to now, six FDA-approved drugs are derived from venom proteins or peptides, with several in clinical trials and many more under preclinical studies (Table 1.2.)

Table 1.2 FDA approved drugs derived from animal venoms

Protein or peptide	Source of venom	Molecular target	Indication	Company	Reference
captopril	Snake (pit viper)	ACE	hypertension	BMS	Cushman *et al.*, 1991
eptifibatide	Snake (pygmy rattle)	integrin receptor	acute coronary syndrome	Merck	O'Shea *et al.*, 2002
tirofiban	Snake (saw-scaled viper)	integrin receptor	acute coronary syndrome	Iroko Cardio & Merck	Menozzi *et al.*, 2005
bivalirudin	Medicinal leech	thrombin	coagulation	The Medicines Co.	Warkentin *et al.*, 2008
ziconitide	Cone snail	CaV 2.2	chronic pain	Azur Pharma & Eisai	Miljanich, 2004
exenatide	Lizard (Gila monster)	GLP-1 receptor	type II diabetes	Amylin & Eli lilly	Barnett, 2007

1.2.2 Scorpion biology

Scorpions are among the most well-known venomous arthropod animals, which belong to the order Scorpiones under the class Arachnids. Evolutionarily, scorpions are one of the oldest creatures and have existed on earth for more than 400 million years since the middle Silurian period. Scorpions are widely distributed all over the world which mostly occupy temperate, desert, and tropical habitats except for Antarctica. Over 1,500 species have been reported so far and assigned to 13 families according to the current higher classification after 2003: *Bothriuridae*, *Buthidae*, *Caraboctonidae*, Chactidae, Chaerilidae, Euscorpiidae, *Hemiscorpiidae*, *Iuridae*, *Microcharmidae*, *Pseudochactidae*, *Scorpionidae*, *Superstitioniidae* and *Vaejovidae* (Williams, 2009). The family *Buthida* is the largest, the most widespread and more importantly the most studied in biomedical research. The *Buthida* family contains more than 500 species and is represented by the genera *Androctonus*, *Buthus*, *Mesobuthus*, *Buthotus*, *Parabuthus* and *Leirus*, which are located in North Africa, Asia, the Middle East, and India (Loret *et al.*, 2001) (Fig 1.4).

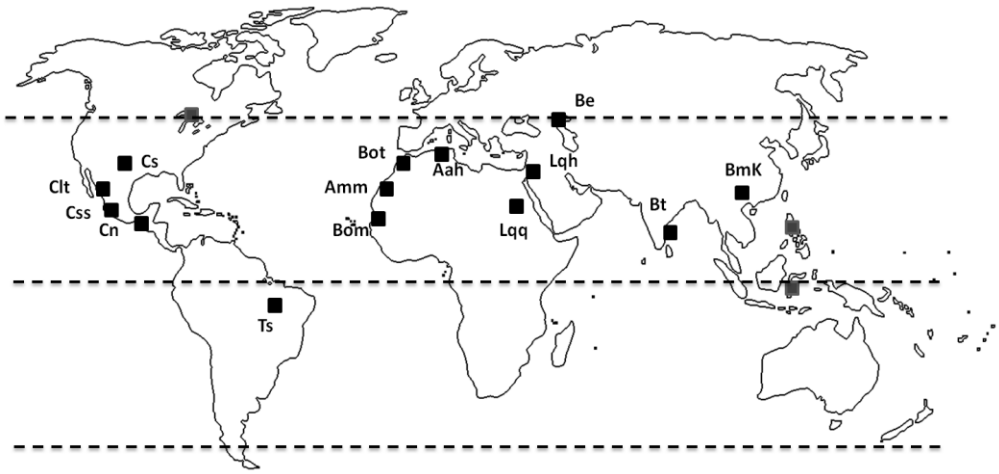

Fig 1.4 Representative geographic distribution of *Buthida* scorpions around the world (redrawn with reference to Loret *et al.*, 2001). Dashed lines indicate equator and 50° latitude north and south. Aah, *Androctonus australis hector*; Amm, *Androctonus mauretanicus mauretanicus*; Be, *Buthus epeus*; *BmK, Buthus martensi Karsh*; *Bom, Buthus occitanus mardochei*; Bot, *Buthus occitanus tunetanus*; Bt, *Buthus tamulus*; Clt, *Centruroides limpidus*; Cn, *Centruroides noxius*; Cs, *Centruroides sculpturatus*; Css, *Centruroides suffuses suffuses*; Lqh, *Leiurus quinquestriatus hebraeus*; Lqq, *Leiurus quinquestriatus quinquestriatus*; Ts, *Tityus serrulatus*.

The scorpion has a variable size of approximately 1-20 cm and is characterized by its segmented morphology. Scorpion comprises 3 parts: the head (prosoma, with a pair of chelae for prey immobilisation, defence and sensory purposes); the abdomen (mesosoma, with 4 legs on each side); the tail (metasoma, with telson and aculeus for venom secretion) (Fig 1.5).

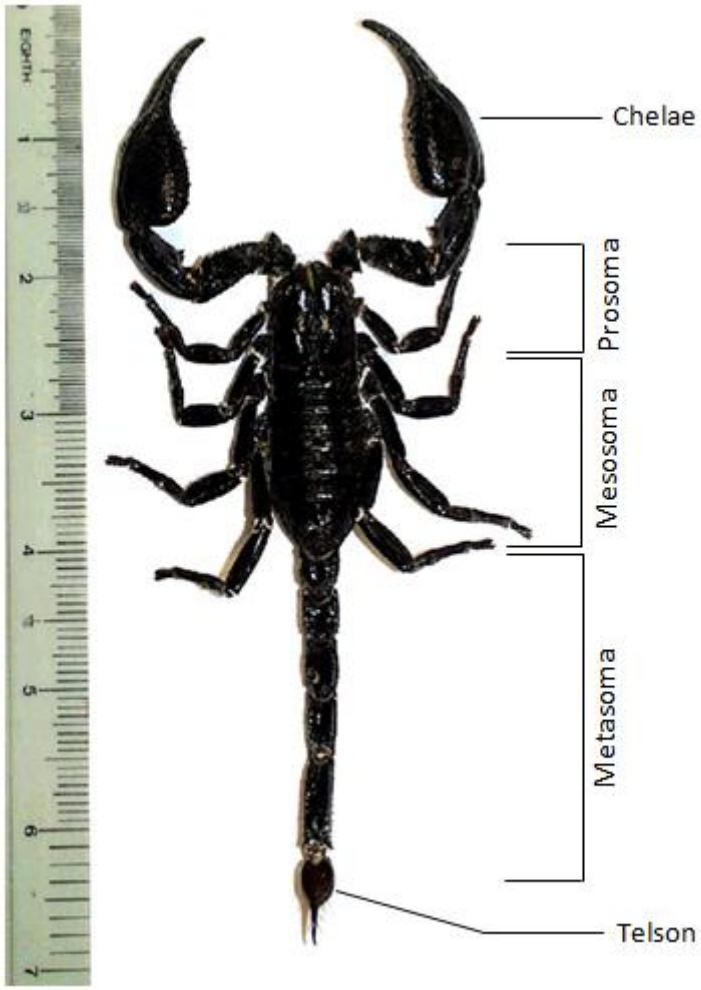

Fig 1.5 Anatomy of scorpion represented by the *Heterometrus spinifer* scorpion (Malaysian black scorpion).

A pair of venom glands is located in the telson, which are segregated by a muscle septum. Each gland has a tortuous lumen, surrounded by folded glandular epithelium. Upon stimulation, the muscle will contract and the venom stored in the lumen will be ejected through the aculeus (Fig 1.6).

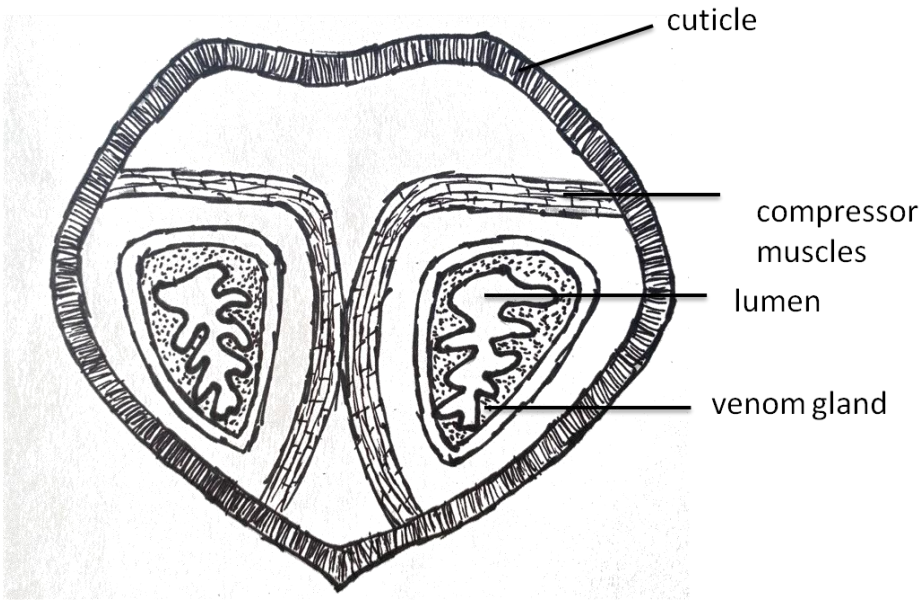

Fig 1.6 Diagram of scorpion venom glands (redrawn based on Hjelle, 1991).

1.2.3 Scorpion venoms and toxins

Scorpion venoms are produced and secreted by the venom glands for offensive or defensive purposes, which are normally milked and collected by electrical stimulation in the laboratory. Scorpion venoms are a complex mixture of water, salts, mucoproteins, lipids, nucleotides, glycoaminoglycans, histamine, serotonin, biogenic amines, low M.W peptides (e.g. neurotoxins), high M.W. proteins (e.g. enzymes), and others (Andreotti *et al.*, 2010). Each

scorpion has its own component profile in the venom and the number varies from dozens to hundreds.

Small peptides (<10 kDa) are the most important components in scorpion venoms, which are believed to be responsible for the intoxication and are widely investigated for biomedical and scientific applications. They are often considered as neurotoxins because the majority of peptides target and modify the ion channels of the excitable cells (e.g. neurons), which makes them valuable tools for ion channel research in neuroscience. Based on the types of targeted ion channels, scorpion venom peptides can be classified into four groups: sodium (Na^+) channel toxins, potassium (K^+) channel toxins, calcium(Ca^{2+}) channel toxins and chloride (Cl^-) channel toxins.

1.2.3.1 Sodium channel toxins (NaScTxs) from scorpion venoms

The scorpion Na^+ channel toxins (NaScTxs) are polypeptides of 60-76 amino acid residues in length (6.5-8.5 kDa), tightly bound by four disulfide bridges (Possani *et al.*, 1999). Current database covers around 200 sequences of putative NaScTxs, which can be found in World Wide Web: SCORPION (Srinivasan *et al.*, 2002a). As Na^+ channel comprises one α subunit and two β subunits, Na^+ toxins are divided into two categories: α- NaScTxs and β-NaScTxs, based on the binding sites and physiological effects. α-NaScTxs bind to the receptor site 3 (a domain in α subunit) in a voltage dependent mode and inhibit the fast inactivation process of sodium channel (Couraud *et al.*, 1982). β-NaScTxs bind to receptor site 4 (a domain in β1 subunit)

independently of voltage and shift the threshold of channel activation to a more hyperpolarized membrane potential. The phyletic preference has been reported among NaScTxs, which principally categorizes NaScTxs into two groups: "Classical"-highly active on mammalian sodium channels, and "anti-insect"- highly active on insect sodium channels. The later toxins are further subdivided into excitatory and depressant insect toxins (Quintero-Hernández *et al.*, 2013).

1.2.3.2 Potassium channel toxins (KTxs) from scorpion venoms

Scorpion venoms are rich sources of potassium channel toxins (KTxs), which block several types of K^+ channels, e.g. voltage-gated K^+ channels (Kv1.x), Ca^{2+} activated K^+ channels of small, intermediate and high conductance. KTxs are structurally categorized into four families: α-, β-, γ- and κ-KTxs, most of which share a conserved cysteine-stabilized α-helical and β-sheet structural motif (CSαβ) (Tytgat *et al.*, 1999; Rodriguez de la Vega *et al.*, 2004). The α-KTx family is considered as the largest in number, with about 140 peptides falling in 26 subfamilies, termed α-KTx_{1-26} and new peptides are described continuously (Diego-García *et al.*, 2013). These peptides are composed of 23-42 amino acid residues with 3 or 4 disulfide bridges. This family of toxins are important blockers of voltage-gated potassium channels and attract much attention in the studies of Kv channel structure-function and Kv related channelopathies (Castle, 2010). The β-KTxs are long-chain peptides with 50-75 amino acid residues. The γ- KTxs are new

interesting short chain peptides mainly targeting hERG channels, which are associated with the cell cycle and proliferation of several cancers (Corona *et al.*, 2002; Asher *et al.*, 2010). The κ-KTxs toxins are characterized by two parallel α-helices linked by two disulfide bridges CSαα, represented by the well known κ-Hefutoxin isolated from *Heterometrus fulvipes* scorpion venom (Srinivasan *et al.*, 2002b). Scorpion potassium channel toxins have improved our understanding of the physiological and patho-physiological functions of potassium channels and contributed to the identification of therapeutic leads for Kv related diseases.

1.2.3.3 Calcium and Chloride channel toxins from scorpion venoms

Different from NaScTxs and KTxs, scorpion venom peptides that target calcium and chloride channels, are scarcely known and have variable amino acid lengths (Possani *et al.*, 2000). Imperatoxin A (IpTxa), purified from *Pandinus imperator* scorpion venom, was the first peptide that was reported to have high affinity to ryanodine receptor (RyR, one type of ligand-activated calcium channels). IpTxa increases the binding of [^{3}H] ryanodine and induces a fast release of calcium from sarcoplasmic reticulum (Valdivia *et al.*, 1992). Subsequently, several IpTxa-like peptides were identified from other scorpion venoms, including Maurocalcin, Hemicalcin and Hadrucalcin (Quintero-Hernández *et al.*, 2013). Kurtoxin, a 63 amino acid peptide from the venom of the scorpion *Parabuthus transvaalicus*, was initially shown to bind with high affinity to T-type voltage-gated calcium channels (Cav3.x). Later, it was found

that it can also interact with T-, L-, N-, and P-type Cav channels in central and peripheral neurons (Chuang *et al.*, 1998; Sidach *et al.*, 2002).

So far, some small peptides that target chloride channels have been identified and characterized. Chlorotoxin (CTX/ClTx), a 36 amino acid small peptide purified from the *Leiurus quinquestriatus* scorpion venom, was initially described as a chloride channel blocker that acts as a paralytic agent for small insects (DeBin *et al.*, 1993). One remarkable finding and application of this toxin is that CTX can specifically bind to the chloride channel on glioma cells and inhibit glioma progression (Lyons *et al.*, 2002). Because of its high affinity, specificity and low toxicity, CTX is considered as a promising agent for imaging and targeted therapies for gliomas. A phase II clinical trial is in progress with ^{131}I-TM-601, a synthetic CTX coupled with radioactive iodine isotope (Mamelak *et al.*, 2006). Other chloride channel inhibitors from scorpion venoms include BmKCT from *Mesobuthus martensi*, Chlorotoxin-like peptide Bs 14 from *Buthus sindicus*, Toxin PBITx1 from *Parabuthus schlechteri*, *et al.* (Ali *et al.*, 1998; Tytgat *et al.*, 1998; Zeng *et al.*, 2000).

1.2.3.4 Scorpion venom peptides with no disulfide bridges

Apart from the ion channel targeted peptides with disulfide bridges, there are a number of non disulfide-bridged peptides (NDBPs) in scorpion venoms (Almaaytah *et al.*, 2014). These peptides show high diversity in both structure and bioactivities. To date more than 40 scorpion venom NDBPs have been isolated and functionally described. The majority of NDBPs are

antimicrobial peptides with a board spectrum of activity against bacteria, yeast, fungi and viruses (Hancock *et al.*, 2006). Hadruin, a 41 amino acid peptide isolated from *Hadrurus aztecus*, was the first to show antimicrobial activities against both Gram-positive and Gram-negative bacteria at low micromolar concentration (10-50 uM) (Torres-Larios *et al.*, 2000). Mucroporin-M1, a modified antimicrobial peptide from scorpion *Lychas mucronatus*, was demonstrated to have antibacterial activity against antibiotic-resistant pathogens (Dai *et al.*, 2008). Another small group of NDBPs are the so called bradykinin potentiating peptides (Bpps). Bradykinin is a vasoactive peptide that plays an important role in the regulation of blood pressure, which can be inactivated by one enzyme, angiotensin converting enzyme and the Bpps are the inhibitors of this enzyme. Peptides T from *Tityus serrulatus*, K-12 from *Buthus occitanus* and BmKbpp from *Mesobuthus martensi Karsch* are examples in this group (Almaaytah *et al.*, 2014).

1.2.3.5 High molecular weight enzymes

The high M.W. proteins in scorpion venoms are mainly diverse enzymes, which are believed to contribute to the venom cytotoxicity or potentiate the envenomation process. Therefore, a good understanding of these enzymes` structures and functions is helpful for anti-venom strategy. In contrast to spider and snake venoms, scorpion venoms exhibit low levels of enzymatic activities (Gwee *et al.*, 2002). The enzymes present in scorpion

venoms include hyaluronidase, phospholipase A2, L-amino acid oxidase and proteases (Petricevich, 2010).

Hyaluronidase:

Hyaluronidase can be found in several venomous species like snake, bee, spider and scorpion. This enzyme can degrade the hyaluronan, an extracellular matrix protein in the soft connective tissues around blood vessels and increase the diffusion of toxins (Girish *et al.*, 2007). Hyaluronidase has been purified from a few scorpion venoms, e.g., *Heterometrus fulvipes*, *Tityus serrulatus* and *Palamneus gravimanus.* BmHYA1, a hyaluronidase isolated from *Mesobuthus martensi*, was shown to remove hyaluronan and modulate the expression of CD44 variant in MDA-MB-231 breast cancer cell (Feng *et al.*, 2008).

Phospholipase A2 (PLA_2):

Phospholipases A2 (PLA_2) are a group of enzymes that hydrolyze the ester bonds of phospholipids into lysophospholipid, fatty acids and others (Burke *et al.*, 2009). PLA_2 can be divided into 4 subfamilies: secretory PLA_2 ($sPLA_2$), cytosolic PLA_2 ($cPLA_2$) calcium-independent PLA_2 ($iPLA_2$) and lipoprotein PLA_2 ($LpPLA_2$) (Six *et al.*, 2000). All the PLA_2s described in scorpion venoms belong to $sPLA_2$, which have low molecular weight (13-15 kDa) and are involved in tissue destruction and inflammation during the action of scorpionism (Valentin *et al.*, 2000). Several scorpion $sPLA_2$ have been identified and characterized, such as Imperatoxin I and Phospholipin from the

venom of the African scorpion *Pandinus imperator*, Phaiodactylipin from wood scorpion (*Anuroctonus phaiodactylus)* and Heteromtoxin from *Heterometrus laoticus* scorpion venom (Zamudio *et al.*, 1997; Incamnoi *et al.*, 2013). These enzymes have diverse biological and pharmacological potentials like anti-coagulant and anti-bacterial activities (Perumal Samy *et al.*, 2007).

Proteases:

Proteases are important proteins in venoms that are involved in the post-translational processing of toxins and promote the spreading of toxins via degradation of matrix proteins (Almeida *et al.*, 2002). Proteases found in scorpion venom glands are quite recently reported with the help of proteomic and transcriptome studies. Two main types of proteases are identified in scorpion venoms: serine proteases and metalloproteases (Valdez-Velázquez *et al.*, 2013). The first metalloprotease purified from scorpion venom was named antarease from Brazilian scorpion *Tityus serrulatus*, which cleaves the vesicle-associated membrane proteins 2 and 8 (VAMP2 and VAMP8) (Fletcher *et al.*, 2010). A serine protease-like protein (BMK-CBP) was also isolated from Chinese red scorpion *Mesobuthus martensi* (Gao *et al.*, 2008).

1.2.3.6 L-amino acid oxidases (LAAOs) from scorpion and snake venoms

L-amino acid oxidases (LAAOs) are a group of flavoenzymes that catalyze oxidative deamination of L-amino acid substrates and form the corresponding α-keto acids, hydrogen peroxide and ammonia (Du *et al.*, 2002). LAAOs can be widely found in nature, including bacteria, fungi, seaweeds and snake venoms. Normally, LAAOs are homodimeric, FAD-binding glycoproteins with 3-4% carbohydrate with molecular weight range 110-150 kDa. However, the de-glycosylation has no effect on enzymatic activities of LAAOs from several snake venoms.

The presence of LAAOs in scorpion venoms is not widely reported while our group and another study showed the LAAO activity in the Chinese red scorpion venom *Mesobuthus martensi (Ahn et al., 2000)*. Snake venoms are the richest source of LAAOs, which are responsible for the yellowish colour for the venoms (de Vieira Santos *et al.*, 2008). Recently, LAAOs have become a research interest in biomedicine because they have multi-biological activities, such as anti-microbial, anti-HIV, anti-coagulant, apoptosis-inducing, edema-inducing and hemorrhagic activities (Tan *et al.*, 2008). Interestingly, some snake venom LAAOs can induce platelet aggregation, like LAAOs from *B. moojeni, Bothrops atrox* and *Trimeresurus jerdonii*. While LAAOs from snake venoms of *Vipera berus berus, Naja naja oxiana* and others, were reported to inhibit platelet aggregation. The mechanisms of such controversial actions on platelet aggregation are not clearly understood (Guo *et al.,* 2012).

The application of LAAOs in cancer research is another recent scientific attempt, by applying the cytotoxic effects of H_2O_2 generated from LAAO enzymatic reaction. It was found that LAAOs from snake venoms of *Ophiophagus hannah*, *Agkistrodon acutus*, *Bothrops jararaca*, *Bothrops atrox*, *Naja naja atra*, etc., inhibited cancer proliferation and induced cancer cell apoptosis in bench studies or in animal experiments. This will be discussed in detail in discussion part.

1.2.4 The anticancer potential of scorpion venoms and toxins

Scorpion envenomation is a risk for public health in tropical and subtropical regions and there is a clear need for the improvement in specific (antivenom) and systematic treatments. However, each coin has two sides and the medical significance of scorpion venoms should not be ignored. Scorpions and scorpion venoms have been applied in traditional medicine for long periods in China, India and Africa. For example, in one Chinese famous pharmacopoeia book "Ben Cao Gang Mu" (Compendium of Materia Medica, A.D. 1578), the dried whole body of scorpion was described as an antiepilepsy and analgesic agent (Shao *et al.*, 2007). Meanwhile, scorpion venoms have the antimicrobial functions against bacteria, fungi, yeasts and viruses. Studies show that scorpion venoms-derived protein Mucroporin-M1 can inhibit the amplification of hepatitis virus B and another peptide Kn2-7 possesses anti-HIV-1 activity (Chen *et al.*, 2012).

The anticancer potential is another recently observed biological property of scorpion venoms and toxins. A number of experimental and preclinical studies have shown that scorpion venoms and toxins can impair cancer growth, induce apoptosis and inhibit cancer metastasis *in vitro* and *in vivo*. Several active molecules with anticancer activities have been purified from scorpion venoms in terms of inhibition of proliferation, cell cycle arrest, induction of apoptosis and decreasing cell migration and invasion. The investigated cancer types include glioma, neuroblastoma, leukemia, lymphoma, breast, lung and prostate cancers (refer to Table 1.3) (Ding *et al.*, 2014).

Among all the scorpions tested in cancer research, *Mesobuthus martensi Karsch* (BmK) scorpion venom is probably the first to be reported to possess antitumor properties. Early in 1980s, a Chinese researcher Zhang Futong extracted a solution from the dried whole body of BmK and administered this to mice with reticulum cell Sarcoma and MA-737 mammary carcinoma. Results showed that the BmK solution can significantly inhibit the tumor growth and decrease DNA content in tumor tissues (Zhang *et al.*, 1987). This innovative study paved the way for the investigation of BmK and other scorpion venoms in cancer therapy. BmK scorpion venom was the most extensively studied in China and several active molecules have been isolated and characterized.

Polypeptide extract from the scorpion venom (PESV), a group of partially purified polypeptides with 50-60 amino acids from the crude venom of BmK, was reported to inhibit cell proliferation and induce cell apoptosis of DU 145 human prostate cancer cells (Zhang *et al.*, 2009b). AGAP, an analgesic-antitumor peptide isolated from BmK with a molecular mass of 6,280 Da, was shown to exert antitumoral activity against mouse S-180 fibro sarcoma and Ehrlich ascites tumor (Liu *et al.*, 2002). AGAP was subsequently indentified as a voltage gated sodium channel scorpion toxin (Cui *et al.*, 2010). A fusion protein SUMO-AGAP, which connected a small ubiquitin-related modifier to AGAP, inhibited cell proliferation and migration of SHG-44 human malignant glioma cells via interfering with the p-AKT, NF-κB, BCL-2, and MAPK signaling pathways (Zhao *et al.*, 2011).

The most notable evidence regarding the anticancer effects of scorpion venoms comes from Chlorotoxin (CTX, mentioned in sention 3.1.3) used in the treatment of glioma. Based on electrophysiological evidence, the chloride ion channel was initially considered to be responsible for the affinity and specificity of CTX to glioma. However, further studies by protein interaction approaches with a recombinant His-CTX, revealed that the principle receptor of CTX is matrix metalloproteinase-2 (MMP-2), a protease that is over-expressed on the surface of glioma cells (Deshane *et al.*, 2003). ^{131}I-TM-601, a synthetic CTX coupled with radioactive iodine isotope produced by Transmolecular, Inc. (Cambridge, MA) has been approved by

FDA, to perform clinical trials imaging and diagnosis of gliomas (Mamelak *et al.*, 2006).

In recent years, several scorpion venoms have been screened for the apoptosis inducing action against cancer cells and some active molecules have been identified and characterized. Bengalin, a 72 kDa protein isolated from the Indian black scropion *Heterometrus bengalensis koch*, was shown to induce apoptosis of human leukemic cells without cytotoxicity to normal human lymphocytes. The damaged nuclei, DNA fragmentation was observed to be accompanied by decreased expression of heat shock protein (HSP) 70 and 90, activation of caspase-3,9 and induced cleavage of poly (ADP-ribose) polymerase (PARP) (Gupta *et al.*, 2010). Two novel apoptogenic peptides with molecular mass of around 30 kDa were purified from *Tityus discrepans* scorpion venom, named Neopladine 1 and Neopladine 2, respectively. Immunohistochemistry studies demonstrated that Neopladines can bind to the cell surface of SKBR3 breast cancer cells, induce the expression of Fas ligand (FasL) and triger cell apoptosis. Whereas, Neopladines had a negligible effect on non-malignant MA104 monkey kidney cells, indicating their potential in the development of anticancer drugs (D'Suze *et al.*, 2010). Another two crude scorpion venoms were also evaluated for the anticancer effects including *Odontobuthus doriae* and *Androctonus crassicauda* against SH-SY5Y human neuroblastoma cells and MCF-7 breast cancer cells. The oxidative stress was proposed to contribute to the cell cycle arrest at S phase and induction of apoptosis (Zargan *et al.*, 2011b, a; Zargan *et al.*, 2011c).

To sum up briefly, the anticancer potential of scorpion venoms and toxins has been screened on various carcinomas, *in vitro* and *in vivo* (summarized in Table 1.3).

Table 1.3 Molecules purified from scorpion venoms with anticancer potential (adapted from Ding *et al.*, 2014)

Molecules	Scorpion species	Tested cancer models	Mechanisms of actions	References
BmK AGAP	*Mesobuthus martensi Karsch*	Mouse fibro sarcoma , Rhrlich ascites tumor，SHG-44 glioma cells	Voltage gated sodium channel, interfering p-AKT, NF-κB, Bcl-2 and MAPK signaling pathway	Liu *et al.*, 2002; Liu *et al.*, 2003; Cao *et al.*, 2010; Cui *et al.*, 2010; Zhao *et al.*, 2011.
BmKCT	*Mesobuthus martensi Karsch*	SHG-44 glioma cells, glioma/SD rat	Inhibit chloride current and selectively target glioma	Zeng *et al.*, 2000; Fan *et al.*, 2010.
Chlorotoxin	*Leiurus quinquestriatus*	Glioma cells, animal models and clinical trials	Suppress chloride current, bind to matrix metalloproteinase-2 (MMP-2)	Lyons *et al.*, 2002; Deshane *et al.*, 2003; Mamelak *et al.*, 2006.
Iberiotoxin	*Mesobuthus tamulus*	MCF-7 breast cancer cells	Block large conductance Ca2+ activated K+ (BK) channel	Ouadid-Ahidouch *et al.*, 2004.
Magatoxin	*Centruroides margartatus*	A549 human lung adenocarcinoma cells and xenograft model	Inhibit Kv 1.3, increase expression of p21Waf1/Cip1 and decrease CdK4	Jang *et al.*, 2011.
Charybdotoxin	*Leiurus quinquestriatus*	NIH3T3 fibroblasts and human melanoma cells	Inhibit cell migration does-dependently	Schwab *et al.*, 1999.
Bengalin	*Heterometrus bengalensis Koch*	human leukemic U937 and K562 cells	Induce caspase apoptosis pathway by loss of mitochondrial	Gupta *et al.*, 2010.

			membrane potential and decreased HSP 70 and 90	
Neopladine 1 & 2	*Tityus discrepans*	SKBR3 breast cancer cell line	Trigger FasL and BcL-2 expression	D'Suze *et al.*, 2010.

It can be concluded that two mechanisms have been described for scorpion venoms in their actions against cancer cells. I), targeting the ion channels to inhibit cell proliferation and metastasis; II), induction of apoptosis by cell cycle arrest, caspase activation, mitochondria depolarization or oxidative stress.

Nevertheless, as a novel search field, much more efforts should be made to extensively evaluate the anticancer effects of scorpion venoms and toxins and understand the mechanisms of action. Currently, only a few scorpion species have been tested and most work is performed in cell culture, not in animal model. Furthermore, the mechanisms are not clearly elucidated and the purification and characterization of active molecules remain a challenge.

1.3 Scope of study

The application of animal venoms and toxins as anticancer agents is a novel frontier in cancer research. Few scorpion venoms have been investigated and the mechanisms are not quite clear. **The hypothesis of this study is that scorpion venoms, particularly the *Hottentotta hottentotta***

scorpion venom, and L-amino acid oxidase from snake venom have antitumoral potential in gastric cancer, based on our preliminary studies.

Objectives of this study:

1. Perform a preliminary screening of the anti-proliferative effects of several crude scorpion venoms in gastric cancer and breast cancer cell lines
2. Evaluate the anticancer effects of *Hottentotta hottentotta* scorpion venom in gastric cancer *in vitro* and *in vivo*.
3. Purify and characterize the anticancer component from *Hottentotta hottentotta* scorpion venom (BHV).
4. Investigate the anticancer effects of L-amino acid oxidase (LAAO) from *Crotalus adamanteus* snake venom in gastric cancer cells. LAAO was the active molecule identified from BHV but there was difficulty in processing BHV from the same source.
5. Elucidate and understand the mechanisms that account for the anti-cancer actions of *Hottentotta hottentotta* scorpion venom and L-amino acid oxidase, including cellular responses, gene and protein targets and mechanistic pathways.

CHAPTER 2

MATERIALS AND METHODS

2. MATERIALS AND METHODS

2.1 Scorpion venom preparation, purification and characterization

2.1.1 Scorpion venom preparation

Crude *Hottentotta hottentotta* scorpion venom was purchased from Latoxan (Valence, France), which was extracted from the scorpions in Mali. *Methbuthus martensii karsch* scorpion venom was purchased from a supplier in Zhejiang Province, P.R. China. Aqueous L-amino acid oxidase from *Crotalus adamanteus* snake venom was purchased from Sigma (Sigma-Aldrich, St. Louis, MO, USA), whose enzymatic activity was described to be more than 15 unit/ml. *Heterometrus bengalensis* and *Pandinus imperator* scorpion venoms were stocks in the laboratory, which were previously lyophilized and kept at 4 °C. The lyophilized crude scorpion venom was dissolved in ice-cold 1 x PBS, pH=7.4. The venom was centrifuged for 30 min at 100,000 rpm to remove any undissolved particles. The supernatant (crude venom solution) was collected and filtered through 0.22 µm syringe filter (Sartorius Stedim Biotech, Goettingen, Germany). The sterile venom solution can be kept at 4 °C for one or two weeks. Otherwise, it was aliquoted into 100 µl/tube and kept at -20 °C for long time storage.

2.1.2 Protein concentration measurement

Protein concentration for scorpion venoms and cell lysate was determined by Bradford method using Bio-Rad Protein Assay (Bio-Rad

Laboratories, Hercules, CA, USA) (Bradford, 1976). This assay is based on the colormetric change of Coomassie Brilliant Blue in response of various concentrations of protein. Briefly, 10 µl of protein samples and protein standards (0.05, 0.1, 0.2, 0.3, 0.4, 0.5 mg/ml BSA) were pipetted into a 96 well plate in triplicates. Subsequently, 200 µl diluted dye reagent (1 part dye diluted with 4 parts distilled water) was added into each well with multi-channel pipet. The protein and dye were mixed well and incubated in dark at room temperature (RT) for 5 to 10 min. At last, the absorbance was measured at 595 nm using SpectraMax® M5 Microplate Reader (Molecular Devices, Sunnyvale, CA, USA). The concentration of protein sample was deduced from the standard curve generated from BSA standards.

2.1.3 Sodium dodecyle sulphate-polyacrylamide gel electrophoresis (SDS-PAGE)

10% resolving gel and 5% stocking gel were prepared following the recipe in Table 2.1. Appropriate amounts of protein sample (normally 20 µg for western blot and 50 µg for venom sample) was mixed with 6 x biomophenol blue loading dye and denatured at 95 ^{o}C for 5 min. SDS-PAGE was run with Mini-Protean 2 apparatus electrophoresis system (Bio-Rad) in 0.25 M Tris-glycin buffer (pH=8.3) at 70 V for 45 min followed by run at 100 V until the loading dye reached the bottom of the resolving gel. PageRuler Prestained Protein Ladder (Pierce, Rockford, IL, USA) was applied to indicate the molecular weight of protein samples. After the run, the separated protein

was transferred onto PVDF membrane for western blot or stained by GelCode Blue Stain Reagent (Pierce) according to manufacturer`s instruction and visualized with Bio-Rad GS-800 calibrated imaging densitometer.

Table 2.1 Recipe of resolving gel and stocking gel

Reagent	10% resolving gel (ml)	5% stacking gel (ml)
dd H2O	4	3.4
30% acylamide	3.3	0.83
1.5 M Tris pH8.8	2.5	-
1.0 M Tris pH6.8	-	0.67
10% SDS	0.1	0.05
10% APS	0.1	0.05
TEMED	0.004	0.005
Total	10	5

2.1.4 Size exclusive gel filtration

Size exclusive gel filtration chromatography normally provides the preliminary separation of proteins based on their molecular size. The prepared crude venom was loaded onto Superdex G75 Hi-load 16/60 gel filtration column (GE healthcare, Buckinghamshire, UK), and the venom fractions were eluted with 50 mM ammonium bicarbonate, pH=8.0, at a flow rate of 1mL/min. The absorbance was monitored at 215, 254, 280 nm simultaneously. Each fraction was collected by pooling the eluted solution together and lyophilized using Modulyo® freeze dryer (Thermo Scientific, Wilmington, DE, USA). Protein concentration of each fraction was determined by the Bradford method and the molecular weight (M.W.) distribution was detected by SDS-PAGE.

2.1.5 Cation exchange chromatography

Based on the cell viability assay, the anticancer component was determined in fraction 1 (BHV-F1). Therefore, the BHV-F1 was processed for secondary purification using 7x35 mm UNOS1 cation exchange column (Bio-Rad). Desalting and buffer exchange was accomplished with Amicon Ultra-15 centrifugal filter device (Millipore, MA, USA). The column was equilibrated with 50 mM sodium acetate, pH=5.0, at a flow rate of 1ml/min, and the elution buffer was 1M NaCl in starting buffer with a gradual increase of gradient from 0% to 100%. The absorbance was monitored at 215, 254 and 280 nm simultaneously.

2.1.6 MALDI-TOF Mass spectrometry

MALDI-TOF-MS (Matrix-Assisted Laser Desorption/Ionization Time of Flight Mass Spectrometry) was applied to determine the protein identity. After BHV was partially purified and separated by SDS-PAGE, the bands of interest were carefully cut out from gel. Next, the samples were submitted to the Protein and Proteomics Center, NUS for further analysis. First, the gel was cut into small pieces, washed, dehydrated and digested into peptides with 11ng/µl trypsin in 25mM ammonium bicarbonate. The peptides were then extracted and eluted with elution solution (0.1% TFA/50% acetonitrile). Peptides extracts were dried on a speed-vac at RT and re-dissolved in 1 µL of matrix solution (5 mg ml of a-cyano-4-hydroxycinnamic acid (CHCA) in 0.1%

TFA, 50% acetonitrile in MilliQ water). Next, the sample was spot onto the MALDI target plate, allowed to air dry and analyzed by ABI 4800 Proteomics Analyzer MALDI-TOF/TOF Mass Spectrometer (Applied Biosystems, Foster City, CA, USA). The GPS explorer™ software v3.6 (Applied Biosystems) was used to retrieve data and create reports. The peptide and protein identification was analyzed using MASCOT search engine v2.1 (Matrix Science) with reference to NCBInr Protein Database.

2.2 Cell culture

MKN-7, MKN-74 and NUGC-3 gastric cancer cell lines were purchased from Japanese Riken Cell Bank (Tsukuba, Japan). MDA-MB-231, T-47D, MCF7 and MCF-12A breast cancer cell lines were obtained from American Tissue Culture Collection (ATCC, Manassas, VA, USA). In this study, the cell maintenance and subculture conditions are listed in Table 2.2. The medium RPMI-1640, DMEM/High Glucose and fetal bovine serum (FBS) came from HyClone (Logan, Utah, US). DMEM F12 plus supplements and trypsin were purchased from Invitrogen (Carlsbad, CA, USA). The cells were grown in an incubator at 37 ^{o}C with 5% CO_2 air flow. Upon reaching 90% confluency, cells were washed with 1 x PBS and detached by trypsin. The enzymatic reaction was stopped by adding complete culture medium and the cells were harvested by centrifugation at 1000 rpm for 5 min. The cells were resuspended in corresponding culture medium and a subcultivation ratio of

1:4 was used. For cell seeding in 96- and 6-well plate, cells were counted with hemocytometer.

For cryopreservation, cells were harvested and resuspended in the respective culture medium containing 20% FBS and 10% dimethylsulfoxide (DMSO). The cells were kept in Cryo 1 ^{o}C Freezing Container (Nalgene, Rochester, NY, USA) and put in -80 ^{o}C freezer overnight before transferring into a liquid nitrogen tank.

Table 2.2 Cell lines, cell maintenances and subculture conditions

Gastric cancer cells		
Cell line	**Medium receipt**	**Subculture condition**
NUGC-3	RPMI + 10%FBS	2 x trypsin* 6-8 min
MKN-7	RPMI + 10%FBS	2 x trypsin 15 min
MKN-74	RPMI + 10%FBS	2 x trypsin 8 min
Breast cancer cells		
Cell line	**Medium receipt**	**Subculture condition**
MDA-MB-231	RPMI + 10%FBS	1 x trypsin 2 min
MCF-7	DMEM + 10%FBS	1 x trypsin 5 min
T-47D	RPMI + 10%FBS	1 x trypsin 5-7 min
MCF-12A	DMEM F12 + cocktail*	5 x trypsin 6 min

*cocktail indicates 5% FBS + 20 ng/ml epidermal growth factor (EGF) + 100 ng/ml cholera toxin + 0.01 mg/ml insulin + 500 ng/ml hydrocortisone + 40 µg/ml gentamicin. 1 x trpysin means 0.05% w/v trypsin.

2.3 Functional studies to evaluate the anticancer effects of scorpion venom and LAAO *in vitro*

2.3.1 Cell proliferation/viability assay

Cell proliferation/viability was determined by alamarBlue® Cell Viability Reagent (Invitrogen). The alamarBlue Reagent is an oxidized form of redox indicator that is blue in colour and non-fluorescent. When incubated with viable cells, the reagent change colour from blue to red and become fluorescent because the viable cells provide a reducing environment. Briefly, 10,000 cells per well were seeded in a 96-well plate. After 24 h of settlement, cells were treated with various concentration of venom or LAAO for another 24 h. Next, cells were washed once with warm PBS and 100 µl new medium containing 10 µl alamarBlue was added to each well. After 1 h-4 h of incubation at 37 ^{o}C in dark, fluorescence was measured with the SpectraMax® M5 Microplate Reader (Molecular Devices) at 570/585nm excitation/emission.

2.3.2 Cytotoxixity determination by Lactate Dehydrogenase (LDH) assay

Cytotoxicity of scorpion venom and LAAO to cancer cells was determined using Cytotoxicity Detection Kit (Roche, Basel, Switzerland) based on the measurement of lactate dehydrogenase (LDH) from damaged cells. Briefly, 10,000 cells per well were seeded in a 96-well plate and received drug treatment for 24 h. 100 µl of 2% Triton X solution was added to cells 10 min

prior to assay as a positive control. The microplate was centrifuged at 250 x g for 10 min and 100 µl of supernatant from each well was transferred into a new plate. 100 µl of freshly prepared reaction mixture (250 µl of Diaphorase/NAD^+ mixture in 11.25 ml of Indotetrazolium chloride + sodium lactate) was added and mixed with the supernatant. The mixture was incubated at RT for 30 min and the absorbance of each sample was read at 492 nm. The cytotoxicity of drugs was calculated using the following formula:

$$Cytotoxicity(\%) = \frac{\text{exp. value} - \text{control value}}{\text{Triton X value} - \text{control value}} \text{x}100$$

2.3.3 Cell cycle analysis

Both floating and adherent cells after treatment with scorpion venom or LAAO were harvested by trypsin-EDTA and centrifugation at 1000 rmp for 5 min. Cells were washed twice with ice-cold PBS, followed by fixation with 70% cold ethanol overnight at 4 °C. Next, the fixed cells were collected and washed twice again. The cell pellet was resuspended in 1 ml propidium iodide (PI) staining reagent, which contains 20 µg PI, 0.2mg RNase A, and 0.1% Triton-X dissolved in PBS. The cells were incubated in the dark for 15 min at RT and analyzed by flow cytometry with CyAn™ ADP Analyzer (Beckman Coulter, Brea, CA, USA) or BD LSRFortessa™ cell analyzer (BD Biosciences, Franklin Lakes, NJ, USA). The data obtained were analyzed using the Summit software version 4.3.

2.3.4 Cell apoptosis detection by Annexin V & PI staining

Cells exposed to scorpion venom or LAAO were harvested by the trypsin-EDTA method and washed twice with ice-cold PBS. FITC Annexin V Apoptosis Detection kit I (BD Bioscience) was applied to detect the cell apoptosis. In apoptotic cells, the membrane phospholipid phosphatidylserine (PS) is translocated from the inner to the outer leaflet of the plasma membrane. The FITC conjugated Annexin V is a 35-36 kDa Ca^{2+} dependent phospholipid-binding protein that has a high affinity for PS and thus serves as a sensitive probe of cell apoptosis analysed by flow cytometry. Since externalization of PS occurs in the earlier stages of apoptosis, the FITC Annexin V staining is used to identify early apoptosis. Briefly, the washed cells were collected by centrifugation and resuspended in 100 µl 1 X Binding Buffer. Then, 5 µl of FITC Annexin V and 5 µl PI were added into each solution. Meanwhile, unstained, Annexin V staining alone and PI staining alone were set as controls, respectively. The cell solution was gently vortex and incubated at RT for 15 min in dark. Finally, 400 µl of 1 X Binding Buffer was added to each tube to stop the reaction and cells were analyzed by flow cytometry within 1 h with CyAn™ ADP Analyzer (Beckman Coulter) or BD LSRFortessa™ cell analyzer (BD Biosciences).

2.3.5 Transmission electron microscopy (TEM)

NUGC-3 cells were seeded on Nunc™ Lab-Tek™ 4-Chambered Coverglass (Thermo Scientific) at a density of 8 x 10^4 cells/well. After 24 h of settlement, cells were treated with BHV for 24 h or LAAO for 12h, respectively. After treatment, medium was removed and cells were washed twice with ice-cold PBS, followed by fixation with 2.5% glutaraldehyde for 1 h at 4 °C. Cells were washed 3 times with ice-cold PBS and post-fixed with 1% osmium tetroxide and potassium ferrocyanide for 1 h at room temperature. Subsequently, cells were dehydrated through an ascending series of ethanol and embedded in araldite for 24 h. 99 nm ultrathin sectioning of samples was performed using the Reichert Ultracut E ultramicrotome. The last step of sample preparation was mounting the cells onto copper grids and doubly stained with uranyl acetate and lead citrate. NUGC-3 cellular ultrastructure was observed under the EM280S transmission electron microscope (Philips, Amsterdam, Netherlands) at a voltage level of 100.0 KeV.

2.3.6 Scanning electron microscopy (SEM)

Lab-Tek™ 4-Chambered Coverglass (Thermo Scientific) was used for seeding NUGC-3 cell at a density of 8 x 10^4 cells/well. NUGC-3 cells were treated with 1.0 µg/ml LAAO for 12 h and washed with 1 x PBS at RT. Cells were then fixed with 2.5% glutraldehyde for 1 h at RT, followed by 3 times of washing with 1 x PBS. Next, cells were dehydrated by being passed through

an ascending series of ethanol (in 25%, 50%, 75%, 95% ethanol for 3 min and in 100% ethanol twice for 5 min, respectively). Samples were then transferred into the Balzers CPD 030 critical point drier (Bal-tec, Liechtenstein) for 1 h as per the manufacturer's instruction. The cover slides were mounted onto the metal stubs with silver paint. Finally, samples were coated with gold for conductivity in a sputter way before being viewed under JSM-6701F, cold field-emission scanning electron microscope (JEOL, Tokyo, Japan) at a voltage level of 10.0 KeV.

2.3.7 Cell migration and invasion assay

NUGC-3 cell migration assay was conducted using 6.5 mm Transwell with 8.0 µm pore polycarbonate membrane inserts (Corning, MA, USA). Firstly, the inserts were re-hydrated by adding 600 µl RPMI 1640 medium containing 20% FBS into lower chamber and 200 µl RPMI 1640 medium into upper chamber and incubating at 37 °C with 5% CO_2 overnight. After re-hydration, the medium was carefully removed. NUGC-3 cells (treated with non-cytotoxic dose of scorpion venom) were harvested by trypsin-EDTA method, pelleted and resuspended in appropriate volume of RPMI 1640 medium to get the concentration of 4 X 10^5 cell/ml. Next, 200 µl of cell suspension containing 8 x 10^4 cells was placed into upper chamber and 600 µl of RPMI 1640 medium with 20% FBS was added into lower chamber as a chemoattractant to attract the cells to migrate through the insert polycarbonate membrane. After incubation for 24 h in the humidified

incubator at 37 °C with 5% CO_2, the inserts were washed twice with 1 x PBS and fixed in 100% methanol for 15 min. Afterwards, the inserts were washed again and kept in the hood for air dry. The dried inserts were subsequently stained with 0.5% (w/v) crystal violate for 30 min. The excess dye was flushed off by rinsing the inserts in clean water twice and the non-migrated cells in the upper chamber were removed using cotton swab. Finally, the migrated cells that adhere to the bottom of the insert were viewed under SMZ 1500 stereomicroscope (Nikon, Yurakucho, Tokyo, Japan). Five fields (1 in centre and 4 in periphery) were chosen to take photo and the cell number was counted using Adobe Photoshop CS5 software.

The cell invasion assay was similar to migration assay using BD Biocoat™ Matrige Invasion Chamber with 8.0 µm PET membrane insert (BD Biosciences). The incubation time for cell invasion assay was 36 h.

2.3.8 Evaluation of Caspase-3 activity

Caspase-3 is a downstream effector caspase, that is activated when caspase-dependent cell apoptosis happens, and in turn executes apoptosis by cleaving various cytoplasmic or nuclear proteins including PARP. In this study, the caspase-3 activity was measured using Caspase-3 Colormetric Assay Kit (Genescript, NJ, USA) based on spectrophotometric detection of the chromophore *p*nitroanilide (*p*NA) after cleavage from the labeled substrate DEVD-*p*NA. DEVD (Asp-Glu-Val-Asp) is an amino acid sequence that can be

preferentially recognized by caspase-3. Briefly, cell apoptosis was induced by treating NUGC-3 cells with 30 µg/ml BHV or 1 µg/ml LAAO for 24 h. 10 µM Doxorubicin was used as positive control. Cells were harvested by trypsin-EDTA method and washed once with ice-cold 1x PBS. 5 x 10^6 cells were collected by centrifugation and lysed in 50 µl lysis buffer containing 10 mM DTT. The solution was incubated on ice for 40 min with vortex every 10 min. The cell lysate was obtained by collecting the supernatant after centrifuging at 10,000 rpm at 4 °C for 10 min. Protein concentration was then determined by the Bradford method. Next, 50 µl of supernatant containing 100 µg protein was transferred into 96-well plate and mixed with another 50 µl 2 x reaction buffer. 5 µl of caspase-3 substract (200 µM final concentration) was added to each sample and mixed well. The plate was incubated in dark at 37 °C for 4 h and the absorbance was read with avSpectraMax® M5 Microplate Reader (Molecular Devices) at 405 nm.

2.3.9 Measurement of mitochondrial membrane potential

Loss of mitochondrial membrane potential (MMP) is one of the key events happening during cell apoptosis (Ly *et al.*, 2003). In this study, NUGC-3 mitochondrial membrane potential was measured using JC-1 (5,5',6,6'-tetrachloro-1,1',3,3'- tetraethyl-imidacarbocyanine iodide) (BioVison, Milpitas, CA, USA). JC-1 is a cationic dye that can stain mitochondria in living cells in a membrane potential dependent fashion. In healthy cells with high MMP, JC-1

spontaneously forms complexes called J-aggregates with red fluorescence. Whereas, in apoptotic cells with low MMP, JC-1 remains in the monomeric form and shows green fluorescence. Briefly, 4 x 10^5 NUGC-3 cells seeded in 6-well plate were treated with 1.0 µg/ml LAAO for 0 h, 3 h, 6 h and 9 h, respectively. For the positive control, CCCP (carbonyl cyanide 3-chlorophenylhydrazone) was applied to treat cells in 50 µM final concentration for 10 min. After treatment, cells were harvested by trypsin-EDTA method and resuspended in 1ml warm medium containing 2 µM JC-1 dye. Cells were incubated at 37 °C, 5% CO2 for 20 min followed by one time wash with 1 x PBS to remove the excess dye. Finally, cells were resuspended in 500 µl PBS and analyzed on BD Accuri™ C6 flow cytometer (BD Biosciences) with red and green fluorescence channels.

2.3.10 Measurement of Oxidative stress

NUGC-3 intracellular oxidative stress was evaluated with 2',7' – dichlorofluorescein diacetate (DCFDA) (Sigma-Aldrich), a fluorogenic dye that measures the level of various reactive oxygen species (ROS) in the cell. After diffusion into the cell, DCFDA is deacetylated by cellular esterases to a non-fluorescent compound, which is later oxidized by ROS into 2', 7' – dichlorofluorescin (DCF). DCF is a highly fluorescent compound and can be detected and quantified by flow cytometry. Briefly, 4 x 10^5 NUGC-3 cells seeded in 6-well plate were treated with 0.5 µg/ml LAAO for 0 h, 1.5 h, 3 h

and 6 h, respectively. Cells were harvested by trypsin-EDTA method and washed once with warm 1x PBS. Cells were pelleted by centrifugation at 1,000 rpm for 5 min and resuspended in 1 ml PBS buffer containing 10 µM DCFDA. The solution was incubated in dark at 37 °C for 30 min. After that, the staining buffer was removed by centrifugation and cells were returned to pre-warmed medium and incubated in cell culture incubator for a short recovery (about 5 min) for cellular esterases to hydrolyze the acetate groups and render the dye which is responsive to oxidation. Finally, cells were collected and resuspended in 1 ml PBS and analyzed by BD Accuri™ C6 flow cytometer (BD Biosciences) with excitation spectra of 495nm. Meanwhile, in this experiment, 50 µM tert-butyl hydroperoxide, tBHP (Sigma-Aldrich) was used as positive control by incubating with NUGC-3 cells for 2 h prior to assay.

2.3.11 Immunofluorescence analysis of AIF translocation

8 x 10^4 NUGC-3 cells were grown in Lab-Tek™ 4-Chambered Coverglass (Thermo Scientific) up to 60-70% confluency and were treated with 1 µg/ml LAAO for 12 h. After treatment, cells were washed twice with 1 x PBS and fixed in 4% paraformaldehyde at RT for 20 min. The fixed cells were washed twice with 0.05% Teween-20 in PBS and treated with 0.2% Triton X-100 in PBS for 5 min at RT for permeabilization. Next, cells were blocked in 1% BSA in 1 x PBS at RT for 1 h, and subsequently incubated in 200 µl AIF antibody (1:200 dilution, Cell signaling, Dancers, MA, USA) diluted in blocking solution, for 1 h at RT. After 3 times of washing with 0.05% Teween-

20 in PBS, cells were incubated in 200 µl Cy5-conjugated anti-rabbit IgG (1:500 dilution, Sigma-Aldrich) for another 1 h at RT in dark. After incubation, cells were washed thrice again and nuclei conterstaining was performed by incubating cells with 4,6-diamidino-2-phenylindole (DAPI) (Vector Laboratories, Burlingame, CA, USA) for 5 min at RT. Finally, cells were covered with 200 µl 1 x PBS and visualized under FluoView™ FV1000 confocal microscope (Olympus, Shinjuku, Tokyo, Japan).

2.4 NUGC-3 xenograft model to assess the anticancer potential of scorpion venom

2.4.1 Establishment of NUGC-3 xenograft model

Female 4-week-old BALB/c-nu/nu mice were obtained from Biological Resource Centre (A·STAR, Singapore). The animals were housed four per plastic cage with free access to water and food under controlled temperature, humidity and lightning (12-12 h light-dark cycle). All manipulations of mice were performed in accordance with the procedures outlined in the Guide for the Care and Use of Laboratory Animals of National University of Singapore. After one week of acclimatisation, 5 x 10^6 NUGC-3 cells in 0.1 ml PBS were inoculated subcutaneously into the left flank of the mice. The tumor growth was monitored and the tumor volume was calculated using the following formula: Tumor volume= maximum diameter x (minimum diameter)^2 x 0.5.

2.4.2 Intratumoral injection of venom

After 3-4 weeks, the tumor has grown to palpable size (100-200 mm^3, shown in Fig 3.14). The mice were randomly divided into 3 groups. The experimental groups were injected intratumorally with BHV of 6.25 µg/mouse and 12.5 µg/mouse, respectively. The control group were injected with equal volume of 1 x PBS. The mice were observed for another one week with measurement of tumor volume using a digital calliper every two days. At the endpoint, all mice were euthanized by CO2 and the tumor was harvested. A very small part of the tumor was cut and kept in RNA*later* (Qiagen, Hilden, NRW, Germany) at -80 °C for RNA and protein use. The rest was put into 10% formaldehyde for following analysis.

2.4.3 Tissue processing, paraffin embedding and microtome sectioning

The animal tissues were automatically processed using ATP700 Tissue Processor (Histo-Line Laboratories, Milano, Italy) with the settings in Table 2.3. Subsequently, the specimen was fixed with wax in the mould and cooled down on the Cryo Console. 5 µm sections of tumor specimens were obtained using Leica RM2165 microtome (Leica Biosystems, Nussloch, Germany).

Table 2.3 Program settings for tissue processing

Step NO.	**1**	**2**	**3**	**4**	**5**	**6**
Reagent	10% formaldehyde	70% alcohol	90% alcohol	100% alcohol	100% alcohol	100% alcohol
Time/h	1.0	1.3	1.3	2.0	2.0	3.0
Step NO.	**7**	**8**	**9**	**10**	**11**	**12**
Reagent	Histoclear	Histoclear	Histoclear	Wax	Wax	Wax
Time/h	2.0	2.0	3.0	2.0	2.0	2.0

2.4.4 Haematoxylin and Eosin staining

The dewaxing of paraffin slides was conducted in accordance with the following steps: Histoclear (2 times)→100% alcohol→90% alcohol→70% alcohol→50% alcohol→ distilled water (3 times).

After dewaxing, slides were kept in Shandon Instant Haematoxylin solution for 5 min followed by washing in distilled water. Differentiation was achieved by immersing slides in differentiating fluid (70% ethanol with a few drops of HCl) for 20 seconds. Then, slides were rinsed in distilled water and checked under a microscope to see if the differentiating process is completed. Sections were blued in tap water for 15 min and rinsed once in distilled water. Next, sections were immersed in 95% alcohol for a while before being stained in Alcoholic Eosin for 20 seconds. Dehydration was completed by quick immersion of slides in 95% alcohol and absolute alcohol for two changes. Finally, slides were cleaned in Histoclear for 3 changes and mounted with coverslip over the section.

2.4.5 *In situ* apoptosis detection

The *in situ* apoptosis in tumor specimen was assessed by the detection of DNA fragmentation based on terminal deoxynucleotidyl transferase (TdT) dUTP nick end labeling (TUNEL) technique. The TumorTACS™ In Situ Apoptosis Detection Kit (Trevigen, MD, USA) was used for this purpose. Firstly, the tumor specimens were deparaffinized as mentioned in section 2.4.4**.** Secondly, the slides were washed in 1 x PBS for 10 min and covered with 50 µl of diluted Proteinase K solution for 5 min. Thirdly, after washing the slides in distilled water twice for 2 min, the specimens were immersed in Quenching solution for 5 min. Fourthly, after being washed in 1 x PBS for 1 min, the specimens were immersed in 1 x TdT Labeling buffer for 5 min. Fifthly, The specimens were covered with 50 µl of Labeling Reaction Mix and incubated at 37 °C in a humidity chamber for 60 min. Sixthly, the reaction was stopped by immersing specimens in 1 x TdT Stop buffer for 5 min. Seventhly, The specimens were washed twice again in 1 x PBS, 2 min each, covered with 50 µl of Strep-HRP Solution and incubated for 10 min at RT in a humidity chamber. Eighthly, the specimens were washed twice in 1 x PBS for 2 min each and stained in DAB solution for 5 min before rinsing 4 times in distilled water for 2 min each and staining in 1% Methyl Green solution for 30 sec. Finally, the slides were dipped 10 times each in distilled water→ distilled water→95% alcohol→100% alcohol → Histoclear→ Histoclear and mounted with coverslip.

2.5 Transcriptomic and proteomic analysis

2.5.1 Quantitative real-time polymerase chain reaction (qRT-PCR)

RNA isolation:

Total RNA was isolated from NUGC-3 human gastric cancer cells using the commercially available RNeasy mini kit (Qiagen) based on the manufacturer's instructions. Cell monolayer grown in 6-well plate was washed once with ice-cold PBS to completely remove the culture medium. 350 µl of Buffer RLT buffer containing 1% of β-mercaptoethanol was added to each well to lyse the cells. Cell scraper may be used to disrupt the cells. Then, the cell lysate was homogenized by being passed through a 23-gauge needle for 5 times. A volume of 70% ethanol was mixed with the lysate and the whole mixture was transferred to an RNeasy spin column and centrifuged for 15 sec at 13,000 rmp. Flow-through was discarded and 700 µl Buffer RW1 was added to spin column to wash RNA, followed by the same centrifugation. The RNA sample was further concentrated by adding 500 µl Buffer RPE to the column and centrifuging at the same speed for 15 sec and 2 min, respectively. Finally, the purified RNA was eluted in 30 µl RNase-free water by centrifugation. The RNA concentration was determined by nanodrop ND-100 spectrophotometer (Thermo Scientific). The quality of RNA was assessed by the ratio of 260 nm /280 nm absorbance.

cDNA synthesis:

Complementary DNA (cDNA) was synthesized using SuperScript® VILO™ cDNA Synthesis Kit (Invitrogen) following the product protocol. Briefly, a 20 µl of reaction system was prepared by mixing 5x VILO Reaction Mix (4 µl), 10x SuperScript Enzyme Mix (2 µl), RNA (up to 2.5 µg), as well as DEPC-treated water. Then, the master mix was incubated at 25 °C for 10 min, followed by 42 °C for 60 min. The reaction was terminated at 85 °C for 5 min. The resultant cDNA was stored at -20 °C until use.

qRT-PCR:

Real time PCR was performed on the HT7900 FAST Real-Time PCR System using FAST SYBR® Green Master Mix (Applied Biosystems). Primers were designed with PRIMER3 software (http://frodo.wi.mit.edu/) and their specificities were verified by the NCBI's Basic Local Alignment Search Tool (BLAST) database (http://blast.ncbi.nlm.nih.gov). The sequences of synthesized primers (1st BASE, Singapore) are listed in Table 2.4. 10 µl PCR reaction mix consisted of 5 µl SYBR green cocktail, 0.5 µl forward primer, 0.5 µl reverse primer, 1 µl cDNA and 3 µl DEPC-treated water. The reaction mixture was added into a 96-well PCR plate. The thermal-cycling conditions were programmed as follows: polymerase activation at 95 °C for 20 sec, followed by 40 cycles of denature at 95 °C for 1 sec and annealing/extension at 60 °C for 20 sec. The dissociation curve was applied to check the specificity of amplification and the existence of primer dimer. Real-time PCR results

were analyzed using the ΔΔCt and $2^{-\Delta\Delta Ct}$ method to calculate the relative gene expression (Livak *et al.*, 2001).

Table 2.4 Sequences of primers used in real-time PCR

Gene	Forward Primer Sequence (5'→3')	Reverse Primer Sequence (5'→3')
ASNS	CGTGTGTCTCCAGCACTGTT	ATCAGCTTGTTTGCCGTCTT
BIRC3	ATGCTTTTGCTGTGATGGTG	TGGGCTGTCTGATGTGGATA
FNTA	CTAACCCGGGATGCTATTGA	ACTCGCCTATGATGCCAAAC
SERPINB 2	GGTCCTGGTGAATGCTGTCT	TGGAAGCAACAAGAACATGC
TNFSF15	CAGGAGTTTGCACCTTCACA	CCAGGCCTAGTTCATGTTCC
SART1	AACCAAAAGCTGGGGAAGAT	CTCCACCAGAGTGCTGACAC
TOP2A	CAGCCCATTGGTCAGTTTGG	AGGACCACCCAGTACCGATT
TUBB	CTGGACCGCATCTCTGTGTA	GTTACCTGCCCCAGACTGAC
ERK1	ACAGTCTCTGCCCTCCAAGA	CTCATCCGTCGGGTCATAGT
ERK2	CCAGACCATGATCACACAGG	CTGGAAAGATGGGCCTGTTA
RSK	TGCACAGCCTGGGTATCATTT	CTGTCCCGCAGAAAGAATAGG
MEK1	CTATGGTGCGTTCTACAGCGA	CCCACGGGAGTTGACTAGGAT
MEK2	CCAAGGTCGGCGAACTCAAA	TCTCAAGGTGGATCAGCTTCC
Raf1	AGTTCAGCAGTTTGGCTATCAG	CACTGTTCTTTGCTTGTTCGG
P70	TTTGAGCTACTTCGGGTACTTGG	CGATGAAGGGATGCTTTACTTCC
Tpl-2	CTCCCCAAAATGGACGTTACC	GGATTTCCACATCAGATGGCTTA
Bcl-2	GAGGATTGTGGCCTTCTTTG	ACAGTTCCACAAAGGCATCC
GAPDH	GAAGGTGAAGGTCGGAGTCAAC G	TGCCATGGGTGGAATCATATTGG

2.5.2 Western blot

Protein extraction:

Cell monolayer or cell pallet was washed twice with ice-cold PBS prior to protein extraction. The extraction buffer consisted of M-PER® Mammalian Protein Extraction Reagent (Pierce), Halt™ Protease and Phosphatase Inhibitor Cocktail (Pierce) and 0.5 M EDTA at a ratio of 100:1:1. Appropriate amount of extraction buffer was added to the cells and the mixture was put on ice for 15 min with gentle shaking. Cell lysate was collected and transferred to a microcentrifuge tube. Then, the protein sample was centrifuged at 13,000 rpm for 10 min at 4 °C to remove debris. The protein in the supernatant was collected and stored at -80 °C.

Western blot:

The extracted proteins were quantified (refer to section 2.1.2), separated on SDS-PAGE gel and transferred onto a polyvinyl difluoride membrane (PVDF, Bio-Rad) via semi-dry transfer method. First, the membrane was rehydrated with absolute methanol and equilibrated in transfer buffer. A sandwich structure was made by putting the gel onto membrane and laying them in between two filter pads. Air bubble between each layer was removed using a glass rod and the protein was transferred at 15 V for 60 min. After protein transfer, the membrane was blocked in 5% non-fat milk for 1 h at RT and washed thrice with 1 x TBST. Diluted primary antibody was added to cover the membrane and incubated overnight at 4 °C.

The membrane was then washed thrice with 1 x TBST followed by incubation with corresponding secondary antibody for 2 h at RT. After washing with TBST and two changes of 1 x TBS, the protein bands were developed with Supersignal West Pico Chemiluminescent substrate (Pierce) and finally visualized on blue X-ray films in dark room. The protein bands were scanned with Bio-Rad GS-800 densitometer and quantified with Quantity-One Image Analysis software (Bio-Rad). The relative expression of target protein was calculated by the ratio of optical density (OD) of target protein to the OD of β-actin. The primary and secondary antibodies used in this study are listed in Table 2.5

Table 2.5 Antibodies used in western blot

Antibody	Source	Host species	Dilution
Cleaved PARP	Cell Signaling	Rabbit	1:1000
Cleaved caspase-3	Cell Signaling	Rabbit	1:1000
Cleaved caspase-8	Cell Signaling	Rabbit	1:1000
Cleaved caspase-9	Cell Signaling	Rabbit	1:1000
Phospho-ERK1/2	Cell Signaling	Rabbit	1:1000
Phospho-MEK1/2	Cell Signaling	Rabbit	1:1000
Phospho-Elk-1	Cell Signaling	Rabbit	1:1000
Phospho-MSK-1	Cell Signaling	Rabbit	1:1000
Phospho-p90RSK	Cell Signaling	Rabbit	1:1000
Bcl-2	Cell Signaling	Rabbit	1:1000
Bax	Cell Signaling	Rabbit	1:1000
Bcl-xl	Cell Signaling	Rabbit	1:1000
Polyclonal Malondialdehyde (MDA)	Abcam Cambridge, UK	Rabbit	1:5000
β-actin	Sigma-Aldrich	Mouse	1:6000
Anti-rabbit IgG	Cell Signaling	Goat	1:2000
Anti-mouse IgG	Sigma-Aldrich	Rabbit	1:10000

2.5.3 Affymetrix Gene Chip® Human Gene 2.0 ST Array

To investigate the gene expression profile after BHV scorpion venom treatment, the cDNA microarray was conducted using Gene Chip® Human Gene 2.0ST Array (Affymetrix, Santa Clara, CA, US). NUGC-3 cells were treated with 5 µg/ml BHV-F1 for 24 h. Total genome RNA was extracted as mentioned in section 2.5.1. After that 6 total RNA samples were submitted to Origen Labs (Singapore) for following analysis.

First, the RNA integrity and quality were checked using spectrophotometric measurement (BioSPEC-Mini, Shimadzu, Nakagyo-ku, Tokyo, JP) and RNA gel electrophoresis analyzed with Agilent Bioanalyzer (Santa Clara, CA, US), according to SOP of Origen Labs. Next, for each sample, 100 ng total RNA was reverse transcribed to cDNA/mRNA, which was subsequently converted to double strand cDNA with a unique DNA/RNA heteroduplex on one end. The cDNA was then amplified via SPIA (Single Primer Isothermal Amplification) and post-SPIA Modification to generate sense target cDNA. Finally, the target cDNA was fragmented, biotin labelled and hybridized to Affymetrix Human Gene 2.0 ST array for 18 h at 45 °C with rotation at 60 rpm. Arrays were then washed and stained using the FS450_0002 fluidics protocol and scanned with an Affymetrix 3000 7G scanner.

For results interpretation, probe intensity data in CEL file were generated from Affymetrix GeneChip Command Console Software (AGCC)

and imported into Expression Console 1.3 software for array quality control. List of target genes was created using Gene Spring GX software (Agilent) with requirement of fold change above 2 and p value less than 0.05. Functional clustering was accomplished with the online Database for Annotation, Visualization and Integrated Discovery (DAVID). The flow chart of whole processes are summarised in Fig 2.1.

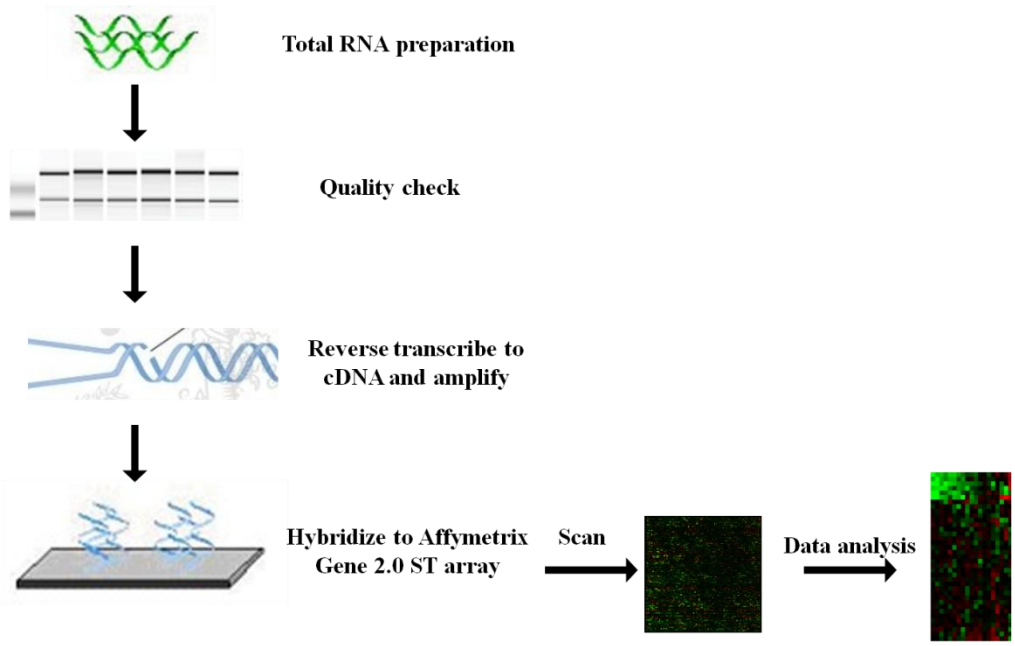

Fig 2.1 Flow chart of Affymetrix DNA microarray

2.5.4 Cancer 10-Pathway Reporter Array

The Cancer 10-Pathway Reporter Array (Qiagen) is a commercial reporter array to measure the activities of ten cancer-related signaling pathways. All reporter assays are based on dual-luciferase technology. Each reporter consists of a mixture of a pathway-focused transcription factor-responsive firefly luciferase construct and a constitutively expressing Renilla

luciferase construct (shown in Fig 2.2). Briefly, first, 50 µl of Opti-MEM® was added to each well to resuspend reporter constructs. Second, 50 µl of diluted Attractene was mixed with resuspended reporter constructs and the mixture was incubated at RT for 20 min. Third, NUGC-3 cells after treatment with scorpion venom were harvested by trypsin method, counted and suspended in 50 µl Opti-MEM containing 10% of FBS. Then, 2 x 10^4 cells were seeded to each well and transfected for 24 h. Forth, after transfection, each well was replaced with complete growth medium and the Dual-Glo® Luciferase Assay was performed (Promega).

Tube	Pathway	Transcription Factor
1	Wnt	TCF/LEF
2	Notch	RBP-Jκ
3	p53/DNA Damage	p53
4	TGFβ	SMAD2/3/4
5	Cell cycle/pRb-E2F	E2F/DP1
6	NFκB	NFκB
7	Myc/Max	Myc/Max
8	Hypoxia	HIF1A
9	MAPK/ERK	Elk-1/SRF
10	MAPK/JNK	AP-1
11	Negative Control	
12	Positive Control	

Fig 2.2 Plate components for Cancer 10-Pathway Reporter Array

2.5.5 Stable Isotopic Labeling using Amino acids in Cell culture (SILAC)

Stable Isotopic Labeling using Amino acids in Cell culture (SILAC) is a novel technique in quantitative proteomics based on Mass spectrum. NUGC-3

cells were cultured in light and heavy medium systems to incorporate the isotopes for labeling. Light medium contained L- Lysine : 2HCl and L-Arginine:HCl (Sigma-Aldrich). Heavy medium contained L- Lysine : 2HCl (U-13**C**6, U15**N**2) and L-Arginine:HCl (U-13**C**6, U15**N**4) (Cambridge Isotope Laboratories, MA, US). Dialyzed FBS was used in this experiment (Therom Scientific). After 6 passages of cell culture for isotope incorporation, cells in heavy medium were treated with 1.0 µg/ml LAAO for 8 h and cell lysates from both culture mediums were harvested using RIPA buffer (Pierce). Protein concentration was determined by Bradford method and samples were mixed in 1:1 ratio. Subsequently, samples were analyzed by Quantitative Proteomics Group in IMCB (A·STAR, Singapore) using LTQ-OrbiTrap (Classic) Mass Spectrometer (Thermo Scientific). The protein quantification was performed with MaxQuent software (Version 1.3.0.5).

2.6 Statistical analysis

In this study, GraphPad Prism 5 (GraphPad Prism, San Diego, CA, USA) was applied for statistical analysis. The Student`s t-test was used to compare the difference between two groups. One way ANOVA with a post-hoc Tukey's Test was performed for the data with 3 or more groups. Two way ANOVA analysis was used in two-factorial experiments. Data were presented as mean+SEM and p value less than 0.05 was considered significant. In this thesis, two levels of significance were shown. * indicates $p<0.05$ and ** indicates $p<0.01$.

CHAPTER 3

RESULTS

3. RESULTS

3.1 Preliminary screening of the anticancer activities of scorpion venoms

3.1.1 The anti-proliferative effects of *Mesobuthus martensi* scorpion venom

This study started with preliminary screening of the anticancer effects of *Mesobuthus martensi karsch* (synonym: *Buthus martensi karsch*, BmK) scorpion venom. The alamarBlue cell viability assay was conducted to evaluate the anti-proliferative effects of BmK to cancer cells. The cell viability/proliferation of 3 cancer cell lines were analyzed after treatment with 0, 1.25, 2.5 and 5 mg/ml BmK crude venom for 24 h, respectively. Results showed that BmK venom only inhibited the viability/proliferation of NUGC-3 human gastric cancer cells significantly at 5 mg/ml while had no effects on MDA-MB-231 and MCF-7 human breast cancer cells (p>0.05) (Fig 3.1).

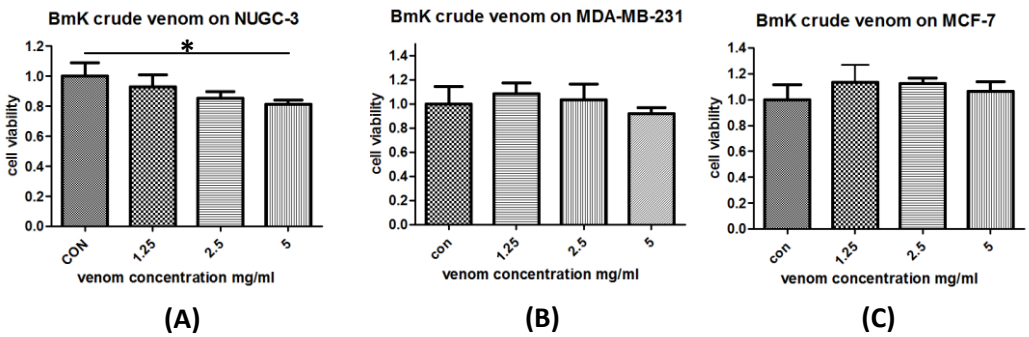

Fig 3.1 AlamarBlue cell viability/proliferation assay of cancer cells after BmK venom treatment. The cell viability of NUGC-3 human gastric cancer cells (A), MDA-MB-231 human breast cancer cells (B) and MCF-7 human breast cancer cells (C) was analyzed after treatment for 24 h and cell viability was normalized with control group. Data are presented as means + SEM. N=3. *, $p < 0.05$.

Since the BmK scorpion venom had inhibitory effect on the NUGC-3 cell proliferation at 5 mg/ml, cell cycle and apoptosis of NUGC-3 cells were examined to further investigate the anticancer effects of BmK in gastric cancer cells. As shown in Fig 3.2, after treatment with 5 mg/ml BmK venom for 24 h, the cell cycle profile changed with 6 percent increase in sub-G1 phase (2.3% vs 8.2%), 9 percent increase in G1 phase (51.1% vs 60.3%) and 11 percent decrease in G2/M phase. Meanwhile, 5 mg/ml of BmK venom treatment also induced a slight increase in apoptosis of NUGC-3 cells (8.4% vs 13.7%).

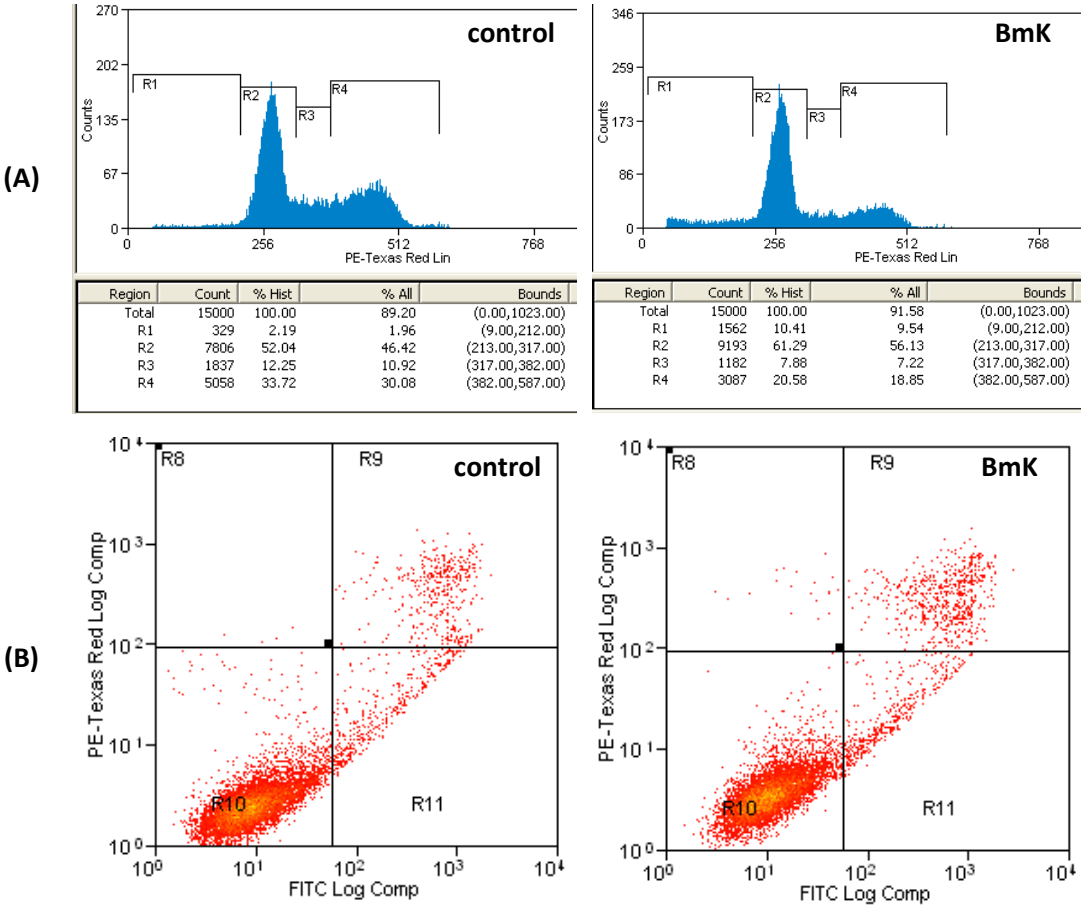

Fig 3.2 Representative profiles of NUGC-3 cell cycle (A) and cell apoptosis (B) analysis by flow cytometry. Cells were treated with 5 mg/ml BmK venom for 24 h. R1, R2, R3 and R4 in (A) indicate sub-G1, G1, S and G2/M phase, respectively. R11 and R9 in (B) indicate early apoptosis and late apoptosis, respectively. Experiment was performed in triplicates.

All these findings indicate that BmK scorpion venom had a significant inhibitory effect on NUGC-3 cell proliferation via cell cycle arrest at sub-G1 and G1 phases and apoptosis enhancement. However, the administrated concentration of BmK venom was high and the anti-proliferative effects were limited.

3.1.2 The anti-proliferative effects of crude venom from *Hottentotta hottentotta, Heterometrus longimanus* and *Pandinus imperator* scorpions

Another three crude scorpion venoms were screened using alamarBlue cell viability/proliferation assay to compare their anti-proliferative effects on NUGC-3 cells, including *Pandinus imperator, Heterometrus longimanus* and *Hottentotta hottentotta* scorpion venoms (short for PIV, HLV and BHV, respectively). Results showed that all these three venoms could decrease NUGC-3 cell viability/proliferation in a dose dependent way (Fig 3.3). The IC50 for 24 h treatment in 96-well plate was 0.9 mg/ml for PIV, 0.3 mg/ml for HLV and 8.1 μg/ml for BHV. Compared with BmK scorpion venom, it can be seen that these three venoms have stronger inhibition activity even at much lower concentration. BHV has the lowest effective concentration and seems the most promising to be developed as anticancer agent. Therefore, BHV was selected for further investigation of the anticancer potential in gastric cancer model.

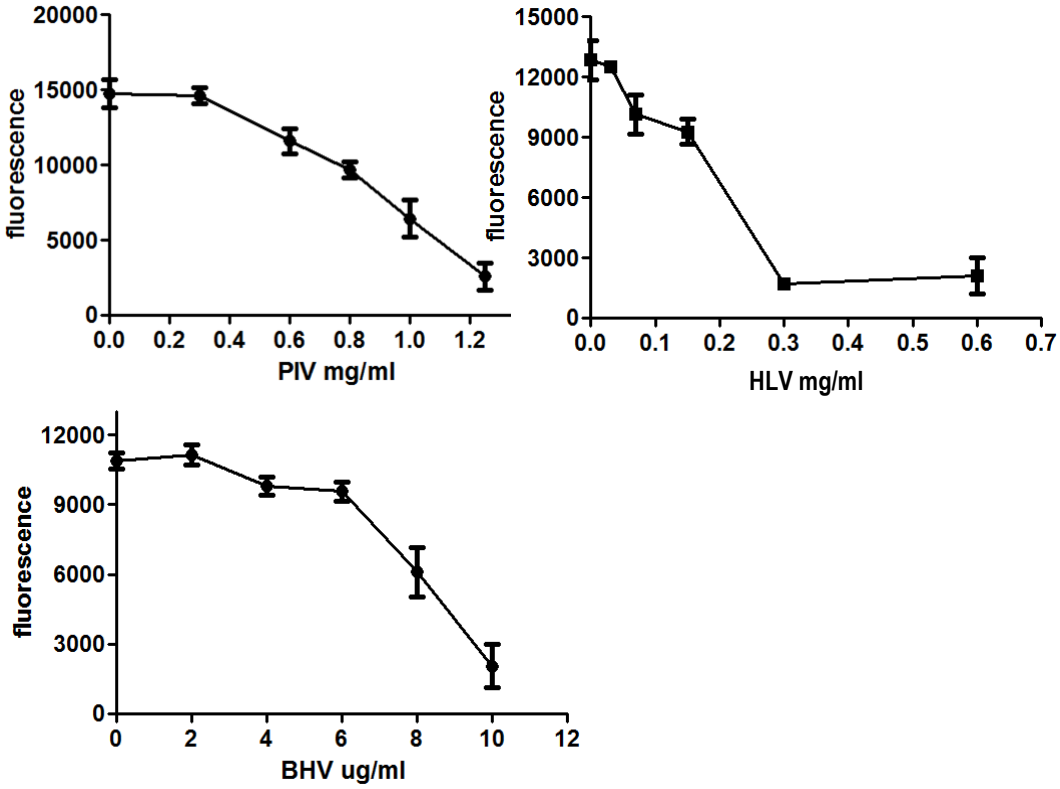

Fig 3.3 AlamarBlue cell viability/proliferation assay of NUGC-3 cells after treatment with PIV, HLV and BHV for 24 h, respectively. The intensity of alamarBlue was read by fluorescence with excitation at 570 nm and emission at 585 nm. Data are presented as means + SEM. N=3.

3.2 Evaluating the anticancer potential of *Hottentotta hottentotta* scorpion venom in gastric cancer

3.2.1 BHV`s inhibition to cell viability/proliferation of gastric cancer cell lines

Based on the observations in the preliminary screening work, the anticancer potential of BHV in gastric cancer will be the focus of this study. First, the cell viability/proliferation of another two gastric cancer cells (MKN-7

and MKN-74) were validated after receiving BHV treatment. Similar to NUGC-3, BHV decreased their cell viability/proliferation dose dependently. Whereas, MKN-7 and MKN-74 seemed more resistant to BHV treatment (Fig 3.4).

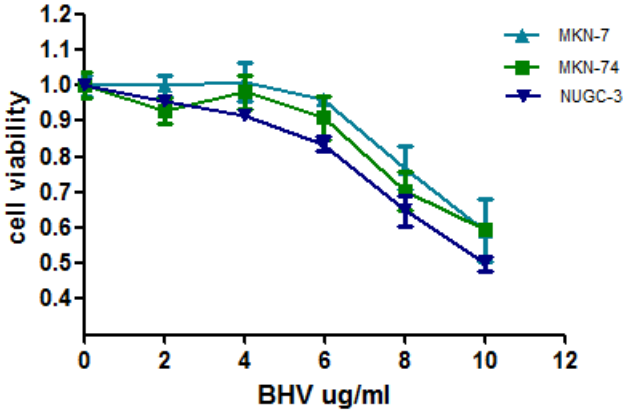

Fig 3.4 AlamarBlue cell viability/proliferation assay of gastric cancer cells after treatment with BHV for 24 h. Data are presented as means + SEM. N=3.

3.2.2 Evaluation of the cytotoxicity of BHV to NUGC-3 cells by LDH assay

The cytotoxicity of BHV to NUGC-3 cells was evaluated by measuring the release of lactate dehydrogenase (LDH) enzyme. Cells were treated with different dose of BHV for 24 h prior to LDH study. Results showed that there was no increase in the amount of released LDH after treatment with less than 8 µg/ml BHV ($p>0.05$), even though the cell viability decreased dose dependently. However, treatment with 10 µg/ml BHV significantly induced the LDH release, indicating the loss of membrane integrity (Fig 3.5). The percentage cytotoxicity was calculated as 49.5% for the 10 µg/ml BHV group.

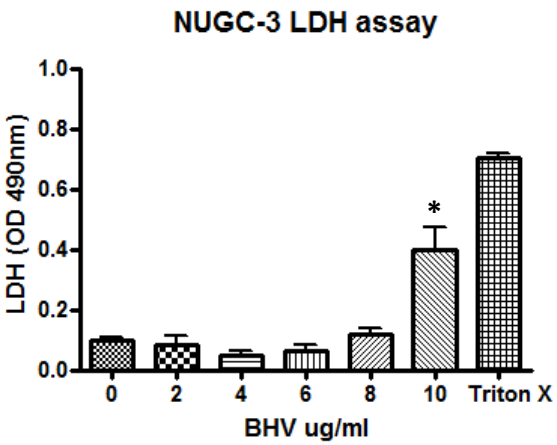

Fig 3.5 BHV cytotoxicity to NUGC-3 cells by LDH assay. Cells were treated for 24 h. 2% (w/v) Triton X was used as positive control. Data are presented as means + SEM. N=3. *, $p < 0.05$

3.2.3 NUGC-3 cell cycle profile after treatment with BHV

To determine BHV`s effect on NUGC-3 cell cycle profile, the fixed cells were stained with PI and analyzed by flow cytometry after treatment with different concentrations of crude venom for 24 h. It was shown that BHV treatment resulted in an increase in sub-G1 phase, which indicates the occurrence of DNA fragmentation. With 7.5 µg/ml of BHV treatment, sub-G1 phase increased from 2.25% to 29.5%. Concomitantly, G2/M phase decreased from 39.5% to 20.7%, and there was a slight decrease in G1 phase (Fig 3.6). Such observations suggested that BHV could induce DNA fragmentation at the sub-G1 phase.

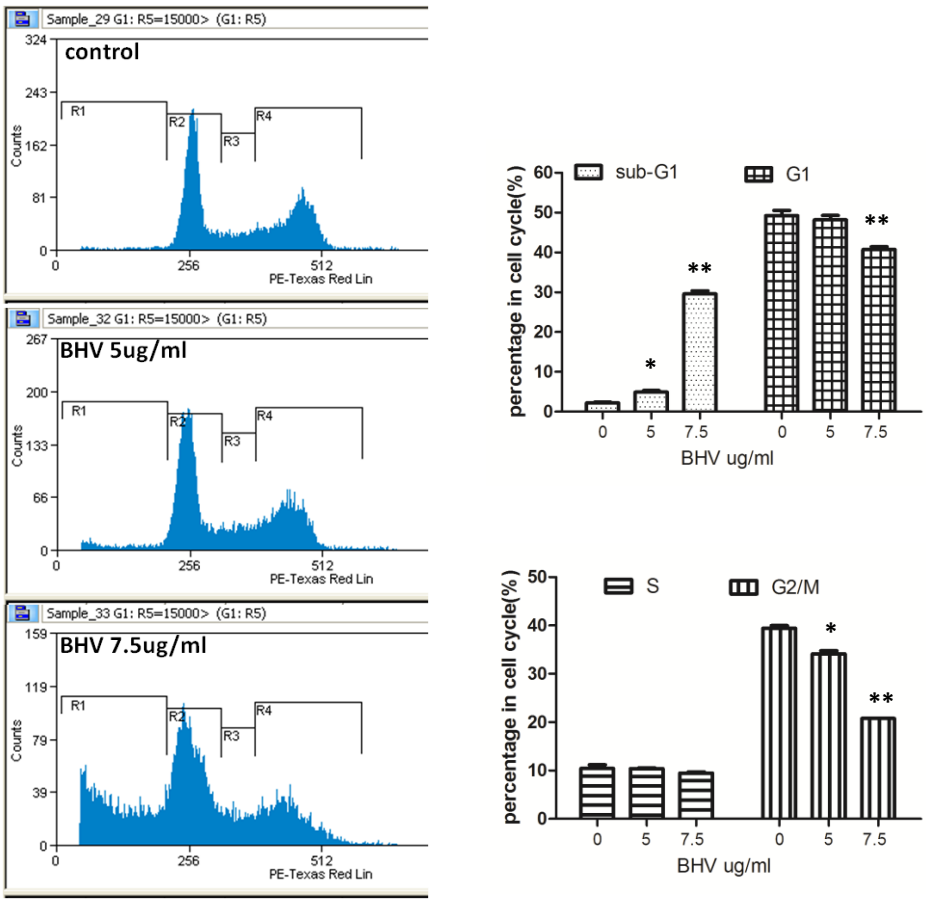

(A) **(B)**

Fig 3.6 BHV treatment induced changes of NUGC-3 cell cycle profile
(A): Representative images of NUGC-3 cell cycle profiles. R1, R2, R3 and R4 indicate sub-G1, G1, S and G2/M phase, respectively. (B): Cell fractions in different cell cycle phases. Data are presented as means + SEM. N=3. *, $p < 0.05$; **, $p < 0.01$.

3.2.4 Morphological changes induced by BHV treatment in NUGC-3 cells

3.2.4.1 NUGC-3 morphology under fluorescence microscope

Acridine orange/Ethidium bromide (AO/EB) staining is a simple way to detect cell morphology using fluorescence light microscope, which is commonly used in the differentiation of early and late apoptosis. In this study,

NUGC-3 cells were treated with 20 µg/ml BHV for 12 h and 24 h, respectively. Different stages of apoptotic morphologies were observed. The control cells were uniformly green from the staining of AO (Fig 3.7-A). Fig 3.7-B showed typical features of early apoptotic cells. Cells were stained green with bright yellowish dots as a consequence of chromatin condensation and nuclear fragmentation. Moreover, the formation of membrane blebbing was also observed. The late apoptotic cells were stained orange red because the cells have lost membrane integrity and EB was incorporated to stain DNA. In addition, late apoptotic cells displayed more condensed nuclei and cell shrinkage (Fig 3.7-C).

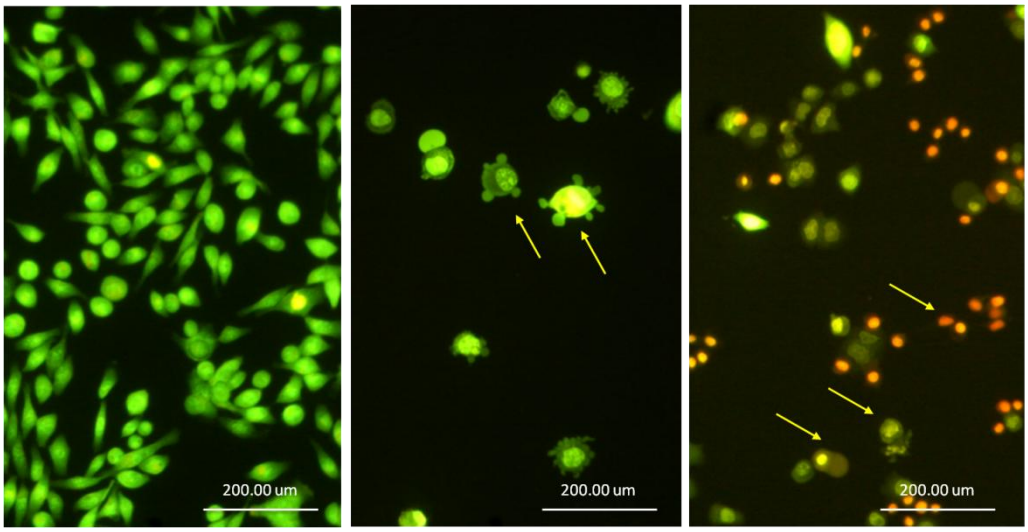

(A): Control **(B): BHV 12 h** **(C): BHV 24 h**

Fig 3.7 NUGC-3 morphological changes after BHV treatment by AO-EB staining. Photos were taken at 200 X magnification. Arrows indicate apoptotic features including yellowish and red colour changes, membrane blebbing, nuclear condensation and cell shrinkage.

3.2.4.2 NUGC-3 morphology under transmission electron microscope (TEM)

TEM was used to visualize the ultrastructural changes induced by BHV treatment. NUGC-3 cells were treated with 20 µg/ml BHV for 24 h. As shown in Fig 3.8-A, the cytoplasmic and nuclear integrity in the control cell was well preserved. For example, chromatin was evenly distributed in nucleus and the cell membrane was intact. The subcellular organelles such as mitochondria could also be seen in the cytoplasm. Comparatively, in BHV treated cells (Fig 3.8-B), the cell integrity was remarkably disrupted. The chromatin was condensed with margination along the nuclear envelope with membrane blebbing, characteristic of early apoptotic cells.

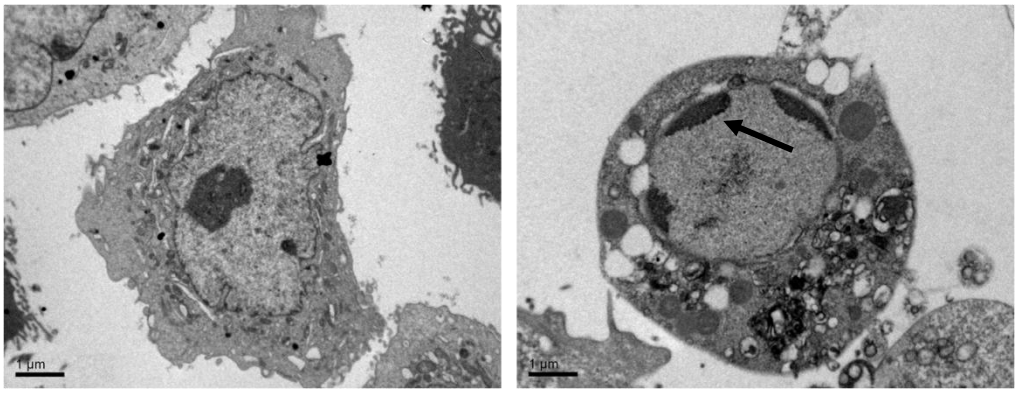

(A) **(B)**

Fig 3.8 Morphological changes seen in NUGC-3 cells after BHV treatment under TEM. (A): untreated NUGC-3 cell. (B): NUGC-3 cell treated with 20 µg/ml BHV for 24 h showing condensed chromatin, membrane blebbing and vacuoles. Scale bar is 1 µm for (A) and (B).

3.2.5 NUGC-3 apoptosis detection by Annexin-V and PI staining

Annexin-V and PI staining is a sensitive method to detect and quantify cell apoptosis based on the externalization of phosphatidylserine (PS). NUGC-

3 cells were treated with 15 µg/ml BHV for 24 h prior to staining with Annexin-V-FITC and PI. Results showed that Annexin-V-FITC signal was considerably increased after BHV treatment, which indicated the occurance of cell apoptosis (Fig 3.9). Compared with untreated cells, late apoptosis (R9) increased significantly from 3.37% up to 29.9% ($p<0.01$) and there was a slight increase in early apoptosis (2.34% vs 5.21%, $p<0.01$).

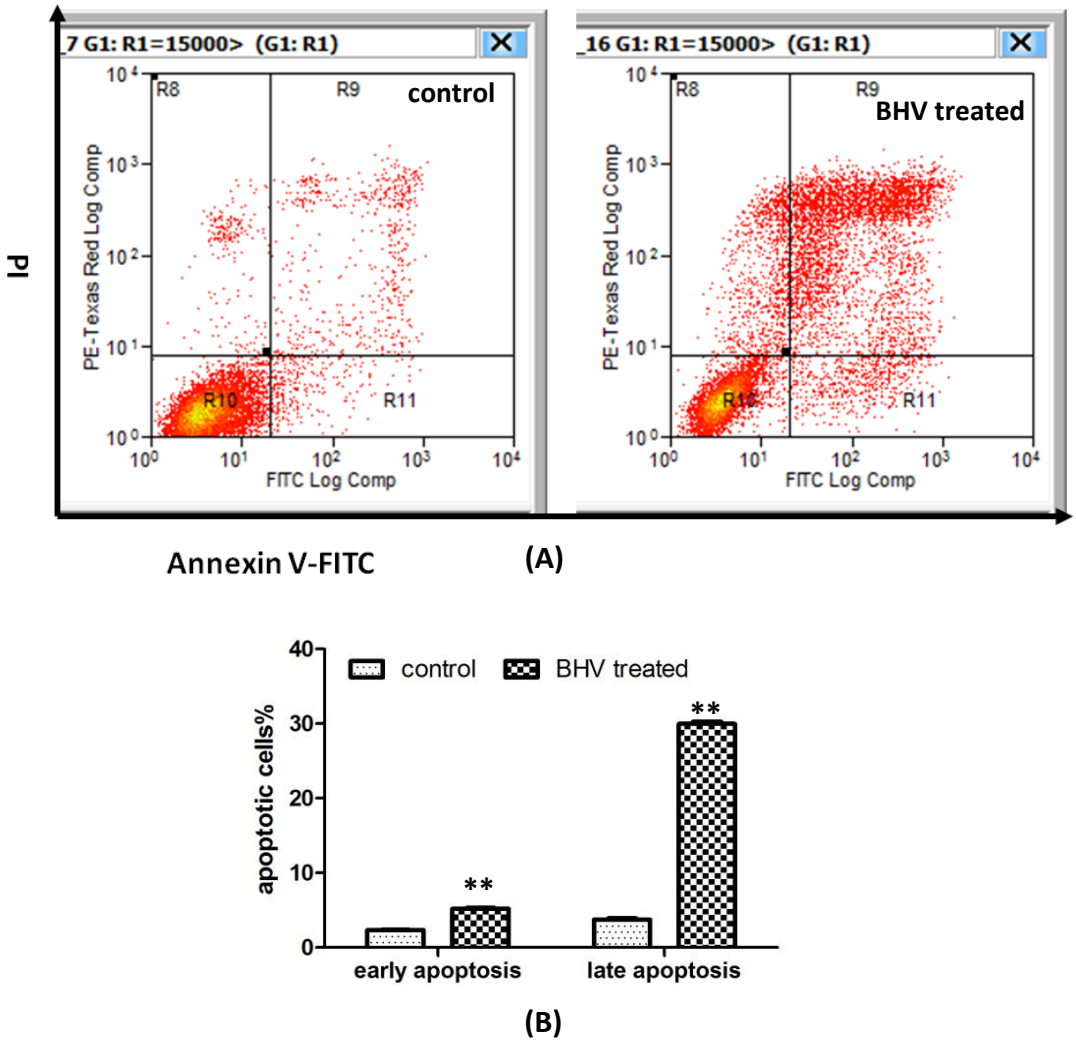

Fig 3.9 Flow cytometric analysis of NUGC-3 cell apoptosis with Annexin V and PI staining. (A): Representative profiles of Annexin-V-FITC and PI signals from flow cytometry. R11 (Annexin-V positive/PI negative) indicates early apoptosis; R9 (Annexin-V positive/PI positive) indicates late apoptosis. (B): Bar chart of the percentage of cells undergoing early and late apoptosis, respectively. Data are presented as means + SEM. N=3. **, $p < 0.01$.

3.2.6 Detection of caspase activation after BHV treatment

3.2.6.1 Western blot analysis of cleaved caspases

Apoptosis is commonly considered to be mediated by the activation of a family of cysteine-containing aspartate-directed proteases called caspases. To prove this hypothesis, the cleaved caspase antibodies were applied in western blot to identify the activation of caspase family members during BHV induced apoptosis. PARP, caspase-3 caspase-8 and caspase-9 are key regulators in the caspase apoptosis pathway. NUGC-3 cells were treated with 30 µg/ml BHV for 24 h and cell lysate was collected for western blot. Unexpectedly, results showed that no cleaved bands were detected for caspase-3, caspase-8 and caspase-9 after BHV treatment and a faint but non-significant cleaved PARP was visualized (Fig 3.10). However, in the positive control group (NUGC-3 treated with Doxorubicin, a chemotherapy drug), obvious bands were seen. Such findings suggested that the apoptosis induced by BHV was not regulated via caspase pathway.

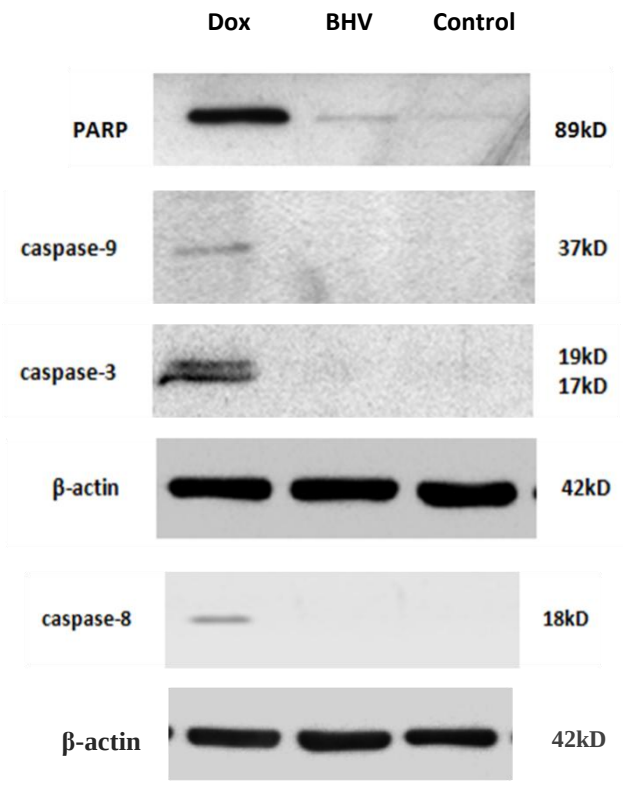

Fig 3.10 Western blot of caspase proteins in NUGC-3 cells after treatment with BHV. β actin was used to normalized the protein loading. BHV, 20 µg/ml. Dox, doxorubicin, 25 µM. Data were representative of two replicates.

3.2.6.2 Caspase-3 activity assay and the influence of pan-caspase inhibitor on NUGC-3 cell viability

To confirm the apoptosis induced by BHV was caspase independent, the caspase-3 activity was measured based on the reaction between caspase-3 and its substrate DEVD-pNA. Results showed that there was no increase in caspase activity in NUGC-3 cells after treatment with BHV (Fig 3.11-A). NUGC-3 cells were pre-treated with the pan-caspase inhibitor z-VAD-fmk for 1 h to inhibit caspase pathway prior to the administration of BHV. However, the pre-treatment with z-VAD-fmk did not have influence on the cell viability, indicating that the inhibition of caspase pathway had no effect on the BHV induced reduction of cell viability (Fig 3.11-B, p=0.16 by Two-way ANOVA). These two experiments further concluded that BHV induced a caspase independent apoptosis in NUGC-3 cells.

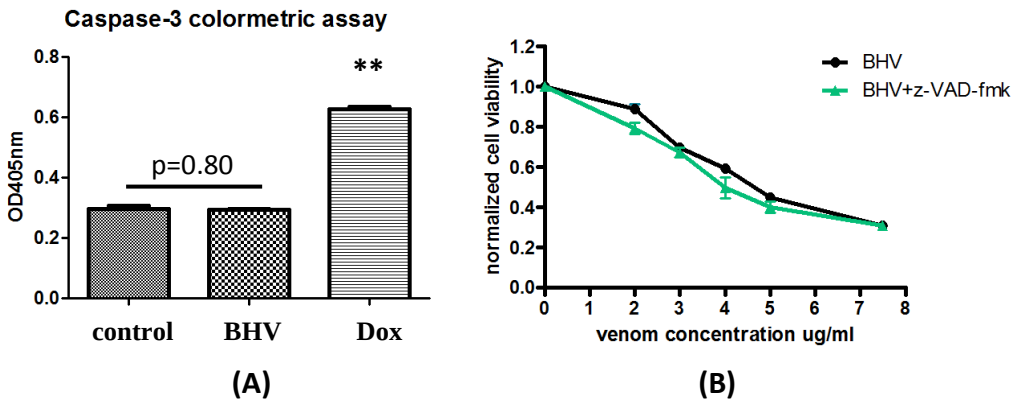

Fig 3.11 Confirmation of caspase independent apoptosis induced by BHV treatment. (A): caspase-3 activity assay. NUGC-3 cells were treated with 30 µg/ml BHV for 24 h. Dox, 25 µM doxorubicin as positive control. (B): NUGC-3 cell viability study after treatment with different concentration of BHV. BHV+z-VAD-fmk indicates cells were pre-treated with 50 µM z-VAD-fmk for 1 h prior to the administration of BHV. Data are presented as means + SEM. N=3. **, $p < 0.01$.

3.2.7 BHV`s effects on NUGC-3 cell migration and invasion

Cell migration and invasion are pivotal cell behaviours involved in cancer metastasis. The effect of BHV treatment on NUGC-3 cell migration was investigated by transwell study. Based on the cell viability study, a non-toxic concentration 2 µg/ml was used in this assay to eliminate the interference of cell viability as influencing migration. Results showed that 2 µg/ml of BHV reduced the cell migration ability through the polycarbonate membrane inserts and the reduction rate reached 55.5 % (p=0.02, Fig 3.12).

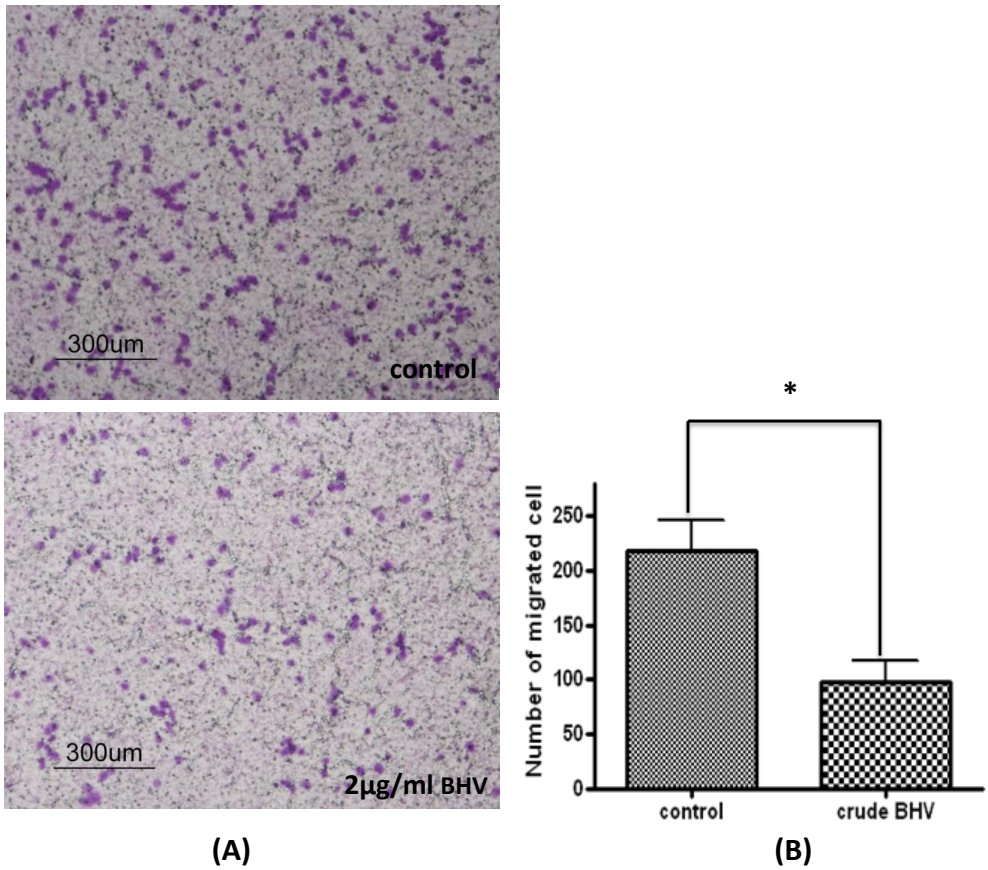

Fig 3.12 NUGC-3 gastric cancer cell migration assay after treatment with BHV. (A): Representative images of migrated NUGC-3 cells. Images were taken at 80 X magnification. (B): Bar chart of migrated cell number. Numbers are the average of 5 counting areas. Data are presented as means + SEM. N=3. *, $p < 0.05$

Similarly, NUGC-3 cell invasion activity was examined using Matrigel assay. There was a significant decreased number of cells that invaded through the matrigel and polycarbonate membrane after crude BHV treatment. The inhibitory effect was up to 90% ($p < 0.01$, Fig 3.13).

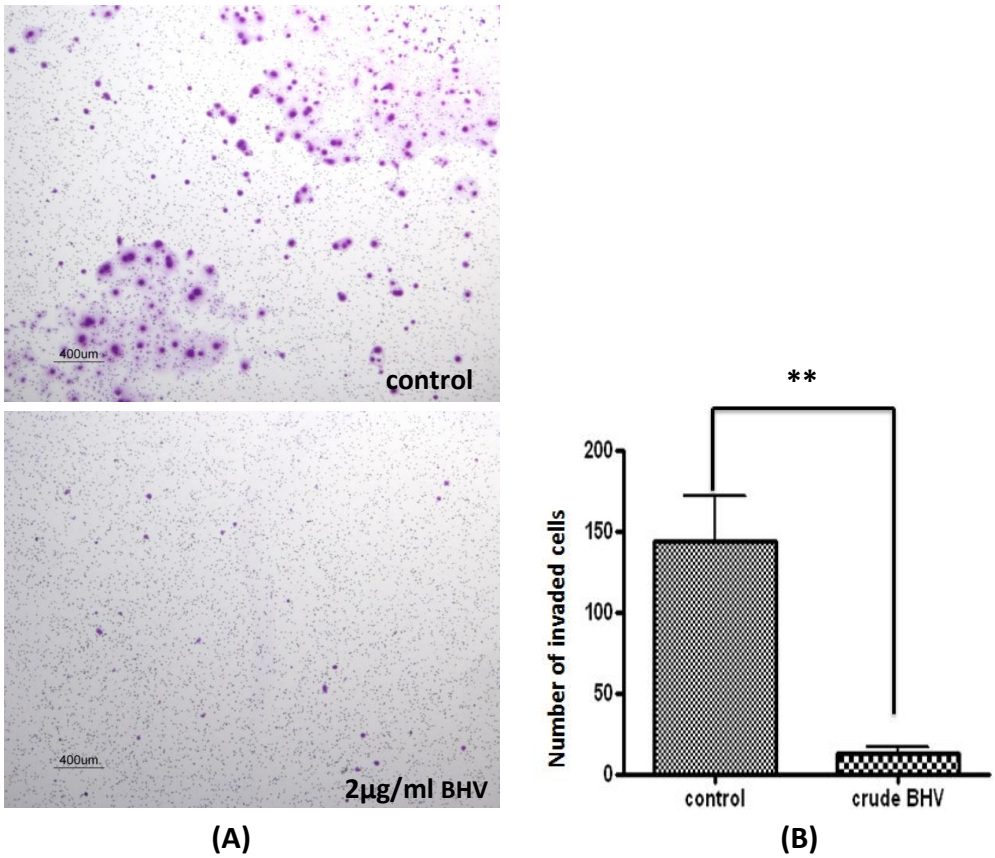

Fig 3.13 NUGC-3 gastric cancer cell invasion assay after treatment with BHV. (A): Representative images of invaded NUGC-3 cells. Images were taken at 80 X magnification. (B): Bar chart of invaded cell number. Numbers are the average of 5 counting areas. Data are presented as means + SEM. N=3. **, $p < 0.01$

3.2.8 The effects of BHV in NUGC-3 xenograft *in vivo* model

NUGC-3 xenograft model was established on BALB/c-nu/nu mice by subcutaneous injection of cancer cells. After 4 weeks, the tumor grew to palpable size (100-200 mm^3, Fig 3.14-A). The non-lethal dose of BHV to mice was determined as lower than 12.5 µg/mouse. The inhibition effect of BHV following injection was evaluated by monitoring the tumor growth. Results showed that 6.25 µg/mouse BHV did not inhibit tumor growth (p=0.06) while 12.5 µg/mouse BHV significantly inhibited tumor growth (p=0.008) (Fig 3.14-B1). The finding was confirmed with a repetitive experiment with injection of 12.5 µg/mouse BHV and the partially purified fraction BHV-F1 (5 µg/mouse) (Fig 3.14-B2).

(A)

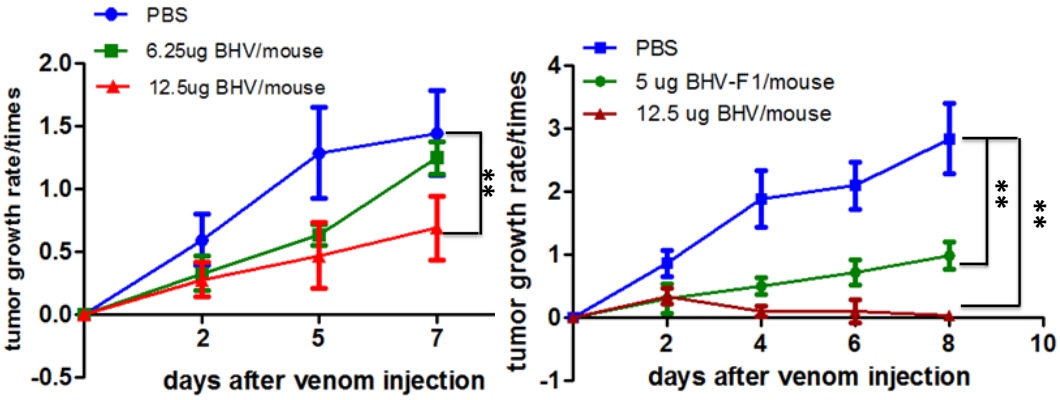

(B1) **(B2)**

Fig 3.14 Tumor growth rate of NUGC-3 xenograft after BHV treatment
(A): Representative image of BALB/c-nu/nu mice bearing NUGC-3 xenograft on the left flank, as shown with arrow. The photo was taken 4 weeks after cancer cell injection.
(B1) and (B2): Tumor growth rate of NUGC-3 xenograft after BHV treatment. Data are presented as means + SEM. N=5 (For group B2-12.5 µg/mouse, N=3). **, $p < 0.01$.

3.2.9 Tumor histology by Haematoxylin and Eosin staining

Histology of tumor sections was observed after staining with Haematoxylin and Eosin. As shown in Fig 3.15, BHV treatment disrupted the tumor homogeneity and induced cavities containing tissue debri (A vs B).

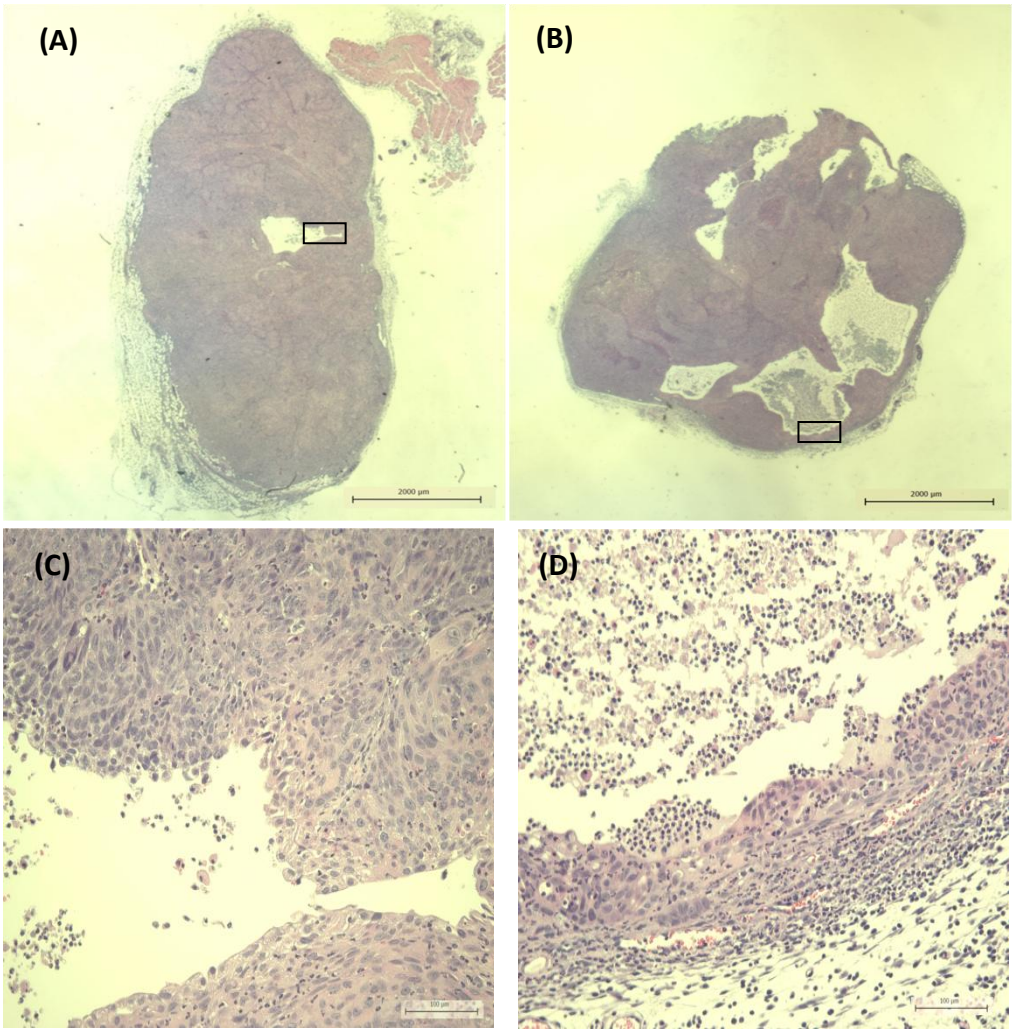

Fig 3.15 Tumor histology with H & E staining. (A) and (B) are representative images of tumor tissues with H&E staining. A, control; B, 12.5 µg/mouse BHV injection. Photos were taken at 12.5 X magnification. Scale bar=2000 µm; (C) and (D) are higher magnified images of the framed area in (A) and (B), respectively. Photos were taken at 200 X magnification. Scale bar=100 µm;

3.2.10 Apoptosis detection in tumor tissues

Apoptosis *in situ* was detected in paraffin embedded tumor sections based on the TdT-mediated dUTP-biotin nick end labeling (TUNEL) assay. Apoptotic cells were stained into brown colour and the healthy cells were stained green. As shown in Fig 3.16, much more apoptosis positive staining was observed in BHV injected tumor specimens. This finding indicated that BHV impaired tumor growth and disrupted tumor histology by the induction of apoptosis *in situ*.

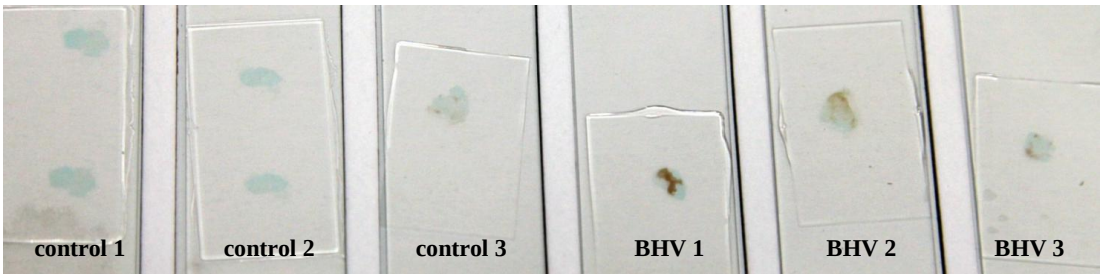

(A)

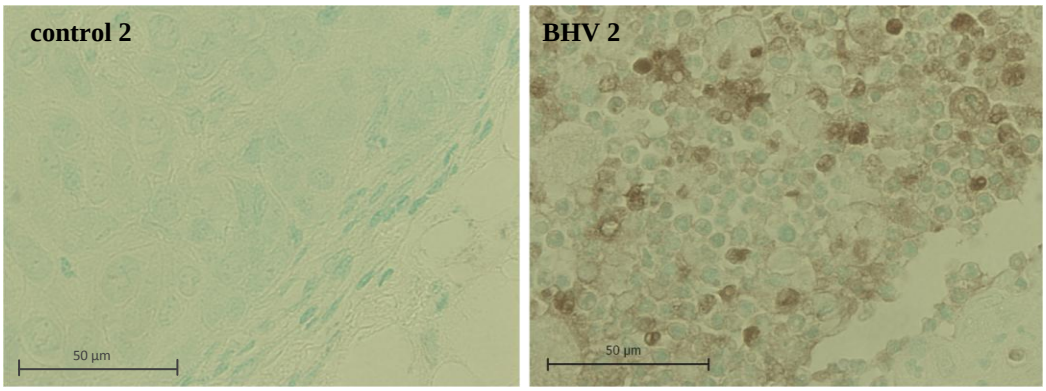

(B)

Fig 3.16 Apoptosis in situ analysis in tumor sections after BHV treatment. (A): Gross view and comparison between control and BHV treated tumor slides. (B): Magnified images showing the apoptotic cells (dark brown) after BHV treatment. Photos were taken at 400 X magnification. Scale bar= 50 µm.

3.3 Investigation of possible mechanisms of BHV anticancer actions

3.3.1 Cancer 10-pathway Reporter Array

Cignal Finder Cancer 10-Pathway Reporter Array was carried out to investigate the activity of ten important pathways in NUGC-3 cancer cells (as described in section 2.5.4). Results showed that among the ten pathways, the activity of five pathways was detected and the rest did not respond. The responsive pathways were NFκB, Myc/Max, Hypoxia, MAPK/ERK and MAPK/JNK, respectively. After BHV treatment, there was a significant decrease in the activity of MAPK/ERK pathway (p=0.02). Whereas, the other four pathways were not significantly changed.

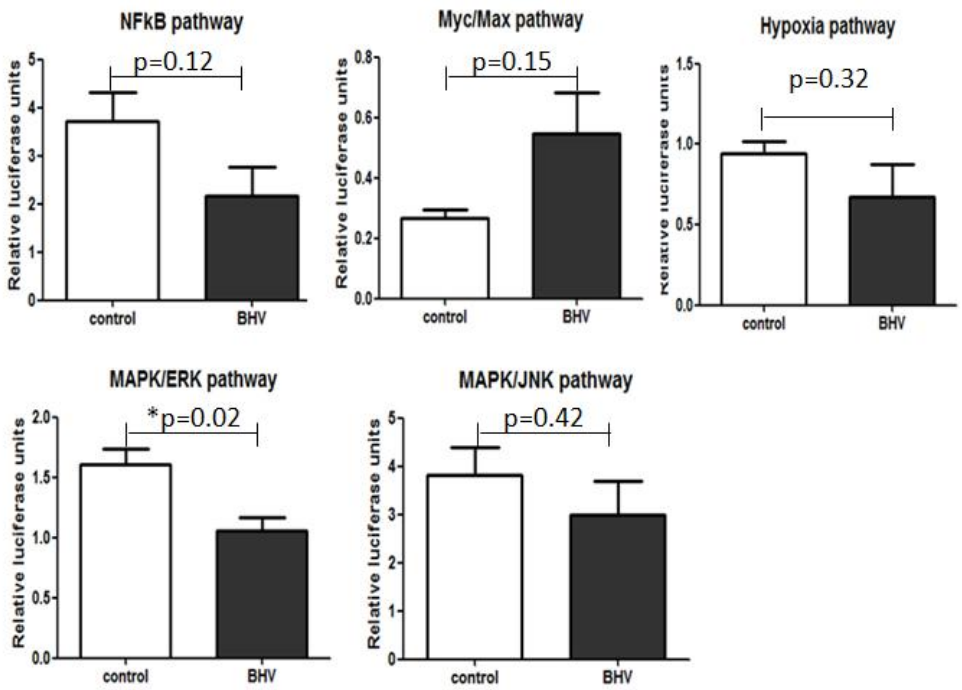

Fig 3.17 Activity of pathways in NUGC-3 cells after BHV treatment by Cancer 10-Pathway Reporter Array. Cells were treated with 20 µg/ml BHV for 24 h. Date are presented as means + SEM. N=4. *, p<0.05.

3.3.2 Expression of genes in MAPK/ERK pathway after BHV treatment

The MAPK/ERK pathway plays an important role in the regulation of cell proliferation and cell apoptosis. The expression of some selected genes in the MAPK/ERK pathway was quantified by real-time PCR. Results showed that most of the genes were down regulated after treatment with BHV, such as ERK1, ERK2, MEK1, Raf1, p70 and RSK. These results indicated the MAPK/ERK pathway was inhibited by BHV.

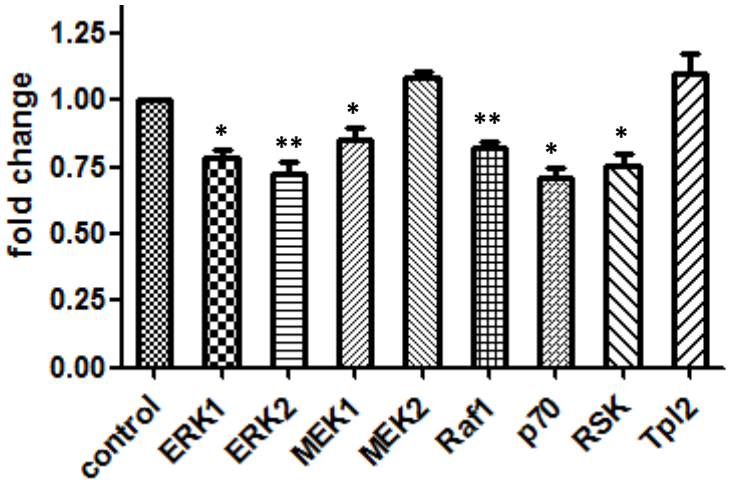

Fig 3.18 Expression of genes in MAPK/ERK pathway by reat-time PCR. NUGC-3 cells were treated with 20 µg/ml BHV for 24 h. GAPDH was used for normalization. Date are presented as means + SEM. N=3. p values were calculated based on each gene expression of untreated cells and the expression of treated cells. *, $p<0.05$. **, $p<0.01$.

3.3.3 Regulation of phosphorylated proteins in MAPK/ERK pathway by BHV treatment

The expression of phosphorylated proteins plays an critical role in the regulation of one pathway`s activity. In this study, the phosphorylated protein expression of several important regulators in MAPK/ERK pathway was validated by western blot. NUGC-3 cells were treated with 30 μg/ml BHV for 24 h and the cell lysates were collected for western blot. Results showed that most of the selected proteins were down regulated. After BHV treatment, the expression of MEK 1/2, MSK-1 and Elk-1 significantly decreased ($p<0.05$) whereas the expression of ERK 1/2 and p90RSK showed a non-significant decrease ($p>0.05$) (Fig 3.19).

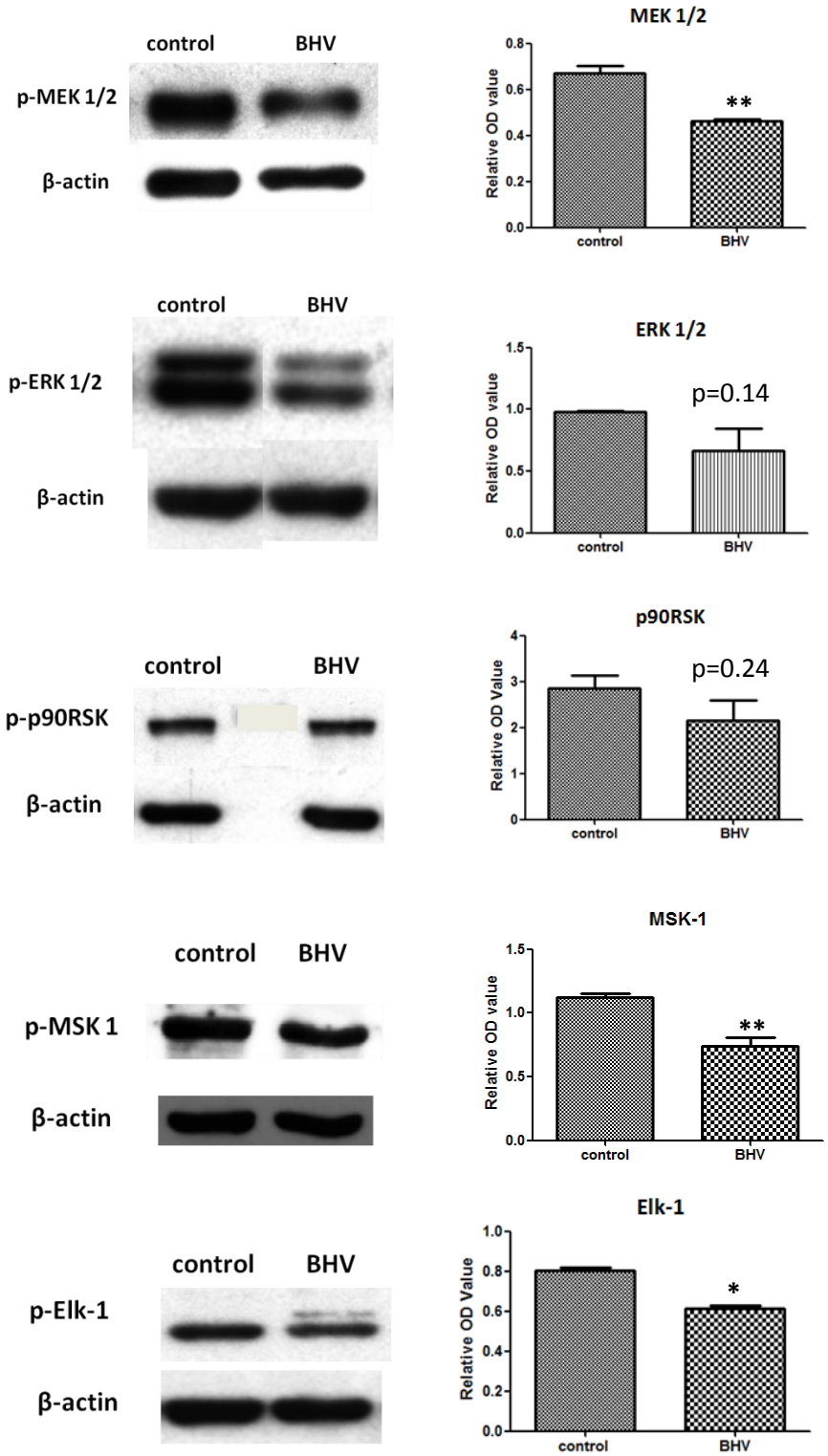

Fig 3.19 Regulation of MAPK/ERK pathway in NUGC-3 cells by BHV analyzed by western blot. NUGC-3 cells were treated with 30 µg/ml BHV for 24 h. β actin was used as loading control. Molecular mass: MEK 1/2 - 45 kDa, ERK 1/2 - 42, 44 kDa, p90RSK - 90 kDa, MSK 1 - 90 kDa, Elk-1 -47 kDa, β actin - 42 kDa. Date are presented as means + SEM. N=3. *, $p<0.05$; **, $p<0.01$.

3.3.4 Affymetrix gene microarray of NUGC-3 cells after BHV-F1 treatment

To better understand the genomic changes induced by BHV, the Affymetrix Gene Chip® Human Gene 2.0 ST Array was performed. NUGC-3 cells were treated with 5 µg/ml BHV-F1 for 24 h and the total RNA was extracted for gene chip. Based on One-Way ANOVA analysis, 140 transcription IDs were considered as differentially expressed (fold change >2 and p value <0.05). The hierarchical clustering of these transcripts is shown in Fig 3.20, which indicates the standardized gene expression level of each gene in each sample. High consistency of the gene expressions of 3 samples in the same group (control or BHV-F1 treated) was observed. Moreover, the differential expression pattern between control and BHV-F1 treated group was also outlined by different colors.

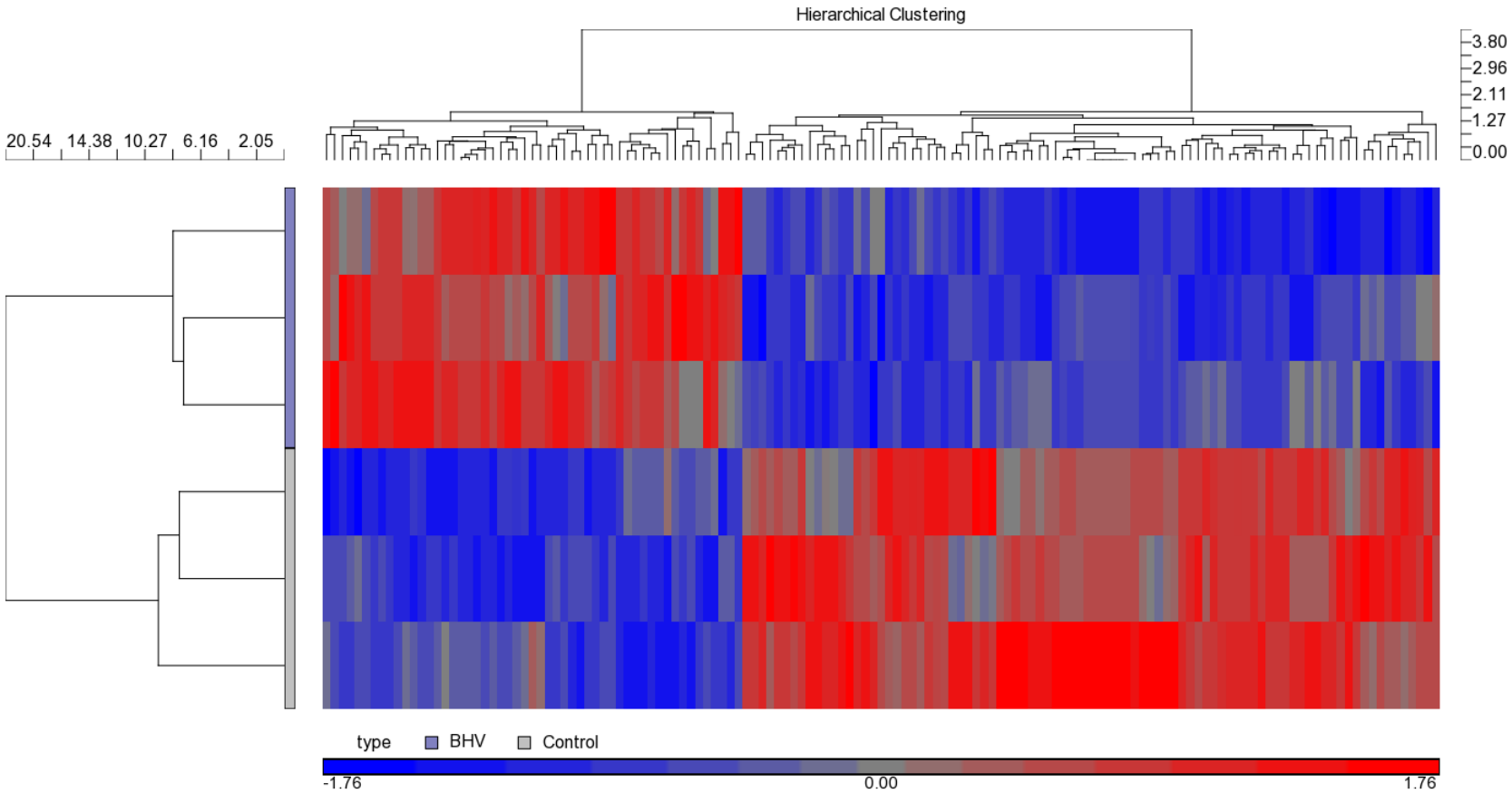

Fig 3.20 Hierarchical clustering of differentially expressed genes from microarray. The gene expression was standardized by shifting genes to mean of zero and scaling to standard deviation of one. Genes with no changes are displayed as a value of zero and colored gray. Up-regulated genes have positive values and displayed in red, whereas down-regulated genes have negative values and displayed in blue.

The microarray data were also analyzed by volcano plot to see the distribution of differentially regulated genes, as shown in Fig 3.21. The results showed that the majority of genes were not changed by BHV-F1 treatment with fold change less than two and among those genes with fold change above two, most were not significant as their p values were more than 0.05. After removing the repetitive and invalid transcription IDs, 65 genes were confirmed as differentially regulated by BHV-F1 treatment. Among these genes, 22 genes were up regulated and 43 genes were down regulated (summarized in Table 3.1).

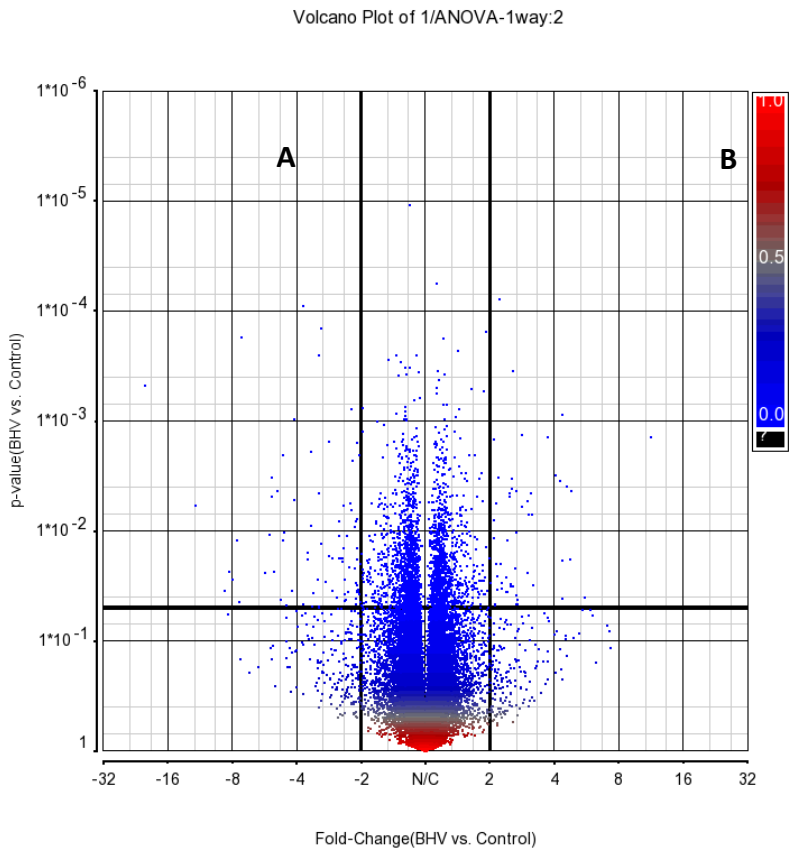

Fig 3.21 Volcano plot of microarray data. The significant genes are indicated out by one horizontal bold blace line (p=0.05) and two vertical bold black lines (fold change > 2 or < -2). The down regulated genes are distributed in zone A and up regulated genes are distributed in zone B.

Table 3.1 List of differentially expressed genes in NUGC-3 cells after BHV-F1 treatment by Affymetrix microarray.

Gene symbol	ENTREZ ID	Description	Fold change	p value
ANAPC5	51433	anaphase promoting complex subunit 5	-14.9854	0.000446
ANGPT2	285	angiopoietin 2	11.49494	0.001509
ANKRD1	27063	ankyrin repeat domain 1	-3.63879	0.018007
ANLN	54443	anillin, actin binding protein	-2.17062	0.008509
ANP32E	81611	acidic (leucine-rich) nuclear phosphoprotein 32 family, member E	-2.18441	0.02323
ASNS	440	asparagine synthetase	2.589586	0.003469
ASPM	259266	asp (abnormal spindle) homolog, microcephaly associated	-2.35799	0.026867
ATP6V1G2	534	ATPase, H+ transporting, lysosomal 13kDa, V1 subunit G2	-2.774	0.001193
BIRC3	330	baculoviral IAP repeat-containing 3	2.389077	0.027975
C6orf48	26797	chromosome 6 open reading frame 48	4.328741	0.004102
CANX	821	calnexin	-7.05307	0.011419
CBX3	11335	similar to chromobox homolog 3	-4.26086	0.004875
CHMP4C	92421	chromatin modifying protein 4C	2.04211	0.014596
COX7B	1349	cytochrome c oxidase subunit VIIb	-2.04037	0.002444
DDX5	1655	DEAD (Asp-Glu-Ala-Asp) box polypeptide 5	-4.41702	0.011417
DNAJA1	3301	DnaJ (Hsp40) homolog, subfamily A, member 1	-3.15604	0.000129
DSCC1	79075	defective in sister chromatid cohesion 1 homolog	-2.08955	0.00115
EGR1	1958	early growth response 1	4.184436	0.001438
EIF3D	8664	eukaryotic translation initiation factor 3, subunit D	-2.85451	0.04928
EIF3F	390282	eukaryotic translation initiation factor 3, subunit F	-3.11397	0.040692
EIF4G2	1982	eukaryotic translation initiation factor 4 gamma, 2	-3.9618	0.030402
ESCO1	114799	establishment of cohesion 1 homolog 1	2.130514	0.026444
FNTA	2339	farnesyltransferase, CAAX box, alpha	5.199527	0.032174
FTH1	2495	ferritin, heavy polypeptide 1	4.362973	0.003489
FTL	2512	ferritin, light polypeptide	2.400792	0.037392
GATC	283459	glutamyl-tRNA(Gln) amidotransferase, subunit C homolog	3.314797	0.027889
GDI2	2665	GDP dissociation inhibitor 2	-3.05096	0.000612
HNRNPA1	3178	heterogeneous nuclear ribonucleoprotein A1-like 3	-6.72359	0.027009
HNRNPD	3184	heterogeneous nuclear ribonucleoprotein D	-2.07645	0.035162
HNRNPK	3190	heterogeneous nuclear ribonucleoprotein K	-2.111	0.008072

HSP90AB1	3326	heat shock protein 90kDa alpha (cytosolic), class B member 1	-3.07199	0.046848
HSPA8	3312	heat shock 70kDa protein 8	-3.85441	0.000141
HSPH1	10808	heat shock 105kDa/110kDa protein 1	-2.76811	0.001413
ILF2	3608	interleukin enhancer binding factor 2, 45kDa	-10.4436	0.005072
KDM2B	84678	lysine (K)-specific demethylase 2B	-2.85705	0.007626
KYNU	8942	kynureninase (L-kynurenine hydrolase)	2.308296	0.046193
LOC285359	285359	phosducin-like 3 pseudogene	-2.93047	0.011587
LOC389765	389765	similar to KIF27C	2.159745	0.033027
LOC648771	648771	similar to 60S ribosomal protein L12	-3.69463	0.029502
NAMPT	10135	nicotinamide phosphoribosyltransferase	4.892851	0.004212
NBEAL1	65065	neurobeachin-like 1	-3.69463	0.029502
ND1	4535	NADH-ubiquinone oxidoreductase chain 1	-2.68821	0.039377
NEAT1	283131	non-protein coding RNA 84	2.997719	0.006362
NONO	4841	non-POU domain containing, octamer-binding	-6.04071	1.89E-05
PARK7	11315	Parkinson disease (autosomal recessive, early onset) 7	-7.18922	0.042892
PRPF8	10594	PRP8 pre-mRNA processing factor 8 homolog	-4.27161	0.008261
PSMB2	5690	proteasome (prosome, macropain) subunit, beta type, 2	-2.48659	0.005686
RIOK3	8780	RIO kinase 3	2.790354	0.00825
RPL10A	4736	ribosomal protein L10a	2.253678	0.016353
RPL18	6141	ribosomal protein L18	-2.57181	0.005058
RPL4	158345	ribosomal protein L4	2.673675	0.001257
SART1	9092	squamous cell carcinoma antigen recognized by T cells	-3.71279	0.001753
SART3	9733	squamous cell carcinoma antigen recognized by T cells 3	-7.01067	0.027671
SBNO1	55206	strawberry notch homolog 1	-2.03721	0.034587
SERPINB2	5055	serpin peptidase inhibitor, clade B (ovalbumin), member 2	2.747522	0.047249
SNORD18C	595098	small nucleolar RNA, C/D box 18C	2.673675	0.001257
STARD7	56910	StAR-related lipid transfer (START) domain containing 7	-2.22616	0.021743
TAF1D	684959	TATA box binding protein (TBP)-associated factor, RNA polymerase I, D,	2.086967	0.011563
TMSB4X	7114	thymosin beta 4, X-linked	-2.12485	0.027562
TNFSF15	9966	tumor necrosis factor (ligand) superfamily, member 15	2.470492	4.98E-05
TOP2A	7153	topoisomerase (DNA) II alpha 170kDa	-2.22287	0.000971
TUBB	203068	tubulin, beta;	-2.15314	0.027179
UBE2L1	7330	ubiquitin-conjugating enzyme E2L 1	-2.27259	0.038651
ZFAS1	441951	ZNFX1 antisense RNA 1	-2.62715	0.003335
ZNF146	7705	zinc finger protein 146	-2.31987	0.018035

The functional classification was accomplished using DAVID functional annotation clustering analysis. These genes were involved in different biological processes including cell cycle, cell apoptosis, membrane organization, cytoskeleton, stress response, DNA repair, oxidation reduction and so on (Table 3.2).

Table 3.2 Functional classification of differentially expressed genes from Affymetrix microarray

Biological processes	Related genes
cell cycle	ANAPC5, ANLN, ASPM, DSCC1, EIF4G2, PSMB2, SART1, TUBB, ESCO1
cell apoptosis	SART1, TOP2A, TUBB, ASNS, BRIC3, FNTA, SERPINB2, TNFSF15, LOC285359
cytoskeleton	ANLN, ASPM, FNTA, CBX3, TMSB4X, TOP2A, TUBB
stress response	HSPH1, HSPA8, HSP90AB1
DNA repair	NONO1, TOP2A, ESCO1
Oxidation reduction	ND1, FTH1, KDM2B, FTL
membrane organization	HSPA8, FTH1, FTL

3.3.5 Validation of apoptosis related genes by real-time PCR

Considering the importance of cell apoptosis induced by BHV in functional studies, real-time PCR was performed to verify the reliability of results of apoptosis related genes obtained from microarray. It was found that the expression of all 8 genes by real-time PCR was in concordance with the microarray data and more up-regulation of ASNS and TNFSF15 was observed (Fig 3.22).

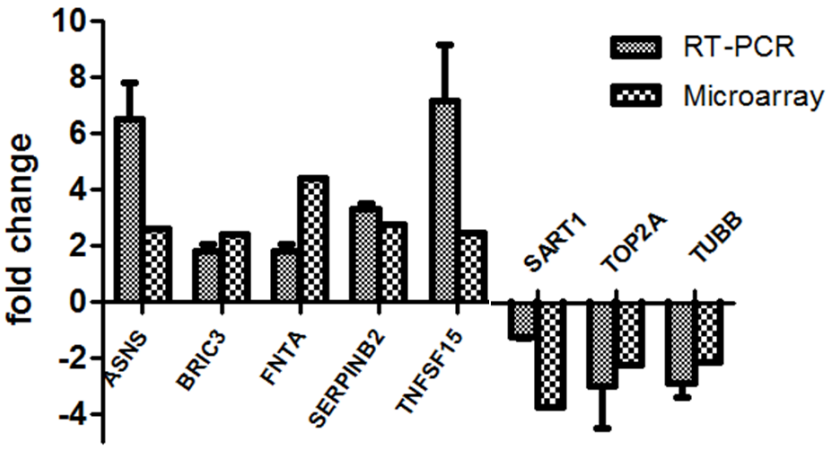

Fig 3.22 Validation of apoptosis related genes from microarray data by real-time PCR. NUGC-3 cells were treated with 5 µg/ml BHV-F1 for 24 h. The RNA samples were as the same as those sent for cDNA microarray. GAPDH was used for normalization. Date are presented as means + SEM. N=3.

3.4 Purification and characterization of the antitumoral agent in BHV

3.4.1 Characterization of crude BHV by SDS-PAGE

The lyophilized crude BHV was dissolved in 1 x PBS and protein concentration was measured with Bradford method, with finding that the proteins accounted for 60% of the total weight of the crude venom. The 10% SDS-PAGE results verified the molecular mass distribution of crude BHV (Fig 3.23). More than 10 bands were separated on the gel with a wide range of M.W., which included small peptides (5~15 kDa), medium size proteins (15~55 kDa) and high M.W. proteins (55~130 kDa).

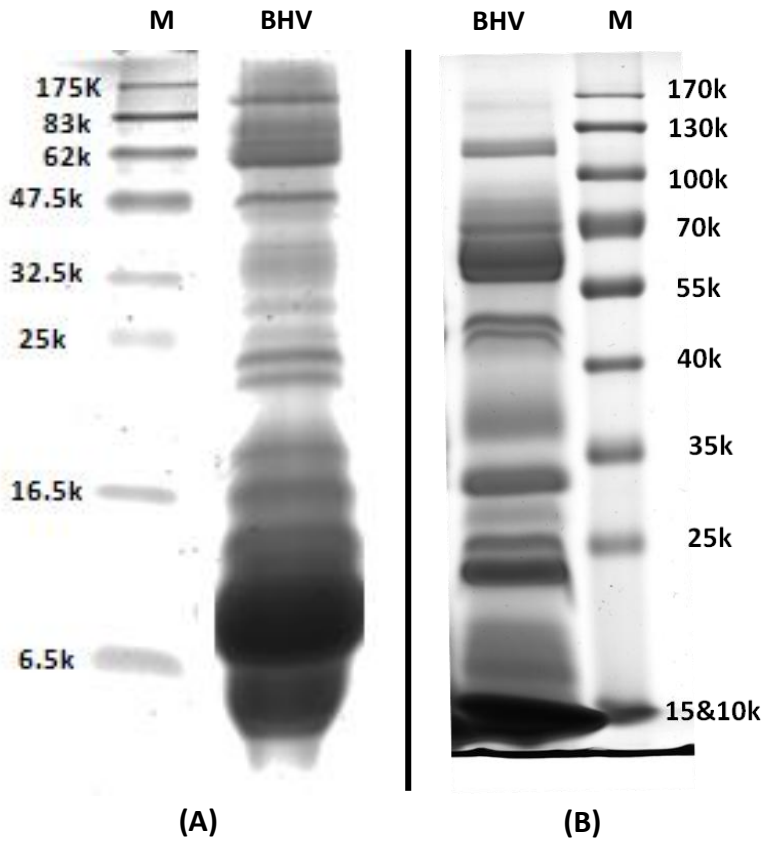

Fig 3.23 10% SDS-PAGE pattern of crude BHV in two different separation conditions. 30 µg crude venom was loaded and M.W. unit is Da.
(A): shorter time running with focus on low M.W. protein separation. Bio-Rad protein ladder was used as standard. (B): longer time running with focus on high M.W. protein separation. PageRuler protein ladder was used as standard.

3.4.2 Size exclusive gel filtration chromatography and SDS-PAGE of fractions

Superdex G75 gel filtration column was used to perform the preliminary separation of crude BHV. Five fractions were obtained, named F1 to F5, respectively (Fig 3.24). Among which, F2 was the most abundant and F5 had the fewest contents. All fractions were collected and lyophilized and each fraction was characterized by SDS-PAGE (Fig 3.25). Results showed that F1 mainly contained high M.W. proteins (>32.5 kDa) with few small bands as well. F2 contained wide range of small and medium proteins (5~32.5 kDa). F3 and F4 contained small peptides around 10 kDa.

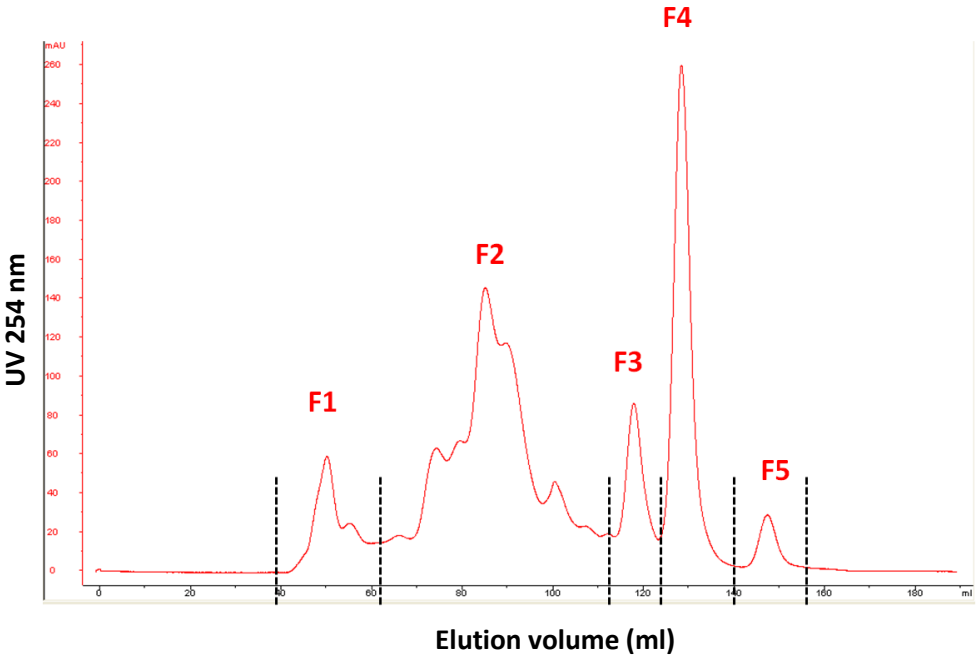

Fig 3.24 Superdex G75 gel filtration chromatography of crude BHV.
100 µg crude venom was loaded each time. Fractions were eluted with 50 mM ammonium bicarbonate, pH=8.0, at a flow rate of 1 mL/min. Five fractions (F1-F5) were separated as shown with dash lines.

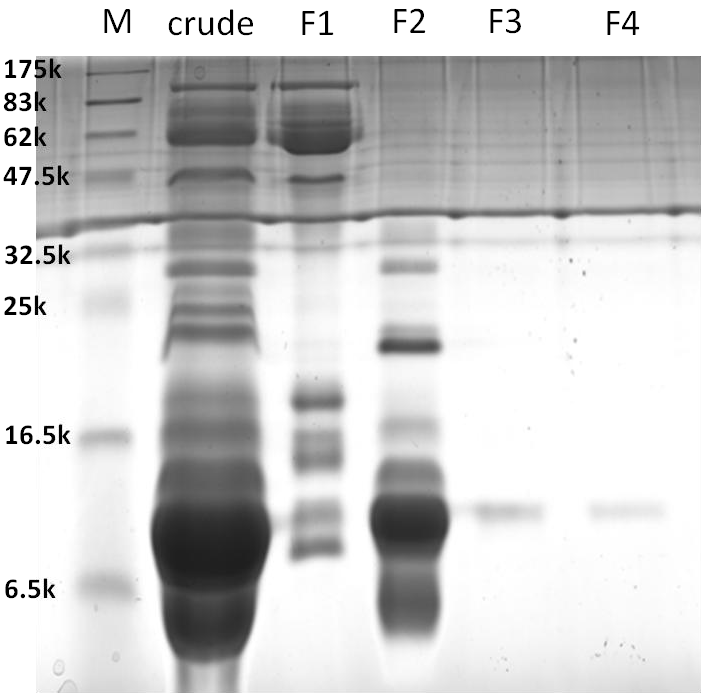

Fig 3.25 10% SDS-PAGE profile of gel filtration fractions. For crude BHV, F1 and F2, 30 µg protein was loaded. For F3 and F4, 2 µg protein was loaded. F5 contained too low protein and was not applied in this experiment.

3.4.3 Test of the inhibition effect of each fraction to NUGC-3 cell viability

To find out which fraction has the anticancer effect and contain the cytotoxic protein, NUGC-3 cell viability study was performed after treatment with each fraction (10 µg/ml). The results showed that F1 almost killed all NUGC-3 cells with viability reduction more than 90%. F2 and F3`s inhibition effect was also significant but were negligible compared with F1`s effect (Fig 3.26-A). Therefore, the cytotoxic protein was confirmed to be located in F1, which deserved further investigations. To verify this finding, different concentration of F1 was applied and a corresponding cell viability inhibition was observed (Fig 3.26-B) with calculated IC 50 around 3 µg/ml.

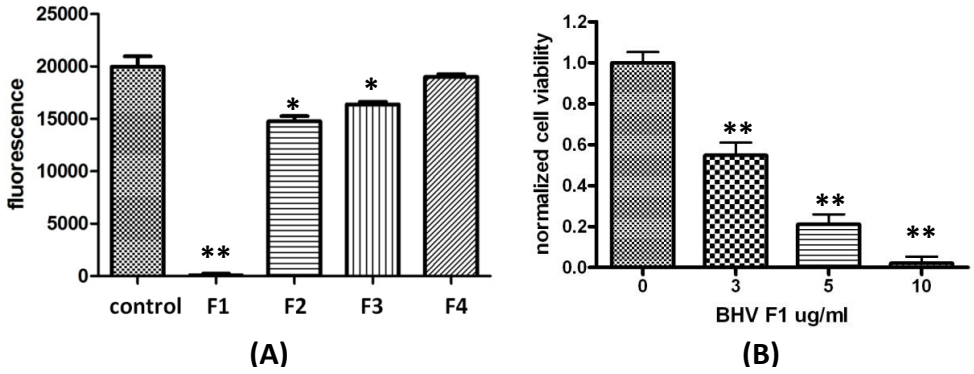

Fig 3.26 NUGC-3 cell viability assay after treatment with gel filtration fractions. (A): NUGC-3 cell viability study after treatment with each fraction after gel filtration (10 µg/ml for 24 h). (B): NUGC-3 cell viability study after treatment with different concentrations of F1 for 24 h. Data are presented as means + SEM. N=3. *, $p<0.05$; **, $p < 0.01$.

3.4.4 Cation exchange chromatography, SDS-PAGE and cell viability test

BHV-F1 was further separated with UNO S1 cation exchange chromatography column (Bio-Rad). A liner NaCl gradient elution resolved the BHV-F1 into another 5 peaks, named BHV-F1-A to BHV-F1-E, respectively (Fig 3.27). BHV-F1-A was the unbound fraction and the rest peaks were eluted fractions. Similarly, 10% SDS-PAGE was performed to characterize protein M.W. distribution in each peak (Fig 3.28) and the inhibition effect of each fraction to NUGC-3 cell viability was examined by alamarBlue assay. Results showed that among all 5 fractions, both fraction 3 and 4 decreased cell viability of NUGC-3 cells, indicating that the targeted proteins were in both fractions (Fig 3.29). This was possibly because BHV-F1-C and BHV-F1-D were not completely separated and there was overlap as shown in the chromatogram.

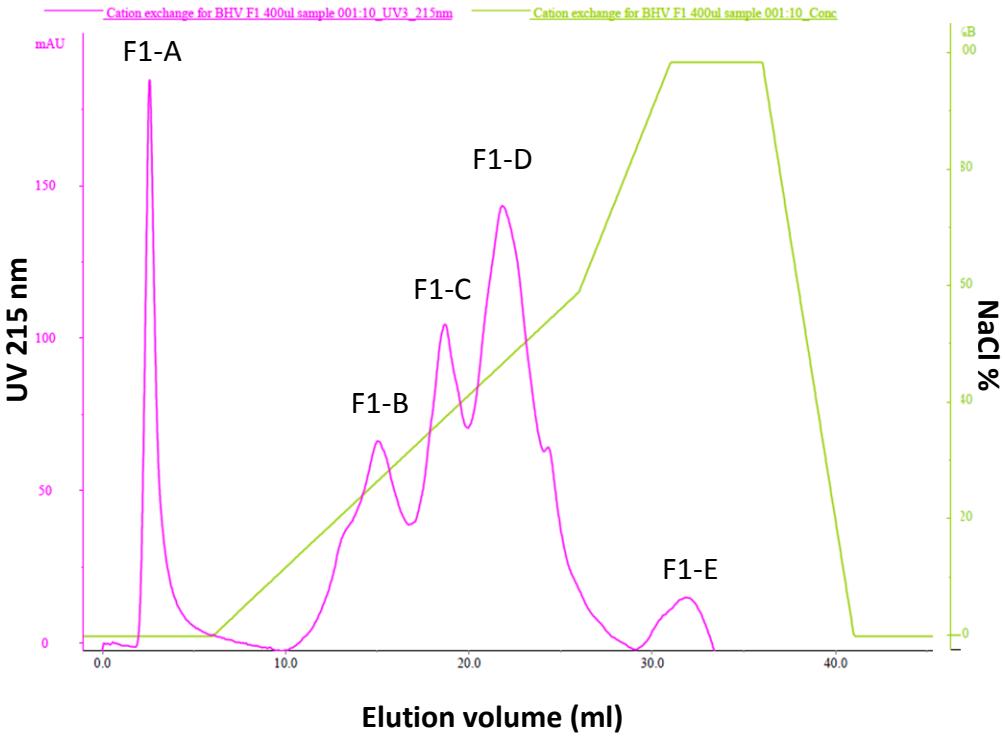

Fig 3.27 UNO S1 cation exchange chromatogram of BHV-F1. BHV-F1 was lyophilized and re-dissolved in starting buffer (50 mM sodium acetate, pH 5.0). The column was equilibrated with starting buffer and the elution was achieved with a liner gradient of 1 M NaCl.

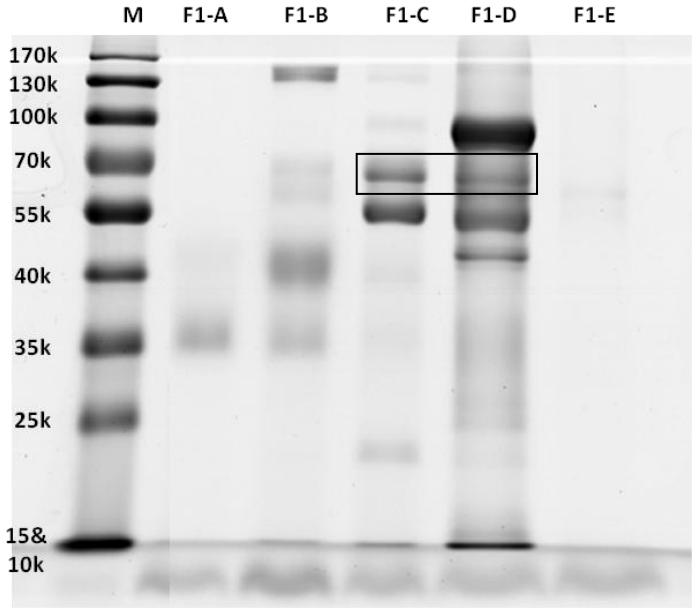

Fig 3.28 10% SDS-PAGE profile of fractions after BHV-F1 separation.
20 µl of each fraction was loaded. Protein concentration: F1-A, 0.04 µg/ml; F1-B, 0.31 µg/ml; F1-C, 0.31 µg/ml; F1-D, 0.88 µg/ml; F1-E, 0.04 µg/ml;

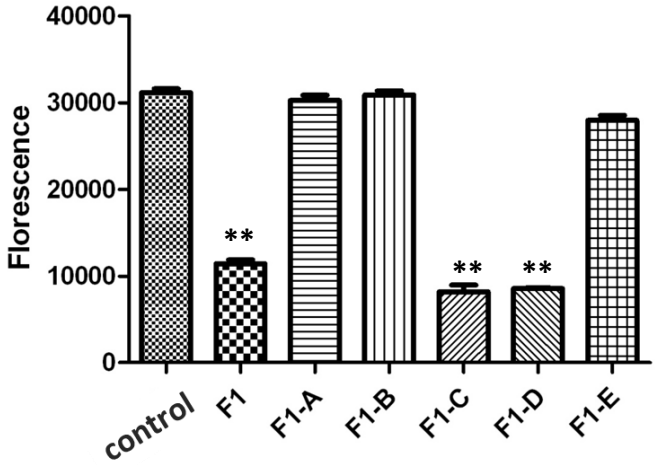

Fig 3.29 NUGC-3 cell viability assay after treatment with fractions after cation exchange chromatography. 10 µl of each fraction was added to 100 ul cell medium and treatment time was 24 h. Protein concentration: F1-A, 0.04 µg/ml; F1-B, 0.31 µg/ml; F1-C, 0.31 µg/ml; F1-D, 0.88 µg/ml; F1-E, 0.04 µg/ml; Data are presented as means + SEM. N=3. **, $p < 0.01$.

3.4.5 Preliminary protein identification results with MALDI-TOF-Mass Spectrometry

Based on the information from SDS-PAGE (Fig 3.28), several suspected bands were cut down from the gel and sent for MALDI-TOF-MS/MS analysis to identify the protein, including a mixed protein band from BHV-F1 named F1-a, two bands from BHV-F1-C named F1-C-a and F1-C-b, and one band from BHV-F1-D, named F1-D-a (Fig 3.30). Mass spectrometry results showed that F1-a contained 3 types of protein, which were Coagulation factor X-activating enzyme heavy chain, Acetylcholinesterase and L-amino acid oxidase. Consistently, the individual band protein identification results indicated that F1-C-a was Acetylcholinesterase, F1-C-b was L-amino acid oxidase and F1-D-a was Coagulation factor X-activating enzyme heavy chain. From the literature review, the L-amino acid oxidase was reported to possess anticancer effect and became our research interest for further study. The mass spectrum of F1-C-b and the protein identification report was shown in (Fig 3.31 and 3.32).

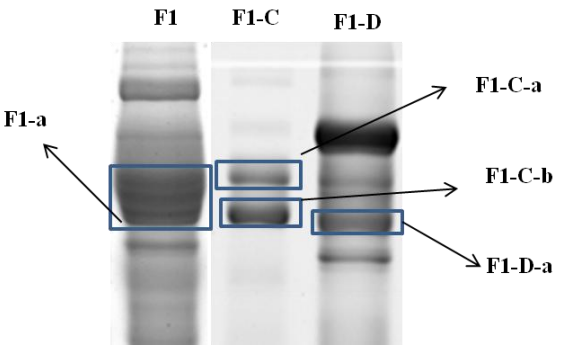

Fig 3.30 Indication of the bands that were cut from PAGE gel for mass spectrometry analysis. The bands cut down from each lane were indicated with rectangles and labelled with the name following arrow`s direction.

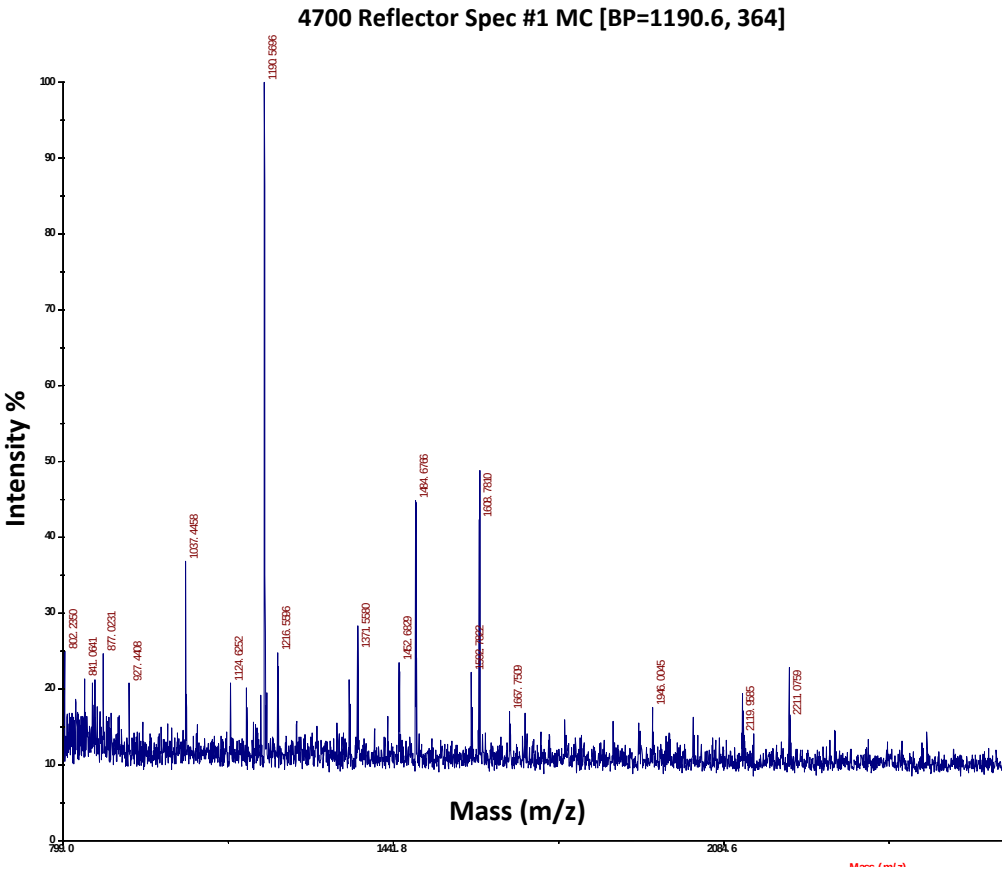

Fig 3.31 Mass spectrum of F1-C-b band

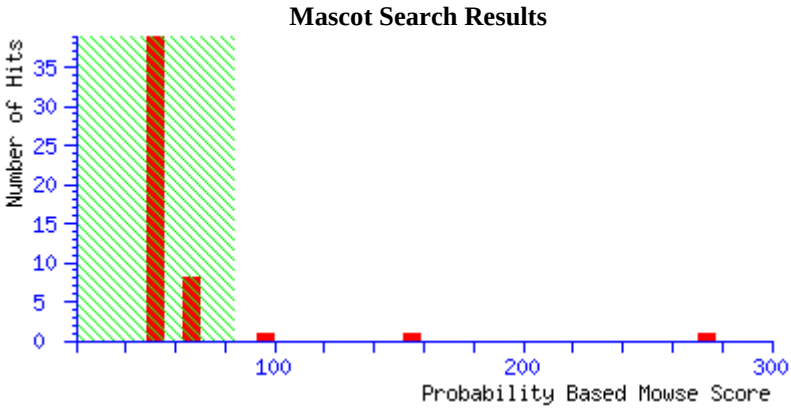

Index

	Accession	Mass	Score	Description
1.	gi|126035649	59116	274	L-amino acid oxidase [Bungarus multicinctus]
2.	gi|123916680	59374	159	RecName: Full=L-amino-acid oxidase; Short=LAAO; Short=LAO; Flags: Precursor
3.	gi|126035653	59069	100	L-amino acid oxidase [Bungarus fasciatus]

Fig 3.32 Probability Based Mowse Score and protein summary report. Ions score is -10*Log(P), where P is the probability that the observed match is a random event. Protein scores greater than 83 are significant (p<0.05).

3.4.6 Detection of LAAO enzymatic activity in crude BHV and BHV-fractions

As the results from mass spectrometry and protein ID blast can only putatively identify the protein, the enzymatic activity test was performed to double confirm that the anticancer protein was LAAO. LAAO can oxidaze L-leucine and form hydrogen peroxide, which can be degraded by horseradish peroxidase (HRP) and produce the absorbance at 490 nm. The results are shown in Fig 3.33. The LAAO enzymatic activity was observed in crude BHV, fraction 1 after gel filtration and BHV-F1-C after BHV-F1 cation exchange separation. Such findings firmly prove that the anticancer protein was LAAO.

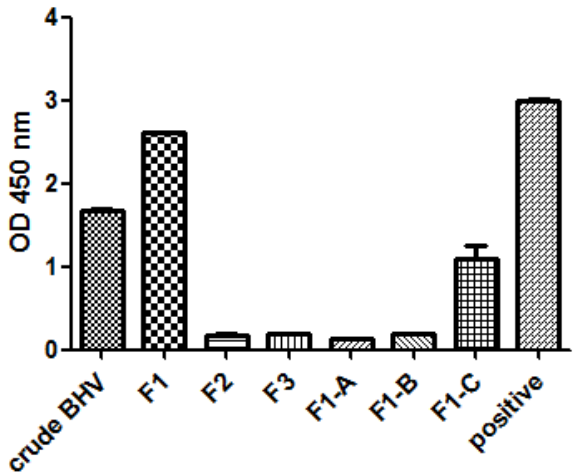

Fig 3.33 LAAO enzymatic activity assay in BHV fractions. 10 µl of samples mixed in 90 µl 50mM Tris-Hcl buffer (pH 8.0) containing 5 mM L-leucine, 2 mM o-Phenylenediamine and 2.5 unit HRP. Reaction mixture was incubated at 37 °C for 1h and terminated by adding 50 µL 2 M H2SO4. Absorbance was read at 450 nm. N=2 for F1 and F1-C; N=3 for the rest

3.5 Investigating the anticancer effects of L amino acid oxidase (LAAO) in gastric cancer

3.5.1 LAAO`s inhibition to cell viability/proliferation of gastric and breast cancer cell lines

Because of the non-availability of LAAO from scorpion venom, LAAO purified from *Crotalus adamanteus* snake venom was used in the following studies. Firstly, its effect on the viability/proliferation of gastric cancer cells (MKN-74, MKN-7, NUGC-3) was analyzed, with results showing that LAAO decreased the cell viability dose dependently. Moreover, an extended study using breast cancer cells (MDA-MB-231, T-47D, MCF-7) and normal breast cells (MCF12A) was also done, showing that LAAO induced more reduction of cancer cell viability, compared with normal cells.

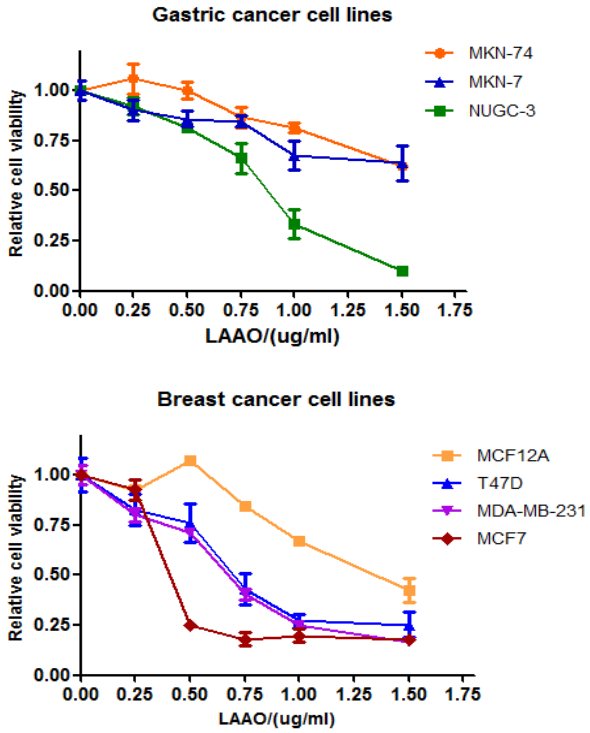

Fig 3.34 AlamarBlue cell viability/proliferation assay of gastric and breast cancer cells after treatment with LAAO for 24 h. Data are presented as means + SEM. N=3.

3.5.2 LAAO cytotoxicity to NUGC-3 cells by LDH assay

The cytotoxicity of LAAO to NUGC-3 cells was evaluated by LDH assay. Results showed that more than 0.5 µg/ml LAAO induced a significant increase of LDH release from cytoplasm to culture medium, which indicated that the plasma membrane had lost its integrity. The cytotoxicity was up to 53.4% for 1.5 µg/ml LAAO treatment.

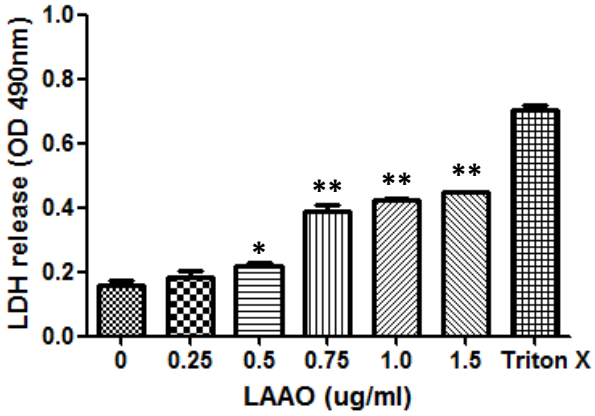

Fig 3.35 LAAO cytotoxicity to NUGC-3 cells by LDH assay. Cells were treated for 24 h. 2% (w/v) Triton X was used as positive control. Data are presented as means + SEM. N=3. *, $p < 0.05$; **, $p<0.01$.

3.5.3 NUGC-3 cell cycle profile after treatment with LAAO

LAAO`s effect on NUGC-3 cell cycle was examined by flow cytometry after fixing and staining with PI. NUGC-3 cells were treated with 1.0 µg/ml and 1.5 µg/ml LAAO for 24 h. Results showed that LAAO treatment induced a percentage increase in G2/M phase (27.3% vs 34.8% vs 38.5%) and a percentage decrease in G1 phase (51.1% vs 42.5% vs 37.5%), indicating a G2/M cell cycle arrest (Fig 3.36). However, no sub-G1 peak was observed for LAAO treatment.

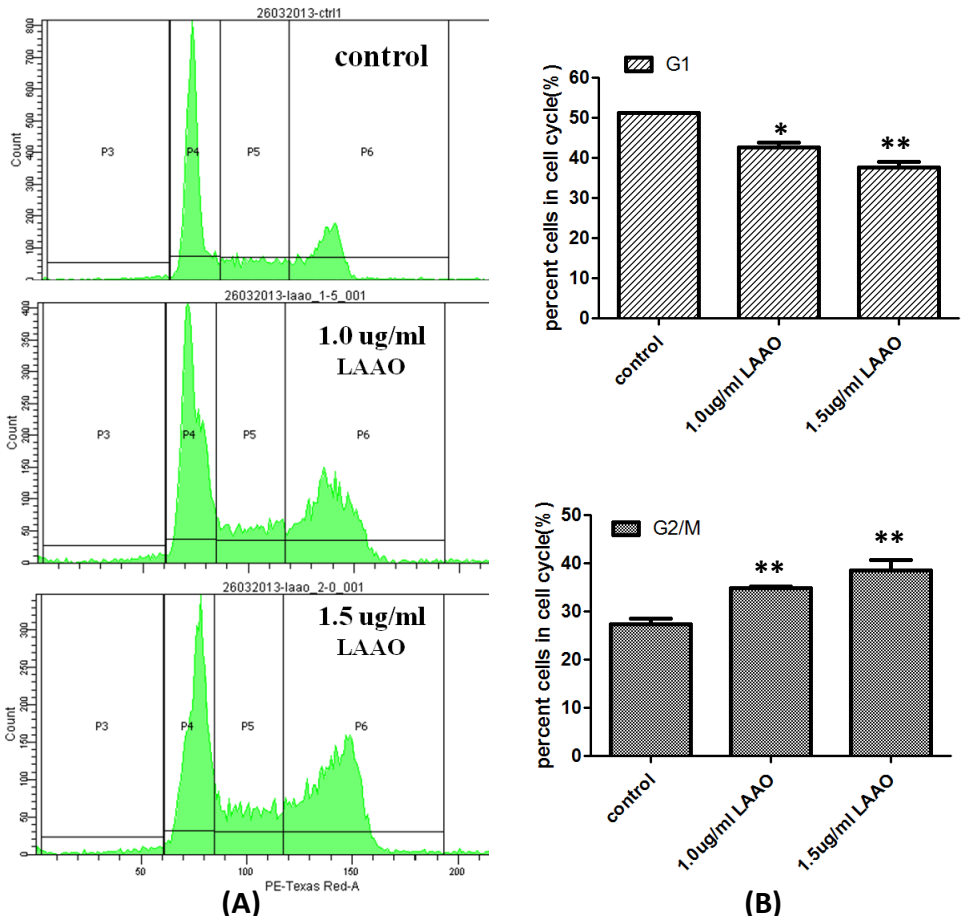

Fig 3.36 LAAO treatment induced the changes of NUGC-3 cell cycle profile (A): Representative images of NUGC-3 cell cycle profiles. P3, P4, P5 and P6 indicate sub-G1, G1, S and G2/M phase, respectively. (B): Cell fractions in different cell cycle phases. Data are presented as means + SEM. N=3. *, $p < 0.05$; **, $p < 0.01$.

3.5.4 NUGC-3 cell apoptosis analysis after treatment with LAAO

The apoptosis induced by LAAO treatment was confirmed and quantified by flow cytometry analysis after staining with Annexin-V-FITC and PI. NUGC-3 cells were treated with 1.0 µg/ml LAAO for 12 h prior to staining with Annexin-V-FITC and PI. Compared with untreated cells, LAAO treatment induced both early apoptosis (2.8% vs 8.1%) and late apoptosis (5.8% vs 44.6%) of NUGC-3 cells (Fig 3.37).

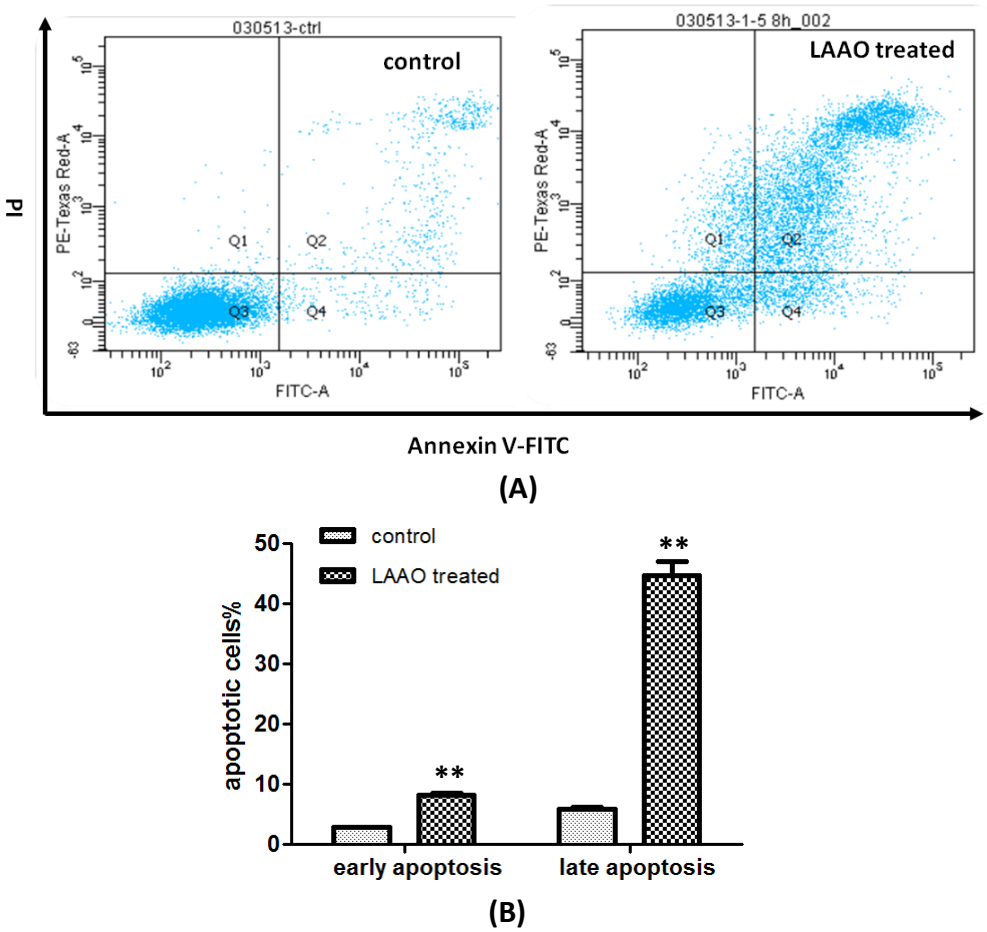

Fig 3.37 Flow cytometry analysis of NUGC-3 cell apoptosis with LAAO treatment. (A): Representative profiles of Annexin-V-FITC and PI signals from flow cytometry. Q4 (Annexin-V positive/PI negative) indicates early apoptosis; Q2 (Annexin-V positive/PI positive) indicates late apoptosis. (B): Bar chart of the percentage of cells undergoing early and late apoptosis, respectively. Data are presented as means + SEM. N=3. **, $p < 0.01$.

3.5.5 Morphological changes induced by LAAO treatment in NUGC-3 cells

In order to detect the morphological changes of NUGC-3 induced by LAAO treatment, with special attention on early characteristics, cells were treated with 1.0 μg/ml LAAO for 12 h. Different approaches were taken to investigate both extracellular and intracellular structure changes, including fluorescence light microscopy, transmission electron microscopy and scanning electron microscopy.

Fluorescence microscopy:

Fig 3.38 reveals the morphological changes of NUGC-3 cells after LAAO treatment under fluorescence light microscope with AO/EB staining. Such changes included nuclear condensation, membrane blebbing and the loss of membrane integrity.

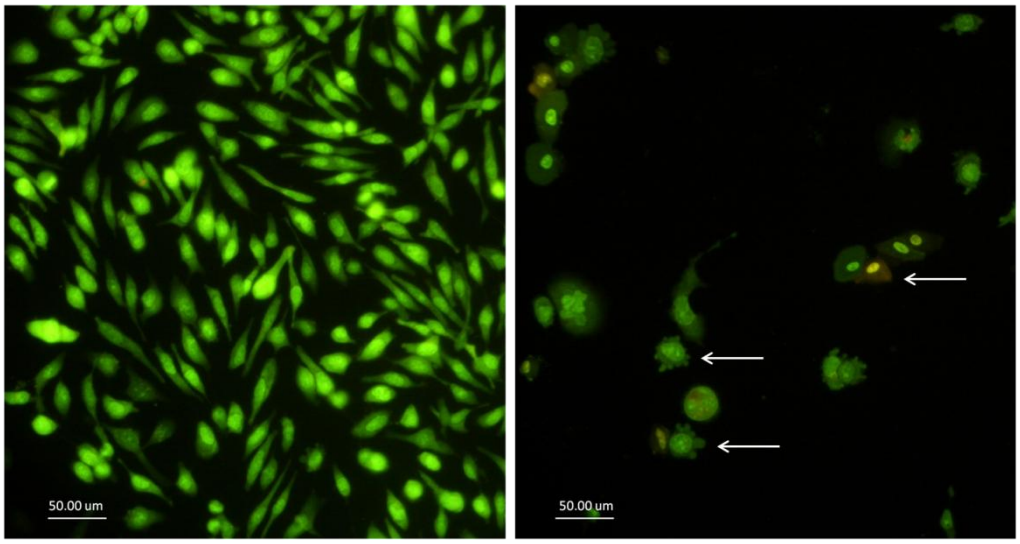

(A) **(B)**

Fig 3.38 NUGC-3 morphological changes after LAAO treatment by AO-EB staining. Photos were taken at 200 X magnification. (A): control; (B): LAAO treated. Arrows indicate apoptotic features such as membrane blebs and nuclear condensation

Scanning electron microscopy (SEM):

SEM was applied to visualize NUGC-3 cell surface structures. As shown in Fig 3.39, the untreated cell had fusiform shape with smooth surface and lots of small contacts. In contrast, after treatment with LAAO, cell became irregularly round and small membrane blebs were formed.

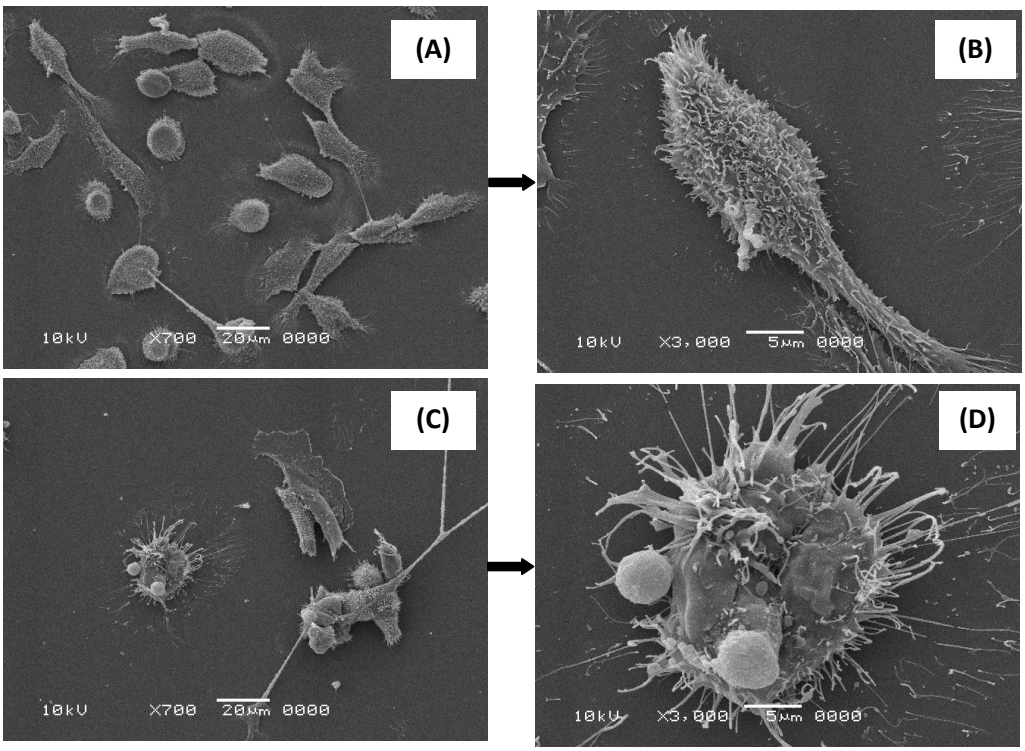

Fig 3.39 Morphological changes of NUGC-3 cells after LAAO treatment under SEM.(A): untreated NUGC-3 cells. (B): a magnified image of the rectangle-framed cell in (A). (C): NUGC-3 cells treated with 1.0 µg/ml LAAO for 12 h. (D): a magnified image of the rectangle-framed cell in (C). Scale bar is 20 µm for (A) and (C), 5 µm for (B) and (D).

Transmission electron microscopy (TEM):

The nuclear and cytoplasmic structure changes induced by LAAO treatment were identified by TEM. For untreated cell, nuclear and cytoplasm integrity was well maintained with loosed chromatins and organelle structures. After treatment with LAAO, obvious chromatin condensation and cytoplasmic vacuoles were visualized (Fig 3.40).

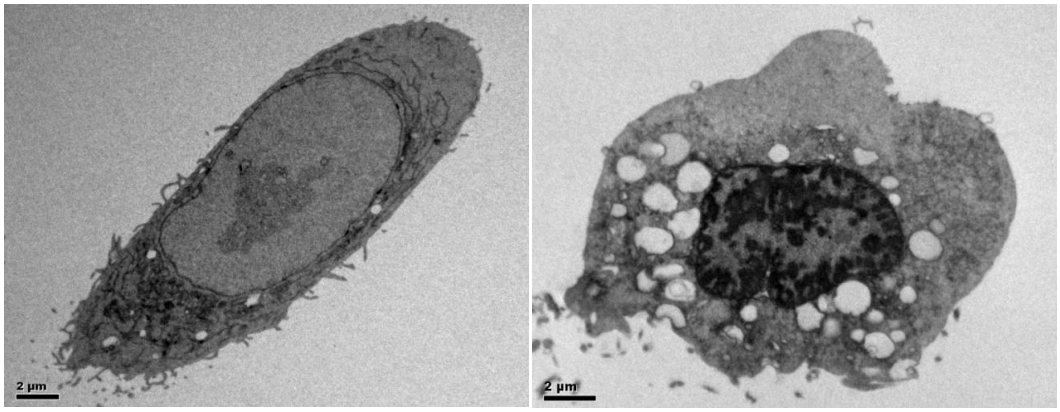

(A) **(B)**

Fig 3.40 NUGC-3 morphological changes after LAAO treatment under TEM (A): untreated NUGC-3 cell. (B): NUGC-3 cells treated with 1.0 µg/ml LAAO for 12 h. Scale bar is 2 µm.

3.5.6 Detection of caspase activation after LAAO treatment

Similar approaches were taken to detect the caspase activation after LAAO treatment. In the western blot, a very faint cleaved band was observed for PARP and caspase-3 in both control and LAAO treated groups. There was no increase in caspase-3 activity in the substrate colourmetric assay (p=0.248) and the pre-treatment with pan-caspase inhibitor z-VAD-fmk did not change the pattern of NUGC-3 cell viability with LAAO treatment (p=0.93 by Two-way ANOVA) (Fig 3.41). All these findings were consistent with BHV work and indicated that LAAO also induced a caspase independent apoptosis in NUGC-3 cells.

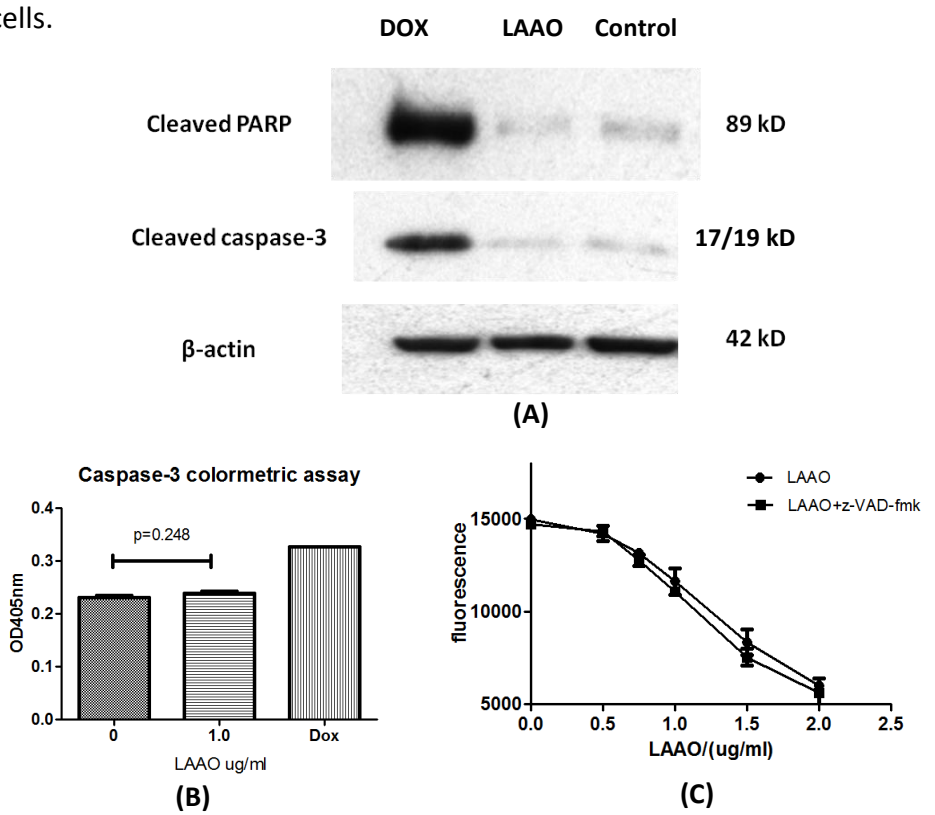

Fig 3.41 Confirmation of caspase independent apoptosis induced by LAAO treatment. (A): western blot of cleaved PARP and caspase-3. β-actin was used to normalized the protein loading. Cells were treated with 1.0 µg/ml LAAO or 25 µM doxorubicin (Dox) for 24 h. Data were representative of two replicates. (B): caspase-3 activity assay. NUGC-3 cells were treated with 1.0 µg/ml BHV for 24 h. Dox, 25 µM doxorubicin as positive control. (C): NUGC-3 cell viability study after treatment with different concentration of LAAO. LAAO+z-VAD-fmk indicates cells were pre-treated with 50 µM z-VAD-fmk for 1 h prior to the administration of LAAO. Data are presented as means + SEM. N=3.

3.5.7 Translocation of apoptosis inducing factor induced by LAAO

Some studies have revealed that caspase independent cell apoptosis could be induced by other factors such as apoptosis inducing factor (AIF), Endonuclease G (Endo G) and apoptotic protease activating factor-1 (Apaf-1) (Tait *et al.*, 2008). The translocation of AIF from mitochondria to nucleus has been reported to play an important role in caspase independent apoptosis. Therefore, in this study, the role of AIF in LAAO induced caspase independent apoptosis of NUGC-3 cells was investigated by immunofluorescence. Shown in Fig 3.42, in untreated NUGC-3 cells, there was no overlap between AIF-Cy5 labelling and DAPI labelling, which indicated that AIF localized in the cytoplasm not in nucleus. In contrast, after treatment with LAAO, the purple merged colour was observed, suggesting the translocation of AIF from cytoplasm (mitochondria) to nucleus.

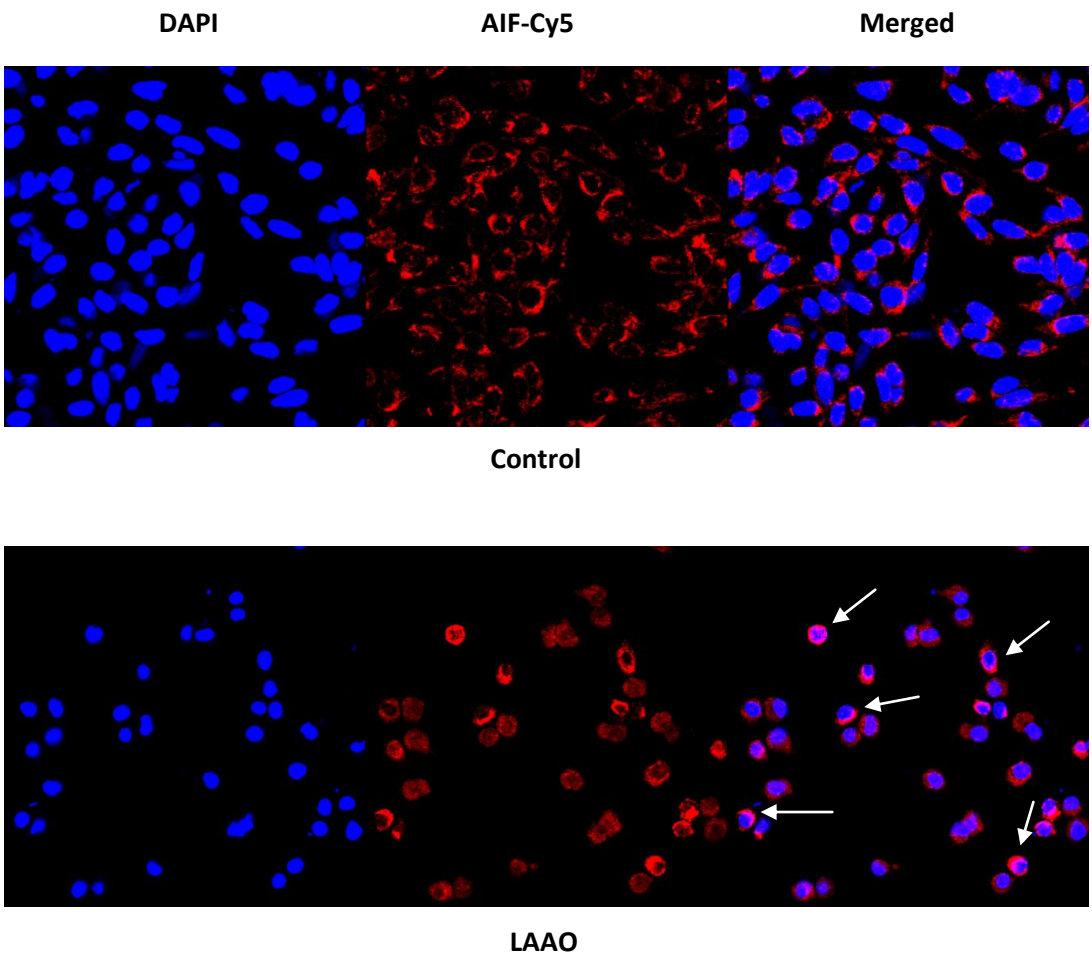

Fig 3.42 Immunofluorescence staining of NUGC-3 cells after LAAO treatment. Cells were treated with 1.0 µg/ml LAAO for 12 h. Photos were taken at 200 X manification. AIF antibody dilution was 1:200 and Cy5-conjugated anti-rabbit IgG dilution was 1:500. Arrows indicate the AIF translocation of AIF from cytoplasm to nucleus.

3.5.8 Loss of mitochondrial membrane potential of NUGC-3 cells after LAAO treatment

Since the translocation of AIF was observed, it was hypothesized that the mitochondria function may also be impaired by LAAO. Thus, the mitochondrial membrane potential (MMP) was measured by JC-1 staining. Shown in Fig 3.43, there was an increase in the JC-1 green fluorescence signal after LAAO treatment, which indicated an increasing percentage of NUGC-3 cells that lost MMP and became depolarized. After 9 h of LAAO treatment, more than 90 percent of NUGC-3 cells had lost the MMP.

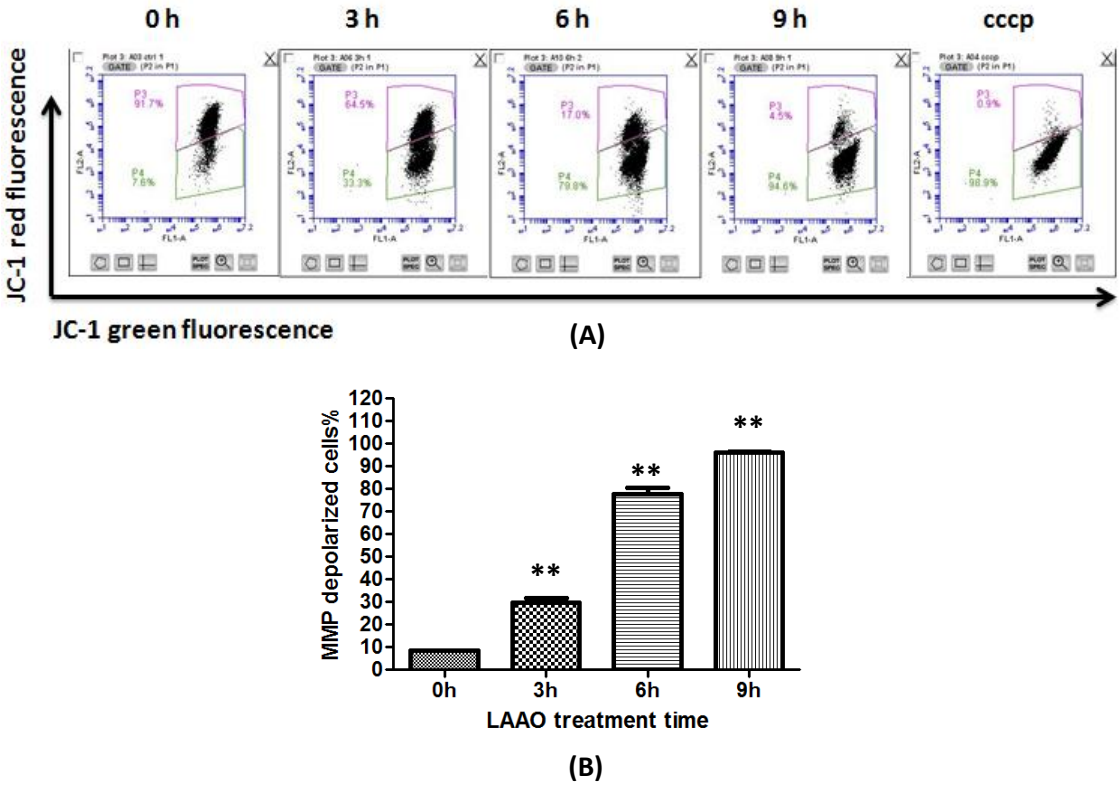

Fig 3.43 Flow cytometry analysis of NUGC-3 cells with JC-1 staining
Cells were treated with 1.0 µg/ml LAAO for 0 h, 3 h, 6 h and 9 h respectively. cccp, carbonyl cyanide m-chlorophenylhydrazone was used as positive control. (A): Representative images of flow cytometry analysis of JC-1 fluorescence. P3 indicates JC-1 red fluorescence and P4 indicates JC-1 green fluorescence. (B): Bar chart of the percentage of MMP depolarized cells (P4). Data are presented as means + SEM. N=3. **, $p < 0.01$.

3.5.9 Measurement of NUGC-3 oxidative stress induced by LAAO

NUGC-3 intracellular oxidative stress was measured by flow cytometry after staining with DCF-DA, the indicator of reactive oxygen species (ROS). Results showed that there was a significant increase in intracellular oxidative level after 3 h of LAAO treatment. However, the DCF signal decreased to the baseline at 6 h time point. This could be because that after 6 h of LAAO treatment, NUGC-3 cells had lost the plasma membrane integrity and the DCF dye has leaked out. This result suggested that LAAO treatment increased the intracellular oxidative stress of NUGC-3 cells.

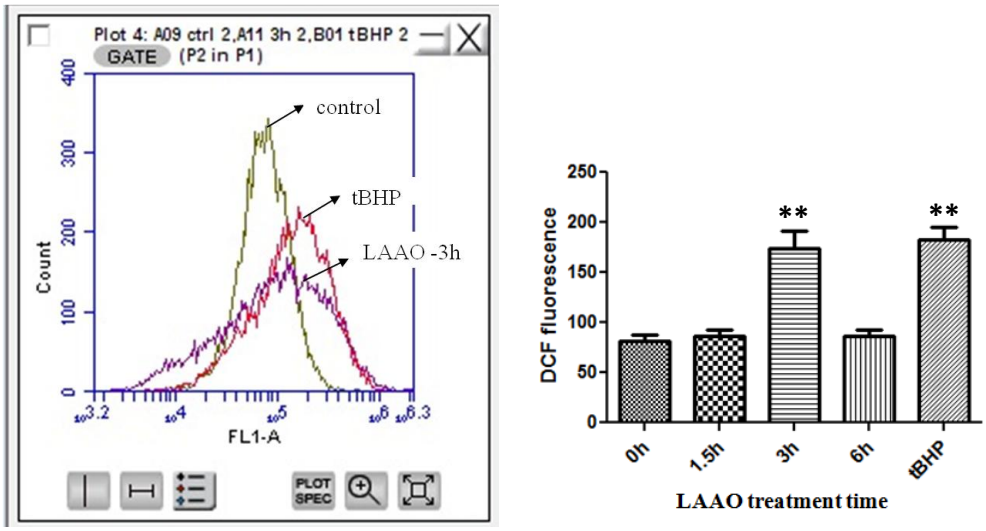

(A) (B)

Fig 3.44 Flow cytometry analysis of NUGC-3 cells stained with DCF-DA
Cells were treated with 0.5 μg/ml LAAO for 0 h, 1.5 h, 3 h and 6 h, respectively. tBHP, tert-butyl hydroperoxide, was used as positive control. (A): Representative images of flow cytometry analysis of DCF fluorescence (FL1-A, 480 nm). The increase shift of DCF peaks was indicated. (B): Bar chart of DCF fluorescence of sample with different treatment time. Data are presented as means + SEM. N=3. **, $p < 0.01$.

Lipid peroxidation is another indicator of cellular oxidative stress. In this study, lipid peroxidation was evaluated by analyzing the malondialdehyde (MDA) modified protein adducts in western blot, which is a byproduct of lipid oxidation and ROS. NUGC-3 whole cell lysate western blot against MDA was shown in Fig 3.45-A. A significant increase of MDA protein adducts was observed after LAAO treatment, particularly the band around 70 KDa. The overall OD values for different duration after LAAO treatment followed a time course increasing trend (Fig 3.45-B, $p<0.05$).

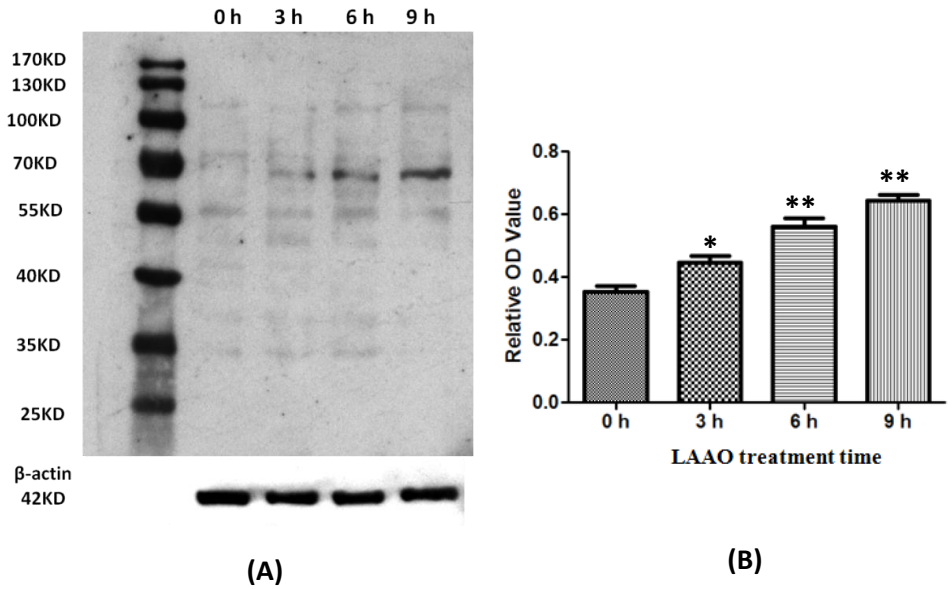

Fig 3.45 Whole cell lysate western blot against MDA. Cells were treated with 0.5 µg/ml LAAO for 0 h, 3 h 6 h and 9 h, respectively. (A): Western blot of MDA protein adducts. MDA antibody dilution was 1: 5000. (B): Bar chart of overall OD values of MDA modified protein adducts in each lane . Data are presented as means + SEM. N=3.*, $p<0.05$; **, $p < 0.01$.

3.5.10 Effects of LAAO on NUGC-3 cell migration and invasion

The effects of LAAO on NUGC-3 cell migration and invasion were explored using Transwell assay. The cells were treated with 0.25 µg/ml LAAO for 24 h prior to migration and invasion assays, a concentration that would not affect NUGC-3 cell proliferation (refer to section 3.4.1). The results showed that LAAO treatment resulted in a 36.6% decrease in the number of migrated cells (Fig 3.46-A, p=0.04) and a 36.9% decrease in the number of invaded cells (Fig 3.46-B, p=0.2).

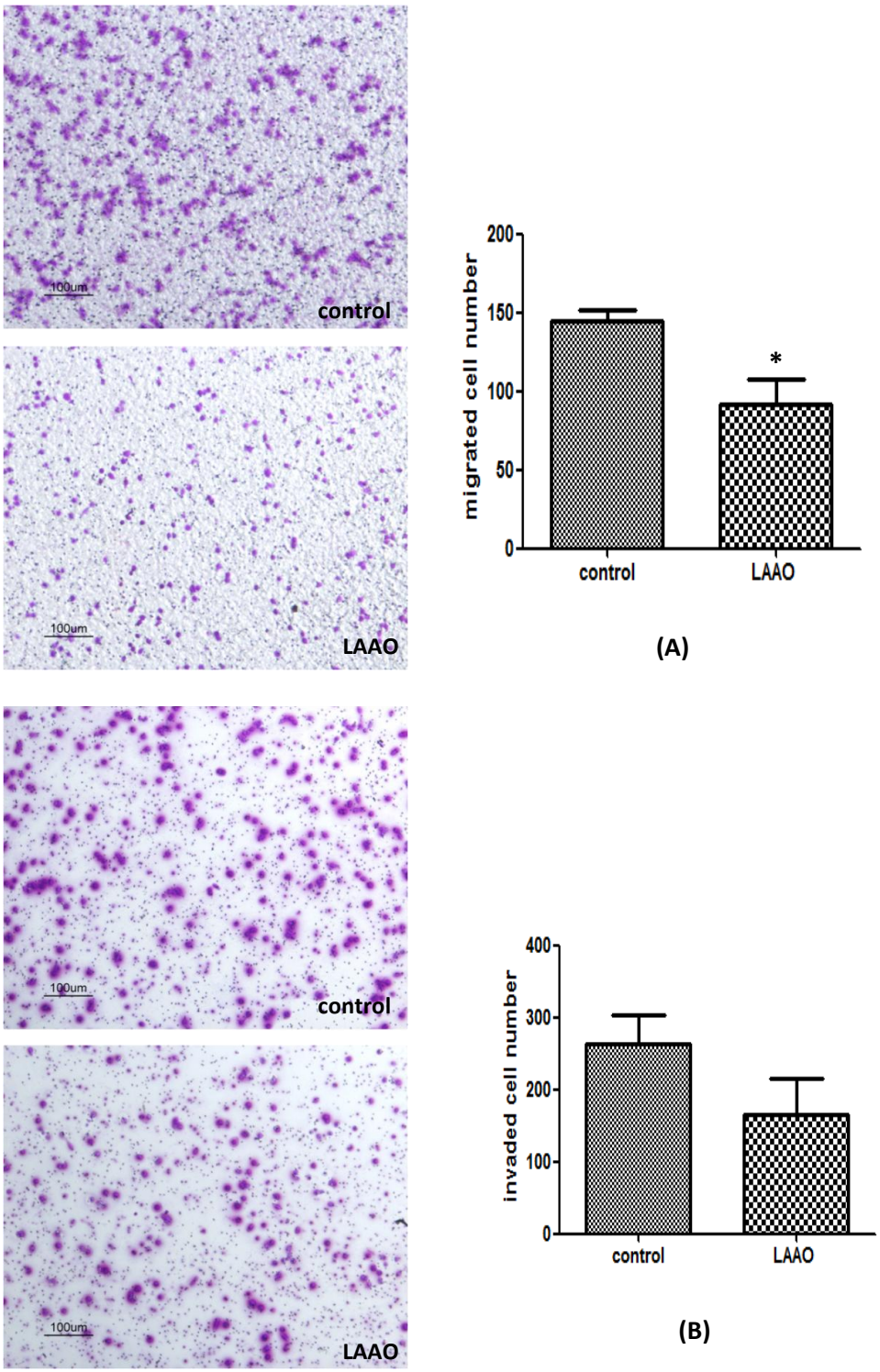

Fig 3.46 NUGC-3 gastric cancer cell migration (A) and invasion (B) assays after treatment with LAAO. Left panel, representative images of migrated NUGC-3 cells. Images were taken at 80 X magnification. Right panel, bar chart of migrated and invaded cell number, respectively. Numbers are the average of 5 counting areas. Data are presented as means + SEM. N=3. *, $p < 0.05$

3.6 Investigation of mechanism in LAAO treated NUGC-3 gastric cancer cells

3.6.1 Expression of genes in MAPK/ERK pathway after LAAO treatment

Based on the observations in BHV work, the regulation of MAPK/ERK pathway was also assessed in NUGC-3 gastric cancer cells after treatment with LAAO. The expression of selected genes in MAPK/ERK pathway was analysed by real time PCR, with the results showing that most of the main regulatory genes in this pathway were inhibited by LAAO treatment, such as ERK1, ERK2, MEK1, Raf1 and RSK (Fig 3.47).

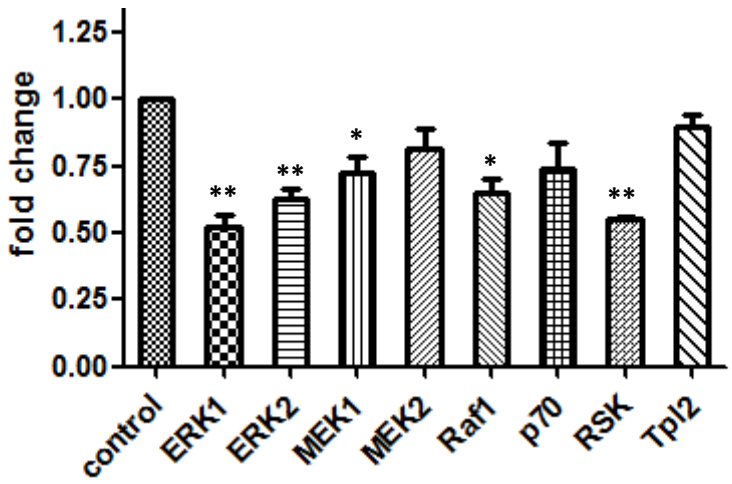

Fig 3.47 Expression of genes in MAPK/ERK pathway by reat-time PCR. NUGC-3 cells were treated with 1.0 µg/ml LAAO for 24 h. GAPDH was used for normalization. Date are presented as means + SEM. N=3. p values were calculated based on each gene expression of untreated cells and the expression of treated cells. *, $p<0.05$. **, $p<0.01$.

3.6.2 Regulation of phosphorylated proteins in MAPK/ERK pathway by LAAO treatment

Similarly, the phosphorylated protein expression of the main regulators in MAPK/ERK pathway was also validated by western blot analysis. The results showed that, after LAAO treatment, the expression of MEK 1/2, MSK-1 and p90RSK was significantly inhibited and ERK 1/2 showed a non-significant decrease (Fig 3.48).

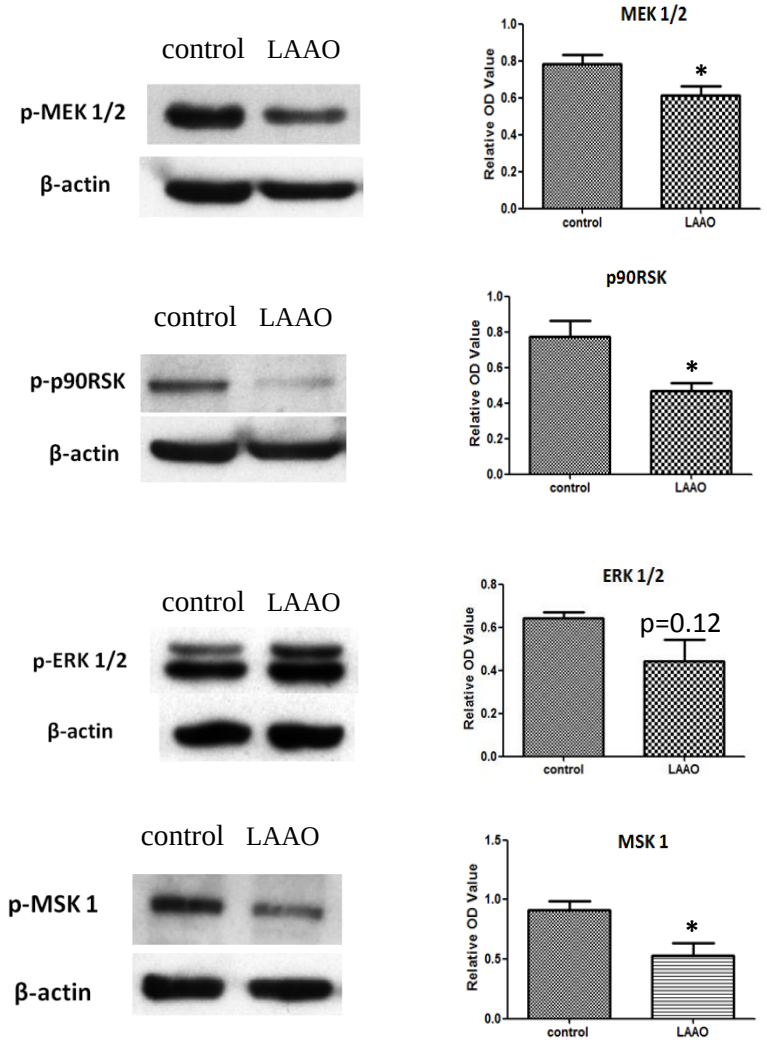

Fig 3.48 Regulation of MAPK/ERK pathway in NUGC-3 cells by LAAO analyzed by western blot. NUGC-3 cells were treated with 1.0 µg/ml LAAO for 24 h. β actin was used as loading control. Molecular mass: MEK 1/2 - 45 kDa, ERK 1/2 - 42, 44 kDa, p90RSK - 90 kDa, MSK 1 - 90 kDa, β actin - 42 kDa. Date are presented as means + SEM. N=3. *, $p<0.05$.

3.6.3 Regulation of Bcl-2 family by LAAO treatment

Bcl-2 family play a critical role in mitochondria function and programmed cell death. Since the loss of mitochondrial membrane potential was observed after LAAO treatment, the expression of Bcl-2 family members was examined by western blot. Results showed that the anti-apoptotic protein Bcl-2 and Bcl-xl were significantly down-regulated and the pro-apoptotic protein Bax was up-regulated with borderline significance (p=0.07) (Fig 3.49).

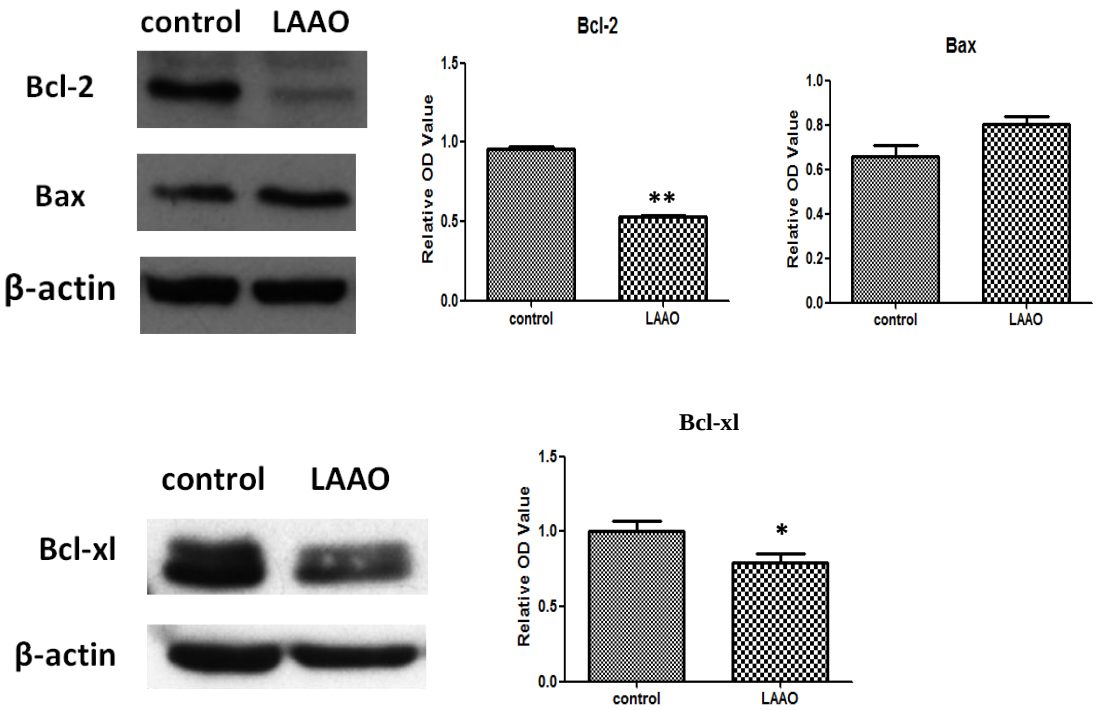

Fig 3.49 Regulation of Bcl-2 family in NUGC-3 cells by LAAO analyzed by western blot. NUGC-3 cells were treated with 1.0 μg/ml LAAO for 24 h. β actin was used as loading control. Molecular mass: Bcl-2, 26 kDa; Bax, 20 kDa; Bcl-xl, 30 kDa; β actin, 42 kDa. Date are presented as means + SEM. N=3. *, p<0.05; **, p<0.01.

3.6.4 Validation of apoptosis related genes from microarray data in LAAO treated NUGC-3 gastric cancer cells

To further validate the role of apoptosis related genes from microarray data, real time PCR was conducted in NUGC-3 cells after treatment with 1.0 µg/ml LAAO for 24 h. The results showed that seven of the eight apoptosis related genes were differentially regulated ($p<0.05$) and presented the same trend as BHV-F1 treatment, except for SART1 (Fig 3.50).

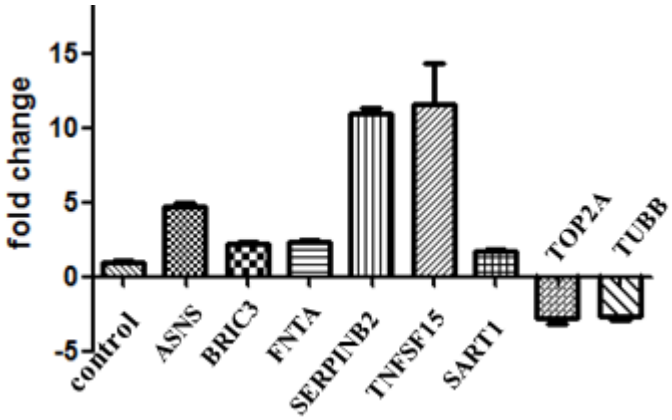

Fig 3.50 Validation of apoptosis related genes in LAAO treated NUGC-3 cells by real-time PCR. NUGC3 cells were treated with 1.0 µg/ml LAAO for 24 h. GAPDH was used for normalization. Date are presented as means + SEM. N=3.

3.6.5 Proteomic regulation of NUGC-3 cells with LAAO treatment by SILAC assay

To further understand the proteomic changes induced by LAAO treatment, the SILAC (Stable Isotopic Labeling using Amino acids in Cell culture) was performed in NUGC-3 cell lysate after treatment with 1.0 µg/ml for 8 h. Experiment was done in duplicate with labeling the LAAO treated cells with heavy and light isotopes, respectively. For results interpretation, up or down regulation with fold change larger than 1.5 was considered as significant. It was found that 9 proteins were up regulated and 108 proteins were down regulated by LAAO treatment.

Table 3.3 List of differentially expressed proteins in NUGC-3 cells after LAAO treatment by SILAC assay.

Protein name	Gene name	Fold change
Putative heat shock protein HSP 90-beta 4	HSP90AB4P	2.1385
Nuclear ubiquitous casein and cyclin-dependent kinase substrate 1	NUCKS1	1.6213
Histone H3.2	HIST2H3A	1.5779
Heterogeneous nuclear ribonucleoproteins C1/C2	HNRNPC;HNRNPCL1	1.5414
Histone H4	HIST1H4A	1.5327
Retinoic acid-induced protein 3	GPRC5A	1.5313
Putative ribosomal RNA methyltransferase NOP2	NOP2	1.5301
Histone H3.3	H3F3A	1.5205
Eukaryotic translation initiation factor 4E-binding protein 1	EIF4EBP1	1.5139
Cystatin-M	CST6	0.65738
BRCA1-associated ATM activator 1	BRAT1	0.65571
Kinesin-like protein KIF22	KIF22	0.65531
Replication factor C subunit 5	RFC5	0.65368
F-actin-capping protein subunit beta	CAPZB	0.64494

F-actin-capping protein subunit alpha-1	CAPZA1	0.63878
Pyrroline-5-carboxylate reductase 2	PYCR2	0.63655
DNA polymerase delta catalytic subunit	POLD1	0.63414
Hepatocyte growth factor receptor	MET	0.63411
G patch domain-containing protein 8	GPATCH8	0.62832
Enoyl-CoA hydratase, mitochondrial	ECHS1	0.62552
Glutamine-rich protein 1	QRICH1	0.62029
Histone-lysine N-methyltransferase MLL;MLL cleavage product N320;	MLL	0.61948
Succinate dehydrogenase [ubiquinone] flavoprotein subunit, mitochondrial	SDHA	0.6122
28S ribosomal protein S35, mitochondrial	MRPS35	0.60941
Glutaredoxin-related protein 5, mitochondrial	GLRX5	0.60612
Isoleucine--tRNA ligase, mitochondrial	IARS2	0.60568
Neurolysin, mitochondrial	NLN	0.60347
Protein LAP2	ERBB2IP	0.60264
3-ketoacyl-CoA thiolase, mitochondrial	ACAA2	0.60133
Pyruvate dehydrogenase E1 component subunit beta, mitochondrial	PDHB	0.59244
Methionine aminopeptidase 1;	METAP1	0.58701
Proteasome maturation protein	POMP	0.58508
Succinyl-CoA ligase [ADP/GDP-forming] subunit alpha, mitochondrial	SUCLG1	0.58052
Enoyl-CoA delta isomerase 1, mitochondrial	ECI1;DCI	0.57272
Heterogeneous nuclear ribonucleoprotein M	HNRNPM	0.5697
Glutathione peroxidase 1	GPX1	0.56895
Melanoma-associated antigen 1	MAGEA1	0.56505
Aspartate--tRNA ligase, mitochondrial	DARS2	0.55745
Serine/threonine-protein kinase PRP4 homolog	PRPF4B	0.55638
Pleckstrin-2	PLEK2	0.55386
Presequence protease, mitochondrial	PITRM1	0.55104
Myosin IC	MYO1C	0.54947
Cytosol aminopeptidase	LAP3	0.54576
Protein transport protein Sec16A	SEC16A	0.54294
Dihydrofolate reductase	DHFR	0.53233
Cellular tumor antigen p53	TP53	0.53046
Centromere protein F	CENPF	0.53045
Plakophilin-2	PKP2	0.52966

Dihydrolipoyllysine-residue acetyltransferase component of pyruvate dehydrogenase complex	DLAT	0.52825
Ras GTPase-activating-like protein IQGAP3	IQGAP3	0.52385
Acetyl-CoA acetyltransferase, mitochondrial	ACAT1	0.52288
Replication protein A 70 kDa DNA-binding subunit	RPA1	0.51943
Deoxyhypusine hydroxylase	DOHH	0.5159
Keratin, type II cuticular Hb1;Keratin, type II cuticular Hb6;Keratin, type II cuticular Hb3	KRT81;KRT86;KRT83	0.51085
Oral-facial-digital syndrome 1 protein	OFD1	0.51046
Chromodomain-helicase-DNA-binding protein 1-like	CHD1L	0.50979
28S ribosomal protein S7, mitochondrial	MRPS7	0.5083
Myosin-9	MYH9	0.50814
Zinc finger protein 36, C3H1 type-like 1	ZFP36L1	0.50441
PCNA-associated factor	KIAA0101;PAF	0.49908
Desmoplakin	DSP	0.49789
Fibronectin;Anastellin;Ugl-Y1;Ugl-Y2;Ugl-Y3	FN1	0.49709
Baculoviral IAP repeat-containing protein 5	BIRC5	0.49495
Aurora kinase B	AURKB	0.49336
Lon protease homolog, mitochondrial;	LONP1	0.48667
Myosin-14	MYH14	0.48518
Nucleobindin-2	NUCB2	0.48378
Replication factor C subunit 1	RFC1	0.48251
28S ribosomal protein S29, mitochondrial	DAP3	0.48
Polymerase delta-interacting protein 2	POLDIP2	0.47749
Glutamine synthetase	GLUL	0.47712
UPF0160 protein MYG1, mitochondrial	C12orf10	0.47384
ESF1 homolog	ESF1	0.46832
Dimethyladenosine transferase 2, mitochondrial	TFB2M	0.45689
Succinyl-CoA ligase [ADP-forming] subunit beta, mitochondrial	SUCLA2	0.44914
Adenylate kinase isoenzyme 4, mitochondrial	AK4	0.4412
Pericentriolar material 1 protein	PCM1	0.43745
HD domain-containing protein 2	HDDC2	0.43556
Receptor-type tyrosine-protein phosphatase F	PTPRF	0.42992
Protein FAM83H	FAM83H	0.42756
Alanine--tRNA ligase, cytoplasmic	AARS	0.42721

28S ribosomal protein S23, mitochondrial	MRPS23	0.42442
28S ribosomal protein S9, mitochondrial	MRPS9	0.42306
Cyclin-dependent kinases regulatory subunit 2	CKS2	0.4178
Mitochondrial-processing peptidase subunit alpha	PMPCA	0.41628
Iron-sulfur cluster assembly enzyme ISCU	ISCU	0.40652
Melanoma-associated antigen 6;Melanoma-associated antigen 2;	MAGEA6;MAGEA 2;	0.40648
28S ribosomal protein S2, mitochondrial	MRPS2	0.39839
Serine/arginine repetitive matrix protein 2	SRRM2	0.38479
Isocitrate dehydrogenase [NAD] subunit alpha	IDH3A	0.38292
Isopentenyl-diphosphate Delta-isomerase 1	IDI1	0.37563
Iron-sulfur cluster assembly 2 homolog, mitochondrial	ISCA2	0.36781
Protein SON	SON	0.34983
Tropomodulin-3	TMOD3	0.34788
Antigen KI-67	MKI67	0.34436
Protein TBRG4	TBRG4	0.33751
Delta-1-pyrroline-5-carboxylate synthase;Gamma-glutamyl phosphate reductase	ALDH18A1	0.33638
Trifunctional enzyme subunit beta, mitochondrial;3-ketoacyl-CoA thiolase	HADHB	0.33277
Ubiquitin-like protein 5	UBL5	0.33193
Isocitrate dehydrogenase [NAD] subunit beta	IDH3B	0.33082
Elongation factor Tu, mitochondrial	TUFM	0.32626
Putative ATP-dependent RNA helicase DHX30	DHX30	0.31263
SRA stem-loop-interacting RNA-binding protein	SLIRP	0.30718
dCTP pyrophosphatase 1	DCTPP1	0.29616
Ribonucleoside-diphosphate reductase subunit M2	RRM2	0.29498
Long chain 3-hydroxyacyl-CoA dehydrogenase	HADHA	0.28884
Glutaminase kidney isoform, mitochondrial	GLS	0.27842
Protein ETHE1, mitochondrial	ETHE1	0.26047
Monofunctional C1-tetrahydrofolate synthase	MTHFD1L	0.25422
ATP-dependent zinc metalloprotease YME1L1	YME1L1	0.24702
Mitochondrial-processing peptidase subunit beta	PMPCB	0.23348
G antigen family D member 2	XAGE1A	0.22967
Leucine-rich PPR motif-containing protein, mitochondrial	LRPPRC	0.21201

1,2-dihydroxy-3-keto-5-methylthiopentene dioxygenase	ADI1	0.19006
AFG3-like protein 2	AFG3L2	0.17198
FAST kinase domain-containing protein 5	FASTKD5	0.13476
Elongation factor G, mitochondrial	GFM1	0.13452

These proteins were also functionally characterized using DAVID functional annotation clustering analysis, which were classified into different groups involved in several interests of cellular processes, such as regulation of cell apoptosis, cell cycle, chromosome organization, cytoskeleton organization, mitochondrial membrane integrity and oxidative reduction (Table 3.4).

Table 3.4 Functional classification of differentially expressed proteins from SILAC assay

Biological processes	Related proteins
cell cycle	CKS2, MKI67, AURKB, BIRC5, CENPF, ERBB2IP, KIF22, MLL, MYH9, POLD1, RPA1, TBRG4, TP53
cell apoptosis	FASTKD5, BIRC5, DAP3, GPX1, MLL, TBRG4, TP53, SON, AARS, PTPRF
Cytoskeleton organization	CKS2, CAPZA1, CHPZB, ERBB2IP, MYH9, OFD1, PCM1, PLEK2, MYO1C, MYH14
Chromosome organization	H3F3A, CENPF, CHD1L, HIST2H3A, HIST1H4A, MLL, RFC1, PRA1, TP53
Oxidation reduction	ADI 1, ALDH18A1, DOHH, DHFR, GPX1, HADHA, IDH3A, IDH3B, PYCR2, PDHB, RRM2, SDHA
Mitochondrial membrane	AFG3L2, ACAT1, ALDH18A1, DC1, HADHA, HDAHB, ACAA2, PMPCA, PMPCB, SDHA, SUCLG1

3.6.6 The validation of proteins involved in MAPK/ERK pathway from SILAC findings

By literature research, it was found that protein EIF4EBP1 (eukaryotic translation initiation factor 4E-binding protein 1, fold change=1.51 after LAAO treatment), HNPNPM (heterogeneous nuclear ribonucleoprotein M, fold change=0.52) and IQGAP3 (IQ motifcontaining GTPase activating protein 3, fold change=0.57) are involved in MAPK/ERK signaling pathway. Consistently, EIF and HNRNP family were also observed to be down-regulated by BHV treatment. Briefly, IQGAP3 is the up-stream activator of ERK pathway and EIF and HNRNP protein family are down-stream translational targets of ERK pathway. EIF4EBP1 can bind with EIF4E protein and inhibit its function. Their background and involvement in ERK pathway will be further discussed in section 4.4.

To double confirm the gene and protein expression of these 3 targets after LAAO treatment, real time PCR and western blot were conducted. Results indicated that EIF4EBP1 was up-regulated by LAAO in both gene and protein level. Both HNRNPM and IQGAP3 were down-regulated by LAAO in gene and protein level (Fig 3.51). Taken together, these evidence further confirm that LAAO exerted the anticancer actions by regulating MAPK/ERK pathway.

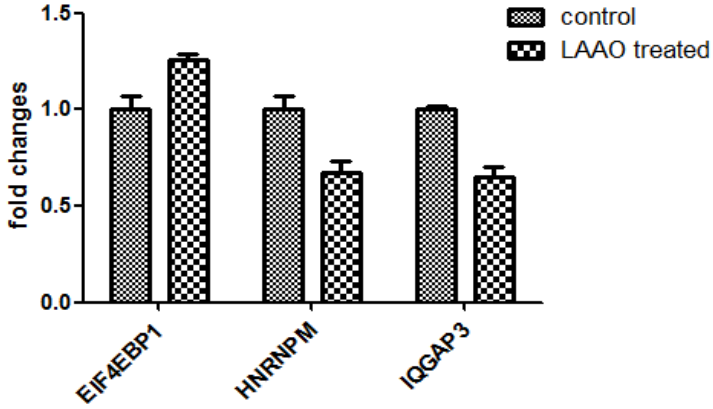

A: RT-PCR

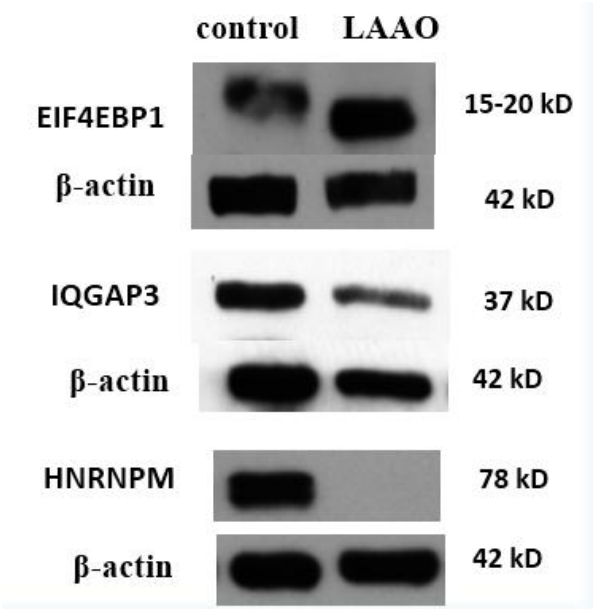

B: western blot

Fig 3.51 Validation of proteins involved in MAPK/ERK pathway by real-time PCR (A) and western blot (B). NUGC3 cells were treated with 1.0 µg/ml LAAO for 24 h. GAPDH and β actin were used for normalization. Date are presented as means + SEM. N=3.

CHAPTER 4

DISCUSSION

4. DISCUSSION

4.1 Anticancer potential of *Hottentotta hottentotta* scorpion venom and L-amino acid oxidase

Animal venoms and toxins from snakes, scorpions, spiders, bees, wasps and ants, have shown wide applications in biopharmacological fields. They have provided rich sources for drug discovery to target various human diseases such as cancer, HIV, hypertension, diabetes, chronic pain, congestive heart failure, stroke, microbial infection, autoimmune disease, and so on (King, 2011). In addition, the peptides isolated from animal venoms, which act on the ion channels, can be applied as channel modulators in the neurophysiology research (Lewis *et al.*, 2003).

The anticancer potential is a new discovery platform for animal venoms and toxins. Over the last three decades, the anticancer activities of a number of crude venoms and the active components from snakes, scorpions, spiders and bees have been extensively investigated in laboratories. Snake venoms and isolated proteins are the earliest and the most studied in anticancer perspective. Several components in the snake venoms have been described to inhibit cancer proliferation, induce cell apoptosis or block angiogenesis, cell adhesion, migration and invasion, such as phospholipase A_2, L-amino acid oxidase, metalloprotease, disintegrin, lectins and peptides (Cardiotoxin III, Cytotoxin P4) (Calderon *et al.*, 2014). Other proteins and peptides purified from animal venoms are promising to become the "leads"

for drug screening, including Chlorotoxin and Bengalin from scorpion venoms, Mellitin from bee venom, Mastoparan from wasp venom, Gomesin and Psalmotoxin 1 from spider venoms, etc. (Heinen *et al.*, 2011).

All these findings have shown that animal venoms and toxins possess anticancer potential by the inhibition of cancer cell proliferation, arrest of cell cycle, induction of cell death, reduction of cancer angiogenesis, cell adhesion, migration or invasion. Such functional studies have been done in a set of malignancies in cell culture or in mouse xenograft model, including leukemia, glioma, melanoma, lymphoma, breast, lung, gastric, prostate cancers and others. The outcome from clinical trial regarding synthetic Chlorotoxin (TM-601) in glioma diagnosis and treatment is also encouraging (Mamelak *et al.*, 2006). All together, it is very promising that animal venoms and toxins could be developed into anticancer agents and deserve further studies.

4.1.1 The anticancer potential of scorpion venoms, in particular BHV

Scorpion venoms and toxins are gaining increasing attention in the investigations of anticancer agents, given that they are rich in proteins and peptides, especially the neurotoxins that act on ion channels in the cell membrane. In this study, four scorpion venoms were screened in the beginning for their anti-proliferative effects on cancer cells (mainly on gastric cancer cells). Results showed that BmK had limitative inhibition effect on NUGC-3 cell proliferation at a high concentration (5 mg/ml), which was probably by cell cycle arrest at G1 and sub-G1 phases and the promotion of

cell apoptosis. Whereas, other 3 scorpion venoms displayed much stronger inhibition effects on NUGC-3 cell proliferation with different IC50 values. Considering that BHV was shown to be the most effective against NUGC-3 with very low IC50 (8.1 µg/ml), BHV was chosen to be further investigated for its anticancer potential in gastric cancer *in vitro* and *in vivo*.

The *Hottentotta hottentotta* scorpion was first reported by Fabricius in 1787, and has been mainly found in Africa and Middle East (supp. Fig 1). The genus *Hottentotta* was originally recognized as *Buthotus,* a subgenus of *Buthus,* and was elevated to an independent genus in 1935 (Werner, 1935). That is why the *Hottentotta hottentotta* venom was abbreviated as BHV (*Buthotus hottentotta* venom) in this study. Only few studies have been performed on this scorpion venom, leaving much unknown with regard to its biological properties in medical usages. It was reported that BHV can activate ryanodine receptor Ca^{2+} release channels of sarcoplasmic reticulum (Valdivia *et al.*, 1991). Another study reported that BHV can stimulate adrenergic nerves with consequent release of transmitter (Gwee *et al.*, 1995). The present study could be one of the first to evaluate its anticancer potential in gastric cancer.

In vitro:

The functional studies to evaluate the anticancer potential of BHV in gastric cancer cell lines *in vitro* included alamarBlue cell viability/proliferation assay, LDH cytotoxicity study, cell cycle analysis, observations of cell

morphological changes under fluorescence microscope and TEM, apoptosis identification by Annexin-V & Propidium iodide staining, cell migration and cell invasion assays. The results showed that BHV induced the apoptotic phenotypes of NUGC-3 cells, which were supported by decrease in cell viability/proliferation, sub-G1 cell cycle arrest, morphological changes like chromatin condensation, membrane blebbing and cell shrinkage, as well as the significant increase in Annexin-V labeling. It needs to mention that the IC50 of BHV from test in 96-well assay was less than 10 µg/ml, while the concentration used in apoptosis studies in 6-well assay was 15 -30 µg/ml. The reason could be that the 50 percent reduction in cell viability may not convert to 50 percent cell apoptosis. Obvious cell apoptosis was observed at higher concentration of BHV administration based on morphological and biochemical judgement. That was why we applied higher concentration of BHV in TEM and western blot experiments.

The apoptosis induction by scorpion venoms and toxins has been widely reported. Wang and Ji observed that BmK crude induced apoptosis of U-251-MG glioma cells at 10 mg/ml (Wang *et al.*, 2005). Another study showed that BmK arrested cell cycle and induced apoptosis of human Jurkat and Raji lymphoma cells (Gao *et al.*, 2009). Polypeptide extract from scorpion venom (PESV), a mixture of 50-60 aa polypeptides purified from BmK venom, was reported to induce apoptosis of DU 145 human prostate cancer cells, which was confirmed by TUNEL assay (Zhang *et al.*, 2009b). Another group of researchers studied the apoptosis inducing activities of *Odontobuthus doriae*

and *Androctonus crassicauda* scorpion venoms on SH-SY5Y human neuroblastoma cells and MCF-7 breast cancer cells, together with the up-regulation of caspase-3 activity and reactive nitrogen intermediates (Zargan *et al.*, 2011b, a; Zargan *et al.*, 2011c). Other evidences could be the cell apoptosis induced by Bengalin and Neopladine 1 and 2, as described in detail in section 1.2.4. In this study, the NUGC-3 cell apoptosis induced by BHV was not only identified by conventional approaches like cell cycle and Annexin V staining, but also confirmed based on morphological changes. The application of TEM and SEM techniques clearly revealed the structural changes of chromatin and cytoplasm, as well as the membrane blebbing. Membrane blebbing is one early morphological characteristic of apoptosis and is associated with the cytoskeleton disruption which leads to the contraction of the actin-myosin complex and the surface protrusion (Mills, 2001; Song *et al.*, 2002).

It was found that different scorpion venoms or toxins induced cell apoptosis with different mechanisms or various intracellular signaling transduction pathways. For example, Bengalin activated mitochondria-caspase apoptotic cascades and inhibited HSP 70 and 90. Neopladine 1 and 2 induced the expression of Fas ligand and triggered cell apoptosis, whereas, BmK killed Jurkat cells by the inactivation of PI3K/Akt pathway via increasing PTEN expression. Moreover, the cell cycle arrest induced by scorpion venoms treatment was found to be distributed in diverse phases of the cell cycle, such as sub-G1 (Bengalin), G1 phase (PESV), S phase (*Androctonus*

crassicauda). These different mechanisms could be due to the difference in venom components among different scorpions and the response from cancer cells would be varied.

On the other hand, when the concentration of BHV was controlled as low as not affecting the cell viability/proliferation, BHV revealed another aspect of anticancer potential, the inhibition of NUGC-3 cell migration and invasion. The effects of scorpion venoms and toxins on cancer cell migration and invasion were seldom reported. SUMO-AGAP, a modified voltage gated sodium channel toxin from BmK venom by combining a small ubiquitin-related modifier, was shown to inhibit the migration of SHG-44 glioma cells by wound healing assay (Zhao *et al.*, 2011). CTX and BmKCT, the two anticancer peptides purified from scorpion venoms that can block the chloride ion channels, were reported to inhibit the migration and invasion of glioma cells by Transwell assays and the metastasis of glioma in rat model, respectively (Soroceanu *et al.*, 1999; Fan *et al.*, 2010). It could be inferred that scorpion toxins could reduce cancer metastasis maybe by the modulation of ion channels in the membrane of cancer cells and

Targeting cancer metastasis is considered as an effective and promising strategy for cancer therapeutics, as neoplastic metastasis is a critical final step in cancer progression and indicates a poor prognosis and intervention efficacy. Recently, a growing body of studies have suggested that there is a strong correlation between the functional expression of ion

channels and cancer migration and invasion (Prevarskaya *et al.*, 2010). A variety of experiments have discussed the involvement of $Ca^{2+,}$ Na^{+}, K^{+}, Cl^{-} and some transporters in the processes of cancer migration and invasion. The mechanisms are poorly understood and one hypothesis was proposed that these ion channels facilitate cancer migration/invasion by the regulation of cell volume and motility (Cuddapah *et al.*, 2011). Specifically, ion channels control the osmotic movement of water by fluxing ions, which results in the extension at the leading edge of migrant cells as a moving force (Schwab *et al.*, 2007). $Na_v1.5$ was reported to be up-regulated in metastatic breast cancer cells and tissues and there was a close link between its activity and the metastatic behaviours of cancer cells, such as endocytosis, directional motility and invasion. Moreover, the strong correlation was observed between $Na_v1.5$ expression and lymph node metastasis in clinical samples (Fraser *et al.*, 2005; Onkal *et al.*, 2009).

As mentioned in section 1.2.3.1-1.2.3.4, scorpion venoms contain abundant ion channel regulators and have the potential for the development of anti-metastasis drugs. As for BHV, a pool of small peptides were identified in gel filtration and SDS-PAGE (Fig 3.23 and Fig 3.24), which may be related to the ion channel regulation. Furthermore, using patch clamp electrophysiological approach, we investigated the existence of voltage gated potassium current in NUGC-3 cells (Supp. Fig 2) and various K^{+} and Na^{+} channels in NUGC-3 cells were also found to be differentially expressed compared with HeLa cells (Supp. Fig 3). Taken together, it can be postulated

that the channel toxins in BHV may be responsible for the inhibitory effects on NUGC-3 cell migration and invasion.

in vivo:

It is commonly recognized that the *in vivo* model plays a crucial role in translational cancer researches and the findings from animal model are more applicable to clinical applications. In this study, the NUGC-3 xenograft model was established on BALB/c-nu/nu mice to evaluate the antitumoral effects of BHV and examine its toxicity to mouse as well. First, 5 BHV venom doses were tested on mice with tumor, which were 100 μg, 50 μg, 25 μg, 12.5 μg and 6.25 μg per mouse, respectively, in a descending order. It was found that 100 μg and 50 μg per mouse BHV injection would kill the mice and doses lower than 25 μg per mouse were safe. By monitoring the mice health conditions like body weight (shown in supp. Table 1), it was confirmed that the doses of 12.5 μg and 6.25 μg per mouse for injection would not produce systemic toxicity to mice and could be applied to evaluate the antitumoral effects of BHV *in vivo*.

The results showed that 12.5 μg/mouse BHV significantly inhibited the tumor growth and histologically disrupted the tumor structure with the formation of more cavities with tissue debris. What is more, the apoptosis was detected mainly in the disruptive tissue areas. Such observations indicated that BHV could inhibit tumor progression *in vivo*.

However, there is certain limitation in the experiment setting. IACUC has a regulation that the tumor on mice cannot exceed 1.5 cm. When it was applicable to give intratumoral injection, the tumor diameter had already reached 0.7 - 1.0 cm and NUGC-3 was an aggressive and fast growing tumor. These two factors limited the observation period to only one week after venom injection. An alternative way to overcome this is to inject the venom intraperitoneally or intravenously when the tumor size is still small.

4.1.2 The anticancer potential of LAAO from snake venom

BHV has been partially purified and characterized by HPLC, SDS-PAGE and mass spectrum, with the identification of LAAO as one active component in BHV in small quantity. Unfortunately, all the available crude venom had been used up and the purification for single protein could not be completed. However, from the literature review, LAAOs are found to share more than 80% sequence similarity (Franca *et al.*, 2007). Therefore, in this study, a commercial source of LAAO purified from *Crotalus adamanteus* snake venom was used to be screened and evaluated for its anticancer effects in gastric cancer.

To date, several snake venom LAAOs have been reported to exert anticancer effects, such as *Ophiophagus hannah* (King Cobra), *Agkistrodon acutus*, *Bothrops jararaca*, *Bothrops atrox*, *Naja naja atra*, as well as a LAAO homolog from parasite-infected fish. ACTX-6, the LAAO isolated from *Agkistrodon acutus* snake venom, induced apoptosis in A549 human lung

cancer cells via the Fas pathway, probably triggered by the ROS initiated JNK and c-Jun phosphorylation (Zhang *et al.*, 2007). Another study showed that LAAO from King Cobra exerted cytotoxicity to murine melanoma, fibrosarcoma, stomach, breast, colorectal and lung cancer cell lines (Ahn *et al.*, 1997). More inspiringly, a new report revealed its relative low toxicity to non-tumourigenic cells (Lee *et al.*, 2013). For *in vivo* study of the anticancer effect of LAAO, the enzyme isolated from *Bothrops jararaca* snake venom was shown to significantly inhibit the growth Ehrlich ascites tumor and prolong the survival time of mouse with tumor (de Vieira Santos *et al.*, 2008). A recent publication demonstrated the antitumoral effects of LAAO from King cobra in PC-3 prostate tumor xenograft, as LAAO induced apoptosis in PC-3 cells and PC-3 tumors, suppression of PC-3 tumor growth and no obvious damage to vital organs (Lee *et al.*, 2014). These evidence suggest that LAAO could be a promising anticancer agent, which deserves further investigation for its application in cancer therapeutics.

In this study, the anticancer potential of LAAO from *Crotalus adamanteus* snake venom was fully investigated. First, the anti-proliferative activity of LAAO to gastric and breast cancer cells was screened. It would appear that LAAO had certain selectivity regarding the cytotoxicity to various cancer cell lines. For instance, more reduction of cell viability was observed on NUGC-3 cells compared with MKN-74 and MKN-7 cells. Pathologically, MKN-74 and MKN-7 are well-differentiated while NUGC-3 is poorly-differentiated. In the test on breast cancer cells, LAAO showed less

cytotoxicity to MCF12A non-tumorigenic breast cells in comparison with MCF-7 (less invasive), T-47D (less invasive) and MDA-MB-231 (invasive) breast cancer cells. However, whether and why LAAO selectively has stronger cytotoxicity against poorly-differentiated cancer cells in gastric cancer are still not clear and need to be further determined.

The toxicity of LAAO to mouse tissues was verified by evaluating liver damage with the measurement of alanine transaminase (ALT) activity in mouse serum one week after LAAO injection. The result demonstrated that there was no change in the ALT activity after LAAO injection, suggesting that LAAO did not cause any damage to mouse liver (supp Fig 3), and appear relatively safe.

For the cell cycle study in NUGC-3 cells, it was found that the cell cycle was arrested at G2/M phase (27.3% vs 38.5%) after treatment with LAAO and there was no increase in sub-G1 phase, indicating that there was no small DNA fragmentation induced by LAAO treatment. This appears to be different from what happened in NUGC-3 cells after treatment with BHV, which induced a significant increase in sub-G1 phase. However, the involvement of G2/M arrest in apoptosis is in agreement with several other studies. Such examples can be the G2/M cell cycle arrest and apoptosis induced by Furanodiene in HepG2 hepatocellular carcinoma cells and Doxorubicin induced G2/M phase arrest in synchronized p388 leukemia cells (Ling *et al.*, 1996; Xiao *et al.*, 2007; Ouyang *et al.*, 2009). The discrepancy of cell cycle

arrests induced by BHV and LAAO could be attributed to the different components in apoptosis inducers, as BHV is a mixture and may contain other factors that enhance small DNA fragmentation.

4.2 Caspase-independent apoptosis, an alternative way to combat cancer

4.2.1 General background

During the past decade, there are accumulative data, which have confirmed caspase-independent apoptosis (CIA) as an alternative modality of cell death, which differs from classic apoptosis, necrosis and autophagy. CIA has been widely reported in cell culture and animal studies. Quite a few *in vitro* studies have indicated the occurrence of CIA, by inducing apoptosis in the presence of caspase inhibitors (e.g. z-VAD-fmk) or in cells genetically expressing caspase inactivation genes like XIAP or p35. For example, as early in 1996, Xiang *et al.* reported that the apoptosis induced by the expression of Bax in Jurkat cells was not prevented by caspase inhibitor z-VAD-fmk (Xiang *et al.*, 1996). Another example is the cell death induced by nitric oxide (NO) in PC12 cells was found not to be inhibited by expression of p35, a baculvirus-encoded caspase inhibitor, indicating the CIA occurred (Okuno *et al.*, 1998). Additionally, a number of natural and synthetic compounds were shown to induce CIA, such as Selenocysteine in MCF-7 breast cancer cells, Ciglitazone in renal epithelial cells, and Artesunate in human myelodysplastic syndrome SKM-1 cells (Kwon *et al.*, 2008; Chen *et al.*, 2009b; Wang *et al.*, 2014). Besides

in vitro evidence, studies on mouse models also revealed the existence of CIA pathways. CHM-1, a synthetic quinolone, inhibited tumor growth and prolonged the survival of mice inoculated with HA22T hepatocellular carcinoma cells, via a CIA pathway mediated by AIF translocation (Wang *et al.*, 2008).

The significance of caspase-independent apoptosis has been increasingly recognized in cancer research as it may unravel novel targets for cancer therapy. Cancer cells have developed diverse strategies to escape apoptosis by the inactivation of caspase-dependent pathway, which is critical for tumor development and adjuvant chemoresistance. For example, the gene mutation of tumor suppressor protein p53 is present in about half of cancer patients (Oren, 1999). In this context, CIA regulates an alternative pathway to kill cancer cells and provides novel targets for the design of more effective chemotherapeutic drugs (Mathiasen *et al.*, 2002; Constantinou *et al.*, 2009). On the other hand, it was described in several experiments that induction of apoptosis by CIA exhibited selective antitumoral activity, with negligible or minor toxicity to noncancerous cells and tissues, indicating the potential clinical implications of CIA in the elimination of the side effects caused by chemotherapy drugs (Wang *et al.*, 2008; Li-Weber, 2009).

4.2.2 Mechanistic pathway in LAAO induced CIA

In this work, the CIA induced in NUGC-3 cells by BHV and LAAO treatment was confirmed by the absence of caspases activation in western

blot, absence of increased caspase-3 activity using DEVD-pNA substrate and the decrease in cell viability in the presence of caspase inhibitor z-VAD-fmk (section 3.2.6.2 and section 3.5.6).

Like classical apoptosis, CIA is largely dependent on activation of other proteases and mitochondrial membrane permeabilization (MMp). Several proteases have been implicated in CIA, such as cathepsin B and D, calpains and serine proteases (Mathiasen *et al.*, 2002). Cathepsins are lysosomal proteases, which participate in CIA by directly cleaving Bid and AIF or translocating Bax and Bid from cytosol to mitochondria (Bidere *et al.*, 2003; Cirman *et al.*, 2004). Calpains reside in cytosol and are activated in response to the elevation in intracellular calcium caused by ER stress (Muruganandan *et al.*, 2006). Similar to cathepsins, calpains can cause the cleavage of AIF in the absence of caspase activation. The serine proteases that are responsible for CIA include granzymes A and B, Omi/Htra2 and apoptotic protease 24 (AP24) (Constantinou *et al.*, 2009).

Numerous studies have indicated that mitochondria play a pivotal role in the control of CIA, given that the AIF translocation from mitochondria to nucleus occurs in most CIA processes. Furthermore, the above mentioned proteases can serve as the upstream triggers of MMp. AIF is a 62 kDa flavoprotein localized in the inner mitochondrial membrane, which has dual functions: mitochondrial oxydoreductase and nuclear proapoptotic factor. Upon death stimulus, AIF is cleaved into a soluble protein of 57 kDa

(truncated AIF, tAIF) and released into cytosol along with MMp. Subsequently, tAIF translocates into nucleus where it cooperates with Endonuclease G and induces DNA fragmentation and CIA (Delavallee *et al.*, 2011).

Several drugs that target AIF mediated CIA have been developed. BZL101 (Bezielle®), an extract from plant *Scutellaria barbatae*, is known to induce CIA by AIF translocation and ROS generation in breast and prostate cancer cells, and the results from a phase I clinical trial showed that BZL101 was safe and had a favorable toxicity profile with encouraging clinical activity in patients (Rugo *et al.*, 2007). Another study showed that Bobel-24 and derivatives triggered CIA in human pancreatic cancer cell lines via lysosomal and mitochondrial death pathway by activation of cathepsin B. Particularly, Bobel-24 was also active against NP9 apoptosis-resistant pancreatic cell line (Parreno *et al.*, 2008).

In this study, the exploration of mechanistic pathway was performed using NUGC-3 cells with LAAO treatment, as LAAO is one active component from BHV and the findings from LAAO should also be applied to BHV. The AIF translocation was first identified by immunofluorescence assay. After treatment with LAAO for 12 h, AIF translocated from cytoplasm into nucleus in most of NUGC-3 cells and a merged blue and red color was clearly observed. However, in this assay, only the nucleus was labelled with DAPI and the mitochondria were not labelled, the original location of AIF in mitochondria was not demonstrated.

Since the mitochondrial membrane permeabilization is necessary for AIF release, the mitochondrial membrane potential (MMP) was examined by JC-1 staining, which acts as a sensitive indicator of low and high MMP. The results showed that, just after 6 h of LAAO treatment, more than 70% NUGC-3 cells had lost MMP and were permeabilized in mitochondrial membrane. This finding is in line with the notion that AIF translocation is dependent on time. The Bcl-2 family members are important for maintaining the integrity of outer mitochondrial membrane. The pro-apoptotic proteins Bax and Bid are responsible for the pore formation in mitochondrial membrane and the initiation of CIA, whereas this may be counteracted by anti-apoptotic protein Bcl-2 (Cabon *et al.*, 2012). Consistently, in this study LAAO was observed to up-regulate Bax expression and down-regulate the expression of Bcl-2 and Bcl-xl.

Many studies have shown that oxidative stress or reactive oxygen or nitrogen species (ROS/RNS) can trigger programmed cell death and several antitumor drugs are known to induce apoptosis by elevating intracellular ROS and affecting mitochondria in cancer cells (Ryter *et al.*, 2007; Guo *et al.*, 2013; Poornima *et al.*, 2013; Yang *et al.*, 2013). More importantly, new emerging evidence indicates the implication of oxidative stress in the initiation of CIA. It is documented that the intracellular ROS eruption induces AIF translocation and triggers CIA in the presence of z-VAD-fmk, accompanied by loss of MMP and inhibition of Bcl-2 (Son *et al.*, 2009; Franke *et al.*, 2010; Yu *et al.*, 2011). It is postulated that the ROS produced by exogenous stimulus causes

mitochondria membrane dysfunction and permeabilization. In turn, such a dysfunction increases the ROS level, which leads to further damage to mitochondria. Therefore, a positive feedback loop for ROS-induced mitochondrial membrane dysfunction is formed (Ma *et al.*, 2014).

In this present study, oxidative stress induced by LAAO treatment was verified by detecting MDA modified protein adducts in western blot and the increase of total intracellular ROS by DCF-DA staining. It was found that 3 h of LAAO treatment or longer can significantly increase the intracellular ROS in NUGC-3 cells, evidenced by increased expression of MDA protein adducts and the right shift of formed DCF fluorescence. However, at 6 h of treatment group, the DCF signal went back to baseline level, which was believed to be because the plasma membrane of NUGC-3 had become permeable at this time and the DCF dye leaked out (Maher *et al.*, 2005).

It is not difficult to understand how LAAO induces intracellular oxidative stress, as H_2O_2 is generated during the oxidation process of LAAO. To confirm the role of LAAO generated ROS in the apoptosis inducing activity of LAAO, a ROS scavenger catalase was applied to check if the apoptosis can be rescued. As shown in supp. Fig 5, reduction of NUGC-3 cell viability was neutralized by 40%. However, catalase cannot completely compensate the anti-proliferative effect of LAAO, indicating that the anticancer activity of LAAO was not attributed to liberated ROS alone. It has previously been

reported that the direct interaction between LAAO and target cells may also play a role (Suhr *et al.*, 1996).

4.3 BHV and LAAO target MAPK/ERK pathway

The mitogen-activated protein kinases (MAPKs) are evolutionarily conserved protein kinase family that transmit extracellular signals to intracellular effectors and regulate a variety of cellular processes, such as proliferation, differentiation, migration, survival and apoptosis (Ravingerova *et al.*, 2003). The diverse exogenous signals include cytokines, growth factors, neurotransmitters, cellular stress and others. The activation of MAPKs is a three-kinase sequential cascade consisting of MAPK kinase kinase (MKKK), MAPK kinase (MKK) and MAPK, which is achieved through the reversible phosphorylation of both threonine and serine residues of the TXY motif in the catalytic domain. MAPKs comprise at least five subfamilies, of which the best known are ERK (extracellular signal-regulated kinase), JNK (c-Jun NH2-terminal kinase) and p38 (Widmann *et al.*, 1999). It is generally described that ERK pathway links to cell proliferation and cell survival. Whereas, JNK and p38 pathways are associated with apoptosis, differentiation and inflammation (Pearson *et al.*, 2001).

The MAPK/ERK pathway is among the most extensively studied MAPK signaling pathways. This pathway starts from the GTP loading of Ras at plasma membrane, followed by the phosphorylated activation of a series of

kinases, namely Ras → Raf (MKKK) → MEK 1/2 (MKK) → ERK 1/2 (MAPK). Upon phosphorylated, ERK 1/2 activates a variety of downstream substrates that participate in various cell behaviors, such as cell growth, cell differentiation, cell apoptosis and cell motility (Lewis *et al.*, 1998). This pathway can be negatively regulated by various proteins, such as dual-specificity phosphatases (DUSPs), cytoplasmic Sprouty protein family, scaffolding/chaperonin proteins such as MEK partner 1 (MP-1), heat shock protein-90 (HSP90), as well as many tumor suppressor proteins (e.g. PTEN, PP2A, DUSP5, RKIP, etc.) (McCubrey *et al.*, 2012). The dysregulation of ERK pathway has been implicated in several neurodegenerative diseases and various malignancies (Kim *et al.*, 2010).

A large number of evidence reveals the aberrant activation of ERK pathway and its role in tumorigenesis. The mutations in growth factor receptors and upstream kinases are widely reported in many neoplasms. For example, the overexpression or oncogenic mutation of epidermal growth factor receptor (EGFR) has been detected in cancers of lung, breast, colon, ovary, etc. (Arteaga, 2002). Ras mutations cover approximately 30% of human tumors and the frequency of *K-RAS* mutation is high in pancreatic cancer (~ 60%) (Prior *et al.*, 2012). *BRAF* is frequently mutated in melanomas (66%) and papillary thyroid tumors (40%) (Davies *et al.*, 2002; Puxeddu *et al.*, 2004). Previously, mutations of MEK and ERK genes were rarely reported while recent studies indicate the somatic mutation of *MEK1* in non-small cell lung cancer and ovarian cancer cell lines (Estep *et al.*, 2007; Pao *et al.*, 2011).

Abnormal activation driven by the mutation or up-regulation of certain components in ERK pathway has been associated with the multiple steps of cancer progression, by regulations of cancer cell proliferation, cell cycle, cell apoptosis, cancer metastasis and angiogenesis, as well as drug resistance (Kohno *et al.*, 2006; Steelman *et al.*, 2010).

In this current study, the inhibition of ERK pathway by BHV was discovered by screening the activity of ten important signaling pathways in cancer. This assay is based on the measurement of the expression of the transcription factor, a downstream target of each specific signaling pathway. The results indicate that MAPK/ERK pathway (Elk-1 as downstream transcription factor) was down-regulated by 34.8%, while no significant change was observed in the activity of MAPK/JNK pathway (AP-1 as transcription factor). To further confirm this notion, the gene expressions of members in ERK pathway were examined by RT-PCR. It was found that both BHV and LAAO significantly decreased the gene expressions of both upstream and downstream ERK members, including Raf-1, MEK-1, ERK-1, ERK-2, p90RSK. Furthermore, the phosphorylated protein expression of ERK members were assessed by western blot, given that only proteins in phosphorylated form work as active signal transducers. The results indicated the phosphorylation level of all members was down-regulated by 20%-40% in both BHV and LAAO treated groups. However, ERK 1/2 (with BHV and LAAO treatment) and p90RSK (with BHV treatment) showed a decrease with non-significance in statistical analysis ($p>0.05$), which may be due to the variations

of OD values between the triplicates. Collectively, these observations surely confirm that the MAPK/ERK pathway was inhibited by BHV and LAAO.

There are two questions to be answered with regard to the inhibition of ERK signaling pathway in NUGC-3 by BHV and LAAO. The first one is how does ERK pathway participate in the regulation of various cellular processes observed in BHV and LAAO treated cells, such as inhibition of cell proliferation, cell migration and invasion and caspase-independent apoptosis? The second one is how does LAAO or BHV exert the inhibitory effect on ERK pathway?

The first question can be addressed by analysing the downstream targets and networks of ERK pathway. After being activated as the final effectors, ERK 1/2 can phosphorylate dozens of substrates in different cell compartments (nucleus, cytoplasm, cytoskeleton). In the nucleus, ERK 1/2 activate a set of transcription factors, such as ternary complex factors (TCFs, e.g. Elk-1, Sap-1), MSKs, ATF-1, c-Fos, c-Myc, Stat 1/3, estrogen receptor, etc.(Kohno *et al.*, 2006). These transcription factors further regulate gene expression and promote cell growth and survival. Moreover, ERK 1/2 also phosphorylate cytoplasmic targets such as p90RSK, which regulates GSK3 and BAD. More importantly p90RSK will translocate into nucleus and phosphorylate SRF (serum response factor), CREB (Cyclic AMP Response Element-Binding protein) and other factors (Hauge *et al.*, 2006). In comparison with our work, we found the down-regulation of Elk-1, p90RSK

and MSK-1, which could be responsible for the anti-proliferation effects of BHV and LAAO, as well as the cell cycle arrest.

Apart from the role in cell proliferation and survival, ERK signaling pathway also mediates cell apoptosis and cell metastasis. The regulation of cell apoptosis by ERK pathway is mainly accomplished via interaction with Bcl-2 family in several ways (Balmanno *et al.*, 2009). For example, p90RSK and MSK can inactivate pro-apoptotic protein BAD by phosphorylation at Ser112. The expressions anti-apoptotic proteins like Bcl-2 and Bcl-xl are also reported to be ERK pathway dependent, which is supported by the fact that MEK inhibitor PD98059 induced a decrease in Bcl-2 and Bcl-xl and promoted apoptosis in pancreatic cancer cells (Boucher *et al.*, 2000). Additionally, ERK 1/2 can target the proteasomal degradation of FOXO3A and thereby repress the FOXO3A-dependent expression of BIM (Yang *et al.*, 2008). All these observations help considerably in understanding how LAAO induces inhibition of the ERK pathway, which participates in mitochondria-mediated caspase-independent apoptosis, associated with decreased expression of Bcl-2 and Bcl-xl, accompanied by the down-regulation of ERK pathway.

Several studies have also shown that the ERK pathway promotes cancer cell migration/invasion by modulating matrix metalloproteinase, myosine light-chain kinase (MLCK) as well as genes involved in epithelial mesenchymal transition (EMT), such as Twist, Snail and Slug. (Klemke *et al.*,

1997; Welch *et al.*, 2000; Chen *et al.*, 2009a; Hong *et al.*, 2011; Nagarajan *et al.*, 2012).

The relationship between LAAO and MAPK pathway has thus far remained elusive. However, some clues can be obtained by analyzing the responses of MAPK pathway towards intracellular ROS. It is commonly described that ROS can trigger the activation of JNK or p38-MAPK pathway, which can facilitate the ROS mediated cell apoptosis (Runchel *et al.*, 2011). Nonetheless, several studies also indicate the role of ERK pathway in response to ROS induction. A non-aromatic B-ring flavonoid (DHEC), isolated from Macrothelypteris viridifrons, induced apoptosis in human colon HT-29 tumor cells via ROS-mitochondrial dysfunction, activation of p38 and JNK and inhibition of phosphorylated ERK (Wei *et al.*, 2011). Similar findings were observed in mycotoxin zearalenone induced apoptosis of RAW267.4 macrophages (Yu *et al.*, 2011). Krifka S *et al.* reviewed the adaptive mechanisms in cell responses to oxidative stress caused by dental resin monomers, finding that the downstream targets of ERK pathway were inhibited, including Elk-1, AFT-2, AFT-3 and c-Jun (Krifka *et al.*, 2013). All these evidence suggest, at least partially, that ROS may result in the down-regulation of ERK pathway. Therefore, it would seem that LAAO suppress the ERK pathway probably via the induction of intracellular ROS. Nevertheless, the direct interaction of LAAO with plasma membrane should also not be ignored.

4.4 Application of cDNA microarray and SILAC to understand the biology of BHV and LAAO-treated NUGC-3 cancer cells

During last two decades, with the advances in bioinformatics (i.e. genomics and proteomics), the systematic analysis of gene and protein expressions of cells or tissues in large scale become realised. Tens of thousands of genes or proteins can be analyzed in one set of experiment. Two such approaches applied in this study are cDNA microarray (gene chip) and SILAC (Stable Isotopic Labeling using Amino acids in Cell culture) techniques. Because of the advantage in time- and cost- efficiency, SILAC and gene chip are now widely used in cancer research to detect oncogenic and tumor suppressor genes/proteins, signaling transduction, biomarkers, treatment targets, and so on (Macgregor *et al.*, 2002; Marimuthu *et al.*, 2013).

4.4.1 Altered genes in BHV treated NUGC-3 gastric cancer cells

In this study, the Affymetrix gene microarray was conducted in NUGC-3 cells after treatment with partially purified BHV (BHV-F1). 69 genes were considered to be differentially regulated by BHV-F1 with the criteria fold change more than 2 and p value less than 0.05. These genes were grouped using DAVID, which helps researchers focus on the genes involved in interested cellular processes such as cell cycle and cell apoptosis. Moreover, these genes were further analyzed by Pathway Studio software to better understand their involvement in various cellular processes. A more extensive

and clearer regulation network was proposed. For example, the genes involved in cell cycle and cell apoptosis analyzed by Pathway Studio are shown in Fig 4.1 and Fig 4.2, respectively. In such networks, the cell processes, involved proteins, protein types and locations, as well as types of regulation (positive or negative) are shown in order.

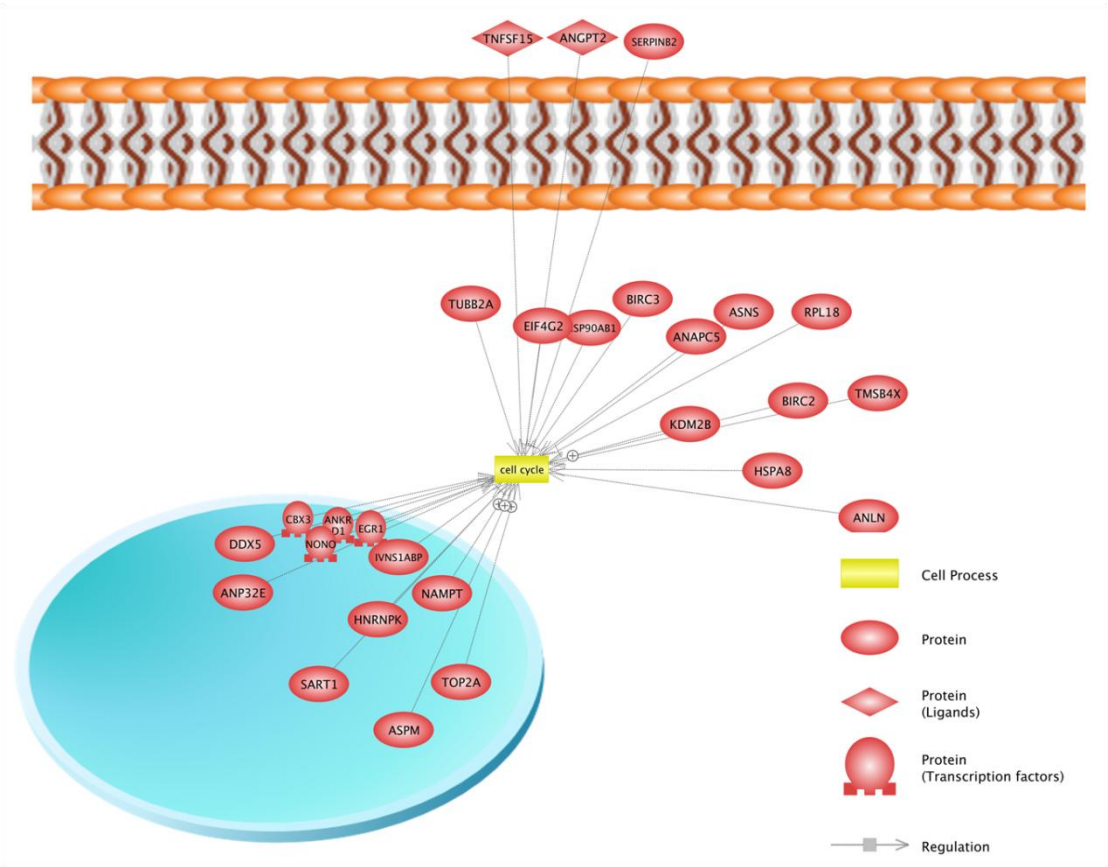

Fig 4.1 Networks of cell cycle related genes analyzed by Pathway Studio.

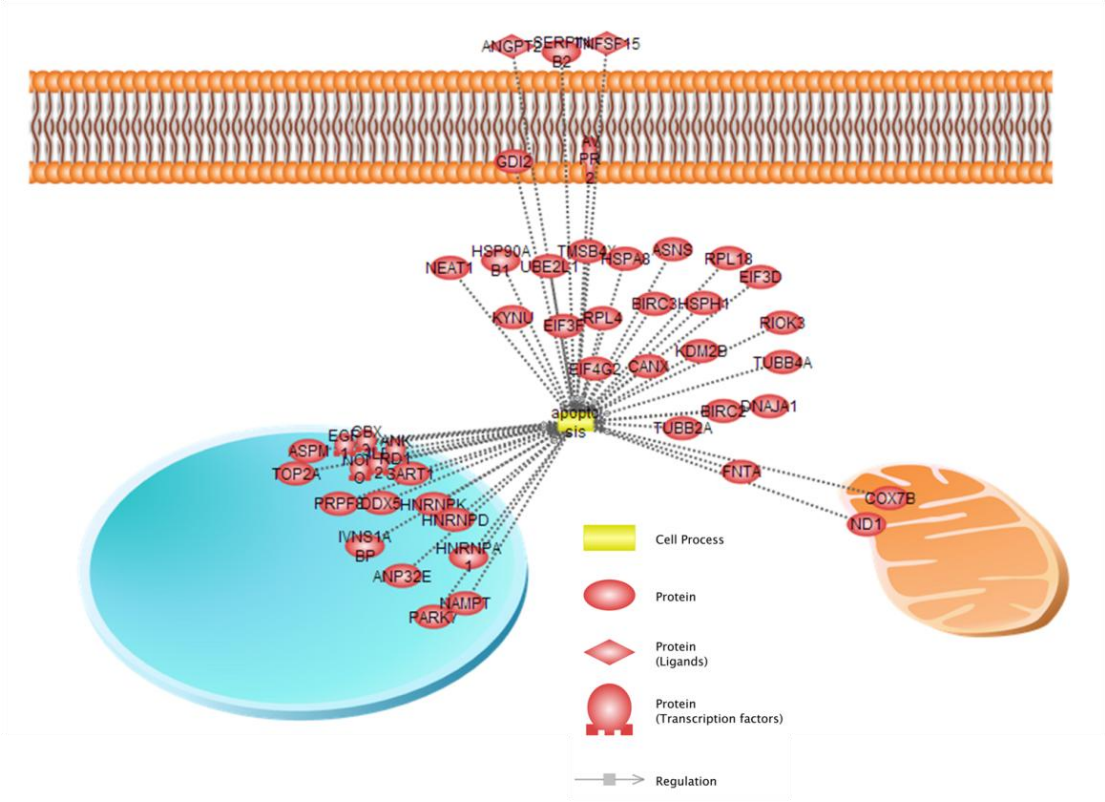

Fig 4.2 Networks of cell apoptosis related genes analyzed by Pathway Studio.

All these gene targets identified from microarray, which are involved in the regulations of cell cycle, apoptosis, cytoskeleton, DNA repair and oxidation reduction, deserve further investigations for novel therapeutic targets. For instance, TOP2A, which encode DNA topoisomerase II, have been implicated in the development of several antitumor agents. A variety of mutations in this gene are associated with the acquirement of drug resistance (Fortune & Osheroff, 2000; Pommier *et al.*, 2010). TUBB, the gene for beta-tubulin, is a major component to assemble microtubules and form cytoskeleton. The anticancer drugs like paclitaxel and vinca alkaloids can target tubulin and kill cancer cells (Hadfield *et al.,* 2003; Pasquier & Kavallaris,

2008). ANAPC5 (anaphase promoting complex subunit 5), which was 15 folds decreased after BHV treatment, is a cell cycle related-E3 ubiquitin ligase that controls progression through mitosis and the G1 phase of the cell cycle (Peters & Jan-Michael, 2002).

Furthermore, by literature review, several genes involved in MAPK/ERK pathway were identified. For example, the eukaryotic translation initiation factors (EIF3D, EIF3F and EIF4G2) are found to be regulated by MAP kinase interacting Ser/Thr kinase 1/2 (MNK 1/2), which are directly activated by ERK 1/2 (Jackson *et al.*, 2010). EIF protein family can bind to 40S ribosome and help maintain 40S and 60S ribosomal subunits, which play an important role in mRNA translation and protein synthesis. Interestingly, EIF3 proteins can also be inhibited by tAIF in cytosol (Kim *et al.*, 2006). Several genes from heterogeneous nuclear ribonucleoproteins (HNRNPA1, HNRNPD and HNRNPK) are also downstream targets of ERK 1/2. HNRNP proteins can function as the substrate of kinases and bind to DNA and RNA in a sequence specific manner, regulating gene translation and mRNA metabolism (Notari *et al.*, 2006). All these gene changes are in agreement with functional observations and signaling studies and further provide new information about mechanisms of actions.

4.4.2 Altered proteins in LAAO treated NUGC-3 gastric cancer cells

In this study, SILAC experiment was performed to examine the protein expression of NUGC-3 cells after treatment with LAAO in a large scale. Results

showed that many of the differentially expressed proteins are related to mitochondria structures and functions (e.g. AFG3L2, ACAT1, ALDH18A1, DC1, HADHA, HDAHB, ACAA2, PMPCA, PMPCB, SDHA and SUCLG1 in Table 3.3), which may be responsible for the mitochondria mediated caspase-independent apoptosis. For example, SDHA which is short for succinate dehydrogenase subunit A, flavoprotein, is involved in complex II of the mitochondrial electron transport chain. The decrease of SDHA was reported Hippi expression induced HeLa cell apoptosis, accompanied by AIF release (Majumder *et al.,* 2006).

Since the treatment agents and conditions are different, the SILAC data cannot be compared with microarray data directly. However, several similarities and consistence are identified. For example, a decreased expression of Ras GTPase-activating-like protein IQGAP3 was observed in SILAC data, which is described as an upstream activator of Ras/ERK pathway (Nojima *et al.*, 2008; Yang *et al.*, 2014). The EIF genes were found to be inhibited in microarray data by BHV and one EIF protein inhibitor EIF4EBP1 (eukaryotic translation initiation factor 4E-binding protein 1) was up-regulated by LAAO treatment. Another protein from HNRNP family (HNRNPM) was also down-regulated by LAAO treatment. Moreover, the down-regulation of heat shock protein family (HSP90AB1, HSPA8 and HSPH1) was observed in BHV treated NUGC-3 cells. A putative heat shock protein HSP90-beta 4 (HSP90AB4P) was also changed by LAAO treatment. HSP family have been

reported to promote cell apoptosis, which was supported by Bengalin induced apoptosis in leukemic cells (Ravagnan *et al.*, 2001; Gupta *et al.*, 2010).

Clearly, the DNA microarray and SILAC can identify a lot of differentially regulated genes and proteins, which provide valuable information to help researchers understand cancer responses to intervention, mechanisms of actions, novel biomarker and anticancer targets. However, how to analyse these hundreds of thousands of genes or proteins is still a challenging task. Nowadays, advanced bioinformatics software and tools have been developed to facilitate researchers to in the analysis of these large volumes of data, including DAVID, KEGG, GeneSpring, Pathway Studio and Partek Genomics Suite.

4.5 Conclusions

In the current study, the anticancer potential of scorpion venoms and snake venom L-amino acid oxidase (LAAO) were screened, evaluated and investigated in gastric cancer *in vitro* and *in vivo*. Particularly, the anticancer effects of *Hottentotta hottentotta* scorpion venoms (BHV) and LAAO from *Crotalus adamanteus* snake venom were extensively studied by various functional analysis and mechanisms detections.

First, the anti-proliferative effects of several scorpion venoms were examined and compared. It was found that scorpion venom from *Mesobuthus martensi karsch* had limited anti-proliferative effects on NUGC-3 gastric cancer cells, and no effect on the proliferation of breast cancer cells.

Comparatively, scorpion venoms from *Hottentotta hottentotta, Heterometrus longimanus* and *Pandinus imperator* exerted stronger inhibition of NUGC-3 cell proliferation, among which BHV was the most promising exhibiting a low IC50.

Next, the anticancer activities of BHV were investigated in both NUGC-3 gastric cancer cell line and a xenograft tumor model. BHV decreased the cell viability/proliferation of NUGC-3 dose-dependently by cell cycle arrest at sub-G1 phase and induction of cell apoptosis, which was confirmed by Annexin V staining. Morphological characteristics of apoptosis such as membrane blebbing and chromatin condensation were observed under fluorescence microscope and TEM. Interestingly, at low concentration, BHV also inhibited cell migration and invasion of NUGC-3 cells. *In vivo*, BHV inhibited the NUGC-3 tumor growth, with histological evidence of disruption of tissue homogeneity and induced apoptosis *in situ*.

Subsequently, BHV crude venom was partially purified and characterized by HPLC, SDS-PAGE and mass spectrum, with the identification of L-amino acid oxidase (LAAO) as the active molecule in BHV. In view of the inability to produce LAAO in BHV from the supplier, a LAAO from *Crotalus adamanteus* snake venom was evaluated for its anticancer effects in NUGC-3 cells. Similar findings including the decrease in cell viability, cell cycle arrest at G2/M phase, induction of apoptosis and the inhibition on cell migration were observed in both BHV and LAAO treated NUGC-3 cells. BHV and LAAO also induced a caspase-independent apoptosis (CIA), which was confirmed in

western blot, caspase-3 activity assay as well as with the presence of pan caspase inhibitor z-VAD-fmk.

The mechanisms and pathways in NUGC-3 gastric cancer cells in response to BHV and LAAO treatment are briefly summarized in as such: BHV/LAAO increases intracellular ROS, which causes mitochondria dysfunction and inhibits MAPK/ERK signaling pathway. Subsequently, AIF translocates from mitochondria to nucleus and initiates a caspase-independent apoptosis. Concomitantly, the inhibition of ERK pathway results in the decrease in cell proliferation/viability, cell cycle arrest, suppression of cell migration and invasion, as well as contribution to cell apoptosis. The proposed regulatory networks are shown in Fig 4.3.

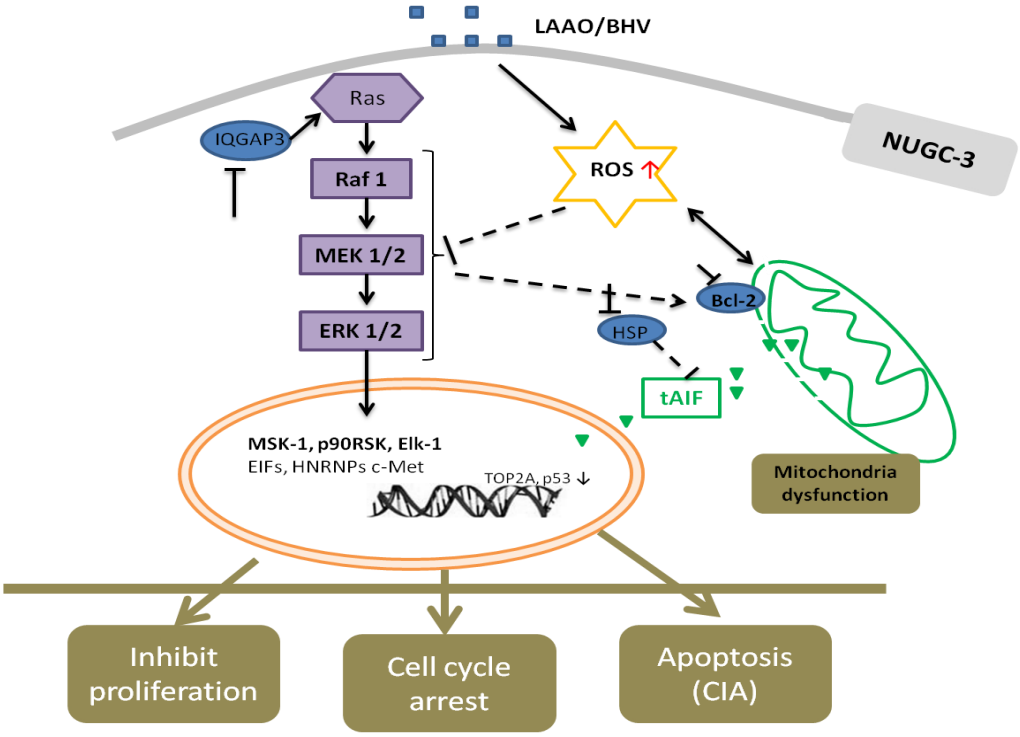

Fig 4.3 Diagram showing the possible mechanistic pathways of how LAAO/BHV exerts the anticancer actions in NUGC-3 cells.

The combination of transcriptomic and proteomic approaches have leaded to the identification of several gene and protein candidates from the microarray data and SILAC analysis, such as EIF, HNRNP and HSP families as well as TUBB, TOP2A and SDHA, which could be important and promising anticancer targets worthy of further studies.

4.6 Future work

The future directions of this study are:

- Further investigation into the selectivity of LAAO to gastric cancer and normal cells. As it was found that LAAO had certain preference to target poorly differentiated gastric cancer cells, future work will include more gastric cancer and normal cell lines to compare the cytotoxicity of LAAO to poorly differentiated and well differentiated gastric cancer cells, and cytotoxicity to cancerous and normal gastric cells.
- Elucidating the mechanism by which LAAO inhibits NUGC-3 cell motility. One interesting finding in this project is the inhibitory effect of LAAO to NUGC-3 cell motility at low concentration. The Cell Motility RT^2 Profiler PCR Array could be employed to elucidate how LAAO may regulate the selected 84 genes involved in NUGC-3 cell migration and invasion.
- Verifying the role of ROS in LAAO induced caspase independent apoptosis. In the present study, the role of ROS activated by LAAO

treatment appears to play an important role in the regulation of MAPK/ERK pathway, mitochondria dysfunction and AIF translocation. Further confirmation could be performed by abrogating ROS formation with catalase.

- Assessing the safety and antitumor activity of LAAO in NUGC-3 xenograft tumor model. The mouse xenograft tumor model is of great importance in the evaluation of LAAO`s anticancer potential. Therefore, this study will continue to assess the safety and efficacy of LAAO in NUGC-3 xenografts. As the present animal model used is a subcutaneous model, an orthotopic model can be employed.
- Validating targeted candidates from the microarray and SILAC data. Several gene/protein candidates have been identified as potential therapeutic targets of gastric cancer from microarray and SILAC assays, including EIFs, HNRNPs, HSPs, TUBB, TOP2A, and SDHA. These candidates will be further validated by RT-PCR, western blot and approaches such as siRNA-mediated silencing of the genes and small inhibitors of the proteins.

REFERENCES

REFERENCES

Ahn MY, Lee BM & Kim YS. (1997). Characterization and cytotoxicity of L-amino acid oxidase from the venom of king cobra (Ophiophagus hannah). *The international journal of biochemistry & cell biology* **29,** 911-919.

Ahn MY, Ryu KS, Lee YW & Kim YS. (2000). Cytotoxicity and L-amino acid oxidase activity of crude insect drugs. *Archives of pharmacal research* **23,** 477-481.

Al Saghie A. (2013). Gastric Cancer: Environmental Risk Factors, Treatment and Prevention. *Journal of Carcinogenesis & Mutagenesis* **S14**.

Albarello L, Pecciarini L & Doglioni C. (2011). HER2 testing in gastric cancer. *Advances in anatomic pathology* **18,** 53-59.

Ali SA, Stoeva S, Schutz J, Kayed R, Abassi A, Zaidi ZH & Voelter W. (1998). Purification and primary structure of low molecular mass peptides from scorpion (Buthus sindicus) venom. *Comparative biochemistry and physiology Part A, Molecular & integrative physiology* **121,** 323-332.

Almaaytah A & Albalas Q. (2014). Scorpion venom peptides with no disulfide bridges: a review. *Peptides* **51,** 35-45.

Almeida FM, Pimenta AMC, De Figueiredo SG, Santoro MM, Martin-Eauclaire MF, Diniz CR & De Lima ME. (2002). Enzymes with gelatinolytic activity can be found in Tityus bahiensis and Tityus serrulatus venoms. *Toxicon* **40,** 1041-1045.

Andreotti N, Jouirou B, Mouhat S, Mouhat L & Sabatier J-M. (2010). Therapeutic Value of Peptides from Animal Venoms. In *Comprehensive Natural Products II*, ed. Liu H-W & Mander L, pp. 287-303. Elsevier, Oxford.

Arteaga CL. (2002). Epidermal growth factor receptor dependence in human tumors: more than just expression? *The oncologist* **7 Suppl 4,** 31-39.

Asher V, Sowter H, Shaw R, Bali A & Khan R. (2010). Eag and HERG potassium channels as novel therapeutic targets in cancer. *World journal of surgical oncology* **8,** 113.

Axon A. (2006). Symptoms and diagnosis of gastric cancer at early curable stage. *Best practice & research Clinical gastroenterology* **20,** 697-708.

Balmanno K & Cook SJ. (2009). Tumour cell survival signalling by the ERK1/2 pathway. *Cell death and differentiation* **16,** 368-377.

Bang YJ, Van Cutsem E, Feyereislova A, Chung HC, Shen L, Sawaki A, Lordick F, Ohtsu A, Omuro Y, Satoh T, Aprile G, Kulikov E, Hill J, Lehle M, Ruschoff J & Kang YK. (2010). Trastuzumab in combination with chemotherapy versus chemotherapy alone for treatment of HER2-positive advanced gastric or gastro-oesophageal junction cancer (ToGA): a phase 3, open-label, randomised controlled trial. *Lancet* **376,** 687-697.

Barnett A. (2007). Exenatide. *Expert opinion on pharmacotherapy* **8,** 2593-2608.

Beghelli S, de Manzoni G, Barbi S, Tomezzoli A, Roviello F, Di Gregorio C, Vindigni C, Bortesi L, Parisi A, Saragoni L, Scarpa A & Moore PS. (2006). Microsatellite instability in gastric cancer is associated with better prognosis in only stage II cancers. *Surgery* **139,** 347-356.

Bidere N, Lorenzo HK, Carmona S, Laforge M, Harper F, Dumont C & Senik A. (2003). Cathepsin D triggers Bax activation, resulting in selective apoptosis-inducing factor (AIF) relocation in T lymphocytes entering the early commitment phase to apoptosis. *The Journal of biological chemistry* **278,** 31401-31411.

Boucher MJ, Morisset J, Vachon PH, Reed JC, Laine J & Rivard N. (2000). MEK/ERK signaling pathway regulates the expression of Bcl-2, Bcl-X-L, and Mcl-1 and promotes survival of human pancreatic cancer cells. *Journal of cellular biochemistry* **79,** 355-369.

Bradford MM. (1976). A rapid and sensitive method for the quantitation of microgram quantities of protein utilizing the principle of protein-dye binding. *Analytical biochemistry* **72,** 248-254.

Burke JE & Dennis EA. (2009). Phospholipase A2 structure/function, mechanism, and signaling. *Journal of lipid research* **50 Suppl,** S237-242.

Cabon L, Galan-Malo P, Bouharrour A, Delavallee L, Brunelle-Navas MN, Lorenzo HK, Gross A & Susin SA. (2012). BID regulates AIF-mediated caspase-independent necroptosis by promoting BAX activation. *Cell death and differentiation* **19,** 245-256.

Calderon LA, Sobrinho JC, Zaqueo KD, de Moura AA, Grabner AN, Mazzi MV, Marcussi S, Nomizo A, Fernandes CF, Zuliani JP, Carvalho BM, da Silva SL, Stabeli RG

& Soares AM. (2014). Antitumoral activity of snake venom proteins: new trends in cancer therapy. *BioMed research international* **2014,** 203639.

Cao P, Yu J, Lu W, Cai X, Wang Z, Gu Z, Zhang J, Ye T & Wang M. (2010). Expression and purification of an antitumor-analgesic peptide from the venom of Mesobuthus martensii Karsch by small ubiquitin-related modifier fusion in Escherichia coli. *Biotechnology progress* **26,** 1240-1244.

Castle NA. (2010). Pharmacological modulation of voltage-gated potassium channels as a therapeutic strategy. *Expert opinion on therapeutic patents* **20,** 1471-1503.

Chen H, Zhu G, Li Y, Padia RN, Dong Z, Pan ZK, Liu K & Huang S. (2009a). Extracellular signal-regulated kinase signaling pathway regulates breast cancer cell migration by maintaining slug expression. *Cancer research* **69,** 9228-9235.

Chen HC, Chen HJ, Khan MA, Rao ZZ, Wan XX, Tan B & Zhang DZ. (2011). Genetic mutations of p53 and k-ras in gastric carcinoma patients from Hunan, China. *Tumour biology* **32,** 367-373.

Chen T & Wong YS. (2009b). Selenocystine induces caspase-independent apoptosis in MCF-7 human breast carcinoma cells with involvement of p53 phosphorylation and reactive oxygen species generation. *The international journal of biochemistry & cell biology* **41,** 666-676.

Chen Y, Cao L, Zhong M, Zhang Y, Han C, Li Q, Yang J, Zhou D, Shi W, He B, Liu F, Yu J, Sun Y, Cao Y, Li Y, Li W, Guo D, Cao Z & Yan H. (2012). Anti-HIV-1 activity of a new scorpion venom peptide derivative Kn2-7. *PloS one* **7,** e34947.

Chiaravalli AM, Feltri M, Bertolini V, Bagnoli E, Furlan D, Cerutti R, Novario R & Capella C. (2006). Intratumour T cells, their activation status and survival in gastric carcinomas characterised for microsatellite instability and Epstein-Barr virus infection. *Virchows Archiv : an international journal of pathology* **448,** 344-353.

Chuang RS, Jaffe H, Cribbs L, Perez-Reyes E & Swartz KJ. (1998). Inhibition of T-type voltage-gated calcium channels by a new scorpion toxin. *Nature neuroscience* **1,** 668-674.

Cirman T, Oresic K, Mazovec GD, Turk V, Reed JC, Myers RM, Salvesen GS & Turk B. (2004). Selective disruption of lysosomes in HeLa cells triggers apoptosis mediated by cleavage of Bid by multiple papain-like lysosomal cathepsins. *The Journal of biological chemistry* **279,** 3578-3587.

Clayburgh DR & Turner JR. (2004). Stomach, Anatomy. In *Encyclopedia of Gastroenterology*, ed. Johnson LR, pp. 458-462. Elsevier, New York.

Constantinou C, Papas KA & Constantinou AI. (2009). Caspase-independent pathways of programmed cell death: the unraveling of new targets of cancer therapy? *Current cancer drug targets* **9,** 717-728.

Corona M, Gurrola GB, Merino E, Cassulini RR, Valdez-Cruz NA, Garcia B, Ramirez-Dominguez ME, Coronas FI, Zamudio FZ, Wanke E & Possani LD. (2002). A large number of novel Ergtoxin-like genes and ERG K+-channels blocking peptides from scorpions of the genus Centruroides. *FEBS letters* **532,** 121-126.

Correa P & Piazuelo MB. (2012). The gastric precancerous cascade. *Journal of digestive diseases* **13,** 2-9.

Corso G, Pedrazzani C, Marrelli D, Pascale V, Pinto E & Roviello F. (2009). Correlation of microsatellite instability at multiple loci with long-term survival in advanced gastric carcinoma. *Archives of Surgery* **144,** 722-727.

Couraud F, Jover E, Dubois JM & Rochat H. (1982). Two types of scorpion receptor sites, one related to the activation, the other to the inactivation of the action potential sodium channel. *Toxicon* **20,** 9-16.

Cuddapah VA & Sontheimer H. (2011). Ion channels and transporters [corrected] in cancer. 2. Ion channels and the control of cancer cell migration. *American journal of physiology Cell physiology* **301,** C541-549.

Cui Y, Liu Y, Chen Q, Zhang R, Song Y, Jiang Z, Wu C & Zhang J. (2010). Genomic cloning, characterization and statistical analysis of an antitumor-analgesic peptide from Chinese scorpion Buthus martensii Karsch. *Toxicon* **56,** 432-439.

Cushman DW & Ondetti MA. (1991). History of the design of captopril and related inhibitors of angiotensin converting enzyme. *Hypertension* **17,** 589-592.

D'Elia L, Rossi G, Ippolito R, Cappuccio FP & Strazzullo P. (2012). Habitual salt intake and risk of gastric cancer: a meta-analysis of prospective studies. *Clinical nutrition* **31,** 489-498.

D'Suze G, Rosales A, Salazar V & Sevcik C. (2010). Apoptogenic peptides from Tityus discrepans scorpion venom acting against the SKBR3 breast cancer cell line. *Toxicon* **56,** 1497-1505.

Dai C, Ma Y, Zhao Z, Zhao R, Wang Q, Wu Y, Cao Z & Li W. (2008). Mucroporin, the first cationic host defense peptide from the venom of Lychas mucronatus. *Antimicrobial agents and chemotherapy* **52,** 3967-3972.

Davies H, Bignell GR, Cox C, Stephens P, Edkins S, Clegg S, Teague J, Woffendin H, Garnett MJ, Bottomley W, Davis N, Dicks E, Ewing R, Floyd Y, Gray K, Hall S, Hawes R, Hughes J, Kosmidou V, Menzies A, Mould C, Parker A, Stevens C, Watt S, Hooper S, Wilson R, Jayatilake H, Gusterson BA, Cooper C, Shipley J, Hargrave D, Pritchard-Jones K, Maitland N, Chenevix-Trench G, Riggins GJ, Bigner DD, Palmieri G, Cossu A, Flanagan A, Nicholson A, Ho JW, Leung SY, Yuen ST, Weber BL, Seigler HF, Darrow TL, Paterson H, Marais R, Marshall CJ, Wooster R, Stratton MR & Futreal PA. (2002). Mutations of the BRAF gene in human cancer. *Nature* **417,** 949-954.

de Vieira Santos MM, Sant'Ana CD, Giglio JR, da Silva RJ, Sampaio SV, Soares AM & Fecchio D. (2008). Antitumoural effect of an L-amino acid oxidase isolated from Bothrops jararaca snake venom. *Basic & clinical pharmacology & toxicology* **102,** 533-542.

DeBin JA, Maggio JE & Strichartz GR. (1993). Purification and characterization of chlorotoxin, a chloride channel ligand from the venom of the scorpion. *The American journal of physiology* **264,** C361-369.

Delavallee L, Cabon L, Galan-Malo P, Lorenzo HK & Susin SA. (2011). AIF-mediated caspase-independent necroptosis: a new chance for targeted therapeutics. *IUBMB life* **63,** 221-232.

Deshane J, Garner CC & Sontheimer H. (2003). Chlorotoxin inhibits glioma cell invasion via matrix metalloproteinase-2. *The Journal of biological chemistry* **278,** 4135-4144.

Dhillon PK, Farrow DC, Vaughan TL, Chow WH, Risch HA, Gammon MD, Mayne ST, Stanford JL, Schoenberg JB, Ahsan H, Dubrow R, West AB, Rotterdam H, Blot WJ & Fraumeni JF, Jr. (2001). Family history of cancer and risk of esophageal and gastric cancers in the United States. *International journal of cancer* **93,** 148-152.

Diego-García E, Peigneur S, Debaveye S, Gheldof E, Tytgat J & Caliskan F. (2013). Novel potassium channel blocker venom peptides from Mesobuthus gibbosus (Scorpiones: Buthidae). *Toxicon* **61,** 72-82.

Ding J, Chua PJ, Bay BH & Gopalakrishnakone P. (2014). Scorpion venoms as a potential source of novel cancer therapeutic compounds. *Experimental Biology and Medicine (Maywood)* **239,** 387-393.

Du XY & Clemetson KJ. (2002). Snake venom l-amino acid oxidases. *Toxicon* **40,** 659-665.

Earle CC & Maroun JA. (1999). Adjuvant chemotherapy after curative resection for gastric cancer in non-Asian patients: revisiting a meta-analysis of randomised trials. *European Journal of Cancer* **35,** 1059-1064.

Edge SB & Compton CC. (2010). The American Joint Committee on Cancer: the 7th edition of the AJCC cancer staging manual and the future of TNM. *Annals of Surgical Oncology* **17,** 1471-1474.

Eslick GD. (2006). Helicobacter pylori infection causes gastric cancer? A review of the epidemiological, meta-analytic, and experimental evidence. *World journal of gastroenterology* **12,** 2991-2999.

Estep AL, Palmer C, McCormick F & Rauen KA. (2007). Mutation analysis of BRAF, MEK1 and MEK2 in 15 ovarian cancer cell lines: implications for therapy. *PloS one* **2,** e1279.

Fan S, Sun Z, Jiang D, Dai C, Ma Y, Zhao Z, Liu H, Wu Y, Cao Z & Li W. (2010). BmKCT toxin inhibits glioma proliferation and tumor metastasis. *Cancer letters* **291,** 158-166.

Feng L, Gao R & Gopalakrishnakone P. (2008). Isolation and characterization of a hyaluronidase from the venom of Chinese red scorpion Buthus martensi. *Comparative biochemistry and physiology Toxicology & pharmacology* **148,** 250-257.

Fletcher PL, Jr., Fletcher MD, Weninger K, Anderson TE & Martin BM. (2010). Vesicle-associated membrane protein (VAMP) cleavage by a new metalloprotease from the Brazilian scorpion Tityus serrulatus. *The Journal of biological chemistry* **285,** 7405-7416.

Fortune JM & Osheroff N. (2000). Topoisomerase II as a target for anticancer drugs: when enzymes stop being nice. *Progress in nucleic acid research and molecular biology* **64,** 221-253.

Franca SC, Kashima S, Roberto PG, Marins M, Ticli FK, Pereira JO, Astolfi-Filho S, Stabeli RG, Magro AJ, Fontes MR, Sampaio SV & Soares AM. (2007). Molecular approaches for structural characterization of Bothrops L-amino acid oxidases with antiprotozoal activity: cDNA cloning, comparative sequence analysis, and molecular modeling. *Biochemical and biophysical research communications* **355,** 302-306.

Franke JC, Plotz M, Prokop A, Geilen CC, Schmalz HG & Eberle J. (2010). New caspase-independent but ROS-dependent apoptosis pathways are targeted in

melanoma cells by an iron-containing cytosine analogue. *Biochemical pharmacology* **79,** 575-586.

Fraser SP, Diss JK, Chioni AM, Mycielska ME, Pan H, Yamaci RF, Pani F, Siwy Z, Krasowska M, Grzywna Z, Brackenbury WJ, Theodorou D, Koyuturk M, Kaya H, Battaloglu E, De Bella MT, Slade MJ, Tolhurst R, Palmieri C, Jiang J, Latchman DS, Coombes RC & Djamgoz MB. (2005). Voltage-gated sodium channel expression and potentiation of human breast cancer metastasis. *Clinical cancer research* **11,** 5381-5389.

Gao F, Li H, Chen YD, Yu XN, Wang R & Chen XL. (2009). Upregulation of PTEN involved in scorpion venom-induced apoptosis in a lymphoma cell line. *Leukemia & Lymphoma* **50,** 633-641.

Gao R, Zhang Y & Gopalakrishnakone P. (2008). Purification and N-terminal sequence of a serine proteinase-like protein (BMK-CBP) from the venom of the Chinese scorpion (Buthus martensii Karsch). *Toxicon* **52,** 348-353.

Girish KS & Kemparaju K. (2007). The magic glue hyaluronan and its eraser hyaluronidase: a biological overview. *Life sciences* **80,** 1921-1943.

Gonzalez CA & Lopez-Carrillo L. (2010). Helicobacter pylori, nutrition and smoking interactions: their impact in gastric carcinogenesis. *Scandinavian journal of gastroenterology* **45,** 6-14.

Gotoda T & Jung H-Y. (2013). Endoscopic resection (endoscopic mucosal resection/ endoscopic submucosal dissection) for early gastric cancer. *Digestive Endoscopy* **25,** 55-63.

Gravalos C & Jimeno A. (2008). HER2 in gastric cancer: a new prognostic factor and a novel therapeutic target. *Annals of oncology* **19,** 1523-1529.

Graziano F, Humar B & Guilford P. (2003). The role of the E-cadherin gene (CDH1) in diffuse gastric cancer susceptibility: from the laboratory to clinical practice. *Annals of oncology* **14,** 1705-1713.

Group HaCC. (2001). Gastric cancer and Helicobacter pylori: a combined analysis of 12 case control studies nested within prospective cohorts. *Gut* **49,** 347-353.

Guo C, Liu S, Yao Y, Zhang Q & Sun MZ. (2012). Past decade study of snake venom L-amino acid oxidase. *Toxicon* **60,** 302-311.

Guo Y, Zhang W, Yan YY, Ma CG, Wang X, Wang C & Zhao JL. (2013). Triterpenoid pristimerin induced HepG2 cells apoptosis through ROS-mediated mitochondrial dysfunction. *Journal of the Balkan Union of Oncology* **18,** 477-485.

Gupta SD, Gomes A, Debnath A & Saha A. (2010). Apoptosis induction in human leukemic cells by a novel protein Bengalin, isolated from Indian black scorpion venom: through mitochondrial pathway and inhibition of heat shock proteins. *Chemico-biological interactions* **183,** 293-303.

Gwee MC, Nirthanan S, Khoo HE, Gopalakrishnakone P, Kini RM & Cheah LS. (2002). Autonomic effects of some scorpion venoms and toxins. *Clinical and experimental pharmacology & physiology* **29,** 795-801.

Gwee MCE, Cheah LS & Gopalakrishnakone P. (1995). Adrenergic nerve stimulation by venom of the scorpion Buthotus hottentota. *Toxicon* **33,** 718-719.

Hadfield JA, Ducki S, Hirst N & McGown AT. (2003). Tubulin and microtubules as targets for anticancer drugs. *Progress in cell cycle research* **5,** 309-325.

Hamilton JP & Meltzer SJ. (2006). A review of the genomics of gastric cancer. *Clinical gastroenterology and hepatology* **4,** 416-425.

Hancock RE & Sahl HG. (2006). Antimicrobial and host-defense peptides as new anti-infective therapeutic strategies. *Nature biotechnology* **24,** 1551-1557.

Handschuh G, Candidus S, Luber B, Reich U, Schott C, Oswald S, Becke H, Hutzler P, Birchmeier W, Hofler H & Becker KF. (1999). Tumour-associated E-cadherin mutations alter cellular morphology, decrease cellular adhesion and increase cellular motility. *Oncogene* **18,** 4301-4312.

Hauge C & Frodin M. (2006). RSK and MSK in MAP kinase signalling. *Journal of cell science* **119,** 3021-3023.

Heinen TE & da Veiga AB. (2011). Arthropod venoms and cancer. *Toxicon* **57,** 497-511.

Hong J, Zhou J, Fu J, He T, Qin J, Wang L, Liao L & Xu J. (2011). Phosphorylation of serine 68 of Twist1 by MAPKs stabilizes Twist1 protein and promotes breast cancer cell invasiveness. *Cancer research* **71,** 3980-3990.

Hu B, El Hajj N, Sittler S, Lammert N, Barnes R & Meloni-Ehrig A. (2012). Gastric cancer: Classification, histology and application of molecular pathology. *Journal of gastrointestinal oncology* **3,** 251-261.

Huang JQ, Zheng GF, Sumanac K, Irvine EJ & Hunt RH. (2003). Meta-analysis of the relationship between cagA seropositivity and gastric cancer. *Gastroenterology* **125,** 1636-1644.

Hudler P. (2012). Genetic aspects of gastric cancer instability. *The Scientific World Journal* **2012,** 761909.

Iacopetta BJ, Soong R, House AK & Hamelin R. (1999). Gastric carcinomas with microsatellite instability: clinical features and mutations to the TGF-beta type II receptor, IGFII receptor, and BAX genes. *The Journal of pathology* **187,** 428-432.

IARC Working Group on the Evaluation of Carcinogenic Risks to Humans. (1994). Schistosomes, liver flukes and Helicobacter pylori. *IARC monographs on the evaluation of carcinogenic risks to humans* **61,** 1-241.

Incamnoi P, Patramanon R, Thammasirirak S, Chaveerach A, Uawonggul N, Sukprasert S, Rungsa P, Daduang J & Daduang S. (2013). Heteromtoxin (HmTx), a novel heterodimeric phospholipase A2 from Heterometrus laoticus scorpion venom. *Toxicon* **61,** 62-71.

Jackson RJ, Hellen CU & Pestova TV. (2010). The mechanism of eukaryotic translation initiation and principles of its regulation. *Nature reviews Molecular cell biology* **11,** 113-127.

Jang SH, Choi SY, Ryu PD & Lee SY. (2011). Anti-proliferative effect of Kv1.3 blockers in A549 human lung adenocarcinoma in vitro and in vivo. *European journal of pharmacology* **651,** 26-32.

Jemal A, Bray F, Center MM, Ferlay J, Ward E & Forman D. (2011). Global cancer statistics. *CA: a cancer journal for clinicians* **61,** 69-90.

Kasper S & Schuler M. (2014). Targeted therapies in gastroesophageal cancer. *European Journal of Cancer* **50,** 1247-1258.

Kawanishi K, Doki Y, Shiozaki H, Yano M, Inoue M, Fukuchi N, Utsunomiya T, Watanabe H & Monden M. (2000). Correlation between loss of E-cadherin expression and overexpression of autocrine motility factor receptor in association

with progression of human gastric cancers. *American journal of clinical pathology* **113,** 266-274.

Kim EK & Choi EJ. (2010). Pathological roles of MAPK signaling pathways in human diseases. *Biochimica et biophysica acta* **1802,** 396-405.

Kim JT, Kim KD, Song EY, Lee HG, Kim JW, Chae SK, Kim E, Lee MS, Yang Y & Lim JS. (2006). Apoptosis-inducing factor (AIF) inhibits protein synthesis by interacting with the eukaryotic translation initiation factor 3 subunit p44 (eIF3g). *FEBS letters* **580,** 6375-6383.

Kim SS, Ruiz VE, Carroll JD & Moss SF. (2011). Helicobacter pylori in the pathogenesis of gastric cancer and gastric lymphoma. *Cancer letters* **305,** 228-238.

King GF. (2011). Venoms as a platform for human drugs: translating toxins into therapeutics. *Expert opinion on biological therapy* **11,** 1469-1484.

Klemke RL, Cai S, Giannini AL, Gallagher PJ, de Lanerolle P & Cheresh DA. (1997). Regulation of cell motility by mitogen-activated protein kinase. *The Journal of cell biology* **137,** 481-492.

Kohno M & Pouyssegur J. (2006). Targeting the ERK signaling pathway in cancer therapy. *Annals of Medicine* **38,** 200-211.

Krifka S, Spagnuolo G, Schmalz G & Schweikl H. (2013). A review of adaptive mechanisms in cell responses towards oxidative stress caused by dental resin monomers. *Biomaterials* **34,** 4555-4563.

Kubicka S, Claas C, Staab S, Kuhnel F, Zender L, Trautwein C, Wagner S, Rudolph KL & Manns M. (2002). p53 mutation pattern and expression of c-erbB2 and c-met in gastric cancer: relation to histological subtypes, Helicobacter pylori infection, and prognosis. *Digestive diseases and sciences* **47,** 114-121.

Kwon CH, Yoon CS & Kim YK. (2008). Ciglitazone induces caspase-independent apoptosis via p38-dependent AIF nuclear translocation in renal epithelial cells. *Toxicology* **244,** 13-24.

Lauren P. (1965). The Two Histological Main Types of Gastric Carcinoma: Diffuse and So-Called Intestinal-Type Carcinoma. An Attempt at a Histo-Clinical Classification. *Acta pathologica et microbiologica Scandinavica* **64,** 31-49.

Lawrence W, Jr. (2004). Gastric adenocarcinoma. *Current Treatment Options in Gastroenterology* **7,** 149-157.

Lee ML, Chung I, Fung SY, Kanthimathi MS & Tan NH. (2014). Anti-Proliferative Activity of King Cobra (Ophiophagus hannah) Venom L-Amino Acid Oxidase. *Basic & clinical pharmacology & toxicology* ***114,*** 336-343.

Lee ML, Fung SY, Chung I, Pailoor J, Cheah SH & Tan NH. (2014). King cobra (Ophiophagus hannah) venom L-amino acid oxidase induces apoptosis in PC-3 cells and suppresses PC-3 solid tumor growth in a tumor xenograft mouse model. *International journal of medical sciences* **11,** 593-601.

Leung WK, Wu MS, Kakugawa Y, Kim JJ, Yeoh KG, Goh KL, Wu KC, Wu DC, Sollano J, Kachintorn U, Gotoda T, Lin JT, You WC, Ng EK & Sung JJ. (2008). Screening for gastric cancer in Asia: current evidence and practice. *The lancet oncology* **9,** 279-287.

Lewis RJ & Garcia ML. (2003). Therapeutic potential of venom peptides. *Nature Reviews Drug Discovery* **2,** 790-802.

Lewis TS, Shapiro PS & Ahn NG. (1998). Signal transduction through MAP kinase cascades. *Advances in cancer research* **74,** 49-139.

Li-Weber M. (2009). New therapeutic aspects of flavones: the anticancer properties of Scutellaria and its main active constituents Wogonin, Baicalein and Baicalin. *Cancer treatment reviews* **35,** 57-68.

Ling YH, el-Naggar AK, Priebe W & Perez-Soler R. (1996). Cell cycle-dependent cytotoxicity, G2/M phase arrest, and disruption of p34cdc2/cyclin B1 activity induced by doxorubicin in synchronized P388 cells. *Molecular pharmacology* **49,** 832-841.

Liu C & Russell RM. (2008). Nutrition and gastric cancer risk: an update. *Nutrition reviews* **66,** 237-249.

Liu YF, Hu J, Zhang JH, Wang SL & Wu CF. (2002). Isolation, purification, and N-terminal partial sequence of an antitumor peptide from the venom of the Chinese scorpion Buthus martensii Karsch. *Preparative biochemistry & biotechnology* **32,** 317-327.

Liu YF, Ma RL, Wang SL, Duan ZY, Zhang JH, Wu LJ & Wu CF. (2003). Expression of an antitumor-analgesic peptide from the venom of Chinese scorpion Buthus martensii karsch in Escherichia coli. *Protein expression and purification* **27,** 253-258.

Livak KJ & Schmittgen TD. (2001). Analysis of relative gene expression data using real-time quantitative PCR and the 2(-Delta Delta C(T)) Method. *Methods* **25,** 402-408.

Look M, Gao F, Low CH & Nambiar R. (2001). Gastric cancer in Singapore. *Gastric Cancer* **4,** 219-222.

Loret E & Hammock B. (2001). Structure and Neurotoxicity of Venoms. In *Scorpion Biology and Research*, ed. Brownell P & Polis G, pp. 204-233. Oxford.

Ly JD, Grubb DR & Lawen A. (2003). The mitochondrial membrane potential (Δψm) in apoptosis; an update. *Apoptosis* **8,** 115-128.

Lyons SA, O'Neal J & Sontheimer H. (2002). Chlorotoxin, a scorpion-derived peptide, specifically binds to gliomas and tumors of neuroectodermal origin. *Glia* **39,** 162-173.

Ma Y, Zhang J, Zhang Q, Chen P, Song J, Yu S, Liu H, Liu F, Song C, Yang D & Liu J. (2014). Adenosine induces apoptosis in human liver cancer cells through ROS production and mitochondrial dysfunction. *Biochemical and biophysical research communications* **448,** 8-14.

Macgregor PF & Squire JA. (2002). Application of microarrays to the analysis of gene expression in cancer. *Clinical chemistry* **48,** 1170-1177.

Maher P & Hanneken A. (2005). The molecular basis of oxidative stress-induced cell death in an immortalized retinal ganglion cell line. *Investigative ophthalmology & visual science* **46,** 749-757.

Majumder P, Chattopadhyay B, Mazumder A, Das P &Bhattacharyya, NP. (2006). Induction of apoptosis in cells expressing exogenous Hippi, a molecular partner of huntingtin-interacting protein Hip1. *Neurobiology of Disease* **22,** 242-256.

Malfertheiner P, Fry LC & Monkemuller K. (2006). Can gastric cancer be prevented by Helicobacter pylori eradication? *Best practice & research Clinical gastroenterology* **20,** 709-719.

Mamelak AN, Rosenfeld S, Bucholz R, Raubitschek A, Nabors LB, Fiveash JB, Shen S, Khazaeli MB, Colcher D, Liu A, Osman M, Guthrie B, Schade-Bijur S, Hablitz DM, Alvarez VL & Gonda MA. (2006). Phase I single-dose study of intracavitary-

administered iodine-131-TM-601 in adults with recurrent high-grade glioma. *Journal of clinical oncology* **24,** 3644-3650.

Marimuthu A, Subbannayya Y, Sahasrabuddhe NA, Balakrishnan L, Syed N, Sekhar NR, Katte TV, Pinto SM, Srikanth SM, Kumar P, Pawar H, Kashyap MK, Maharudraiah J, Ashktorab H, Smoot DT, Ramaswamy G, Kumar RV, Cheng Y, Meltzer SJ, Roa JC, Chaerkady R, Prasad TS, Harsha HC, Chatterjee A & Pandey A. (2013). SILAC-based quantitative proteomic analysis of gastric cancer secretome. *Proteomics Clinical applications* **7,** 355-366.

Mathiasen IS & Jaattela M. (2002). Triggering caspase-independent cell death to combat cancer. *Trends in molecular medicine* **8,** 212-220.

McCubrey JA, Steelman LS, Chappell WH, Abrams SL, Montalto G, Cervello M, Nicoletti F, Fagone P, Malaponte G, Mazzarino MC, Candido S, Libra M, Basecke J, Mijatovic S, Maksimovic-Ivanic D, Milella M, Tafuri A, Cocco L, Evangelisti C, Chiarini F & Martelli AM. (2012). Mutations and deregulation of Ras/Raf/MEK/ERK and PI3K/PTEN/Akt/mTOR cascades which alter therapy response. *Oncotarget* **3,** 954-987.

Meng Z, Yang P, Shen Y, Bei W, Zhang Y, Ge Y, Newman RA, Cohen L, Liu L, Thornton B, Chang DZ, Liao Z & Kurzrock R. (2009). Pilot study of huachansu in patients with hepatocellular carcinoma, nonsmall-cell lung cancer, or pancreatic cancer. *Cancer* **115,** 5309-5318.

Menozzi A, Merlini PA & Ardissino D. (2005). Tirofiban in acute coronary syndromes. *Expert review of cardiovascular therapy* **3,** 193-206.

Miljanich GP. (2004). Ziconotide: neuronal calcium channel blocker for treating severe chronic pain. *Current medicinal chemistry* **11,** 3029-3040.

Mills JC. (2001). Mechanisms underlying the Hallmark features of the execution-phase of apoptosis. In *Advances in Cell Aging and Gerontology*, ed. Mark P. Mattson SEVMR, pp. 1-38. Elsevier.

Ming SC. (1977). Gastric carcinoma. A pathobiological classification. *Cancer* **39,** 2475-2485.

Morabito A, Carillio G & Longo R. (2009). Systemic treatment of gastric cancer. *Critical reviews in oncology/hematology* **70,** 216-234.

Muruganandan S & Cribb AE. (2006). Calpain-induced endoplasmic reticulum stress and cell death following cytotoxic damage to renal cells. *Toxicological sciences* **94,** 118-128.

Nagarajan D, Melo T, Deng Z, Almeida C & Zhao W. (2012). ERK/GSK3beta/Snail signaling mediates radiation-induced alveolar epithelial-to-mesenchymal transition. *Free radical biology & medicine* **52,** 983-992.

Nagini S. (2012). Carcinoma of the stomach: A review of epidemiology, pathogenesis, molecular genetics and chemoprevention. *World journal of gastrointestinal oncology* **4,** 156-169.

Nobili S, Bruno L, Landini I, Napoli C, Bechi P, Tonelli F, Rubio CA, Mini E & Nesi G. (2011). Genomic and genetic alterations influence the progression of gastric cancer. *World journal of gastroenterology* **17,** 290-299.

Nojima H, Adachi M, Matsui T, Okawa K & Tsukita S. (2008). IQGAP3 regulates cell proliferation through the Ras/ERK signalling cascade. *Nature Cell Biology* **10,** 971-978.

Notari M, Neviani P, Santhanam R, Blaser BW, Chang JS, Galietta A, Willis AE, Roy DC, Caligiuri MA, Marcucci G & Perrotti D. (2006). A MAPK/HNRPK pathway controls BCR/ABL oncogenic potential by regulating MYC mRNA translation. *Blood* **107,** 2507-2516.

O'Shea JC & Tcheng JE. (2002). Eptifibatide: a potent inhibitor of the platelet receptor integrin glycoprotein IIb/IIIa. *Expert opinion on pharmacotherapy* **3,** 1199-1210.

Okuno S, Shimizu S, Ito T, Nomura M, Hamada E, Tsujimoto Y & Matsuda H. (1998). Bcl-2 prevents caspase-independent cell death. *The Journal of biological chemistry* **273,** 34272-34277.

Onkal R & Djamgoz MB. (2009). Molecular pharmacology of voltage-gated sodium channel expression in metastatic disease: clinical potential of neonatal Nav1.5 in breast cancer. *European journal of pharmacology* **625,** 206-219.

Oren M. (1999). Regulation of the p53 tumor suppressor protein. *The Journal of biological chemistry* **274,** 36031-36034.

Ottini L, Falchetti M, Lupi R, Rizzolo P, Agnese V, Colucci G, Bazan V & Russo A. (2006). Patterns of genomic instability in gastric cancer: clinical implications and perspectives. *Annals of oncology* **17 Suppl 7,** vii97-102.

Ouadid-Ahidouch H, Roudbaraki M, Ahidouch A, Delcourt P & Prevarskaya N. (2004). Cell-cycle-dependent expression of the large Ca2+-activated K+ channels in breast cancer cells. *Biochemical and biophysical research communications* **316,** 244-251.

Ouyang G, Yao L, Ruan K, Song G, Mao Y & Bao S. (2009). Genistein induces G2/M cell cycle arrest and apoptosis of human ovarian cancer cells via activation of DNA damage checkpoint pathways. *Cell Biology International* **33,** 1237-1244.

Panzini I, Gianni L, Fattori PP, Tassinari D, Imola M, Fabbri P, Arcangeli V, Drudi G, Canuti D, Fochessati F & Ravaioli A. (2002). Adjuvant chemotherapy in gastric cancer: a meta-analysis of randomized trials and a comparison with previous meta-analyses. *Tumori* **88,** 21-27.

Pao W & Girard N. (2011). New driver mutations in non-small-cell lung cancer. *The lancet oncology* **12,** 175-180.

Parkin DM. (2006). The global health burden of infection-associated cancers in the year 2002. *International journal of cancer* **118,** 3030-3044.

Parreno M, Casanova I, Cespedes MV, Vaque JP, Pavon MA, Leon J & Mangues R. (2008). Bobel-24 and derivatives induce caspase-independent death in pancreatic cancer regardless of apoptotic resistance. *Cancer research* **68,** 6313-6323.

Pasquier E & Kavallaris M. (2008). Microtubules: a dynamic target in cancer therapy. *IUBMB Life* **60,** 165-170.

Pearson G, Robinson F, Beers Gibson T, Xu BE, Karandikar M, Berman K & Cobb MH. (2001). Mitogen-activated protein (MAP) kinase pathways: regulation and physiological functions. *Endocrine reviews* **22,** 153-183.

Perumal Samy R, Gopalakrishnakone P, Thwin MM, Chow TK, Bow H, Yap EH & Thong TW. (2007). Antibacterial activity of snake, scorpion and bee venoms: a comparison with purified venom phospholipase A2 enzymes. *Journal of applied microbiology* **102,** 650-659.

Peters & Jan-Michael. (2002). The Anaphase-Promoting Complex: Proteolysis in Mitosis and Beyond. *Molecular Cell* **9,** 931-943.

Petricevich VL. (2010). Scorpion venom and the inflammatory response. *Mediators of inflammation* **2010,** 903295.

Pommier Y, Leo E, Zhang H & Marchand C. (2010). DNA topoisomerases and their poisoning by anticancer and antibacterial drugs. *Chemistry & biology* **17,** 421-433.

Poornima P, Quency RS & Padma VV. (2013). Neferine induces reactive oxygen species mediated intrinsic pathway of apoptosis in HepG2 cells. *Food chemistry* **136,** 659-667.

Possani LD, Becerril B, Delepierre M & Tytgat J. (1999). Scorpion toxins specific for Na+-channels. *European journal of biochemistry* **264,** 287-300.

Possani LD, Merino E, Corona M, Bolivar F & Becerril B. (2000). Peptides and genes coding for scorpion toxins that affect ion-channels. *Biochimie* **82,** 861-868.

Power DG, Kelsen DP & Shah MA. (2010). Advanced gastric cancer--slow but steady progress. *Cancer treatment reviews* **36,** 384-392.

Prevarskaya N, Skryma R & Shuba Y. (2010). Ion channels and the hallmarks of cancer. *Trends in molecular medicine* **16,** 107-121.

Prior IA, Lewis PD & Mattos C. (2012). A comprehensive survey of Ras mutations in cancer. *Cancer research* **72,** 2457-2467.

Puxeddu E, Moretti S, Elisei R, Romei C, Pascucci R, Martinelli M, Marino C, Avenia N, Rossi ED, Fadda G, Cavaliere A, Ribacchi R, Falorni A, Pontecorvi A, Pacini F, Pinchera A & Santeusanio F. (2004). BRAF(V599E) mutation is the leading genetic event in adult sporadic papillary thyroid carcinomas. *The Journal of clinical endocrinology and metabolism* **89,** 2414-2420.

Quintero-Hernández V, Jiménez-Vargas JM, Gurrola GB, Valdivia HH & Possani LD. (2013). Scorpion venom components that affect ion-channels function. *Toxicon* **76,** 328-342.

Ravagnan L, Gurbuxani S, Susin SA, Maisse C, Daugas E, Zamzami N, Mak T, Jaattela M, Penninger JM, Garrido C & Kroemer G. (2001). Heat-shock protein 70 antagonizes apoptosis-inducing factor. *Nature Cell Biology* **3,** 839-843.

Ravingerova T, Barancik M & Strniskova M. (2003). Mitogen-activated protein kinases: a new therapeutic target in cardiac pathology. *Molecular and cellular biochemistry* **247,** 127-138.

Resende C, Thiel A, Machado JC & Ristimaki A. (2011). Gastric cancer: basic aspects. *Helicobacter* **16 Suppl 1,** 38-44.

Rodriguez de la Vega RC & Possani LD. (2004). Current views on scorpion toxins specific for K+-channels. *Toxicon* **43,** 865-875.

Rugo H, Shtivelman E, Perez A, Vogel C, Franco S, Tan Chiu E, Melisko M, Tagliaferri M, Cohen I, Shoemaker M, Tran Z & Tripathy D. (2007). Phase I trial and antitumor effects of BZL101 for patients with advanced breast cancer. *Breast cancer research and treatment* **105,** 17-28.

Runchel C, Matsuzawa A & Ichijo H. (2011). Mitogen-activated protein kinases in mammalian oxidative stress responses. *Antioxidants & redox signaling* **15,** 205-218.

Ryter SW, Kim HP, Hoetzel A, Park JW, Nakahira K, Wang X & Choi AM. (2007). Mechanisms of cell death in oxidative stress. *Antioxidants & redox signaling* **9,** 49-89.

Schwab A, Nechyporuk-Zloy V, Fabian A & Stock C. (2007). Cells move when ions and water flow. *European journal of physiology* **453,** 421-432.

Schwab A, Reinhardt J, Schneider SW, Gassner B & Schuricht B. (1999). K(+) channel-dependent migration of fibroblasts and human melanoma cells. *Cellular physiology and biochemistry* **9,** 126-132.

Scott AM, Allison JP & Wolchok JD. (2012). Monoclonal antibodies in cancer therapy. *Cancer immunity* **12,** 14.

Shao J, Kang N, Liu Y, Song S, Wu C & Zhang J. (2007). Purification and characterization of an analgesic peptide from Buthus martensii Karsch. *Biomedical chromatography* **21,** 1266-1271.

Shiao YH, Rugge M, Correa P, Lehmann HP & Scheer WD. (1994). p53 alteration in gastric precancerous lesions. *The American journal of pathology* **144,** 511-517.

Sidach SS & Mintz IM. (2002). Kurtoxin, a gating modifier of neuronal high- and low-threshold ca channels. *The Journal of neuroscience* **22,** 2023-2034.

Six DA & Dennis EA. (2000). The expanding superfamily of phospholipase A(2) enzymes: classification and characterization. *Biochimica et biophysica acta* **1488,** 1-19.

Smith I, Procter M, Gelber RD, Guillaume S, Feyereislova A, Dowsett M, Goldhirsch A, Untch M, Mariani G, Baselga J, Kaufmann M, Cameron D, Bell R, Bergh J, Coleman R, Wardley A, Harbeck N, Lopez RI, Mallmann P, Gelmon K, Wilcken N, Wist E, Sanchez Rovira P & Piccart-Gebhart MJ. (2007). 2-year follow-up of trastuzumab after adjuvant chemotherapy in HER2-positive breast cancer: a randomised controlled trial. *Lancet* **369,** 29-36.

Son YO, Jang YS, Heo JS, Chung WT, Choi KC & Lee JC. (2009). Apoptosis-inducing factor plays a critical role in caspase-independent, pyknotic cell death in hydrogen peroxide-exposed cells. *Apoptosis* **14,** 796-808.

Song Y, Hoang BQ & Chang DD. (2002). ROCK-II-induced membrane blebbing and chromatin condensation require actin cytoskeleton. *Experimental cell research* **278,** 45-52.

Soroceanu L, Manning TJ, Jr. & Sontheimer H. (1999). Modulation of glioma cell migration and invasion using Cl(-) and K(+) ion channel blockers. *The Journal of neuroscience* **19,** 5942-5954.

Srinivasan KN, Gopalakrishnakone P, Tan PT, Chew KC, Cheng B, Kini RM, Koh JL, Seah SH & Brusic V. (2002a). SCORPION, a molecular database of scorpion toxins. *Toxicon* **40,** 23-31.

Srinivasan KN, Sivaraja V, Huys I, Sasaki T, Cheng B, Kumar TK, Sato K, Tytgat J, Yu C, San BC, Ranganathan S, Bowie HJ, Kini RM & Gopalakrishnakone P. (2002b). kappa-Hefutoxin1, a novel toxin from the scorpion Heterometrus fulvipes with unique structure and function. Importance of the functional diad in potassium channel selectivity. *The Journal of biological chemistry* **277,** 30040-30047.

Steelman LS, Abrams SL, Shelton JG, Chappell WH, Basecke J, Stivala F, Donia M, Nicoletti F, Libra M, Martelli AM & McCubrey JA. (2010). Dominant roles of the Raf/MEK/ERK pathway in cell cycle progression, prevention of apoptosis and sensitivity to chemotherapeutic drugs. *Cell Cycle* **9,** 1629-1638.

Suerbaum S & Michetti P. (2002). Helicobacter pylori infection. *The New England journal of medicine* **347,** 1175-1186.

Suhr SM & Kim DS. (1996). Identification of the snake venom substance that induces apoptosis. *Biochemical and biophysical research communications* **224,** 134-139.

Tait SWG & Green DR. (2008). Caspase-independent cell death: leaving the set without the final cut. *Oncogene* **27,** 6452-6461.

Tan NH & Fung SY. (2008). Snake Venom L-Amino Acid Oxidases and Their Potential Biomedical Applications. *Malaysian Journal of Biochemistry and Molecular Biology* **16,** 1-10.

Torres-Larios A, Gurrola GB, Zamudio FZ & Possani LD. (2000). Hadrurin, a new antimicrobial peptide from the venom of the scorpion Hadrurus aztecus. *European journal of biochemistry* **267,** 5023-5031.

Tsukuma H, Oshima A, Narahara H & Morii T. (2000). Natural history of early gastric cancer: a non-concurrent, long term, follow up study. *Gut* **47,** 618-621.

Tytgat J, Chandy KG, Garcia ML, Gutman GA, Martin-Eauclaire MF, van der Walt JJ & Possani LD. (1999). A unified nomenclature for short-chain peptides isolated from scorpion venoms: alpha-KTx molecular subfamilies. *Trends in pharmacological sciences* **20,** 444-447.

Tytgat J, Debont T, Rostoll K, Muller GJ, Verdonck F, Daenens P, van der Walt JJ & Possani LD. (1998). Purification and partial characterization of a 'short' insectotoxin-like peptide from the venom of the scorpion Parabuthus schlechteri. *FEBS letters* **441,** 387-391.

Uchino S, Tsuda H, Maruyama K, Kinoshita T, Sasako M, Saito T, Kobayashi M & Hirohashi S. (1993). Overexpression of c-erbB-2 protein in gastric cancer. Its correlation with long-term survival of patients. *Cancer* **72,** 3179-3184.

Valdez-Velázquez LL, Quintero-Hernández V, Romero-Gutiérrez MT, Coronas FIV & Possani LD. (2013). Mass Fingerprinting of the Venom and Transcriptome of Venom Gland of Scorpion Centruroides tecomanus. *PloS one* **8,** e66486.

Valdivia HH, Fuentes O, el-Hayek R, Morrissette J & Coronado R. (1991). Activation of the ryanodine receptor Ca2+ release channel of sarcoplasmic reticulum by a novel scorpion venom. *The Journal of biological chemistry* **266,** 19135-19138.

Valdivia HH, Kirby MS, Lederer WJ & Coronado R. (1992). Scorpion toxins targeted against the sarcoplasmic reticulum Ca(2+)-release channel of skeletal and cardiac muscle. *Proceedings of the National Academy of Sciences of the United States of America* **89,** 12185-12189.

Valentin E & Lambeau G. (2000). What can venom phospholipases A2 tell us about the functional diversity of mammalian secreted phospholipases A2? *Biochimie* **82,** 815-831.

Van Cutsem E, Moiseyenko VM, Tjulandin S, Majlis A, Constenla M, Boni C, Rodrigues A, Fodor M, Chao Y, Voznyi E, Risse ML & Ajani JA. (2006). Phase III study of docetaxel and cisplatin plus fluorouracil compared with cisplatin and fluorouracil as first-line therapy for advanced gastric cancer: a report of the V325 Study Group. *Journal of clinical oncology* **24,** 4991-4997.

Vizoso FJ, Corte MD, Alvarez A, Garcia I, del Casar JM, Bongera M, Gonzalez LO, Garcia-Muniz JL & Allende MT. (2004). Membranous levels of c-erbB-2 oncoprotein in gastric cancer: their relationship with clinicopathological parameters and their prognostic significance. *The International journal of biological markers* **19,** 268-274.

Vleminckx K, Vakaet L, Jr., Mareel M, Fiers W & van Roy F. (1991). Genetic manipulation of E-cadherin expression by epithelial tumor cells reveals an invasion suppressor role. *Cell* **66,** 107-119.

Wang SW, Pan SL, Huang YC, Guh JH, Chiang PC, Huang DY, Kuo SC, Lee KH & Teng CM. (2008). CHM-1, a novel synthetic quinolone with potent and selective antimitotic antitumor activity against human hepatocellular carcinoma in vitro and in vivo. *Molecular cancer therapeutics* **7,** 350-360.

Wang WX & Ji YH. (2005). Scorpion venom induces glioma cell apoptosis in vivo and inhibits glioma tumor growth in vitro. *Journal of neuro-oncology* **73,** 1-7.

Wang XQ, Terry PD & Yan H. (2009). Review of salt consumption and stomach cancer risk: epidemiological and biological evidence. *World journal of gastroenterology* **15,** 2204-2213.

Wang Y, Yang J, Chen L, Wang J, Luo J, Pan L & Zhang X. (2014). Artesunate induces apoptosis through caspase-dependent and -independent mitochondrial pathways in human myelodysplastic syndrome SKM-1 cells. *Chemico-biological interactions* **219C,** 28-36.

Warkentin TE, Greinacher A & Koster A. (2008). Bivalirudin. *Thrombosis and haemostasis* **99,** 830-839.

Watabe H, Mitsushima T, Yamaji Y, Okamoto M, Wada R, Kokubo T, Doi H, Yoshida H, Kawabe T & Omata M. (2005). Predicting the development of gastric cancer from combining Helicobacter pylori antibodies and serum pepsinogen status: a prospective endoscopic cohort study. *Gut* **54,** 764-768.

Wei A, Zhou D, Xiong C, Cai Y & Ruan J. (2011). A novel non-aromatic B-ring flavonoid: isolation, structure elucidation and its induction of apoptosis in human

colon HT-29 tumor cell via the reactive oxygen species-mitochondrial dysfunction and MAPK activation. *Food and chemical toxicology* **49,** 2445-2452.

Weinstein S, Dart R, Staples A & White J. (2009). Envenomations: an overview of clinical toxinology for the primary care physician. *American family physician* **80,** 793-802.

Welch DR, Sakamaki T, Pioquinto R, Leonard TO, Goldberg SF, Hon Q, Erikson RL, Rieber M, Rieber MS, Hicks DJ, Bonventre JV & Alessandrini A. (2000). Transfection of constitutively active mitogen-activated protein/extracellular signal-regulated kinase kinase confers tumorigenic and metastatic potentials to NIH3T3 cells. *Cancer research* **60,** 1552-1556.

Werner F. (1935). Scorpiones, Pedipalpi. In *Bronns Klassen und Ordnungen des Tierreich*, ed. Bronn HG, pp. 1-490. Leipzig.

White RM, Levine MS, Enterline HT & Laufer I. (1985). Early gastric cancer. Recent experience. *Radiology* **155,** 25-27.

Widmann C, Gibson S, Jarpe MB & Johnson GL. (1999). Mitogen-activated protein kinase: conservation of a three-kinase module from yeast to human. *Physiological reviews* **79,** 143-180.

Williams SC. (2009). Scorpions. In *Encyclopedia of Insects (Second Edition)*, ed. Resh VH & Cardé RT, pp. 904-909. Academic Press.

Xiang J, Chao DT & Korsmeyer SJ. (1996). BAX-induced cell death may not require interleukin 1 beta-converting enzyme-like proteases. *Proceedings of the National Academy of Sciences of the United States of America* **93,** 14559-14563.

Xiao Y, Yang FQ, Li SP, Gao JL, Hu G, Lao SC, Conceicao EL, Fung KP, Wangl YT & Lee SM. (2007). Furanodiene induces G2/M cell cycle arrest and apoptosis through MAPK signaling and mitochondria-caspase pathway in human hepatocellular carcinoma cells. *Cancer biology & therapy* **6,** 1044-1050.

Yamada Y. (2013). Molecular therapy for gastric cancer. *Chinese Clinical Oncology* **2,** 5.

Yang JY, Zong CS, Xia WY, Yamaguchi H, Ding QQ, Xie XM, Lang JY, Lai CC, Chang CJ, Huang WC, Huang H, Kuo HP, Lee DF, Li LY, Lien HC, Cheng XY, Chang KJ, Hsiao CD, Tsai FJ, Tsai CH, Sahin AA, Muller WJ, Mills GB, Yu DH, Hortobagyi GN & Hung MC.

(2008). ERK promotes tumorigenesis by inhibiting FOXO3a via MDM2-mediated degradation. *Nature Cell Biology* **10,** 138-148.

Yang L, Wang P, Wang H, Li Q, Teng H, Liu Z, Yang W, Hou L & Zou X. (2013). Fucoidan derived from Undaria pinnatifida induces apoptosis in human hepatocellular carcinoma SMMC-7721 cells via the ROS-mediated mitochondrial pathway. *Marine drugs* **11,** 1961-1976.

Yang Y, Zhao W, Xu QW, Wang XS, Zhang Y & Zhang J. (2014). IQGAP3 promotes EGFR-ERK signaling and the growth and metastasis of lung cancer cells. *PloS one* **9,** e97578.

Yu JY, Zheng ZH, Son YO, Shi X, Jang YO & Lee JC. (2011). Mycotoxin zearalenone induces AIF- and ROS-mediated cell death through p53- and MAPK-dependent signaling pathways in RAW264.7 macrophages. *Toxicology in vitro* **25,** 1654-1663.

Zagouri F, Papadimitriou CA, Dimopoulos MA & Pectasides D. (2011). Molecularly targeted therapies in unresectable-metastatic gastric cancer: a systematic review. *Cancer treatment reviews* **37,** 599-610.

Zamudio FZ, Conde R, Arevalo C, Becerril B, Martin BM, Valdivia HH & Possani LD. (1997). The mechanism of inhibition of ryanodine receptor channels by imperatoxin I, a heterodimeric protein from the scorpion Pandinus imperator. *The Journal of biological chemistry* **272,** 11886-11894.

Zargan J, Sajad M, Umar S, Naime M, Ali S & Khan HA. (2011a). Scorpion (Androctonus crassicauda) venom limits growth of transformed cells (SH-SY5Y and MCF-7) by cytotoxicity and cell cycle arrest. *Experimental and molecular pathology* **91,** 447-454.

Zargan J, Sajad M, Umar S, Naime M, Ali S & Khan HA. (2011b). Scorpion (Odontobuthus doriae) venom induces apoptosis and inhibits DNA synthesis in human neuroblastoma cells. *Molecular and cellular biochemistry* **348,** 173-181.

Zargan J, Umar S, Sajad M, Naime M, Ali S & Khan HA. (2011c). Scorpion venom (Odontobuthus doriae) induces apoptosis by depolarization of mitochondria and reduces S-phase population in human breast cancer cells (MCF-7). *Toxicology in vitro* **25,** 1748-1756.

Zeng XC, Li WX, Zhu SY, Peng F, Zhu ZH, Wu KL & Yiang FH. (2000). Cloning and characterization of a cDNA sequence encoding the precursor of a chlorotoxin-like peptide from the Chinese scorpion Buthus martensii Karsch. *Toxicon* **38,** 1009-1014.

Zhang FT, Xu ZS & Qi YX. (1987). A preliminary research of the antineoplasia effects induced by Buthus martensii of Chinese drug-I. Observation of the effect on mice with tumor. *Journal of Gannan Medical University* **6,** 1-5.

Zhang J, Yang PL & Gray NS. (2009). Targeting cancer with small molecule kinase inhibitors. *Nature reviews Cancer* **9,** 28-39.

Zhang L & Cui L. (2007). A cytotoxin isolated from Agkistrodon acutus snake venom induces apoptosis via Fas pathway in A549 cells. *Toxicology in vitro* **21,** 1095-1103.

Zhang YY, Wu LC, Wang ZP, Wang ZX, Jia Q, Jiang GS & Zhang WD. (2009b). Anti-proliferation Effect of Polypeptide Extracted from Scorpion Venom on Human Prostate Cancer Cells in vitro. *Journal of clinical medicine research* **1,** 24-31.

Zhao Y, Cai X, Ye T, Huo J, Liu C, Zhang S & Cao P. (2011). Analgesic-antitumor peptide inhibits proliferation and migration of SHG-44 human malignant glioma cells. *Journal of cellular biochemistry* **112,** 2424-2434.

APPENDICES

Supp. Fig 1 Image *of Hottentotta hottentotta* scorpion. The copyright belongs to František Kovařík and the permission is obtained.

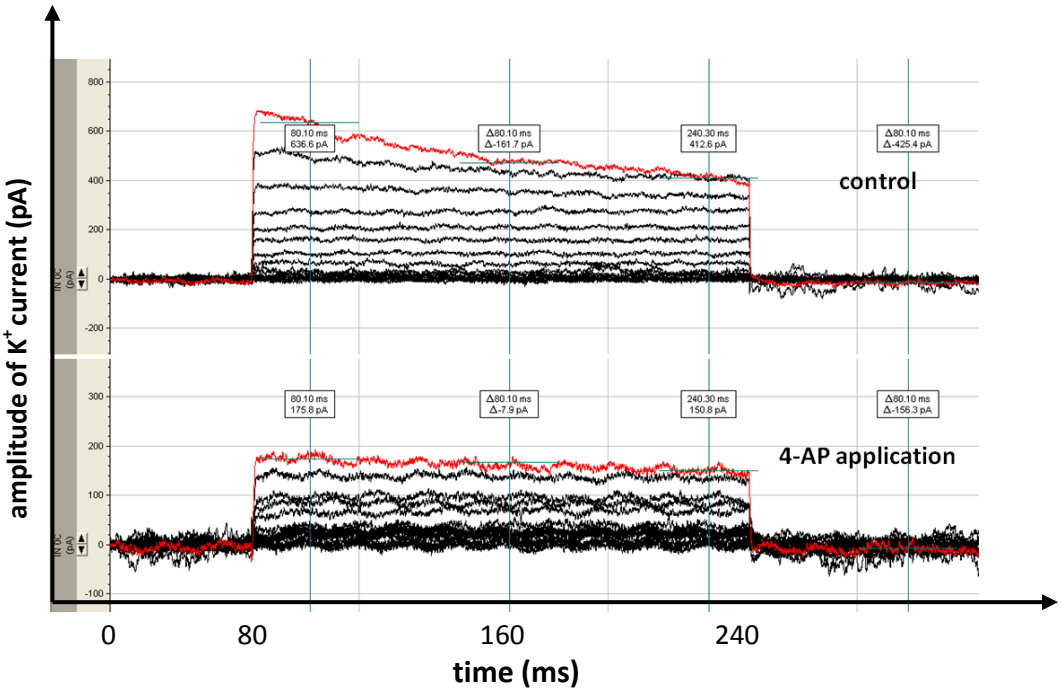

Supp. Fig 2 Identification of voltage-gated potassium channels in NUGC-3 cells by path clamp. 4-AP, 4-aminopyridine (1mM), as inhibitor of voltage gated potassium channels.

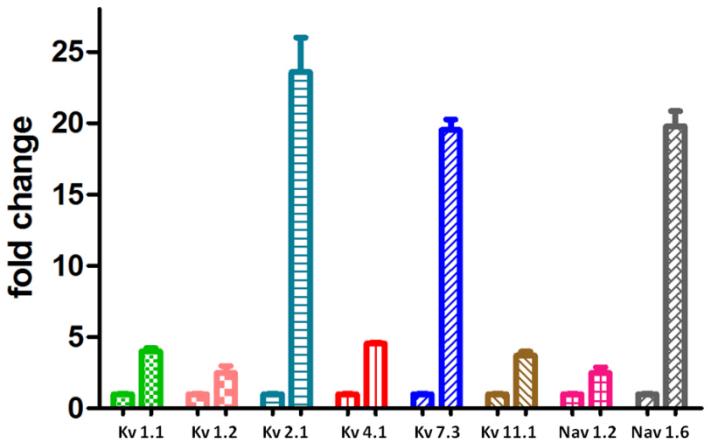

Supp. Fig 3 Gene expression of voltage gated ion channels in NUGC-3 cells by real time PCR. The fold change was normalized with the gene expression in HeLa cells. Data are presented as means + SEM. N=3.

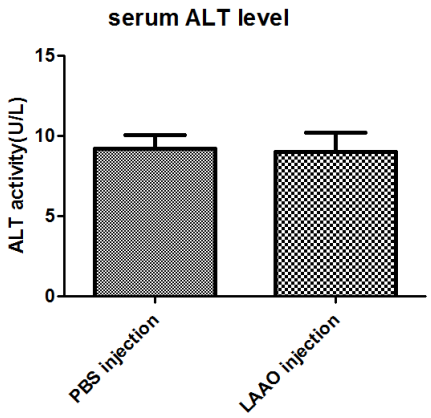

Supp. Fig 4 Measurement of mouse serum alanine transaminase (ALT) activity**.** Alanine Transaminase Activity Assay Kit was applied in this experiment (Cayman Chemical, MI, USA).Data are presented as means + SEM. N=3. p=0.90.

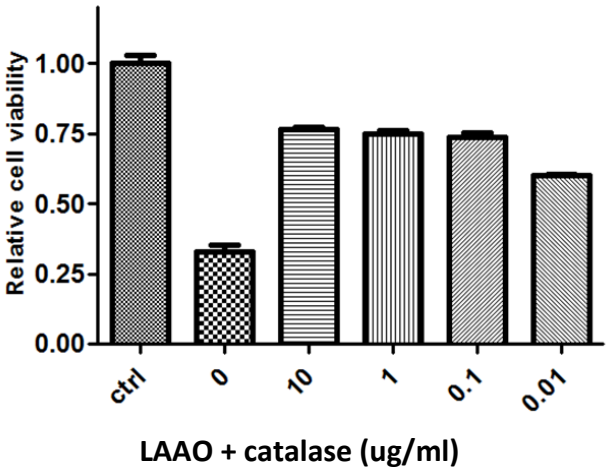

Supp. Fig 5 Role of catalase in LAAO induced reduction of cell viability of NUGC-3 cells. NUGC-3 cells were treated with 1 ug/ml LAAO and various concentrations of catalase for 24 h. Cell viability was analyzed by alamarBlue assay. Data are presented as means + SEM. N=3.

Supp. Table 1 Record of body weight of mice after BHV injection

Group	Labeling	body weight (g)			
control	G1--	19	19	20	20
	G5++	17	18	18	19
	G4L	18	17	18	17
	G2++	18	19	19	18
	G4 R	17	19	18	18
6.25 ug/mouse BHV	G5 L	17	17	18	17
	G6 R	19	19	20	20
	G4 ++	18	18	18	18
	G1 L	18	17	18	18
	G3 L	17	17	17	17
12.5 ug/mouse BHV	G6 --	19	20	20	19
	G3 ++	18	17	18	17
	G6 L	19	18	19	19
	G1 R	18	17	18	18
	G3 R	19	19	20	20
Time (day)		**Day 0**	**Day 2**	**Day 4**	**Day 7**

Minireview

Scorpion venoms as a potential source of novel cancer therapeutic compounds

Jian Ding, Pei-Jou Chua, Boon-Huat Bay and P Gopalakrishnakone

Venom and Toxin Research Programme, Department of Anatomy, Yong Loo Lin School of Medicine, National University of Singapore, Singapore 117 597

Corresponding author: P Gopalakrishnakone. Email: gopalakrishnakone_pon@nuhs.edu.sg

Abstract

Scorpions and their venoms have been used in traditional medicine for thousands of years in China, India and Africa. The scorpion venom is a highly complex mixture of salts, nucleotides, biogenic amines, enzymes, mucoproteins, as well as peptides and proteins (e.g. neurotoxins). One of the recently observed biological properties of animal venoms and toxins is that they possess anticancer potential. An increasing number of studies have shown that scorpion venoms and toxins can decrease cancer growth, induce apoptosis and inhibit cancer progression and metastasis *in vitro* and *in vivo*. Several active molecules with anticancer activities, ranging from inhibition of proliferation and cell cycle arrest to induction of apoptosis and decreasing cell migration and invasion, have been isolated from scorpion venoms. These observations have shed light on the application of scorpion venoms and toxins as potential novel cancer therapeutics. This mini-review focuses on the anticancer potential of scorpion venoms and toxins and the possible mechanisms for their antitumor activities.

Keywords: Scorpion, venoms and toxins, anticancer potential, apoptosis

***Experimental Biology and Medicine* 2014; 239: 387–393. DOI: 10.1177/1535370213513991**

Introduction

The scorpion, which is one of the oldest creatures known, has existed on earth for more than 400 million years. Scorpions are known to be widely distributed all over the world, and there are over 1500 species that have been reported thus far.[1] Scorpions have developed a negative reputation due to their stings and envenomation, usually resulting in pain, swelling, hypertension, cardiac arrhythmia and other systemic manifestations.[2] Scorpion envenomation is a public health hazard in tropical and subtropical regions. More than 1,200,000 scorpion stings are reported to occur yearly with the number of deaths possibly exceeding 3250 per year worldwide. There is therefore, the need for improvement in specific (antivenom) and systematic treatments.[3]

However, human beings have also derived benefits from the scorpion. In China, fried scorpions are popularly consumed as food, and scorpion or snake wines are used to strengthen the immune system.[4] The scorpion and its venom have been applied in traditional medicine for thousands of years in China, India and Africa. For example, in China, the dried whole bodies of scorpions have been widely used as an antiepilepsy and analgesic agent since the Song Dynasty (A.D. 960-1279).[5,6] The *Buthidae* family of scorpions has been widely studied for medical applications. The scorpion venom is a highly complex mixture produced from the venom gland to immobilize/paralyze the prey or to defend against predators. The venom which is found in the telson contains salts, nucleotides, biogenic amines, enzymes such as phospholipase, hyaluronidase, L-amino acid oxidase, metalloproteinase, serine protease, mucoproteins, as well as small peptides which are known to interact with various ion channels in excitable cell membranes, making them good candidates for drug design in the pharmaceutical industry.[7,8] A number of antimicrobial peptides have also been isolated and reported to be bioactive against bacteria, fungi, yeasts and viruses including Mucroporin-M1 which inhibits the amplification of hepatitis virus B and Kn2-7 which possesses anti-HIV-1 activity.[9,10]

This mini-review explores the significance of scorpion venoms as anticancer agents and provides biological insights into their mechanism (s) of action.

Scorpion venoms as potential cancer therapeutics

According to the World Health Organization, cancer has replaced heart disease to become the leading cause of

mortality worldwide, leading to 7.6 million deaths (around 13% of all deaths) in 2008.[11] Cancers of the lung, stomach, liver, colon and breast are known to be the highest contributors to cancer mortality each year. Even though treatment for cancer improved considerably over the past decade resulting in increased patient survival and better quality of life, early screening and diagnosis still play a very important role in improving the patient's survival rate, since many cancers have a high chance of cure if detected early and treated adequately.[12] Surgical resection of the primary tumor and regional lymph nodes is the main and most effective way to treat most patients with solid tumors.[13] Adjuvant and neo-adjuvant therapies (chemotherapy and radiotherapy) are known to benefit patients by increasing their survival remarkably. However, the side effects and risks of treatment resistance and toxicity are of major concern. Newly emerging targeted therapy opens a novel avenue for surgical oncologists and clinicians to better understand the molecular mechanism of cancer and provide alternative and effective approaches to combat cancer.[14]

One of the recently discovered biological properties of scorpion venom and toxin is that they possess anticancer potential. An increasing number of experimental and preclinical investigations have demonstrated that crude scorpion venom and some purified proteins and peptides can impair cancer proliferation, arrest cell cycle, induce cell apoptosis and inhibit cancer metastasis in *in vitro* or *in vivo* setting. The anticancer effect and efficacy of scorpion venoms have been tested in glioma, neuroblastoma, leukemia, lymphoma, breast, lung and prostate cancer.[15,16]

Chinese red scorpion (*Buthus martensii Karsch*) venom

Buthus martensii Karsch (BmK) (Figure 1), also known as Chinese red scorpion, belongs to the *Buthidea* family and can be extensively found from north western China to Mongolia and Korea. The medical use of BmK scorpion dates back to the Song Dynasty of China (A.D. 960-1279). To date, this scorpion venom has been well described as having antiepileptic, analgesic, anti-rheumatic and anticancer potential.[5,6,15,16] Among all the scorpions used in cancer research, BmK is probably the first to have been reported to possess antitumor properties.[16] BMK scorpion venom has been well studied in China, with several active molecules having been isolated and characterized, making this scorpion venom a good source for the development of anticancer agents.

Figure 1 *Buthus martensii Karsch* (Chinese red scorpion). Specimen from Jiangsu Province, PR China. Arrow indicates telson, the venom-producing gland. (A color version of this figure is available in the online journal)

In 1987, Zhang Futong, extracted a solution from the dried whole body of the BmK scorpion (Quan Xie in traditional Chinese medicine) and administered the extract subcutaneously to mice with reticulum cell sarcoma and MA-737 mammary carcinoma at a dose of 0.04 g/mouse every other day for five times.[17] On the 8th day following administration, the inhibitory rate of growth was 55.5% in reticulum cell sarcoma and 30.4% in mammary carcinoma, respectively. There was a decrease in DNA content in the tumor tissues after BmK venom treatment. This seminal finding formed the basis for the escalating reports on the anticancer potential of BmK scorpion venom.

Several groups later described the anticancer effects of the crude scorpion venom of BmK *in vitro* or *in vivo*. However, scientific literatures on the BMK venom which are published in Chinese will not be included in this review. Wang and Ji observed that the crude venom extract from BmK induced apoptosis of malignant glioma U251-MG cells *in vitro* especially at a dose of 10 mg/mL but was not cytotoxic to BEL7404 hepatocellular carcinoma cells and C400 Chinese hamster ovary cells.[18] For the *in vivo* study, BmK venom was assessed using severe combined immunodeficiency mice bearing U251-MG tumor xenografts. Both tumor volumes and weights were significantly reduced compared with the control group after 20 mg/kg BmK venom treatment for 21 days. The authors proposed ion channels as targets for BmK venom in glioma cells. Another study by Gao et al.[19] found that BmK venom could also inhibit growth of human Jurkat and Raji lymphoma cells by arresting the cell cycle and inducing apoptosis as evidenced by Annexin-V and propidium iodide staining and flow cytometry assay. Treatment with the BmK venom has been demonstrated to inactivate the PI3K/Akt signal pathway by increasing phosphatase and tensin homolog (PTEN) expression in Raji cells, whereas, in Jurkat cells, a PTEN-negative cell line, up-regulation of p27 (a cell cycle inhibitor) may partially account for the anticancer effect.[19]

In light of several reports on the anticancer potential of BmK crude venom, researchers attempted to purify and isolate the anticancer agent in BmK venom with techniques such as size-exclusive gel filtration, ion exchange chromatography and high-performance liquid chromatography.[20] Polypeptide extract from the scorpion venom (PESV), a group of polypeptides comprising 50–60 amino acids extracted from crude venom of BmK, was reported to induce growth inhibition and apoptosis of DU 145 human prostate cancer cell.[21] PESV treatment on DU 145 cells resulted in a significantly dose-dependent inhibition of proliferation with G1 phase arrest in cell cycle, accompanied by enhanced expression of p27 and a decrease in cyclin E. PESV treatment also induced a high apoptosis index, which was verified by the TdT-mediated dUTP-biotin nick-end labeling (TUNEL) assay and probably due to an

increase in pro-apoptotic protein Bax. A recent study reported that another partially purified component from BmK scorpion venom (SVCIII), obtained after gel filtration with a molecular weight of approximate 70–80 kDa, could inhibit cell proliferation of THP-1 and Jurkat human leukemia cells and caused cell cycle arrest at G1 phase.[22] A decrease of cyclin D1 expression was observed in a dose-dependent manner after SVCIII treatment. The antiproliferative effect has been attributed to the suppression of NF-κB activation.

Two anticancer peptides have been purified and characterized from BmK scorpion venom. Early in 2002, Liu and colleagues first isolated an analgesic-antitumor peptide (AGAP) from BmK scorpion venom with a series of purification steps.[23] This peptide had a relative molecular mass of 6280 Da and exerted antitumor effects in the mouse S-180 fibro sarcoma model and Ehrlich ascites tumor model. The AGAP gene was determined, cloned and expressed in the *Escherichia coli* system in 2003 by the same group (GeneBank No. AF464898) and the protein showed effective analgesic and antitumor activities.[24] Subsequently, BmK AGAP was classified as a voltage-gated sodium channel scorpion toxin and three transcription regulatory elements were elucidated in the BmK AGAP intron.[25] A recombinant fusion protein SUMO-AGAP which combined a small ubiquitin-related modifier to AGAP was proven to have antitumor activity.[26] Further study showed that SUMO-AGAP inhibited cell proliferation and migration of SHG-44 human malignant glioma cells by inducing cell cycle arrest and interfering with the p-Akt, NF-κB, Bcl-2 and MAPK signaling pathways.[27]

BmKCT, another purified anticancer peptide from BmK with 68% homology to chlorotoxin (a promising antiglioma toxin that will be discussed later), was cloned from a cDNA library made from the venom glands of the BmK scorpion.[28] BmKCT contains 59 amino acid residues and comprises a mature toxin of 35 residues with four disulfide bridges and a signal peptide of 24 residues. Subsequently, the recombinant peptide of BmKCT was shown to inhibit the growth of glioma cells (SGH-44) dose-dependently with IC50 value of approximately 0.28 μM while showing no toxicity to normal astrocytes under the same condition.[29] Whole-cell patch-clamp technique indicated that the chloride current in SHG-44 glioma cells was inhibited by BmKCT in a voltage-dependent manner (up to 55.86% inhibition at 0.14 μM treatment) and histological analysis of tissues from BmKCT-treated mice showed that the brain was one of the targets of this toxin. Furthermore, *in vivo* evidence from Fan et al. using the glioma/SD rat model[30] demonstrated that BmKCT toxin inhibited glioma proliferation and tumor metastasis and ^{131}I-labeled or Cy5.5-conjugated BmKCT selectively targeted the glioma *in situ*. All these observations provide evidence for the potential therapeutic application of BmKCT for glioma diagnosis and treatment.

Two scorpion enzymes, isolated by our research group from BmK scorpion venom, have also been reported to possess anticancer potential. One is the serine proteinase-like protein named BmK-CBP, which can dose-dependently bind with human breast cancer cells MCF-7.[31] The other, BmHYA1, a homogeneous hyaluronidase from the BmK scorpion, was shown to modulate the expression of CD44, a cell surface marker in the MDA-MB-231 breast cancer cell line.[32]

Scorpion venom targeted ion channels

A novel and promising field of cancer research is targeting Na^+, K^+, Ca^{2+} and Cl^- ion channels in cancer, given that altered or abnormal expression and activity of ion channels are related to cancer processes and pathology including cell volume and motility, cell proliferation and death, as well as cell adhesion, migration and invasion. Moreover, blocking ion channel activity can impair cancer growth and metastasis.[33,34]

Functional expression of voltage-gated sodium channels has been reported to be associated with several strongly metastatic carcinomas, such as breast and prostate cancer, as evidenced by their over-expression in aggressive cancer-derived cell lines and biopsies as well as its role in controlling multiple steps of metastatic cascades.[35] Fraser and co-workers[36] observed that functional expression of $Na_v1.5$ was up-regulated in metastatic human breast cancer cells and tissues, and its activity could potentiate cellular behaviours linked to metastasis, such as directional motility, endocytosis and invasion. Also, a strong correlation was found between $Na_v1.5$ expression and lymph node metastasis in a clinical study. Similar findings were also observed for the involvement of $Na_v1.7$ in prostate cancer.[37–39]

Compared to Na^+ channels, K^+ channels are mainly implicated in cancer cell proliferation and survival. There is a tight relationship between K_v expression and cell proliferation and apoptosis, but the underlying mechanism is still not clear. Generally, by regulating the membrane potential, K_v channels can control the Ca^{2+} fluxes and cell volume, and therefore exert their role in cell cycle regulation and cell death.[40] A number of K_v channels have been detected to be abnormally expressed in many primary cancers. $K_v1.3$ has been analyzed in gliomas, colon, prostate and breast cancers.[41] The aberrant expression of $K_v1.3$ was observed to promote cancer cell growth. The roles of K_v 1.5, $K_v10.1$ and $K_{Ca}3.1$ have been studied in gliomas, colon cancer and melanoma. $K_v11.1$, also known as hERG, is expressed in several cancers, including leukemia, neuroblastoma, stomach and colorectal cancers. The blockage of $K_v11.1$ with a channel inhibitor or siRNA interference can impair cell proliferation *in vitro* and reduce cell invasiveness, making it a novel therapeutic target for cancer.[42]

Among the peptides found in scorpion venoms, the most well-studied are the long-chain toxins with 60–70 amino acid residues cross-linked by four disulfide bridges, which interact with Na^+ channels. Short-chain toxins with 30–40 amino acid residues are known to modulate K^+ or Cl^- (chloride ion) channels.[43] Compared to massive Na^+ or K^+ channel toxins, only few calcium channel-related toxins (with a variable number of amino acids) have been purified or cloned from scorpion venoms.[44]

Chlorotoxin (CTX), a 36–amino acid small peptide, first purified from the *Leiurus quinquestriatus* scorpion venom in 1993, contains a single tyrosine residue that is available for

radioiodination, eight cysteine residues, and four disulfide bonds.[45] Originally, CTX was described as a Cl^- channel blocker that acts as a paralytic agent for small insects and other arthropods. CTX had been largely applied as a tool in the study of voltage-gated chloride channel until the seminal findings of Ullrich and co-workers in cancer research.[46,47] They adapted the whole cell patch-clamp recording technique to identify and characterize the voltage-activated outwardly-rectifying Cl^- currents in human astrocytoma/glioblastoma cells. Cl^- currents were observed in all tumor cells of glial origin (primary cultures of six freshly resected brain tumors and seven established human astrocytoma cell lines), while interestingly they were absent in normal non-malignant glial cells or non-glial tumors such as melanoma, breast, rhabdomyosarcoma and neuroblastoma. Their study also demonstrated that CTX could block the Cl^- current and inhibit cell proliferation of astrocytoma cells.

The specifically expressed Cl^- channel in glioma and its high affinity and sensitivity to CTX led to the use of this peptide by Soroceanu and colleagues to target gliomas in 1989.[48] They showed that biotinylated and fluorescence-tagged CTX and CTX-conjugated molecules had specific staining for glioma cells *in vitro*, *in situ* and in patient biopsies. Another survey of over 200 tissue biopsies from patients with various malignancies also suggest that CTX bind to the surface of gliomas and other embryologically related tumors of neuroectodermal origin but not to normal brain.[49] Furthermore, CTX has been reported to significantly reduce the glioma cell migration dose-dependently and inhibited cell invasion into fetal brain aggregates at 5 μM concentration.[50]

The receptor of CTX was initially believed to be related to the Cl^- channel from electrophysiological evidence (as described above). Further studies with a recombinant His-CTX revealed that the principal receptor is matrix metalloproteinase-2 (MMP-2), a proteinase that is present on the surface of glioma cells, and specifically over-expressed in gliomas and related cancers, but normally not expressed in brain.[51] CTX could inhibit the enzymatic activity and reduce the expression of MMP-2, causing disruption of chloride channels and Cl^- currents. A synthetic CTX coupled with radioactive iodine isotope (^{131}I-TM-601), produced by Transmolecular, Inc. (Cambridge, MA) has been approved by the US Food and Drug Administration for tumor imaging and diagnosis. Preclinical and Phase I clinical trials have been completed in recurrent glioma patients, with the conclusion that intracavitary dose of ^{131}I-TM-601 is safe and minimally toxic, and that ^{131}I-TM-601 binds malignant glioma with high specificity and for long duration.[52] A Phase II trial using a higher dose of radioactivity and repeated local administrations is currently in progress. Because CTX binds tumor with high affinity and specificity and shows low toxicity, it represents a promising diagnostic agent for imaging and targeted therapies for gliomas and other cancers.

Apart from CTX, several other scorpion toxins associated with ion channels have been purified and investigated in cancer research. Iberiotoxin (IbTX), a 37-amino acid neurotoxin from the Indian red scorpion *Mesobuthus tamulus*, has been reported to block the large conductance Ca^{2+} activated K^+ (BK) channel and induce a slight depolarization in MCF-7 human breast cancer cells. Cells treated with IbTX (500 nM) were observed to accumulate in S phase of the cell cycle but did not alter the cell proliferation rate.[53] Another experiment showed that blockade of the BK channels by IbTX inhibited K^+ currents and growth of PC-3 prostate cancer cells.[54] Margatoxin (MgTX), which is isolated from the venom of *Centruroides margartatus* scorpion, sharing a sequence homology and structural similarity with IbTX, has a high affinity and specificity against Kv1.3. Jang et al. found that MgTX can significantly inhibit the proliferation of A549 human lung adenocarcinoma cells by regulating the G1/S cell cycle progression. Western blot analysis showed increased expression of p21Waf1/Cip1 and decreased levels of CdK4 after 1 nM MgTX treatment. The antiproliferative effect of MgTX was also verified in a nude mice xenograft model, as confirmed by a reduction of tumor volume after injecting MgTX into the tumor tissues.[55]

Charybdotoxin (ChTX), another peptide isolated from *Leiurus quinquestriatus* scorpion venom, is structurally similar to IbTX and MgTX and acts as an inhibitor of Ca^{2+}-activated K^+ channel. Studies revealed that ChTX can inhibit the migration of NIH3T3 fibroblasts and human melanoma cells dose-dependently by up to 61%, possibly by depolarizing the cell membrane potential and reducing the electrochemical driving force for Ca^{2+} entry, which is important in the cell migration process.[56] However, in the same study, it was also observed that ChTX did not influence the disruption of the epithelial layer of renal cells by human melanoma cells, suggesting that K^+ channel activity was not involved in melanoma invasion.

Recent studies on the anticancer potential of scorpion venoms and toxins

Research on animal venoms and toxins has attracted greater interest because of advances in genomic and proteomic approaches such as the venomous systems genome project.[57] In addition, new emerging research regarding the relationship between ion channels and cancer progression and therapy has paved the way for novel clinical applications for scorpion venoms and toxins, given that scorpion venoms contain many disulfide-rich peptides and proteins which display high specificity, good permeability and stability against cancer cells.[58] In the last decade, more evidence has accumulated regarding the anticancer effect of scorpion venoms and toxins from different species and targeting assorted cancers.

In 2007, Gupta et al.[59] reported the antiproliferative and apoptogenic activities induced by *Heterometrus bengalensis Koch* (Indian black scorpion) against human leukemic U937 and K562 cell lines, characterized by cell cycle arrest, membrane blebbing, chromatin condensation and DNA degradation. The molecule of interest was subsequently purified and named Bengalin, a 72-kDa protein with an N-terminal sequence that shared no similarity with any protein in the scorpion toxin database. The IC50 of Bengalin was determined as 3.7 μg/mL and 4.1 μg/mL for U937 and K562 human leukemic cells, respectively, without affecting

normal human lymphocytes. Bengalin induced apoptosis as confirmed by damaged nuclei, sub G1 peak, DNA fragmentation as well as decreased telomerase activity. Furthermore, Bengalin caused the loss of mitochondrial membrane potential, decreased the expression of heat shock protein (HSP) 70 and 90, activated caspase-3, 9 and induced cleavage of poly (ADP-ribose) polymerase.[60] These observations indicated activation of a mitochondrial death cascade, involving inhibition of HSPs by Bengalin.

Two peptides named neopladine 1 and neopladine 2, isolated from *Tityus discrepans* scorpion venom, were reported to be effective in inducing apoptosis and necrosis of SKBR3 breast cancer cells with negligible effect on non-malignant MA104 monkey kidney cells.[61] Immunohistochemistry showed that neopladines bind to the surface of SKBR3 cell and triggered FasL and Bcl-2 expression. We have also found that the Indian red scorpion (*Mesobuthus tamulus)* venom decreased the cell viability of human breast cancer cells dose-dependently with minimal cytotoxic effect on normal breast epithelial cells *in vitro* (unpublished data).

Another research finding showed that scorpion venom from *Odontobuthus doriae* inhibited cell growth and induced apoptosis in SH-SY5Y human neuroblastoma cells and MCF-7 breast cancer cells.[62,63] Moreover, *Odontobuthus doriae* venom increased intracellular oxidative stress as evidenced by an increase in reactive nitrogen intermediates and depression of glutathione and catalases in MCF-7 cells, which may contribute to the induction of apoptosis. The cytotoxicity of another scorpion venom *Androctonus crassicauda* was also screened using MCF-7 and SH-SY5Y cell lines.[64] Similarly, *Androctonus crassicauda* venom caused the suppression of cell growth by S-phase cell cycle arrest and induced apoptosis by increasing nitric oxide production, thereby, activating caspase-3 and depolarizing mitochondrial membrane. The above findings suggest that the *Odontobuthus doriae* and *Androctonus crassicauda* scorpion venoms may be potential sources for isolating effective anticancer molecules.

Cytotoxic proteins such as Bengalin and Neopladine 1 and 2 with molecular weight more than 10 kDa are able to inhibit cell viability and induce apoptosis or necrosis in cancer cells while showing negligible cytotoxicity to normal cells. Hence, such proteins are promising for developing as anticancer drugs.

Besides cancer therapy, scorpion venoms have also been applied in diagnostic imaging of tumor, mainly based on the conjugates of CTX and its homological peptides (e.g. BmKCT) to delineate the tumor margins. Researchers have combined CTX with other radioactive or fluorescence molecules, such as ^{131}I, Cy5.5, and iron oxide nanoparticles coated with polyethylene glycol, and synthesized various probes that can be detected by γ-camera, single photon emission computed tomography or magnetic resonance imaging.[52,65,66] Due to the binding specificity of CTX and the use of nanovectors, the CTX-conjugated probes can cross the blood-brain barrier and work as imaging agents in tumors of the central nervous system. In addition, the CTX-conjugated nanoparticles are now being developed as a carrier of DNA in gene therapy in glioma.[67]

Conclusion

In summary, the anticancer effects of scorpion venoms and toxins have been reported for several scorpion species and in different cancer types, in both *in vitro* and *in vivo* settings. Scorpion venoms with anticancer properties and possible mechanisms of action are summarized in Table 1. It can be clearly seen that the anticancer effects are achieved mainly via targeting ion channels on cell membrane, or exerting antiproliferative or apoptotic activities by cell cycle arrest or induction of caspase-dependent apoptosis pathways.

Currently, only a few scorpion species have been investigated for anticancer effects. As many of the studies have been carried out in the *in vitro* setting, testing the antitumor potential of scorpion venoms/toxins in animal models is important for preclinical research work and drug design. Although purification and characterization of the active components which exert anticancer effects from crude venoms still remain a challenge, there is potential for the use of scorpion venoms as novel cancer therapeutics.

Table 1 Summary of the important molecules with anticancer potential and possible mechanisms

Molecules	Scorpion species	Tested cancer models	Possible mechanisms	References
BmK AGAP	*Buthus martensii Karsch*	Mouse fibro sarcoma, Rhrlich ascites tumor, SHG-44 glioma cells	Voltage gated sodium channel toxin, interfering p-AKT, NF-κB, Bcl-2 and MAPK signaling pathway	23–27
BmKCT	*Buthus martensii Karsch*	SHG-44 glioma cells, glioma/SD rat	Inhibit chloride current and selectively target glioma	28–30
Chlorotoxin	*Leiurus quinquestriatus*	Glioma cells, animal models and clinical trials	Inhibit chloride current, bind to matrix metalloproteinase-2 (MMP-2)	48–52
Iberiotoxin	*Mesobuthus tamulus*	MCF-7 breast cancer cells	Block large conductance Ca2+ activated K+ (BK) channel	53, 54
Magatoxin	*Centruroides margartatus*	A549 human lung adenocarcinoma cells and xenograft model	Inhibit Kv 1.3, increase expression of p21Waf1/Cip1 and decrease CdK4	55
Charybdotoxin	*Leiurus quinquestriatus*	NIH3T3 fibroblasts and human melanoma cells	Inhibit cell migration does-dependently	56
Bengalin	*Heterometrus bengalensis Koch*	human leukemic U937 and K562 cells	Induce caspase apoptosis pathway by loss of mitochondrial membrane potential and decreased HSP 70 and 90	59, 60
Neopladine 1 and 2	*Tityus discrepans*	SKBR3 breast cancer cell line	Trigger FasL and BcL-2 expression	61

Author contributions: JD wrote the first draft of the paper and made subsequent revisions. PJC, BHB and PG gave comments and suggestions during the writing of the paper and made amendments to the pre-final draft. All authors reviewed the final draft of the manuscript before submission.

ACKNOWLEDGEMENT

This work was supported by Grant NMRC/EDG/1013/2010. JD is a recipient of the National University of Singapore Research Scholarship.

REFERENCES

1. Simard MJ, Watt DD. *Venoms and toxins*. Stanford: Stanford University Press, 1990
2. Bawaskar HS, Bawaskar PH. Scorpion sting: update. *J Assoc Physicians India* 2012;**60**:46–55
3. Chippaux JP, Goyffon M. Epidemiology of scorpionism: a global appraisal. *Acta tropica* 2008;**107**:71–9
4. Ye HY, Liu JX, Zen J, Huang XH, Zhu ZP, Lai F. The Chronic Effect of Snake Wine on the Anti-inflammatory. *J Gannan Med Coll* 2003;**23**:123–6
5. Zhou XH, Yang D, Zhang JH, Liu CM, Lei KJ. Purification and N-terminal partial sequence of anti-epilepsy peptide from venom of the scorpion Buthus martensii Karsch. *Biochem J* 1989;**257**:509–17
6. Shao J, Kang N, Liu Y, Song S, Wu C, Zhang J. Purification and characterization of an analgesic peptide from Buthus martensii Karsch. *Biomed Chromatogr* 2007;**21**:1266–71
7. Andreotti N, Jouirou B, Mouhat S, Mouhat L, Sabatier JM. *Comprehensive Natural Products II*. Oxford: Elsevier, 2010
8. Ahn MY, Ryu KS, Lee YW, Kim YS. Cytotoxicity and L-amino acid oxidase activity of crude insect drugs. *Arch Pharm Res* 2000;**23**:477–81
9. Zhao Z, Hong W, Zeng Z, Wu Y, Hu K, Tian X, Li W, Cao Z. Mucroporin-M1 inhibits hepatitis B virus replication by activating the mitogen-activated protein kinase (MAPK) pathway and down-regulating HNF4alpha in vitro and in vivo. *J Biol Chem* 2012;**287**:30181–90
10. Chen Y, Cao L, Zhong M, Zhang Y, Han C, Li Q, Yang J, Zhou D, Shi W, He B, Liu F, Yu J, Sun Y, Cao Y, Li Y, Li W, Guo D, Cao Z, Yan H. Anti-HIV-1 activity of a new scorpion venom peptide derivative Kn2-7. *PLoS One* 2012;**7**:e34947
11. Jemal A, Bray F, Center MM, Ferlay J, Ward E, Forman D. Global cancer statistics. *CA Cancer J Clin* 2011;**61**:69–90
12. Srinivas PR, Kramer BS, Srivastava S. Trends in biomarker research for cancer detection. *The Lancet Oncology* 2001;**2**:698–704
13. Reed M. Principles of cancer treatment by surgery. *Surgery (Oxford)* 2009;**27**:178–81
14. Malinowsky K, Wolff C, Gundisch S, Berg D, Becker K. Targeted therapies in cancer - challenges and chances offered by newly developed techniques for protein analysis in clinical tissues. *J Cancer* 2010;**2**:26–35
15. Gomes A, Bhattacharjee P, Mishra R, Biswas AK, Dasgupta SC, Giri B. Anticancer potential of animal venoms and toxins. *Indian J Exp Biol* 2010;**48**:93–103
16. Heinen TE, da Veiga AB. Arthropod venoms and cancer. *Toxicon* 2011;**57**:497–511
17. Zhang FT, Xu ZS, Qi YX. A preliminary research of the antineoplasia effects induced by Buthus martensii of Chinese drug-I. Observation of the effect on mice with tumor. *J Gannan Med Coll* 1987;**6**:1–5
18. Wang WX, Ji YH. Scorpion venom induces glioma cell apoptosis in vivo and inhibits glioma tumor growth in vitro. *J Neurooncol* 2005;**73**:1–7
19. Gao F, Li H, Chen YD, Yu XN, Wang R, Chen XL. Upregulation of PTEN involved in scorpion venom-induced apoptosis in a lymphoma cell line. *Leukemia Lymphoma* 2009;**50**:633–41
20. Deutscher MP. *Protein purification : guide to protein purification*. San Diego: Academic Press, 1990
21. Zhang YY, Wu LC, Wang ZP, Wang ZX, Jia Q, Jiang GS, Zhang WD. Anti-proliferation effect of polypeptide extracted from scorpion venom on human prostate cancer cells in vitro. *J Clin Med Res* 2009;**1**:24–31
22. Song X, Zhang G, Sun A, Guo J, Tian Z, Wang H, Liu Y. Scorpion venom component III inhibits cell proliferation by modulating NF-kappa B activation in human leukemia cells. *Exp Ther Med* 2012;**4**:146–50
23. Liu YF, Hu J, Zhang JH, Wang SL, Wu CF. Isolation, purification, and N-terminal partial sequence of an antitumor peptide from the venom of the Chinese scorpion Buthus martensii Karsch. *Prep Biochem Biotechnol* 2002;**32**:317–27
24. Liu YF, Ma RL, Wang SL, Duan ZY, Zhang JH, Wu LJ, Wu CF. Expression of an antitumor-analgesic peptide from the venom of Chinese scorpion Buthus martensii karsch in Escherichia coli. *Protein Expr Purif* 2003;**27**:253–8
25. Cui Y, Liu Y, Chen Q, Zhang R, Song Y, Jiang Z, Wu C, Zhang J. Genomic cloning, characterization and statistical analysis of an antitumor-analgesic peptide from Chinese scorpion Buthus martensii Karsch. *Toxicon* 2010;**56**:432–9
26. Cao P, Yu J, Lu W, Cai X, Wang Z, Gu Z, Zhang J, Ye T, Wang M. Expression and purification of an antitumor-analgesic peptide from the venom of Mesobuthus martensii Karsch by small ubiquitin-related modifier fusion in Escherichia coli. *Biotechnol Prog* 2010;**26**:1240–4
27. Zhao Y, Cai X, Ye T, Huo J, Liu C, Zhang S, Cao P. Analgesic-antitumor peptide inhibits proliferation and migration of SHG-44 human malignant glioma cells. *J Cell Biochem* 2011;**112**:2424–34
28. Zeng XC, Li WX, Zhu SY, Peng F, Zhu ZH, Wu KL, Yang FH. Cloning and characterization of a cDNA sequence encoding the precursor of a chlorotoxin-like peptide from the Chinese scorpion Buthus martensii Karsch. *Toxicon* 2000;**38**:1009–14
29. Fu YJ, Yin LT, Liang AH, Zhang CF, Wang W, Chai BF, Yang JY, Fan XJ. Therapeutic potential of chlorotoxin-like neurotoxin from the Chinese scorpion for human gliomas. *Neurosci Lett* 2007;**412**:62–7
30. Fan S, Sun Z, Jiang D, Dai C, Ma Y, Zhao Z, Liu H, Wu Y, Cao Z, Li W. BmKCT toxin inhibits glioma proliferation and tumor metastasis. *Cancer Lett* 2010;**291**:158–66
31. Gao R, Zhang Y, Gopalakrishnakone P. Purification and N-terminal sequence of a serine proteinase-like protein (BMK-CBP) from the venom of the Chinese scorpion (Buthus martensii Karsch). *Toxicon* 2008;**52**:348–53
32. Feng L, Gao R, Gopalakrishnakone P. Isolation and characterization of a hyaluronidase from the venom of Chinese red scorpion Buthus martensi. *Comp Biochem Physiol C Toxicol Pharmacol* 2008;**148**:250–7
33. Arcangeli A, Crociani O, Lastraioli E, Masi A, Pillozzi S, Becchetti A. Targeting ion channels in cancer: a novel frontier in antineoplastic therapy. *Curr Med Chem* 2009;**16**:66–93
34. Prevarskaya N, Skryma R, Shuba Y. Ion channels and the hallmarks of cancer. *Trends Mol Med* 2010;**16**:107–21
35. Onkal R, Djamgoz MB. Molecular pharmacology of voltage-gated sodium channel expression in metastatic disease: clinical potential of neonatal Nav1.5 in breast cancer. *Eur J Pharmacol* 2009;**625**:206–19
36. Fraser SP, Diss JK, Chioni AM, Mycielska ME, Pan H, Yamaci RF, Pani F, Siwy Z, Krasowska M, Grzywna Z, Brackenbury WJ, Theodorou D, Koyuturk M, Kaya H, Battaloglu E, De Bella MT, Slade MJ, Tolhurst R, Palmieri C, Jiang J, Latchman DS, Coombes RC, Djamgoz MB. Voltage-gated sodium channel expression and potentiation of human breast cancer metastasis. *Clin Cancer Res* 2005;**11**:5381–9
37. Fraser SP, Salvador V, Manning EA, Mizal J, Altun S, Raza M, Berridge RJ, Djamgoz MB. Contribution of functional voltage-gated Na+ channel expression to cell behaviors involved in the metastatic cascade in rat prostate cancer: I. Lateral motility. *J Cell Physiol* 2003;**195**:479–87
38. Mycielska ME, Fraser SP, Szatkowski M, Djamgoz MB. Contribution of functional voltage-gated Na+ channel expression to cell behaviors involved in the metastatic cascade in rat prostate cancer: II. Secretory membrane activity. *J Cell Physiol* 2003;**195**:461–9
39. Diss JK, Stewart D, Pani F, Foster CS, Walker MM, Patel A, Djamgoz MB. A potential novel marker for human prostate cancer: voltage-gated sodium channel expression in vivo. *Prostate Cancer Prostatic Dis* 2005;**8**:266–73

40. Becchetti A. Ion channels and transporters in cancer. 1. Ion channels and cell proliferation in cancer. *Am J Physiol Cell Physiol* 2011;**301**:C255–65
41. Felipe A, Vicente R, Villalonga N, Roura-Ferrer M, Martinez-Marmol R, Sole L, Ferreres JC, Condom E. Potassium channels: new targets in cancer therapy. *Cancer Detect Prev* 2006;**30**:375–85
42. Asher V, Sowter H, Shaw R, Bali A, Khan R. Eag and HERG potassium channels as novel therapeutic targets in cancer. *World J Surg Oncol* 2010;**8**:113
43. Goudet C, Chi CW, Tytgat J. An overview of toxins and genes from the venom of the Asian scorpion Buthus martensi Karsch. *Toxicon* 2002;**40**:1239–58
44. Zhijian C, Yun X, Chao D, Shunyi Z, Shijin Y, Yingliang W, Wenxin L. Cloning and characterization of a novel calcium channel toxin-like gene BmCa1 from Chinese scorpion Mesobuthus martensii Karsch. *Peptides* 2006;**27**:1235–40
45. DeBin JA, Maggio JE, Strichartz GR. Purification and characterization of chlorotoxin, a chloride channel ligand from the venom of the scorpion. *Am J Physiol* 1993;**264**:C361–9
46. Ullrich N, Sontheimer H. Biophysical and pharmacological characterization of chloride currents in human astrocytoma cells. *Am J Physiol* 1996;**270**:C1511–21
47. Ullrich N, Gillespie GY, Sontheimer H. Human astrocytoma cells express a unique chloride current. *Neuroreport* 1996;**7**:1020–4
48. Soroceanu L, Gillespie Y, Khazaeli MB, Sontheimer H. Use of chlorotoxin for targeting of primary brain tumors. *Cancer Res* 1998;**58**:4871–9
49. Lyons SA, O'Neal J, Sontheimer H. Chlorotoxin, a scorpion-derived peptide, specifically binds to gliomas and tumors of neuroectodermal origin. *Glia* 2002;**39**:162–73
50. Soroceanu L, Manning TJ Jr, Sontheimer H. Modulation of glioma cell migration and invasion using Cl(−) and K(+) ion channel blockers. *J Neurosci* 1999;**19**:5942–54
51. Deshane J, Garner CC, Sontheimer H. Chlorotoxin inhibits glioma cell invasion via matrix metalloproteinase-2. *J Biol Chem* 2003;**278**:4135–44
52. Mamelak AN, Rosenfeld S, Bucholz R, Raubitschek A, Nabors LB, Fiveash JB, Shen S, Khazaeli MB, Colcher D, Liu A, Osman M, Guthrie B, Schade-Bijur S, Hablitz DM, Alvarez VL, Gonda MA. Phase I single-dose study of intracavitary-administered iodine-131-TM-601 in adults with recurrent high-grade glioma. *J Clin Oncol* 2006;**24**:3644–50
53. Bloch M, Ousingsawat J, Simon R, Schraml P, Gasser TC, Mihatsch MJ, Kunzelmann K, Bubendorf L. KCNMA1 gene amplification promotes tumor cell proliferation in human prostate cancer. *Oncogene* 2007;**26**:2525–34
54. Ouadid-Ahidouch H, Roudbaraki M, Ahidouch A, Delcourt P, Prevarskaya N. Cell-cycle-dependent expression of the large Ca2+-activated K+ channels in breast cancer cells. *Biochem Biophys Res Commun* 2004;**316**:244–51
55. Jang SH, Choi SY, Ryu PD, Lee SY. Anti-proliferative effect of Kv1.3 blockers in A549 human lung adenocarcinoma in vitro and in vivo. *Eur J Pharmacol* 2011;**651**:26–32
56. Schwab A, Reinhardt J, Schneider SW, Gassner B, Schuricht B. K(+) channel-dependent migration of fibroblasts and human melanoma cells. *Cell Physiol Biochem* 1999;**9**:126–132
57. Menez A, Stocklin R, Mebs D. 'Venomics' or: The venomous systems genome project. *Toxicon* 2006;**47**:255–9
58. King GF. Venoms as a platform for human drugs: translating toxins into therapeutics. *Expert Opin Biol Ther* 2011;**11**:1469–84
59. Gupta SD, Debnath A, Saha A, Giri B, Tripathi G, Vedasiromoni JR, Gomes A. Indian black scorpion (Heterometrus bengalensis Koch) venom induced antiproliferative and apoptogenic activity against human leukemic cell lines U937 and K562. *Leuk Res* 2007;**31**:817–25
60. Gupta SD, Gomes A, Debnath A, Saha A. Apoptosis induction in human leukemic cells by a novel protein Bengalin, isolated from Indian black scorpion venom: through mitochondrial pathway and inhibition of heat shock proteins. *Chem Biol Interact* 2010;**183**:293–303
61. D'Suze G, Rosales A, Salazar V, Sevcik C. Apoptogenic peptides from Tityus discrepans scorpion venom acting against the SKBR3 breast cancer cell line. *Toxicon* 2010;**56**:1497–505
62. Zargan J, Sajad M, Umar S, Naime M, Ali S, Khan HA. Scorpion (Odontobuthus doriae) venom induces apoptosis and inhibits DNA synthesis in human neuroblastoma cells. *Mol Cell Biochem* 2011;**348**:173–81
63. Zargan J, Umar S, Sajad M, Naime M, Ali S, Khan HA. Scorpion venom (Odontobuthus doriae) induces apoptosis by depolarization of mitochondria and reduces S-phase population in human breast cancer cells (MCF-7). *Toxicol In Vitro* 2011;**25**:1748–56
64. Zargan J, Sajad M, Umar S, Naime M, Ali S, Khan HA. Scorpion (Androctonus crassicauda) venom limits growth of transformed cells (SH-SY5Y and MCF-7) by cytotoxicity and cell cycle arrest. *Exp Mol Pathol* 2011;**91**:447–54
65. Veiseh M, Gabikian P, Bahrami SB, Veiseh O, Zhang M, Hackman RC, Ravanpay AC, Stroud MR, Kusuma Y, Hansen SJ, Kwok D, Munoz NM, Sze RW, Grady WM, Greenberg NM, Ellenbogen RG, Olson JM. Tumor paint: a chlorotoxin:Cy5.5 bioconjugate for intraoperative visualization of cancer foci. *Cancer Res* 2007;**67**:6882–8
66. Fu Y, An N, Li K, Zheng Y, Liang A. Chlorotoxin-conjugated nanoparticles as potential glioma-targeted drugs. *J Neurooncol* 2012;**107**:457–62
67. Huang R, Ke W, Han L, Li J, Liu S, Jiang C. Targeted delivery of chlorotoxin-modified DNA-loaded nanoparticles to glioma via intravenous administration. *Biomaterials* 2011;**32**:2399–406